Engineering lipid nanocapsule systems for intracellular delivery of anticancer drugs

Paola Sánchez Moreno

Tesis Doctoral

Programa de doctorado de Biomedicina

UNIVERSIDAD DE GRANADA

Editor: Editorial de la Universidad de Granada
Autor: Paola Sánchez Moreno
D.L.: GR 1848-2014
ISBN: 978-84-9083-031-4

Editor: Editorial Universidad de Granada

Autor: Paola Sánchez Moreno

D.L.:

ISBN:

Engineering lipid nanocapsule systems for intracellular delivery of anticancer drugs

por

Paola Sánchez Moreno

Directores del trabajo:

Juan Luis Ortega Vinuesa
Prof. Titular de Física Aplicada

José Manuel Peula García
Prof. Titular de Física Aplicada

Houria Boulaiz Tassi
Prof. Titular de Embriología y Anatomía Humana

Trabajo presentado para aspirar al grado de Doctor por la Universidad de Granada

Granada, Enero 2014

La doctoranda Paola Sánchez Moreno y los directores de tesis Juan Luis Ortega Vinuesa, José Manuel Peula García y Houria Boulaiz garantizamos, al firmar esta tesis doctoral, que el trabajo ha sido realizado por el doctorando bajo la dirección de los directores de la tesis y hasta donde nuestro conocimiento alcanza, en la realización del trabajo, se han respetado los derechos de otros autores a ser citados, cuando se han utilizado sus resultados o publicaciones.

Granada, Enero 2014

Directores de la tesis: Doctorando:

Fdo.: Juan Luis Ortega Vinuesa Fdo.: Paola Sánchez Moreno

Fdo.: José Manuel Peula García

Fdo.: Houria Boulaiz Tassi

A mi abuela Pepa

A mis padres y mis hermanos,
por su amor incondicional

Agradecimientos

Y aquí me encuentro finalmente escribiendo mi parte favorita de la tesis, de nuestra tesis, porque sin vuestra ayuda y apoyo habría sido imposible. Es muy difícil expresar en unas hojas lo agradecida que estoy por todo lo que me habéis dado todas las personas que habéis aparecido en mi camino estos años. Espero de corazón que os lleguen estas palabras sinceras de gratitud. Imaginadlas gigantes, en mayúscula y luminosas.

Quiero comenzar dando las gracias a la persona que me abrió las puertas de esta etapa maravillosa de mi vida, José Antonio Masegosa conocido en el I.E.S Alquivira como "El Físico", mi profesor de física del instituto que pensó en mí como la persona idónea para esta posición en la que, me contaba, se iba a trabajar en investigación relacionada con el cáncer, mi sueño desde hacía mucho tiempo.

Gracias a mis directores de tesis Juan Luis, Peula y Houria por guiarme y darme la libertad necesaria para crecer como científica, escuchar mi opinión y siempre tenerla en cuenta. Siempre me habéis hecho sentir capaz y competente para esta profesión y me he sentido muy valorada. Peula y Juan Luis sois dos personas excepcionales, además de ser los bioquímicos montañeros más guapos del departamento. Y la dulce Houria, gracias por tus consejos, tu transparencia y por cuidarme como una hermana mayor. Incluyo en este grupo a mis directores de tesis no oficiales, Antonio Martín y Juan Marchal. Gracias de corazón Antonio por confiar en mí desde el principio, por subirme en tu barco y llevarme de la mano durante los primeros años y por las miles de risas que hemos compartido, haciendo mención especial al congreso en Zaragoza. Gracias Juan por tu disponibilidad absoluta, tu optimismo y por trasmitirme tu pasión por la ciencia. Hemos hecho un equipo genial, ¡Abrazo grupal!

Gracias a todos los componentes del grupo de Física de Fluidos y Biocoloides. El trabajar en una disciplina diferente a la biología y en un ambiente ejemplar como el que conseguís mantener día tras día ha hecho expandir mi mente e interiorizar este sistema de trabajo como el modelo a seguir en cualquier posición futura. A Roque por ser una de las personas más inquieta y apasionada que he conocido y a María José por cuidarnos tanto. Gracias a mis queridísimos Conrado y Jose Antonio, no os imagináis cuánto os aprecio y cuántas cosas me habéis enseñado, ambos tenéis un corazón gigante. Gracias a Fernando, Julia, Alberto, Curro, Cabrerizo, Emilia, Pepe Callejas, Juan de Vicente, Natalia, Miguel Ángel, Juan Carlos, Miguel Heredia, Ana Belén, Arturo y María; gracias a todos por darme vuestras sonrisas, consejos, cariño o conversaciones tan inspiradoras. Y a ti Delfi, no sé cómo darte las gracias. Has sido mi ángel de la guarda y mi IMO, incluso me diste el empujón en Oporto para conseguir la estancia en Dublín que ha cambiado el rumbo de mi vida; nunca me quitaré las gafas de la perspectiva diferente que me has regalado. Gracias desde lo más profundo de mi corazón.

Bajando de la primera planta del departamento y pasando el péndulo entro en la sala de becarios en la que me encuentro a mis compañeros, con los que he pasado tan grandes momentos. Empezando por mis Migueles: mil gracias Miguel Wulff por enseñarme tanto sobre ciencia y mundo chanante y por los momentos surrealistas en tu coche rumbo a la Venta del Peral, con las ventanas bajadas y la melena al viento (tú no), junto a nuestro amado Punset que nos explicaba a todo volumen que en un universo paralelo podríamos tener un coche con aire acondicionado, pero no seríamos tan guays. Gracias Miguel Peláez por tus preguntas trascendentales de super físico friki sin respuesta para una modesta bióloga, por tu humor inteligente y tus cuentos del Japón con banda sonora incluida. Gracias Juan Pablo por todas las conversaciones y por ser más bueno que el pan y a Azahara por enseñarme tanto, por ser una mujer y científica excelente y por descubrirme y traer a la sala con frecuencia la butter cream; gracias a los dos

además por ser los mejores compañeros de juergas. Gracias a Pablo por tan buenos ratos de fiesta y en la sala, por coger el teléfono y comerte todos los dulces (que tantos kilos me habrían supuesto). También a la parte mejicana de la sala que tanto nos ha enriquecido: César, el supuesto rockero puro que bailó y disfrutó todas las canciones de la verbena de Orce, incluyendo la de "se va el caimán"; Carmen, la mujer de roble, por darme un gran lección de vida; Felipe por tu ingenio que tanto me ha hecho reír; Efrén y Yadira por mostrarme siempre vuestra sonrisa. Mil gracias a mis queridísimas super científicas, deportistas y grandes personas: Ame, por ayudarme tanto, y Miri por regalarme tanta música y consejos. Gracias a Germán, por transmitirme tu filosofía de vida que me ha aportado tantas reflexiones y por ser tan verde (en el sentido ecológico de la palabra), a José Antonio por tu arte, salero y humildad, a Miguel por las enriquecedoras conversaciones sobre software libre que algún día usaré y a Leo por ser tan dulce y cariñosa. Y gracias también a los que llegaron más tarde pero no con menos fuerza: Diego porque, resumidamente, eres un sol; mi rubiales bonico, Alvariño; mi maravillosa Teresa que en tan poco tiempo me has robado el corazón, y gracias también a Irene, Keshbad, Daniel e Inma por los, aunque cortos, intensos ratos juntos.

Además del grupo de Física aplicada quiero dar las gracias a mi otro grupo, del departamento de Anatomía y Embriología Humana ubicado en el país "Far far away" también conocido como el Campus de la Salud, donde se encuentran mis compañeros biólogos. Muchas gracias a Manu por tu optimismo para afrontar las cosas, a Cynthia, que eres un primor de los primores, a mi maestro de los cultivos celulares Alberto, a la mujer más tímida y responsable, Elena, y a la mujer más fiestera, cañera y divertida, Eleno. Gracias también a Blanca porque tú también me encantas, a la joya de la corona Esther, a Marian por tu apoyo científico y por estar siempre ahí para lo que necesitamos y a Macarena por tu coherencia y principios. Muchas gracias Milán por abrirme las puertas de tu casa en Cork y hacerme pasar

unos días inolvidables, gracias también a Angelina Ina por tu inmensa sonrisa y dulce carácter y al gran fichaje nuevo, Carmen USA. Quiero hacer especial mención a Gemita; compañera durante la carrera, juntas también de alumnas internas en Genética (mil gracias a Rober, Chuchi y Belén que nos enseñásteis a manejarnos en el laboratorio) y compañeras estos años durante el doctorado. Gracias por toda la ayuda que me has dado a nivel profesional durante ya no sé cuántos años día tras día y por cuidarme tantísimas veces las células haciendo una estupendo papel de tita Gema. Pero te quiero dar las gracias sobre todo por ser mi amiga, por cuidarme, darme tu confianza y por estar siempre. Y aquí incluyo a Tomás Justicia, uno de mis artistas preferidos, porque pasaste muy rápido de ser el novio de Gema a ser también mi amigo y eres una de las personas más buenas que conozco.

Thanks, heartfelt thanks to all the people I have met in Dublin, my irish family, during my research stay. You made this experience one of the best in my life. Thanks a million to the amazing people in the Centre for BioNano Interactions (CBNI): Margarita, Tiago, Pippo, John Ah, Fengjuan, Pitek, Linda, Daithi, Louise, Prado, Potti, Bogumila, Daniele, Simona, Eugene, Chris, Marco, Sergio, Dong, Sha, Kanlaya, Delyan, Larry, Miglena, Paolo, Rong, Cristina and Sandra; and thanks as well to my housemates and people outside the CBNI: Adam, Jenny, Audrey, Ben, Gabriela, Joan, Jovana, Luis, Kate, Himanshu and Kiran. Thanks to the professor Kenneth Dawson for giving me this opportunity and specially I want to thank Anna Salvati, thank you very much for supervising and strongly supporting me.

Quiero dar las gracias también a mis tres citometristas preferidos; los dos de la UGR, Jaime Lazuén y Gustavo Ortiz, y el de la University College Dublin, Alfonso Blanco, por tantas geniales conversaciones científicas y no tan científicas que echo tanto de menos desde que me enseñasteis a volar sola. Y también a los microscopistas Raquel Marrero, Mohamed Tassi y Ana Santos, por simpatiquísimos que sois. Así como a Pedro e Irene del departamento de Química-Física de la UGR

con los que he tenido el placer de trabajar los últimos meses del doctorado y ojalá hubiese conocido antes.

Tengo que agradecer el apoyo financiero recibido bajo los proyectos MAT2010-20370 y MAT2007-66662-C02-01 del Ministerio de Educación, Cultura y Deporte.

Fuera del ámbito profesional, me gustaría dar las gracias a mis amigas de toda la vida, las niñangas: Ana, Bea, Clara, Laura, Mª Ángeles, MºLoli, Merces, Rosa y el niñango, Jose. Son tantas y tantas cosas que es imposible describir porqué os estoy tan agradecida. Simplemente gracias por vuestra amistad y por hacerme reír un millón de veces al día.

Las gracias más grandes del mundo para mis padres y mis hermanos por dármelo todo. Por darme vuestro amor infinito, por apoyarme en todas mis decisiones y respetarme cuando no compartís mi opinión, por estar siempre conmigo por mucho que nos alejemos, por ilusionaros con mis cosas como si fueran vuestras y por lo feliz que me hace cada día hablar con vosotros y ser consciente de la familia tan increíble que tengo. Os quiero con locura.

Gracias en general a toda mi familia, tan grande y con gente tan bonita, por los valores que me seguís transmitiendo y por compartir tantas cosas, estar tan unidos y apoyarnos siempre. Especialmente quiero dar las gracias a mis tíos Mari Tere y Antonio, que tantas veces me habéis llevado a Orce para desconectar y una vez allí me habéis hecho pasar ratos increíbles, y a mi prima Tere, más hermana que prima.

Finalmente, gracias a la persona con la que he decidido emprender mi nueva aventura y con la que he compartido el final de ésta, Mattia. Gracias a las

miles de millones de casualidades que se han tenido que dar para que se cruzaran nuestros caminos porque desde que lo hicieron y empezamos a caminar juntos, aunque a veces más lejos de lo que nos gustaría, me siento la persona más afortunada y feliz del mundo. Ti amo ciccio!

Granada, 9 de enero del 2014

Contents:

Resumen

A pesar de todo el esfuerzo invertido en la investigación del cáncer y aunque se han conseguido numerosos avances, en la mayoría de los casos se continúan usando terapias convencionales como puede ser la quimioterapia. El mayor inconveniente que presenta este tratamiento, además de la baja solubilidad en medio acuoso de muchos fármacos antitumorales, es la inespecificidad en su suministro, afectando indiscriminadamente tanto células sanas como cancerígenas, de modo que los pacientes sufren una gran cantidad de efectos secundarios. Con el avance de la nanotecnología y su aplicación en la medicina, han surgido nuevas oportunidades y se han desarrollado distintos sistemas a escala nanométrica que mejoran la liberación intracelular de los fármacos que transportan.

En este contexto, las nanocápsulas lipídicas presentan una elevada capacidad para encapsular y transportar fármacos liposolubles en su núcleo oleoso que se protege del exterior mediante una corteza compuesta por fosfolípidos, otros surfactantes y moléculas con grupos funcionales que añaden una alta versatilidad en cuanto a la modificación superficial permitiendo la vectorización del nanosistema. De esta forma, el objetivo principal de esta tesis ha sido el desarrollo de nanocápsulas lipídicas con distintas características superficiales que sean capaces de transportar fármacos liposolubles. Adicionalmente, se han puesto a punto dos estrategias de vectorización superficial diferentes, una de ellas mediante ácido fólico y la otra mediante anticuerpos monoclonales. Todos los nanosistemas sintetizados han sido caracterizados físico-químicamente para comprender en profundidad el comportamiento de estas nanocápsulas en condiciones fisiológicas simuladas y se han realizado ensayos *in vitro* utilizando distintas líneas celulares tumorales y sanas para para analizar su captación celular y estudiar el efecto citotóxico de los fármacos encapsulados.

Abstract

Despite all the effort made in the field of cancer research and although many advances have been achieved, in most cases conventional therapies, including chemotherapy, are still the choice. The main disadvantage of this treatment, in addition to the low solubility of many antitumor drugs, is the lack of specificity when they are supplied, affecting indiscriminately both healthy and cancer cells, so the patients suffer many side effects. Progress in nanotechnology and its application in medicine have provided new opportunities and different colloidal systems capable to improve the intracellular delivery of the drugs that they transport have been developed.

In this context, lipid nanocapsules present a high ability to encapsulate and transport lipophilic drugs in their oily core, which is protected by a shell composed by phospholipids, other surfactants and molecules with functional groups that add a high versatility in terms of surface modification allowing the vectorization of the nanosystems. Therefore the main objective of this thesis has been the development of lipid nanocapsules able to carry lipophilic drugs, presenting different surface characteristics. Additionally two strategies of surface vectorization have been developed using, independently, folic acid and monoclonal antibodies. All the nanosystems synthesized have been physico-chemically characterized to fully understand the behavior of these nanocapsules under simulated physiological conditions, and *in vitro* assays have been carried out in different tumor and healthy cell lines with the aim of studying their cellular uptake and the cytotoxic effect of the encapsulated drugs.

Chapter 1. Introduction

The term "Nanotechnology" refers to the design, characterization and application of structures, devices and systems by controlling shape and size at atomic, molecular and supramolecular level (1). Advances in nanotechnology have led to the development of new nanomaterials whose physico-chemical properties differ from those of their larger counterparts due to their higher surface-to-volume ratio. These novel properties make them excellent candidates for biomedical applications. Nanotechnology is a new discipline of science and engineering that has led to innovative approaches in many areas of medicine. Its applications in the screening, diagnosis, and treatment of diseases are collectively referred to as "nanomedicine", an emerging field that has the potential to revolutionize individual and population-based health this century (2). In contrast to conventional therapies, where the basic approach is to remove diseased cells faster than healthy cells, nanomedicine attempts to use sophisticated approaches to either kill specific cells or repair them, one cell at a time (3). It is now possible to provide therapy at a molecular level with the help of nanoparticles, treating diseases and adding light to our understanding of their pathogenesis. Nanomedicine can be considered a

refinement of molecular medicine, integrating innovations in genomics and proteomics on the road to a more personalized medicine, so as to allow improved treatment efficacies for many diseases.

1.1. Nanomedicine: origin and advantages over more traditional medical approaches

The advent of nanomaterials was forecast as long ago as 1959 by Richard P. Feynman, "the man who dared to think small" (4). Feynman proposed using machine tools to make smaller machine tools and so on until the atomic level (5). Nowadays, over fifty years later, nanomedicine is playing a growing part in pharmaceutical research and development, primarily in the form of nanoparticle-based delivery systems for drugs and imaging agents, connecting a broad range of disciplines –engineering, biology, physics and chemistry– and leading to numerous publications and patents (see Figure 1).

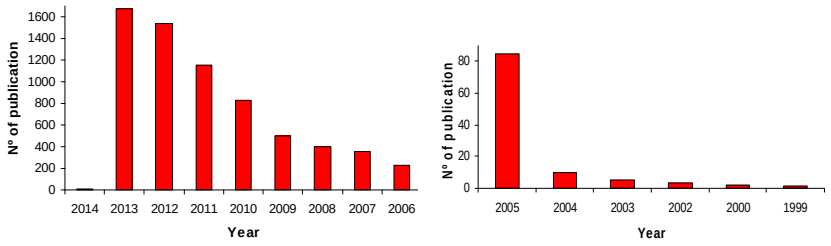

Figure1. Evolution of publications related to nanomedicine over time. Search performed in PubMed database using the term "nanomedicine" as a key word. (http://www.ncbi.nlm.nih.gov/pubmed/?term=nanomedicine)

Nanomedicine applications are grouped in three interrelated areas: analytical/diagnostic tools, regenerative medicine and drug delivery.

1.1.1. Nanomolecular diagnostics

Nanomolecular diagnostics is the use of nanobiotechnology in molecular diagnostics (6) and can be termed 'nanodiagnostics'. Nanodiagnostic tools are developed to meet the rigorous demands of the clinical laboratory for sensitivity, and therefore earlier disease detection and cost-effectiveness.

In a diagnostic assay usually a recognition element (eg. nucleic acid, enzyme, antibody, receptor, tissue, cell, aptamer) interacts with a compound or microorganism of interest and the physical property of a label (such as pH, electron transfer, heat, potential, mass, optical properties) is used to detect this event. In heterogeneous formats, a support might be used to immobilize the recognition element (7). Nanostructures are deployed either as a label or as a support. Due to their small sizes, they can detect very few molecules in solution offering lowest limits of detection and thereby improving sensitivity. Furthermore, conventional labels (such as fluorescent dyes) can be immobilized on nanostructures improving the detection signal and thus the sensitivity of the diagnostic assay. Some examples of nanostructures as diagnostic tools that bring in marked improvements over prevalent classical assays are nanobiosensors, microarrays, latex immunoaggregation assays, biochips of different elements (DNA, proteins or cells) and lab-on-a-chip devices (2).

1.1.2. Regenerative nanomedicine

Tissue engineering brings together principles and innovations from engineering and the life sciences for the improvement, repair or replacement of tissue/organ function. Nanotechnology has the potential to provide instruments that can accelerate progress in the field of tissue engineering and reconstruction, which will greatly enhance and contribute to the field of regenerative medicine (8).

There have been great strides made in using nanomedicine to enhance the functions of cells necessary to regenerate a diverse number of tissues (such as bone, blood vessels, skin, teeth, the nervous system, cornea and the heart among others). In this context, Liu et al. explored the use of silver nanoparticles (AgNPs) on skin excisional wound healing. The *in vitro* and *in vivo* experiments revealed that AgNPs could increase the rate of wound closure through the promotion of proliferation and migration of keratinocytes and by driving the differentiation of fibroblasts into myo-fibroblast for wound contraction (9). Moreover, the mechanical function in healed skin after treatment with AgNPs had similar elastic force, collagen deposition, as well as collagen fibrils alignment to normal skin (10). These results indicated that AgNPs could regulate remodeling process during skin tissue regeneration.

Other applications of nanotechnology in regenerative medicine include the design and development of nanomaterials to mimic extracellular matrices and form scaffolds, an artificial extracellular matrix suitable for tissue formation, using various materials, such as collagen, calcium sulfate and chitosan hydroxyapatite (11-14), or superparamagnetic iron oxide nanoparticles developed to track the migration of mesenchymal stem cells (15). These can be further modified, e.g. for bone repair, with the addition of nanoparticles like boron, growth factors, and/or stem cells (16-18). The various nano-based scaffolds acted on bone matrix to promote recruitment of circulating stem cells, induce proliferation and eventual differentiation into mature osteoblasts.

1.1.3. Drug delivery

Nanoparticle-based drug delivery systems present a large number of advantages for enhancing the activity and overcoming problems associated with traditional therapies.

The biological activity of a substance therapeutically active (a drug) depends, above all, on the nature of the interaction with the target tissue or organ. The interaction occurs when the drug is in the desirable place and in the right quantity to achieve the desired response, which means that the therapeutic agent should be released at a specific location in the body and at a controllable speed. This can be achieved if the active ingredient is suitably formulated prior to administration.

Typically drugs are orally taken, because oral is the most convenient route and usually the safest and least expensive (19), but a large number of drugs cannot be administered by this route because the amount absorbed through the gastrointestinal membrane is too small to produce a therapeutic effect. For these and other difficulties, many drugs should be administered by alternative routes such as parenteral, topical or inhaled route, among others. Parenteral route is particularly important because it avoids many of the problems associated with oral drug delivery because the drug directly reaches to the blood. But intravenous injection of poorly soluble drugs may cause embolization of blood vessels due to drug aggregation, and it often shows local toxicity as a result of high drug concentrations at the site of deposition (20).

Often, conventional dosage forms require repeated administration in order to maintain the drug concentration in the blood to a level high enough to ensure a therapeutic effect. Chronic administration may be inconvenient for the patient, leading to poor compliance with the prescribed dosing regimen. A tool to fix this and other problems associated with repeated administration of a drug is the medical application of nanotechnology.

The greatest advantage of nanotechnology lies in its potential to create novel structures with enhanced abilities to translocate through cell membranes, thereby, enhancing their delivery efficiency. The benefits of developing nanoparticles as drug delivery systems include enhancement of pharmacological activity (21), solubility (many drug molecules can be incorporated in the particle matrix) (22), stability and bioavailability (designing nanoparticles with optimal size and surface characteristics to increase their circulation time in the bloodstream) (23), protection from toxicity and physical and chemical degradation, sustained delivery (24), feasibility of variable routes of administration (25), facilitation of the drug transport across critical and specific barriers (26), etc. Engineering materials on this scale allow for novel medical therapies which are able to release the associated drug to the target tissue in a controlled manner, improving the specificity and resulting in decreased side effects for patients (27). Furthermore the diverse platforms of nanotechnology can be utilized to combine different drugs into a single nanotherapeutic agent for synergistic therapeutic benefits.

1.2. Nanoparticles for therapeutic molecules delivery in cancer therapy

Cancer is currently the third most common cause of death in the world after heart and infectious diseases. According to the estimation of World Cancer Research Fund International based on GLOBOCAN 2008 (the latest year available) and the European cancer mortality predictions for the year 2013, three most common cancers among men are prostate, lung and colorectal cancer while in women, breast, lung and colorectal cancer are the most frequent types of cancer. As stated in the American Cancer Society in the United States in 2013 (28), the prostate (in males) and breast (in females) cancer have the highest frequency of new cases of cancer. Figure 2 shows the estimated data of predicted deaths by cancer in the European Union for five leading cancer types by gender (29).

Cancer results from a group of cells that begin to grow abnormally by disregarding the normal division rules of cell division. Because of their uncontrolled growth and proliferation, these cancer cells (caused by multiple changes in gene expression) establish an autonomous tumor tissue. The main cause of cancer lethality is the spreading of malignant tumor cells, called metastasis (30).

In cancer therapy, undoubtedly the first and the most important step is diagnosis. In the case of patients with solid tumors, the first step of treatment is usually the surgery, to remove cancer cells. Then, to destroy any possible remnants of the tumor, the area should be irradiated and, at the same time or later, cytotoxic drugs can be used to kill residual cancer cells and possible metastases.

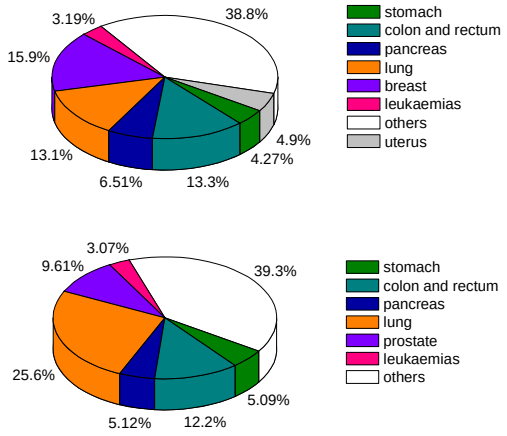

Figure 2. Leading cancer types for the estimated deaths by gender, A) Females B) Males. European Union, 2013.

Conventional anticancer therapies are distributed nonspecifically in the body where they damage both cancerous and normal cells in a state of division, thereby limiting the dose achievable within the tumor and also resulting in

suboptimal treatment due to excessive toxicities. Many effective drugs are hydrophobic, or if soluble, never reach their destination. While the search for efficacious anti-cancer therapeutics continues, it becomes increasingly clear that nanovehicles designed to specifically accumulate in the sites of the body where they are needed in order to improve pharmacotherapeutic outcomes, can play an essential role to formulate effective treatment plans. The main objective of the application of nanomedicines in cancer is to increment therapeutic effectiveness, increasing bioavailability profiles and enabling the administration of lower doses while obtaining lower toxicity rates and rising the quality of patient health (31). Other objective is to overcome the development of multiple drug resistance mechanisms that make this treatment ineffective in a high percentage of cancer cases because cancer cells can evade the cytotoxicity (32-33).

Anticancer nanomedicines require the integration of drugs into nanostructured drug delivery platforms. These platforms are submicron-sized particles (10 – 1000 nm in diameter) (34), devices or systems that can be made using a variety of materials (including polymers, lipids, viruses and organometallic compounds, among others) (35). Moreover all nanoparticle based drug delivery vectors must be able to both transport and release the drug to a specific location. They can be classified by their physical form or functional properties, both of which should be adapted to the specific needs of the drug to be delivered, and the intended therapeutic use (36).

Even though nanomedicine is a relatively new branch of science, many novel nanoparticle drug delivery platforms have been developed over the past three decades. These platforms generally fall into the following categories: polymer-based drug carriers, lipid-based drug carriers, viral nanoparticles, carbon nanotubes, ceramic nanoparticles, magnetic nanoparticles and metal-based nanoparticles. Figure 3 shows some examples of drug delivery platforms.

Polymer-based drug carriers

Polymer therapeutics have been extensively investigated as therapeutic carriers. They encompass polymer–protein conjugates, drug-polymer conjugates and supramolecular drug-delivery systems. Many polymers have been proposed as drug delivery carriers, but only a few of them have been accepted into clinical practice.

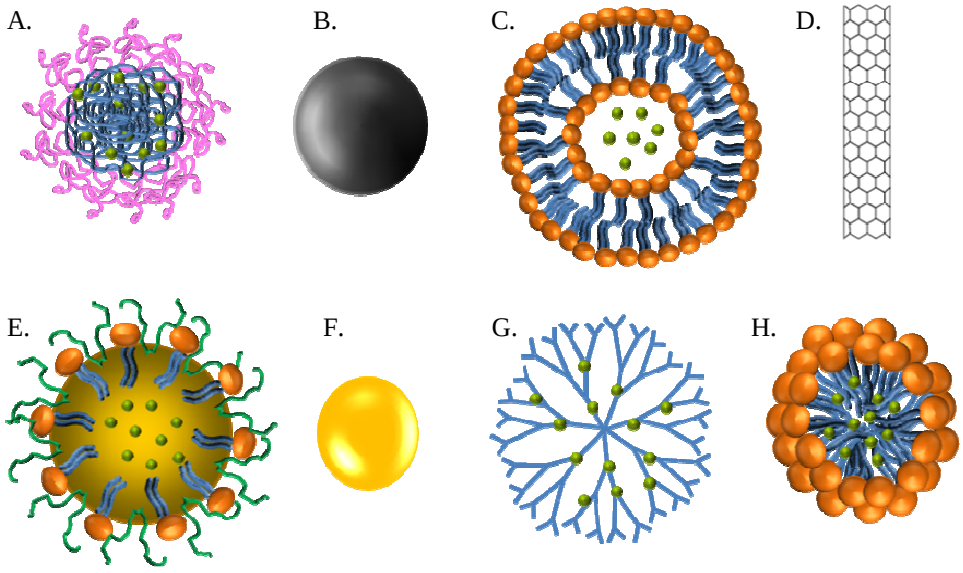

Figure 3: Examples of drug delivery platforms: A) Polymeric nanoparticle. B) Magnetic nanoparticle. C) Liposome. D) Carbon nanotube. E) Nanoemulsion. F) Gold nanoparticle. G) Dendrimer. H) Micelle.

Biodegradable polymers are highly preferred due to its grand bioavailability, better encapsulation, control release and less toxic properties. Incorporation of hydrophobic drugs to polymer chains enhances their water-solubility and changes their biodistribution pattern (37). Mucoadhesive materials like chitosan can be used

to increase intimacy of contact between the drug-containing polymer and cell membranes (38).

Several types of polymer-based drug carriers have been tested as potential drug delivery systems, including polymeric nanoparticles, dendrimers, hydrogels and micelles.

a) Polymeric nanoparticles

Polymeric nanoparticles are engineered from biocompatible and biodegradable polymers and they have been synthesized using various methods based on the needs of its application and the type of drugs to be encapsulated (39). These particles are solid matrix systems in which the drug is dispersed within the particle or conjugated to the polymeric backbone. Polymeric nanoparticles have been formulated to encapsulate either hydrophilic or hydrophobic small drug molecules, as well as macromolecules such as proteins and nucleic acids. Numerous nanoparticles are in pre-clinical or clinical development (40). For example nanoparticles comprising of hydrophobic copolymers such as poly (lactic-co-glycolic acid) (PLGA) and polyalkylcyanoacrylate (PACA) have been used to coencapsulate chemotherapeutic agents and inhibitors of the Multidrug Resistance mechanism (MDR) for delivery to various cancers (41).

b) Hydrogels

Hydrogels are hydrophilic polymer networks that vary in their structures. The former, referred to as the first network, has a linear structure while the second network, called latter, is a polymeric network with three-dimensional covalent crosslinking. Covalent bonds between chains affect polymer properties and thus make these polymers convenient for use as drug carriers in the form of micro- or

nano-particles. They may absorb from 10-20% (an arbitrary lower limit) up to thousands of times their dry weight in water, a property attributed to the presence of hydrophilic groups in their structure (42). Some hydrogels possess features of fluid transport and stimulus responsive characteristics (e.g., pH, temperature and light) (43).

A number of synthetic hydrogels have also been studied for anticancer drug delivery purposes. Cheng et al. prepared thermosensitive hydrogels based on poly (γ-ethyl-l-glutamate)-poly(ethylene glycol)-poly(γ-ethyl-l-glutamate) triblock copolymers (PELG-PEG-PELG) for localized and sustained delivery of paclitaxel (PTX) *in vivo*. The results demonstrated that the PTX-incorporated hydrogels could efficiently suppress the tumor growth, and did not result in obvious damage to normal organs (44).

c) Dendrimers

Dendrimers are synthetic polymers having highly branched structure consisting of an initiator core and multiple layers with active terminal groups. Each layer is called a generation (the core is denoted as generation zero) and they are formed of repeating units (45). Due to this specific molecular structure the bioactive agents may be encapsulated into the interior of the dendrimers (46) or chemically attached/physically adsorbed onto the dendrimer surface.

Dendrimers show increasing promise as drug-delivery vectors and can be generated with a wide range of scaffold structures, sizes and surface functionalities. Ren et al. have developed a poly (amidoamine) (PAMAM) dendrimer for simultaneous co-delivery of gene therapy and chemotherapy agents. 5-fluorouracil (5-FU) was encapsulated in the cavities of the dendrimer core via hydrogen bonds while an antisense microRNA (miR-21) was complexed to the surface (47).

Synchronous delivery of the two therapeutic agents was achieved resulting in synergistic anticancer efficacy, apoptotic activity, and decreased migration ability of the cancer cells compared to each agent alone.

d) Micelles

Polymeric micelles are formulated through a self-assembly process using block-copolymers consisting of two or more polymer chains with different hydrophilicity. These copolymers spontaneously assemble into a core-shell structure in an aqueous environment. Hydrophobic blocks form the core where the drug is carried while the hydrophilic blocks form the shell. Polymeric micelles are usually more stable in blood than liposomes and other surfactant micelles because some amphiphilic copolymers have a considerably lower critical micelle concentration value. Due to such unique properties, polymeric micelles have been well demonstrated as effective drug carriers. Wang et al. demonstrated the specific binding to target cells (MCF-7 breast cancer cell line) of paclitaxel-loaded micelles targeted with a MCF-7 cell-specific phage protein (48). Moreover, recently Kea and collaborators have designed micelles loaded with both thioridazine (which has been reported to kill cancer stem cells) and doxorrobicin, providing a promising strategy for breast cancer treatment by targeting both cancer cells and cancer stem cells with this combination therapy (49).

Lipid-based drug carriers

a) Liposomes

Liposomes are spherical lipid vesicles wich consist of an aqueous volume entrapped by one or more bilayers of natural or synthetic amphiphilic lipid molecules (50). Liposomes became one of the first nanoparticulate platforms for

drug delivery because of their unique characteristics. They can encapsulate and protect from external conditions both hydrophilic and hydrophobic therapeutic agents and they can be coated with polymers and functionalized with specific ligands to target specific cells (51). Drugs can be encapsulated in liposomes either in the phospholipid bilayer, in the entrapped aqueous volume or at the bilayer interface. Among the "first generation" vectors (not specifically targeted), liposomal drug delivery is certainly the most successfully used in the clinic. Doxil®, a pegylated liposomal formulation with doxorubicin, was the first liposomal drug formulation approved by the Food and Drug Administration, USA (FDA) for the treatment of AIDS associated with Kaposi's sarcoma in 1995 (52). Today, there are some formulations approved for clinical use and many more in clinical and preclinical development (53).

b) Solid lipid nanoparticles

Solid lipid nanoparticles (SLN) were developed at the beginning of the 1990s by Mueller and coworkers, and Gasco and coworkers. They are particles with a size range between 50 and 1000 nm composed of a biocompatible/biodegradable lipid matrix made from solid lipids (i.e., lipids that are solid at room temperature and also at body temperature) and stabilized by surfactants (54). SLN has many advantages for drug delivery, such as good tolerability, biodegradability, amenability to encapsulate hydrophilic and hydrophobic drugs, low cost of solid lipids as compared to phospholipids, targeting effect on the brain and a high bioavailability by ocular administration (55-56).

The application of SLN formulations for anticancer drug delivery has overcome many obstacles commonly seen in conventional cancer chemotherapy. Various anticancer drugs, including etoposide (57), methotrexate (58), and idarubicin (59) have been incorporated into SLN and evaluated. Conventional

administration routes (e.g. intravenous route) have shown relatively low tumor uptake. For this reason, various alternative application routes, such as duodenal, subcutaneous and pulmonary routes have been studied (60).

c) Nanoemulsions

Lipid based nanoemulsions are colloidal dispersions of oil and water which typically possess a dispersed phase distributed within a continuous phase that is stabilized by surfactants and co-surfactants at the oil/water interface (61). Thermodynamically stable nanoemulsions form spontaneously with minimum mechanical energy required.

Because our research focuses on the study of nanoemulsions with different interfacial composition, three sections of this chapter (1.6, 1.7 and 1.8) have been devoted to extensively analyze this system.

Virus based nanoparticles

Viruses can be regarded as living nanoparticles with a core–shell structure. The infectious agents are in the core surrounded by a shell comprised of proteins or proteins embedded in lipid membranes (51). They range in sizes from 10 nm to over a micron and can be found in a variety of distinctive shapes (most abundantly icosahedrons, spheres and tubes). They can either be isolated directly after coat protein expression in eukaryotic cells, or assembled *in vitro* from coat protein subunits purified from any recombinant host, from mammalian cells to bacteria (62).

Virus-like particles offer the great advantages of morphological uniformity, biocompatibility, and easy functionalization, and they have been extensively used

for drug delivery, vaccines and gene therapy due to their high gene transfection efficiency and fusogenic cell receptor-binding properties.

Oncolytic viruses are engineered to self-amplifying and replicate selectively within cancer cells and induce toxic effects such as cell lysis and apoptosis, while leaving normal nontransformed cells intact (or nearly so) (63). It is becoming clear that their targeted infection of the tumor has the potential to create an "inflammatory storm" that arouses the innate and adaptive immune responses against tumors (64).

Carbon nanotubes

Carbon nanotubes (CNTs) are allotropes of carbon with a cylindrical nanostructure. Nanotubes have been constructed with length-to-diameter ratio of up to 28,000,000:1 (65). CNT can be imaginatively produced by rolling up a single layer of graphene sheet (single-walled CNT; SWNT) or by rolling up many layers to form concentric cylinders (multi-walled CNT; MWNT) (66).

Although CNT have several unique properties, nonfunctionalized (pristine) CNT are poorly soluble and highly cytotoxic. Their functionalization with more soluble and biocompatible materials has been studied demonstrating that allows enhancing solubility in water with consequent enhancement of their biocompatibility. Functionalized carbon nanotubes have been successfully investigated for several biomedical applications such as proteins, nucleic acids and drug carriers (67-69). The potential of CNTs for delivery of anticancer agents might be attributed to their exclusive physicochemical properties, especially their ability for crossing various biological barriers without generating an immunogenic response and toxic effects. Application of CNTs for the delivery of drugs to their site of action has become one of the main areas of interest for different research

groups. In this context, *in vitro* delivery of paclitaxel attached to single-walled CNTs showed higher efficacy in suppressing tumor growth than delivery of paclitaxel alone. This suggests that higher concentrations of paclitaxel were delivered to breast cancer cells using SWCNT-paclitaxel conjugates in comparison with delivery of paclitaxel alone (70). Furthermore, Liu et al. demonstrated that the control release of the chemotherapeutic drug 7-Ethyl-10-hydroxy-camptothecin (SN38) by SWCNTs conjugated with antibody C225, can achieve targeted therapy against EGFR over-expressed colorectal cancer cells, suggesting that SWCNT could be a good carrier for targeting therapy (71).

Ceramic nanoparticles

Ceramic nanoparticles are typically composed of inorganic compounds such as silica, titania, and alumina (72). However, the nanoparticle core is not limited to just these materials; rather metals, metals oxides and metal sulfides can also be used (73). They are generally bioinert and have porous structures. These nanoparticles have been proposed as drug delivery vehicles to carry drugs for various cancer therapies because these particles can be easily engineered with the desired size, shape and porosity (74-75). They present advantages including the simple conditions required for the preparative processes and the high stability. There are no swelling or porosity changes with a change in pH, and they are not vulnerable to microbial attack (76). They can also be easily funtionalized by various molecules due to the presence of negative charge on the surface. Mesoporous silica nanoparticles of around 100-130 nanometers of diameter were loaded with camptothecin and targeted with folic acid and a dramatic improvement of the potency of tumor suppression (two different human pancreatic cancer xenografts on mice) was obtained (77).

Metal based nanoparticles

Metal nanoparticles can be synthesized in extremely small sizes of around 50 nm and thus, the large surface area provides the ability to carry a relatively higher dose of drugs. One of the most commonly used are gold nanoparticles (AuNPs) because they are biocompatible, easy to synthesize, characterize, and surface modify. The presence of surface plasmon resonance (SPR) bands is responsible for their large absorption and scattering cross-sections, which are 4 to 5 orders of magnitude larger than that of conventional dyes (78). Thus, gold nanoparticles are new agents that are being evaluated for biological sensing, drug delivery, and cancer treatment (79). Recently, it has been shown that AuNPs inhibit the proliferation of cancer cells by abrogating MAPK-signaling and reverse epithelial-mesenchymal transition (EMT) in cancer cells by reducing secretion of a number of proteins involved in EMT. As a consequence, an inhibition of tumor growth and metastasis in two separate orthotopic models of ovarian cancer were observed (80). Additionally potential applications of AuNPs have been recently studied and administrated in phase I & II clinical trials for cancer treatment (81).

Other typical metallic nanoparticles are core-shell magnetic nanoparticles. They consist of a metal or metallic oxide core coated with inorganic or polymeric shell to improve their stability and render the particle biocompatible (82). Metal nanoparticles can be used as thermal release triggers when irradiated with infrared light or excited by an alternating magnetic field. In magnetic drug targeting, magnetic carrier particles with surface-bound drugs are injected into the vascular systems and then captured at the tumor via a locally applied magnetic field. Several studies have demonstrated application of magnetic nanoparticles for drug delivery. Chen et al. developed a magnetic drug delivery system that may find potential applications in cancer treatment, in which doxorubicin chemically bonded to Fe_3O_4 nanoparticles, were embedded in a polyethylene glycol functionalized porous silica

shell (83). Other group used external magnets to demonstrate that gold-coated iron oxide nanoparticles with the active component of cisplatin can be accumulated in specific regions, and that cell growth inhibition was localised to those areas (84).

Currently many other metal-based nanoparticles, as well as various hybrid surface-functionalized nanoparticles, are being extensively used for drug-delivery applications, such as platinum (85), silver, and palladium nanoparticles (86-87). Quantum dots, fluorescent semiconductor nanocrystals, have been also extensively investigated for drug delivery and imaging (88). They combine small size, versatile surface chemistry and outstanding optical properties (89).

1.3. Drug delivery strategies

One of the main objectives of nanomedicine is to overcome the shortcomings of classical chemotherapy including firstly, the non-specific action of the drugs, leading them to damage both tumor and non-tumor cells in a state of division, and increasing the probability of adverse side effects. Secondly, the low concentration of active substance at targeted site, resulting in poor therapeutic effect. Therefore, it is evident the need to target the drug to the tissue or organ of interest rather than allow free systemic circulation.

Nanotechnology offers the possibility of designing novel therapies with greater cell specificity that act selectively on target site. This allows the administration of smaller but more effective doses, minimizing adverse effects.

1.3.1. Passive targeting

Passive targeting refers to the accumulation of a drug or drug-carrier system at a specific site due to physicochemical or pharmacological factors. This type of targeting relies on the disease pathology and the features of tumor tissues, which may preferentially aid accumulation of a drug in target tissues and hence, decrease non-specificity. It is commonly accepted that the vasculature of tumors is different from that of the surrounding tissue. In comparison with normal well organized vessels, the tumor angiogenesis results in a high vascular density, extensive vascular permeability, defective vascular architecture, and impaired lymph clearance from the interstitial spaces of tumor tissue, all of which improve retention of a drug.

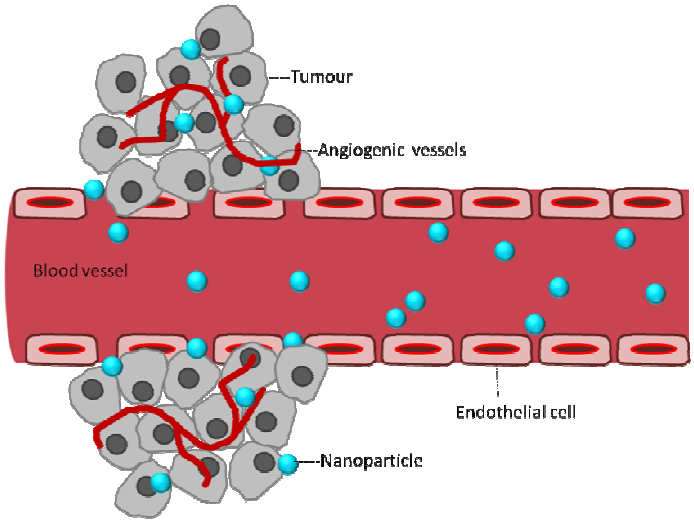

Figure 4: Schematic representation of passive tissue targeting, achieved by extravasation of nanoparticles through increased permeability of tumour vasculature (EPR effect).

The intracellular space of the angiogenic tumor vasculature is estimated to have an average pore size of 100–600 nm, significantly larger than the spaces found in normal endothelial cells within the normal blood vessels, which are typically <6

nm wide (90). This differentiated structure of tumor vessels and this particular tumor vascular permeability, known as "enhanced permeation and retention effect" (EPR), is important in delivery of macromolecular anti-cancer agents and nanomedicines (see Figure 4). EPR has demonstrated enhanced activity and reduced toxicity of many anticancer nanomedicines compared with free anticancer drugs (91-92). However, there is significant heterogeneity within and between tumor types.

1.3.2. Active targeting. Potential targeting ligands

Paul Ehrlich suggested the concept of drug targeting a century ago and coined the term "magic bullet", referring to an entity consisting of two components. The first one should recognize and bind the target, hence providing precise transport of the drug, while the second one should provide a therapeutic

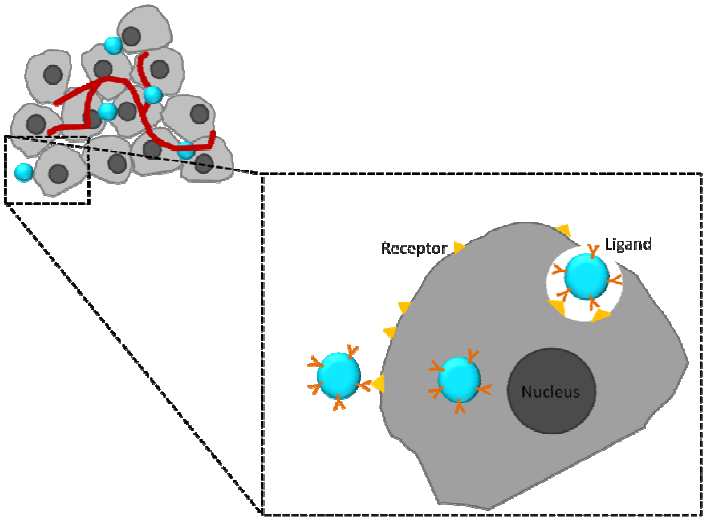

Figure 5: Schematic representation of active targeting which can be achieved by functionalizing the surface of nanoparticles with ligands that promote cell-specific recognition and binding.

action. Since this concept, many efforts have been made in cancer therapy with the goal of designing targeted therapeutic agents against cancer cells (93). Active targeting involves the use of peripherally conjugated targeting moieties for enhanced delivery of nanoparticle systems.

Tumor cells overexpress many tumor-specific receptors because a rapidly growing tumor requires various nutrients and vitamins. To achieve effective tumor-specific drug delivery, nanoparticles are functionalized with targeting ligands that bind to those receptors, which may help internalization upon binding (see Figure 5).

Other targets that are employed to achieve tumor-selective localization of drug nanocarriers are those expressed on endothelial cells of tumor blood vessels. The angiogenesis dependency of tumor growth is a promising target for the development of therapies that control tumor expansion (94-95) by the inhibition of the growth of new tumor-feeding blood vessels. Anti-angiogenesis approaches are effective in limiting tumor growth, with the transformed endothelial cells of the neovasculature as the main targets. Cancer cells are deprived of nutrients and oxygen with the consequent destruction of the tumor. The main angiogenic targets, explored by nanoparticle systems for therapeutic benefit, include the vascular endothelial growth factor receptors (VEGFRs), αvβ3 integrins, matrix metalloproteinase receptors (MMPs), and vascular cell adhesion molecule-1 (VCAM-1) (96).

The types of ligand used to target nanosystems against cancer cells include a wide range of synthetic and natural compounds of different chemical classes. Some of the most widely used are monoclonal antibodies (mAb) and other proteins

(such as transferrin), nucleic acids (aptamers), small molecules (hyaluronic acid, folic acid) and peptides.

Monoclonal antibodies (mAb) were the first and are still the preferred class of targeting molecules. The first mAb to gain FDA approval for the treatment of cancer was Rituximab in 1997, a chimeric mAb for the treatment of B-cell non-Hodgkin's lymphoma. Trastuzumab, in 1998, a humanised mAb for the treatment of HER2 expressing breast cancer, quickly followed. Cetuximab, which binds to epidermal growth factor receptors (EGFR), was approved for treating colorectal cancer in 2004 and head/neck cancer in 2006. Bevacizumab, a tumor angiogenesis inhibitor that binds to vascular endothelial growth factor (VEGF), was approved for treating colorectal cancer in 2004. Recent studies have tried to encapsulate chemotherapeutic drugs into nanoparticles and then functionalize the particle surface with mAbs to maintain targeting efficacy (97-100). The conjugated antibodies enhance uptake and cytotoxic potency of the nanoparticles.

Transferrin receptors are overexpressed on cell surfaces when metabolic processes are increased. It has been reported that the membrane transferrin receptor-mediated endocytosis of the complex of transferrin bound iron and transferrin receptor, is the major route of cellular iron uptake via clathrin-coated pits, with subsequent traffic to endosomal compartments. This uptake pathway has been exploited for the delivery of anti-tumor drugs, proteins, and therapeutic genes with successful results (101-103).

Aptamers are RNA or DNA oligonucleotides that fold by intramolecular interactions into unique three-dimensional conformations capable of binding to target antigens with high affinity and specificity analogous to antibodies. They have many favorable characteristics including small size (20 to 80 bases), lack of immunogenicity, and ease of isolation (104). The most important success of

aptamers so far has been the development of aptamers FDA approved that are able to bind VEGF, a protein involved in angiogenesis (105). The conjugation of aptamers to drug delivery nanoparticles resulted in increased targeting and more efficient therapeutics, as well as more selective diagnostics (106).

Hyaluronic acid (or hyaluronan) (HA) is a linear, negatively charged and natural polysaccharide found in the extracellular matrix and synovial fluids of the body. It is responsible for various functions within the extracellular matrix such as cell growth, differentiation, and migration. It has been shown that the HA level is elevated in various cancer cells. The higher concentration of HA in cancer cells is believed to form a less dense matrix, thus, enhancing the cells motility as well as invasive ability into other tissues. Hyaluronic acid has been investigated as a targeting moiety of the drug conjugates or nanoparticles for cancer therapy, because it can specifically bind to various cancer cells that over-express CD44, an HA receptor (107-109).

Folic acid belongs to the vitamin B family and it is not produced endogenously by mammalian cells. It is important in the formation of new cells because is an essential precursor for the synthesis of nucleic acids and some amino acids. Folate requires internalization by cells via either receptor-mediated endocytosis or a carrier-based uptake mechanism. There are two membrane bound folic acid receptors, FR-α and FR-β. FR-α is overexpressed on a large number of human cancers tumors including malignancies of the ovary, brain, kidney, breast, and lung and it has a high affinity for folic acid which results in high uptake by FR positive cells (110). Folic acid binds to tumor cells 20-times more than normal epithelial cells or fibroblasts. Because of these attractive characteristics, folate conjugation has become a widely used strategy for targeting drug delivery systems (111-113).

Peptide-based targeting of tumor-associated receptors has emerged as potential tumor-specific chemotherapeutic agents. Peptides are attractive ligands because high-affinity sequences can be discovered through screening of combinatorial libraries. Cell permeating and fusogenic peptides from pathogens or toxins and peptides, randomly derived from technologies such as phagedisplay, are also commonly used for targeting purposes (114). Among single nuclear localization (NLS) peptides, trans-activating transcriptional activator (TAT) peptide has been shown to be an efficient molecule for translocating nanoparticles into cell nuclei via the binding import receptors, importin α and β. In a recent publication a peptide has been used to conjugate onto mesoporous silica nanoparticles for nuclear-targeted drug delivery of doxorubicin for the first time (115). Lipid nanoparticles functionalized with targeting peptides are among the most often studied (116).

1.4. Intravenously administered nanoparticles

For parenterally administered drugs, interactions with blood components, systemic distribution and kinetics are of great importance. In a successful intravenous treatment, therapeutic agents should pass a series of biological barriers including hepatic and renal clearance, enzymolysis and hydrolysis, as well as cellular uptake, endosomal/lysosomal degradation, and spleen filtration. The efficiency can be also affected in the case of anticancer drugs by their poor solubility, low stability, and high toxicity for normal tissues and cells.

Nanomaterial carriers are able to improve the biodistribution and prolonged blood circulation of therapeutics, which significantly increase the pharmaceutical efficacy, and decrease the usage dose. *In vivo* fate of drug on parenteral administration is no longer determined by the properties of the drug, but by the type of the drug delivery system.

The filtration of blood through the kidneys effectively removes nanoparticles with diameters smaller than 10-20 nm, and the filtration through inter endothelial slits in walls of the splenic sinus removes particles larger than 200nm. Liver fenestrations found in the sinusoids also temporarily remove nanoparticles from the circulation. These blood filters suggest that the size of nanoparticles should be no smaller than 20 nm and no larger than 200 nm if long circulation within the blood is desired.

The mononuclear phagocyte system (MPS), comprised of phagocytic cells, primarily monocytes and macrophages, plays a vital role in clearing the nanoparticles. MPS has large populations taking residence in the spleen, liver and lymph nodes. The recognition of nanoparticles by these cells is greatly enhanced following a process called opsonization. The opsonization process is the adsorption of protein entities capable of interacting with specific plasma membrane receptors on monocytes and various subsets of tissue macrophages, thus, promoting particle recognition by these cells (117), whereas the absence of opsonins in the adsorption pattern and the presence of dysopsonins lead to the circulation of particles in the bloodstream. Properties such as nanoparticle size, surface charge, hydrophobicity/hydrophilicity, and the steric effects of particle coating, can dictate nanoparticle compatibility with the immune system.

1.4.1 Protein corona: what cells see of particles

When nanosystems are in a physiological environment, they rapidly adsorb biomolecules such as proteins and lipids on their surface forming a protein "corona" (see Figure 6), a biomolecular interface organization that may be loosely divided into two components named the "hard" and "soft" coronas, with (respectively) "long" and "short" typical exchange times. The corona will change

composition if the nanoparticle moves to another compartment or fluid. Tenzer and colleagues found that the corona formed rapidly after the particles had been mixed with plasma and it could be detected already at the first measurement point (at 30 s) (118).

This corona that is surrounding the particle changes its original surface charge and chemistry, size, solubility, aggregation and hence, changes the dialogue of nanoparticles with the cells, influencing the trafficking, *in vivo* biodistribution and cellular uptake because these proteins absorbed on the surface interact with cells through receptors on cell plasma membrane (119).

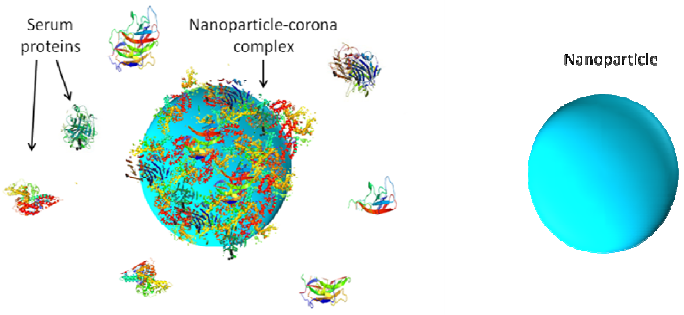

Figure 6: Schematic representation of protein corona developed on the surface of nanoparticles in the presence of serum proteins.

Protein corona influences the macrophage capture. Macrophage scavenger receptors are a broad group of phagocytic receptors that are responsible for the elimination of blood-borne viruses, pathogens, and negatively charged ligands. For example opsonins such as IgG, complement factors, and fibrinogen promote the phagocytosis, removal of nanoparticles from the bloodstream and concentration in the liver and spleen, while dyopsonins such as albumin and apolipoprotein help the longer circulation of nanoparticles in the body (55). Human serum albumin, when

adsorbed on the surface of polystyrene microparticles, was reported to inhibit their phagocytosis by dendritic cells (120).

For many NPs, while removal from the bloodstream is a question of minutes, interaction with cells of distant organs may be relevant hours or days after exposure. Nanoparticles functionalized with hydrophilic polymers such as polyethylene glycol (PEG) and poloxamers show improved circulation lifetime properties and decreased macrophage recognition of many types of nanoparticle by preventing protein absorption (121). Plasma protein absorption is influenced in the case of PEGylated nanoparticles by the length and density of the polymer.

It has been claimed that the protein corona can cover/eliminate the targeting moieties on the surface of nanomaterials and, thus, strongly reduces the targeting capability and recognition of the targeting ligand by cellular receptors (122). Therefore, understanding the interaction of cell plasma membrane and the protein corona around nanoparticles is essential in designing nanoparticle-based targeting drug delivery and treatments.

1.4.2. "Passports" to avoid immune system clearance

Nanoparticles can be engineered to avoid the immune system clearance and increase the circulating half life in blood. One important reason to search for this is to provide a long-circulating drug reservoir from which the drug can be released into the vascular compartment in a continuous and controlled manner.

A relatively successful approach for prolonging the circulation times of colloidal particles in the blood is to create a steric surface barrier of sufficient density. Poloxamer and poloxamines have been investigated to reduce adsorption of proteins and blood opsonins and thus, increasing half life of nanosystems.

Poloxamers, also known as Pluronic®, and poloxamines or Tetronic®, are amphiphilic nonionic block polymers of hydrophobic propylene oxide (PO) and hydrophilic ethylene oxide (EO). Poloxamers consist of a hydrophobic central polyoxypropylene (POP) molecule, which is flanked on both sides by two hydrophilic chains of polyoxyethylene (POE) yielding structures of the (POE)a (POP)b (POE)a type, as it is shown in Figure 7. Poloxamines are tetrafunctional block copolymers with four POE–POP blocks joined together by a central ethylene diamine bridge (123). The absorption of these molecules onto the surface of the nanoparticles via their hydrophobic POP fragments provide stability to the particle suspension by a repulsion effect through a steric mechanism of stabilization, because this type of absorption leaves the hydrophilic POE extended outwards from the particle surface in a mobile state. Nanoparticles engineered with poloxamers and poloxamines exhibit reduced adsorption of proteins and blood opsonins (124) and, as a result, they resist ingestion by phagocytic scavenger cells and remain in the systemic circulation for prolonged period.

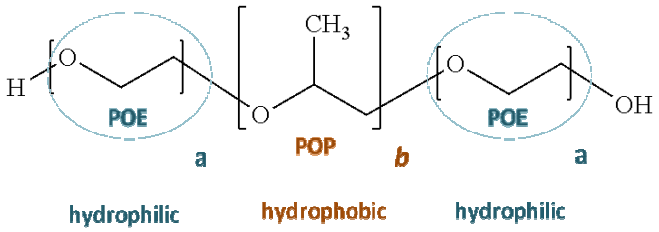

Figure7: Structure of Pluronics.

Other property presented by poloxamers and poloxamines is the inhibition of multidrug resistance (125-126). This phenomenon is the ability of tumour cells to develop resistance to the cytotoxic effects of several chemically unrelated

anticancer drugs, associated with the overexpression of proteins such as P-glycoprotein and multidrug-resistance-associated protein (127).

The addition of poly (ethylene glycol) (PEG) has been widely used to increase the circulating half life of nanoparticles and it is the preferred method of "masking" nanoparticles from immune recognition. This process is also known as PEGylation (128). PEG is a linear polyether diol that exhibits a low degree of immunogenicity and antigenicity (129). The polymer backbone is essentially chemically inert, and the terminal primary hydroxyl groups are available for derivatization. Surface modification of nanoparticles with PEG and its derivatives can be performed by adsorption, incorporation during the production of nanoparticles, or by covalently linking to the surface of particles (117). The addition of PEG can add protein/opsonization resistance properties by preventing interactions between the particle surface and the plasma proteins, although adsorption is not completely avoided. Various studies have been conducted to determine how a change in the thickness and density of a PEG coating affects opsonization and biodistribution, showing that the extent of protein adsorption depends on the PEG size and grafting density, suggesting conformational transition of PEGs between mushroom and brush states when PEG density increase (130-131).

Recent progress has shown that it may be possible to disguise nanomaterials as "self", avoiding the blood clearance by phagocytic cells, by using a novel peptide sequence mimicking, the "marker of self" CD47 protein (132).

1.5. Clinical trials

The approval of drugs for human use by the Food and Drug Administration (FDA) through the Center for Drug Evaluation and Research

(CDER) is a time-consuming and expensive process, and approval rates are low (133). In general, the FDA drug approval process can be separated into preclinical, clinical and postmarketing phases. To date, there are five clinically approved nanoparticle chemotherapeutics for cancer and many more under preclinical and clinical investigation (53).

Liposomal anthracyclines were the first nanoparticle therapeutics approved for clinical use. The anthracyclines (including doxorubicin, daunorubicin, epirubicin and idarubicin) are highly effective against a wide range of cancers. Today, there are three clinically approved liposomal formulations of anthracyclines: pegylated liposomal doxorubicin (PLD; DOXIL in the United States, Caelyx elsewhere), non-pegylated liposomal doxorubicin (NPLD; Myocet) and liposomal daunorubicin (DaunoXome) (134).

Moreover, Abraxane was approved by the FDA for the treatment of breast cancer. It is an albumin-bound 130-nm nanoparticle formulation of paclitaxel, a poorly soluble in water drug effective against different types of cancers. (135).

Finally, another clinically accepted nanosystem is the polymeric micelle formulation of paclitaxel (Genexol-PM), with a diameter of 20-50 nm and composed of block copolymers of PEG and poly-(D,L-lactic acid) (136). Currently is approved for the treatment of breast and lung cancers in Korea.

Many others therapeutics are undergoing clinical investigation. Most of them are liposomes, polymeric nanoparticles, micelles and lipid nanoparticles, transporting different anticancer drugs such as platinum drugs (cisplatin, carboplatin, and oxaliplatin), alkaloids (vincristine, camptothecin derivatives and taxanes), or small interfering RNA (siRNA) among others (53). A 2006 global

survey conducted by the European Science and Technology Observatory (ESTO) revealed that over 150 companies are developing nanoscale therapeutics (137).

1.6. Nanoemulsions and surfactants

Emulsions can be defined as a heterogeneous mixture of at least two immiscible liquids. In an emulsion, one liquid (disperse phase) is dispersed throughout another liquid (continuous phase) in the form of droplets. Depending on the nature of the dispersed and the continuous phase, different types of emulsions can be distinguished (see Figure 8): oil-in-water (O/W), where the oil is the dispersed phase and water is the dispersion medium, or water-in-oil (W/O) where water is the dispersed phase and oil is the continuous one. If the dispersed phase represents an emulsion itself, the systems formed are called multiple emulsions (O/W/O, W/O/W, and so forth) (138).

The interface of emulsions is stabilized by the presence of an emulsifier or surfactant (surface-active agents), that remains immobilized between the different phases acting as a film former, reducing interfacial tension and/or providing a mechanical barrier against coalescence, thereby stabilizing the emulsion. Surfactants are molecules that present both a polar (hydrophilic) and a nonpolar (hydrophobic) region. This type of structure with a water insoluble fragment and a water soluble moiety is called amphiphilic or amphipathic.

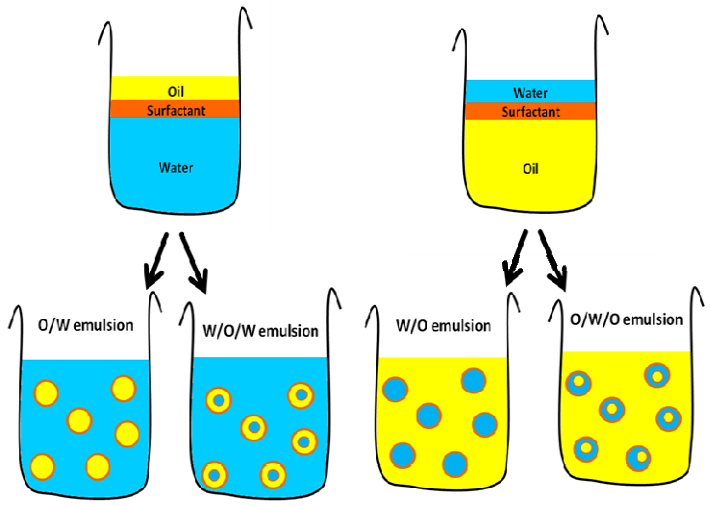

Figure 8: Different types of emulsions according to the nature of the dispersed and continuous phases.

Emulsions are usually classified into two main categories: microemulsions and nanoemulsions. Nanoemulsions, also called Windsor system microemulsions or miniemulsions, are emulsions with a mean droplet diameter in the nanometer scale. There is ambiguity in terms of the size range that may vary depending on the authors. Some authors consider 500 nm as the upper limit (61, 139), while other authors consider 200 nm (140) or even 100 nm (141). However it is generally accepted that droplet diameters in nanoemulsions are less than ~200− 300 nm in size, and from a thermodynamic point of view is a non-equilibrium state. Nevertheless, the kinetics of destabilization is so slow that they can be considered kinetically stable, as opposed to microemulsions, which are thermodynamically stable and may range up to ~1 μm in size (142-144). Such emulsions are typically formed through spontaneous emulsification techniques. The components (e.g., oil, water and surfactants) as well as the emulsification procedure are altered to vary the nanosystem nature that is formed (145).

The dispersed O-phase in most nanoemulsions is typically composed by vegetable oils (fatty acyls) or middle chain triacylglycerols. Surfactants may include nonionic block copolymers, lecithin (charged), and alcohols. Traditionally, nanoemulsions have been prepared using phospholipids as emulsifier molecules. They are ionic surfactants that offer electrostatic stabilization (146-147). Doplets repel each other because they are composed by the same phospholipids that provide particles with net charges of the same sign. When two different phases are in contact, if one of the phases is a charged nanoparticle and the other one is an electrolyte solution, the ions dissolved in the medium with opposite charge to the particle surface tend to surround the particle in order to keep the neutrality of the solution. The arrangement of charges located in one phase and those fixed in the particle surface form what is called the electric double layer (148). Electrokinetic phenomena is a generic term applied to effect associated with the relative movement of the ionic solution near charged interfaces. One of these electrokinetic phenomena is the electrophoresis that appears when an uniform electric field is applied and the particle velocity in the steady state is measured. Electrophoretic mobility of a particle is proportional to the zeta potential, which is the potential existing in the shear plane of the moving particles (149).

The stability of nanoemulsions stabilized with ionic surfactants is compromised in the presence of high ionic strength media. That is the case of physiological conditions. At high salt concentrations the accumulation of counterions near the interface screens the charge of the particles, causing a decrease in the zeta potential value provoked by the double-layer compression, and subsequently reducing the stability of nanoemulsions because the repulsion between particles is decreased (149-150). The use of non-ionic surfactants has attracted special attention in order to solve these problems, in spite of the stability that they cause does not have an electrical origin.

Non-ionic surfactants are also called steric surfactants because when they are absorbed at the particle surface the nanoparticles are stabilized preventing other particles by means of steric repulsion (151). Steric surfactants possess bulky groups protruding into the disperse/continuous medium, which creates a brush-like barrier around the droplets. When two droplets approach each other, the free movement of these flexible groups is hindered by interpenetration of the adsorbed layers, resulting to an entropic repulsion (152). Among others, triblock copolymers such as poloxamers, already described above as "passports" to avoid the immune clearance, are a well known example of steric surfactants. Poloxamers, contrary to ionic surfactants, are unaffected by high electrolyte concentrations, and therefore their nanoemulsions can be safely used in many industrial and pharmaceutical applications where high ionic strength values are needed (153).

Although the nanoparticles developed in this thesis are classified in the group of nanoemulsions, they are also usually referred to as lipid nanocapsules, because morphologically they are formed by an oily core surrounded by a polymeric shell (thick steric barrier at the droplet interface) (142). However, some authors reserve nanocapsule nomenclature for structures formed by a more rigid polymeric shell prepared by interfacial polymerization or interfacial nano-deposition (154-155). It should be noted that the terminology used in this PhD dissertation has been, mainly, lipid nanocapsules, but other general terms have also been employed as nanoemulsions, nanocarriers, nanoparticles or nanosystems.

1.7 Colloidal stability of nanoemulsions

Nanoemulsions are part of a more general class of two-phase mesoscopic systems called colloids that are classified in two classes called lyophobic and lyophilic colloids. Thus, their stability patterns are governed by the physical properties and behaviour of general colloidal dispersions.

In lyophobic colloids, in which our nanoemulsions are included, there is little interaction between the particles in the dispersed phase and the surrounding medium. Due to the small droplet size, they present a large surface area. Because of an excess of free surface energy, lyophobic colloids are thermodynamically unstable; that is, they show a constant tendency to aggregate accompanied by a decrease in the exposed area and the free energy of the system.

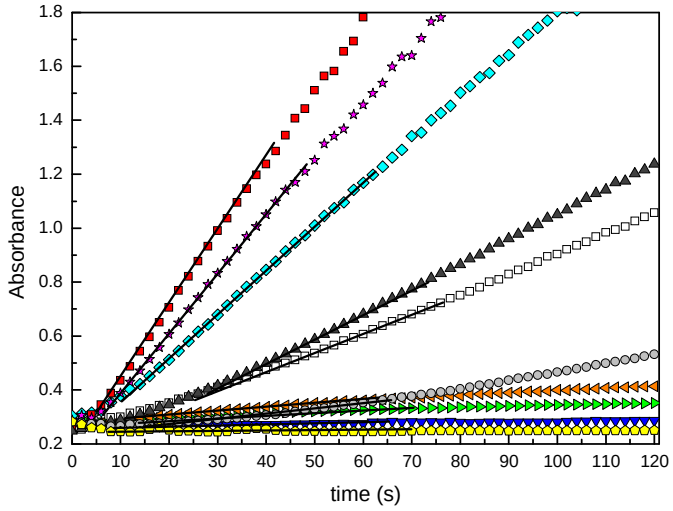

Figure 9. Variation of the optical absorbance (λ = 570 nm) with time for a hydrophilic colloidal system at different NaCl concentrations: 0.003 M (blue inverted triangles ▼), 0.005 M (green right-pointing arrowheads ▶), 0.008 M (orange left-pointing arrowheads ◀), 0.013 M (white squares □), 0.02 M (cyan diamonds ◆), 0.04 M (red squares ■), 0.055 M (pink stars ★), 0.09 M (dark triangle ▲), 0.13 M (grey circle ●), and 0.5 M (yellow pentagons ⬟). The black straight lines represent the initial slopes (dAbs/dt) that are necessary to calculate the Fuchs factor "W".

A theory to describe the aggregation stability of lyophobic colloids was first stablished by Derjaguin, Landau, Verwey, and Overbeek, and it is known as DLVO theory (156-157). According to the classical DLVO theory, increased salinity triggers the coagulation of lyophobic colloidal systems. During aggregation, the

turbidity of the system increases when the average size of the scattering particles enlarges. Figure 9 shows a typical aggregation experiment of a colloidal system partially hydrophilic.

As can be seen, an increment of the salt concentration speeds up the aggregation kinetics, as predicted by the DLVO theory. However, in hydrophilic systems, the kinetics may slow down if the salinity is increased even more. This "anomalous" behaviour is not explained by the DLVO theory, and the origin of this phenomenon must be sought in the repulsive hydration forces.

Information on the kinetics-aggregation constant "*k*" of dimmer formation can be derived from these curves. The initial slopes of the *absorbance vs. time* curves (dAbs/dt) can be directly related to *k* by (158):

$$\frac{dAbs}{dt} = \frac{\left(C_2/2 - C_1\right) N_0^2 \, l}{2.3} k \qquad (1)$$

where C_1 and C_2 are the scattering cross-sections of a monomer and a dimmer, respectively, N_0 is the initial particle concentration, and l is the optical path through the cuvette. Nevertheless, stability is usually evaluated by calculating the Fuchs factor (W), instead of calculating the *k* values by using Equation 1. Fuchs factor (also called "stability factor") is related to the number of collisions that must suffer two colliding particles before they keep definitively stuck (159).

Therefore, when $W = 1$ the system is completely unstable, while $W = \infty$ indicates total stability. Fuchs factor can be calculated at every salt concentration from the curves shown in Figure 10 by using the following equation:

$$W = \frac{k_f}{k_s} = \frac{(dAbs/dt)_f}{(dAbs/dt)_s} \qquad (2)$$

where "k_f" refers to the fastest aggregation-kinetics constant, and the subscript "s" refers to slower coagulation rates. This is shown in Figure 10, where the dependence of W on the salt concentration has been plotted.

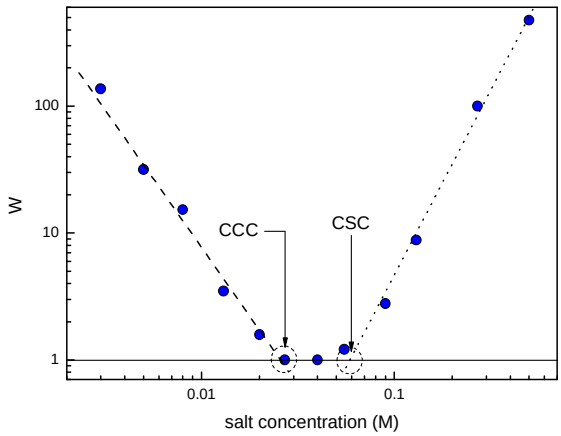

Figure 10. From those experimental data shown in Figure 9, one can derive the Fuchs factor "W" as a function of salt concentration. The dashed line serves to guide the eye for locating the CCC value, while the dotted line is for the CSC.

The critical coagulation concentration (CCC) and the critical stabilization concentration (CSC) are fundamental parameters in colloidal-stability studies. The CCC value is the minimum salt concentration needed to make the interaction energy barrier acting between the surface of two colliding particle vanish. It is related to destabilization processes and it indirectly gives information on the surface-charge density of the particles; a low CCC means low stability caused by a low surface-charge density. However, the CSC value – defined as the minimum salt concentration at which the system begins to re-stabilize when salinity is increased

even more because the energetic barriers grows again – is associated with the surface hydrophilicity. This kind of restabilization phenomenon at high salt concentrations is well known in hydrophilic colloidal systems and it is governed by hydration forces (160-162). Briefly, the microscopic origin of these forces must be sought in the local order of water and hydrated ions located near any hydrophilic surface. The hydration of the surface and ions reduces the free energy of the system if it is hydrophilic. An overlap of the ordered-solvent layers near two mutually approaching surfaces creates a repulsive structural force. Before two particles can collapse, a partial dehydration of the surface polar groups and the ions located near the interface must occur, which leads to an increase in the system energy, resulting in a repulsive force that avoids particle contact and prevents the coagulation of the system. Since this force is dependent on the local concentration of hydrated ions, the repulsive interaction among two colliding particles increases with salinity. This is the explanation of the fact that an instable system at low or moderate ionic strength may become stable when the salt concentration increases to high values. It should be noted that CSC values increase when the hydrophilicity decreases; hence a low CSC value means high hydrophilicity. Therefore, there are two important aggregation parameters (CCC and CSC) that give information about two crucial surface characteristics: charge density and hydrophilicity.

1.8. Nanoemulsions in cancer therapy. Advantages as drug delivery carriers

The use of nanoemulsions as delivery systems is gaining interest in the pharmaceutical industry.

Nanoemulsions were first developed for total parenteral nutrition with the aim of helping patients to overcome a critical nutrition state by providing them with triglycerides (163).

During recent years more innovative nanoemulsion formulations have been developed varying the different components such as the emulsifier and/or the emulsified oil nature (164). The combination of the advantages of traditional parenteral emulsions (mainly biocompatibility and biodegradability) with the new functionalities has led to the first marketed drug delivery systems based on nanoemulsions and several formulations are nowadays commercialized. Examples include etomidate (Etomidat-Lipuro®) and diazepam (Diazepam-Lipuro®) (165).

The main advantages of nanoemulsions in the field of drug delivery systems for hydrophobic drugs are: inexpensive and easy-to-scale production, low toxicity, independence of dilution, high content of the lipid phase and reduced side effects (166).

Nanoemulsions have shown a strong potential for drug delivery in the treatment of cancer, being capable of delivering high concentration of chemotherapy drugs to cancerous tissues improving their bioavailability. The oil phase of the nanoemulsion acts as solubilizer for the lipophilic compound thereby enhancing the solubility of the drug in an emulsion system. Therefore, less amount of the drug has to be administered in comparison to an aqueous solution. By exposing the tissue to lower concentration of the drug and by avoiding a tissue irritating vehicle, the pain associated with the intravenously administered drugs can be minimised (167). In addition, because lipophilic drugs are incorporated within the innermost oil phase, they are sequestered from direct contact with body fluids and tissues, which may help to overcome the pharmacokinetic mismatch associated with that particular chemotherapeutic agent (168).

Nanoemulsions have been investigated in cancer treatment to enhance the transdermal bioavailability of poorly soluble anticancer drugs. For example celecoxib nanoemulsions were prepared and pharmacokinetic studies on rats were

developed showing that transdermally applied nanoemulsions increased the bioavailability as compared to an oral capsule formulation (169). Oral administered nanoemulsions have also been developed to enhance the oral bioavailability of hydrophobic drugs like paclitaxel (170), tamoxifen citrate (171) and raloxifene hydrochloride (172), among others. Studies about nanoemulsions for parenteral administration have been developed showing attractive results. For example the recently developed parenteral lipid nanoemulsions used as a platform for the concurrent delivery of tocotrienol rich fraction of vitamin E, which previously showed anticancer activity (173). Promising results have also been shown by the pegylated nanoemulsions loaded with lycobetaine (LBT)-oleic acid ionic complex against lung cancer, which showed higher LBT levels in blood and longer circulation time, decreased LBT concentration in the heart, liver, and kidney, higher growth inhibitory effect, and longer survival compared to free LBT (174).

1.9. References

1. Wong KKY, Liu XL. Silver nanoparticles-the real "silver bullet" in clinical medicine. *Medchemcomm.* 2010 Aug;1(2):125-31.

2. Boulaiz H, Alvarez PJ, Ramirez A, Marchal JA, Prados J, Rodriguez-Serrano F, et al. Nanomedicine: Application Areas and Development Prospects. International *Journal of Molecular Sciences*. 2011 May;12(5):3303-21.

3. Wong KKY, Liu XL. Nanomedicine: a primer for surgeons. *Pediatr Surg Int.* 2012 Oct;28(10):943-51.

4. Appenzeller T. The Man Who Dared to Think *Small.* Science. 1991 Nov 29;254(5036):1300-1.

5. Feynman RP. There's plenty of room at the bottom. *Eng Sci* (CalTech) 1960;23:22-36.

6. Alexis F, Pridgen E, Molnar LK, Farokhzad OC. Factors affecting the clearance and biodistribution of polymeric nanoparticles. *Mol Pharm.* 2008 Jul-Aug;5(4):505-15.

7. Jain KK. Nanodiagnostics: application of nanotechnology in molecular diagnostics. *Expert Rev Mol Diagn.* 2003 Mar;3(2):153-61.

8. Atala A, Lanza R, Nerem R, Thomson JA. Principles of Regenerative Medicine. 2nd ed Academic Press; London, UK. 2011:733–1105.

9. Liu XL, Lee PY, Ho CM, Lui VCH, Chen Y, Che CM, et al. Silver Nanoparticles Mediate Differential Responses in Keratinocytes and Fibroblasts during Skin Wound Healing. *Chemmedchem*. 2010 Mar;5(3):468-75.

10. Kwan KHL, Liu XL, To MKT, Yeung KWK, Ho CM, Wong KKY. Modulation of collagen alignment by silver nanoparticles results in better mechanical properties in wound healing. *Nanomed-Nanotechnol*. 2011 Aug;7(4):497-504.

11. Hu NM, Chen ZG, Liu X, Liu HY, Lian XJ, Wang XM, et al. Mechanical properties and in vitro bioactivity of injectable and self-setting calcium sulfate/nano-HA/collagen bone graft substitute. *J Mech Behav Biomed*. 2012 Aug;12:119-28.

12. Smith LA, Ma PX. Nano-fibrous scaffolds for tissue engineering. *Colloids Surf B Biointerfaces*. 2004 Dec 10;39(3):125-31.

13. Kavya KC, Dixit R, Jayakumar R, Nair SV, Chennazhi KP. Synthesis and Characterization of Chitosan/Chondroitin Sulfate/Nano-SiO2 Composite Scaffold for Bo e Tissue Engineering. *J Biomed Nanotechnol*. 2012 Feb;8(1):149-60.

14. Polini A, Pisignano D, Parodi M, Quarto R, Scaglione S. Osteoinduction of Human Mesenchymal Stem Cells by Bioactive Composite Scaffolds without Supplemental Osteogenic Growth Factors. *Plos One*. 2011 Oct 12;6(10).

15. Zhu WZ, Li X, Qi JP, Tang ZP, Wang W, Wei L, et al. Experimental Study of Cell Migration and Functional Differentiation of Transplanted Neural Stem Cells Co-labeled with Superparamagnetic Iron Oxide and Brdu in an Ischemic Rat Model. *Biomed Environ Sci*. 2008 Oct;21(5):420-4.

16. Wu CT, Miron R, Sculean A, Kaskel S, Doert T, Schulze R, et al. Proliferation, differentiation and gene expression of osteoblasts in boron-containing associated with dexamethasone deliver from mesoporous bioactive glass scaffolds. *Biomaterials*. 2011 Oct;32(29):7068-78.

17. Zanello LP, Zhao B, Hu H, Haddon RC. Bone cell proliferation on carbon nanotubes. *Nano Lett*. 2006 Mar;6(3):562-7.

18. Sahoo S, Ang LT, Goh JCH, Toh SL. Growth factor delivery through electrospun nanofibers in scaffolds for tissue engineering applications. *J Biomed Mater Res A*. 2010 Jun 15;93A(4):1539-50.

19. Guo JH, Skinner GW, Harcum WW, Barnum PE. Pharmaceutical applications of naturally occurring water-soluble polymers. *Pharm Sci Technol To*. 1998 Sep;1(6):254-61.

20. Park JH, Lee S, Kim JH, Park K, Kim K, Kwon IC. Polymeric nanomedicine for cancer therapy. *Progress in Polymer Science*. 2008 Jan;33(1):113-37.

21. Farokhzad OC, Langer R. Impact of nanotechnology on drug delivery. *Acs Nano*. 2009 Jan 27;3(1):16-20.

22. Merisko-Liversidge E, Liversidge GG, Cooper ER. Nanosizing: a formulation approach for poorly-water-soluble compounds. *Eur J Pharm Sci*. 2003 Feb;18(2):113-20.

23. Jokerst JV, Lobovkina T, Zare RN, Gambhir SS. Nanoparticle PEGylation for imaging and therapy. *Nanomedicine (Lond)*. 2011 Jun;6(4):715-28.

24. Jain TK, Morales MA, Sahoo SK, Leslie-Pelecky DL, Labhasetwar V. Iron oxide nanoparticles for sustained delivery of anticancer agents. *Mol Pharm.* 2005 May-Jun;2(3):194-205.

25. Uner M, Yener G. Importance of solid lipid nanoparticles (SLN) in various administration routes and future perspectives. *Int J Nanomed.* 2007;2(3):289-300.

26. Ye D, Raghnaill MN, Bramini M, Mahon E, Aberg C, Salvati A, et al. Nanoparticle accumulation and transcytosis in brain endothelial cell layers. *Nanoscale.* 2013 Nov 21;5(22):11153-65.

27. Davis ME. Design and development of IT-101, a cyclodextrin-containing polymer conjugate of camptothecin. *Adv Drug Deliver Rev.* 2009 Nov 12;61(13):1189-92.

28. Siegel R, Naishadham D, Jemal A. Cancer statistics, 2013. *Ca-Cancer J Clin.* 2013 Jan-Feb;63(1):11-30.

29. Malvezzi M, Bertuccio P, Levi F, La Vecchia C, Negri E. European cancer mortality predictions for the year 2013. *Ann Oncol.* 2013 Mar;24(3):792-800.

30. Fidler IJ. Tumor heterogeneity and the biology of cancer invasion and metastasis. *Cancer Res.* 1978 Sep;38(9):2651-60.

31. Vizirianakis IS. Nanomedicine and personalized medicine toward the application of pharmacotyping in clinical practice to improve drug-delivery outcomes'. *Nanomed-Nanotechnol.* 2011 Feb;7(1):11-7.

32. Jabr-Milane LS, van Vlerken LE, Yadav S, Amiji MM. Multi-functional nanocarriers to overcome tumor drug resistance. *Cancer Treat Rev.* 2008 Nov;34(7):592-602.

33. Shapira A, Livney YD, Broxterman HJ, Assaraf YG. Nanomedicine for targeted cancer therapy: Towards the overcoming of drug resistance. *Drug Resist Update.* 2011 Jun;14(3):150-63.

34. Sahoo SK, Labhasetwar V. Nanotech approaches to delivery and imaging drug. *Drug Discov Today.* 2003 Dec 15;8(24):1112-20.

35. Cho KJ, Wang X, Nie SM, Chen Z, Shin DM. Therapeutic nanoparticles for drug delivery in cancer. *Clin Cancer Res.* 2008 Mar 1;14(5):1310-6.

36. Hervella P, Lozano V, Garcia-Fuentes M. Nanomedicine: New Challenges and Opportunities in Cancer Therapy. *J Biomed Nanotechnol.* 2008 Sep;4(3):276-92.

37. Duncan R. Polymer conjugates as anticancer nanomedicines. *Nat Rev Cancer.* 2006 Sep;6(9):688-701.

38. Garcia-Fuentes M, Alonso MJ. Chitosan-based drug nanocarriers: Where do we stand? *J Control Release.* 2012 Jul 20;161(2):496-504.

39. Pinto Reis C, Neufeld RJ, Ribeiro AJ, Veiga F. Nanoencapsulation I. Methods for preparation of drug-loaded polymeric nanoparticles. *Nanomedicine.* 2006 Mar;2(1):8-21.

40. Brigger I, Dubernet C, Couvreur P. Nanoparticles in cancer therapy and diagnosis. *Adv Drug Deliver Rev.* 2012 Dec;64:24-36.

41. Lee JH, Nan A. Combination drug delivery approaches in metastatic breast cancer. *J Drug Deliv.* 2012;2012:915375.

42. Hoffman AS. Hydrogels for biomedical applications. *Adv Drug Deliver Rev.* 2012 Dec;64:18-23.

43. Bettinger CJ, Weinberg EJ, Kulig KM, Vacanti JP, Wang YD, Borenstein JT, et al. Three-dimensional microfluidic tissue-engineering scaffolds using a flexible biodegradable polymer. *Adv Mater.* 2006 Jan 19;18(2):165-+.

44. Cheng Y, He C, Ding J, Xiao C, Zhuang X, Chen X. Thermosensitive hydrogels based on polypeptides for localized and sustained delivery of anticancer drugs. *Biomaterials.* 2013 Dec;34(38):10338-47.

45. Kesharwani P KJ, Narendra Kumar Jain. Dendrimer as nanocarrier for drug delivery. *Progress in Polymer Science.* 2013.

46. Lee CC, Gillies ER, Fox ME, Guillaudeu SJ, Frechet JMJ, Dy EE, et al. A single dose of doxorubicin-functionalized bow-tie dendrimer cures mice bearing C-26 colon carcinomas. P Natl Acad Sci USA. 2006 Nov 7;103(45):16649-54.

47. Ren Y, Kang CS, Yuan XB, Zhou X, Xu P, Han L, et al. Co-delivery of as-miR-21 and 5-FU by Poly(amidoamine) Dendrimer Attenuates Human Glioma Cell Growth in Vitro. *J Biomat Sci-Polym E.* 2010;21(3):303-14.

48. Wang T, Petrenko VA, Torchilin VP. Paclitaxel-Loaded Polymeric Micelles Modified with MCF-7 Cell-Specific Phage Protein: Enhanced Binding to Target Cancer Cells and Increased Cytotoxicity. *Mol Pharmaceut.* 2010 Jul-Aug;7(4):1007-14.

49. Kea VWLN, Shu-Jun Gao, Yen Wah Tong, James L. Hedrick,Yi Yan Yang. Co-delivery of thioridazine and doxorubicin using polymeric micelles for targeting both cancer cells and cancer stem cells. 2013.

50. Torchilin VP. Recent advances with liposomes as pharmaceutical carriers. *Nat Rev Drug Discov.* 2005 Feb;4(2):145-60.

51. Zhang L, Gu FX, Chan JM, Wang AZ, Langer RS, Farokhzad OC. Nanoparticles in medicine: Therapeutic applications and developments. *Clin Pharmacol Ther.* 2008 May;83(5):761-9.

52. Northfelt DW, Dezube BJ, Thommes JA, Miller BJ, Fischl MA, Friedman-Kien A, et al. Pegylated-liposomal doxorubicin versus doxorubicin, bleomycin, and vincristine in the treatment of AIDS-related Kaposi's sarcoma: Results of a randomized phase III clinical trial. *J Clin Oncol.* 1998 Jul;16(7):2445-51.

53. Wang AZ, Langer R, Farokhzad OC. Nanoparticle Delivery of Cancer Drugs. *Annual Review of Medicine*, Vol 63. 2012;63:185-98.

54. Lim SB, Banerjee A, Onyuksel H. Improvement of drug safety by the use of lipid-based nanocarriers. *J Control Release.* 2012 Oct 10;163(1):34-45.

55. Joshi MD, Muller RH. Lipid nanoparticles for parenteral delivery of actives. Eur *J Pharm Biopharm.* 2009 Feb;71(2):161-72.

56. Parveen S, Misra R, Sahoo SK. Nanoparticles: a boon to drug delivery, therapeutics, diagnostics and imaging. *Nanomed-Nanotechnol.* 2012 Feb;8(2):147-66.

57. Reddy LH, Sharma RK, Chuttani K, Mishra AK, Murthy RSR. Influence of administration route on tumor uptake and biodistribution of etoposide loaded solid lipid nanoparticles in Dalton's lymphoma tumor bearing mice. J Control Release. 2005 Jul 20;105(3):185-98.

58. Paliwal R, Rai S, Vaidya B, Khatri K, Goyal AK, Mishra N, et al. Effect of lipid core material on characteristics of solid lipid nanoparticles designed for oral lymphatic delivery. Nanomed-Nanotechnol. 2009 Jun;5(2):184-91.

59. Zara GP, Bargoni A, Cavalli R, Fundaro A, Vighetto D, Gasco MR. Pharmacokinetics and tissue distribution of idarubicin-loaded solid lipid nanoparticles after duodenal administration to rats. J Pharm Sci. 2002 May;91(5):1324-33.

60. Cai S, Yang QH, Bagby TR, Forrest ML. Lymphatic drug delivery using engineered liposomes and solid lipid nanoparticles. Adv Drug Deliver Rev. 2011 Sep 10;63(10-11):901-8.

61. Fernandez P, Andre V, Rieger J, Kuhnle A. Nano-emulsion formation by emulsion phase inversion. Colloid Surface A. 2004 Dec 20;251(1-3):53-8.

62. Garcea RL, Gissmann L. Virus-like particles as vaccines and vessels for the delivery of small molecules. Curr Opin Biotech. 2004 Dec;15(6):513-7.

63. Ma YJ, Nolte RJM, Cornelissen JJLM. Virus-based nanocarriers for drug delivery. Adv Drug Deliver Rev. 2012 Jun 15;64(9):811-25.

64. Melcher A, Parato K, Rooney CM, Bell JC. Thunder and Lightning: Immunotherapy and Oncolytic Viruses Collide. Mol Ther. 2011 Jun;19(6):1008-16.

65. Sahithi K, Swetha M, Ramasamya K, Sriniyasan N, Selyamurugan N. Polymeric composites containing carbon nanotubes for bone tissue engineering. Int J Biol *Macromol*. 2010 Apr 1;46(3):281-3.

66. Bianco A, Kostarelos K, Prato M. Applications of carbon nanotubes in drug delivery. *Curr Opin Chem Biol*. 2005 Dec;9(6):674-9.

67. Fabbro C, Ali-Boucetta H, Da Ros T, Kostarelos K, Bianco A, Prato M. Targeting carbon nanotubes against cancer. *Chem Commun*. 2012;48(33):3911-26.

68. Meng LJ, Zhang XK, Lu QH, Fei ZF, Dyson PJ. Single walled carbon nanotubes as drug delivery vehicles: Targeting doxorubicin to tumors. *Biomaterials*. 2012 Feb;33(6):1689-98.

69. Herrero MA, Toma FM, Al-Jamal KT, Kostarelos K, Bianco A, Da Ros T, et al. Synthesis and Characterization of a Carbon Nanotube-Dendron Series for Efficient siRNA Delivery (vol 131, pg 9843, 2009). *J Am Chem Soc*. 2010 Feb 10;132(5):1731-.

70. Liu Z, Chen K, Davis C, Sherlock S, Cao QZ, Chen XY, et al. Drug delivery with carbon nanotubes for in vivo cancer treatment. *Cancer Res*. 2008 Aug 15;68(16):6652-60.

71. Lee PC, Chiou YC, Wong JM, Peng CL, Shieh MJ. Targeting colorectal cancer cells with single-walled carbon nanotubes conjugated to anticancer agent SN-38 and EGFR antibody. *Biomaterials*. 2013 Nov;34(34):8756-65.

72. Savage DJ, Liu XW, Curley SA, Ferrari M, Serda RE. Porous silicon advances in drug delivery and immunotherapy. *Curr Opin Pharmacol*. 2013 Oct;13(5):834-41.

73. Faraji AH, Wipf P. Nanoparticles in cellular drug delivery. *Bioorgan Med Chem.* 2009 Apr 15;17(8):2950-62.

74. Kar M, Tiwari N, Tiwari M, Lahiri M, Sen Gupta S. Poly-L-Arginine Grafted Silica Mesoporous Nanoparticles for Enhanced Cellular Uptake and their Application in DNA Delivery and Controlled Drug Release. *Part Part Syst Char. 2013 Feb;30(2):166-79.*

75. Ferris DP, Lu J, Gothard C, Yanes R, Thomas CR, Olsen JC, et al. Synthesis of Biomolecule-Modified Mesoporous Silica Nanoparticles for Targeted Hydrophobic Drug Delivery to Cancer Cells. *Small.* 2011 Jul 4;7(13):1816-26.

76. Roy I, Ohulchanskyy TY, Pudavar HE, Bergey EJ, Oseroff AR, Morgan J, et al. Ceramic-based nanoparticles entrapping water-insoluble photosensitizing anticancer drugs: A novel drug-carrier system for photodynamic therapy. *J Am Chem Soc.* 2003 Jul 2;125(26):7860-5.

77. Lu J, Li ZX, Zink JI, Tamanoi F. In vivo tumor suppression efficacy of mesoporous silica nanoparticles-based drug-delivery system: enhanced efficacy by folate modification. *Nanomed-Nanotechnol.* 2012 Feb;8(2):212-20.

78. Huang XH, Jain PK, El-Sayed IH, El-Sayed MA. Gold nanoparticles: interesting optical properties and recent applications in cancer diagnostic and therapy. *Nanomedicine.* 2007 Oct;2(5):681-93.

79. Kumar A, Ma HL, Zhang X, Huang KY, Jin SB, Liu J, et al. Gold nanoparticles functionalized with therapeutic and targeted peptides for cancer treatment. *Biomaterials.* 2012 Feb;33(4):1180-9.

80. Arvizo RR, Saha S, Wang EF, Robertson JD, Bhattacharya R, Mukherjee P. Inhibition of tumor growth and metastasis by a self-therapeutic nanoparticle. P *Natl Acad Sci* USA. 2013 Apr 23;110(17):6700-5.

81. Thakor AS, Jokerst J, Zavaleta C, Massoud TF, Gambhir SS. Gold Nanoparticles: A Revival in Precious Metal Administration to Patients. *Nano Lett.* 2011 Oct;11(10):4029-36.

82. Arruebo M, Fernandez-Pacheco R, Ibarra MR, Santamaria J. Magnetic nanoparticles for drug delivery. *Nano Today*. 2007 Jun;2(3):22-32.

83. Chen FH, Zhang LM, Chen QT, Zhang Y, Zhang ZJ. Synthesis of a novel magnetic drug delivery system composed of doxorubicin-conjugated Fe3O4 nanoparticle cores and a PEG-functionalized porous silica shell. *Chem Commun.* 2010;46(45):8633-5.

84. Wagstaff AJ, Brown SD, Holden MR, Craig GE, Plumb JA, Brown RE, et al. Cisplatin drug delivery using gold-coated iron oxide nanoparticles for enhanced tumour targeting with external magnetic fields. *Inorg Chim Acta.* 2012 Dec 1;393:328-33.

85. Rieter WJ, Pott KM, Taylor KML, Lin WB. Nanoscale coordination polymers for platinum-based anticancer drug delivery. *J Am Chem Soc.* 2008 Sep 3;130(35):11584-+.

86. Sun XM, Li YD. Colloidal carbon spheres and their core/shell structures with noble-metal nanoparticles. *Angew Chem Int Edit.* 2004;43(5):597-601.

87. Sun YG, Mayers BT, Xia YN. Template-engaged replacement reaction: A one-step approach to the large-scale synthesis of metal nanostructures with hollow interiors. *Nano Lett.* 2002 May;2(5):481-5.

88. Chen ML, He YJ, Chen XW, Wang JH. Quantum Dots Conjugated with Fe3O4-Filled Carbon Nanotubes for Cancer-Targeted Imaging and Magnetically Guided Drug Delivery. *Langmuir.* 2012 Nov 27;28(47):16469-76.

89. Probst CE, Zrazhevskiy P, Bagalkot V, Gao XH. Quantum dots as a platform for nanoparticle drug delivery vehicle design. *Adv Drug Deliver Rev.* 2013 May;65(5):703-18.

90. Sakhrani NM, Padh H. Organelle targeting: third level of drug targeting. *Drug Des Dev Ther.* 2013;7:585-99.

91. Miller T, Breyer S, van Colen G, Mier W, Haberkorn U, Geissler S, et al. Premature drug release of polymeric micelles and its effects on tumor targeting. *Int J Pharmaceut.* 2013 Mar 10;445(1-2):117-24.

92. Meng H, Xue M, Xia T, Ji ZX, Tarn DY, Zink JI, et al. Use of Size and a Copolymer Design Feature To Improve the Biodistribution and the Enhanced Permeability and Retention Effect of Doxorubicin-Loaded Mesoporous Silica Nanoparticles in a Murine Xenograft Tumor Model. *Acs Nano.* 2011 May;5(5):4131-44.

93. Muro S. Challenges in design and characterization of ligand-targeted drug delivery systems. *J Control Release.* 2012 Dec 10;164(2):125-37.

94. Arvizo RR, Rana S, Miranda OR, Bhattacharya R, Rotello VM, Mukherjee P. Mechanism of anti-angiogenic property of gold nanoparticles: role of nanoparticle size and surface charge. *Nanomed-Nanotechnol.* 2011 Oct;7(5):580-7.

95. Giri S, Karakoti A, Graham RP, Maguire JL, Reilly CM, Seal S, et al. Nanoceria: A Rare-Earth Nanoparticle as a Novel Anti-Angiogenic Therapeutic Agent in Ovarian Cancer. *Plos One.* 2013 Jan 31;8(1).

96. Byrne JD, Betancourt T, Brannon-Peppas L. Active targeting schemes for nanoparticle systems in cancer therapeutics. *Adv Drug Deliver Rev.* 2008 Dec 14;60(15):1615-26.

97. Taheri A, Dinarvand R, Atyabi F, Ghahremani MH, Ostad SN. Trastuzumab decorated methotrexate-human serum albumin conjugated nanoparticles for targeted delivery to HER2 positive tumor cells. European *Journal of Pharmaceutical Sciences.* 2012 Sep 29;47(2):331-40.

98. Wang LN, Su WJ, Liu Z, Zhou MQ, Chen S, Chen YA, et al. CD44 antibody-targeted liposomal nanoparticles for molecular imaging and therapy of hepatocellular carcinoma. *Biomaterials.* 2012 Jul;33(20):5107-14.

99. Abdelghany SM, Schmid D, Deacon J, Jaworski J, Fay F, McLaughlin KM, et al. Enhanced Antitumor Activity of the Photosensitizer meso-Tetra(N-methyl-4-pyridyl) Porphine Tetra Tosylate through Encapsulation in Antibody-Targeted Chitosan/Alginate Nanoparticles. *Biomacromolecules.* 2013 Feb;14(2):302-10.

100. Kanapathipillai M, Mammoto A, Mammoto T, Kang JH, Jiang E, Ghosh K, et al. Inhibition of Mammary Tumor Growth Using Lysyl Oxidase-Targeting Nanoparticles to Modify Extracellular Matrix. *Nano Lett.* 2012 Jun;12(6):3213-7.

101. Davis ME, Zuckerman JE, Choi CHJ, Seligson D, Tolcher A, Alabi CA, et al. Evidence of RNAi in humans from systemically administered siRNA via targeted nanoparticles. *Nature*. 2010 Apr 15;464(7291):1067-U140.

102. Bae S, Ma K, Kim TH, Lee ES, Oh KT, Park ES, et al. Doxorubicin-loaded human serum albumin nanoparticles surface-modified with TNF-related apoptosis-inducing ligand and transferrin for targeting multiple tumor types. *Biomaterials*. 2012 Feb;33(5):1536-46.

103. Hong MH, Zhu SJ, Jiang YY, Tang GT, Sun C, Fang C, et al. Novel anti-tumor strategy: PEG-hydroxycamptothecin conjugate loaded transferrin-PEG-nanoparticles. *J Control Release*. 2010 Jan 4;141(1):22-9.

104. Farokhzad OC, Cheng JJ, Teply BA, Sherifi I, Jon S, Kantoff PW, et al. Targeted nanoparticle-aptamer bioconjugates for cancer chemotherapy in vivo. *P Natl Acad Sci USA*. 2006 Apr 18;103(16):6315-20.

105. Kaiser PK. Antivascular endothelial growth factor agents and their development: Therapeutic implications in ocular diseases. *Am J Ophthalmol*. 2006 Oct;142(4):660-8.

106. Farokhzad OC, Jon SY, Khademhosseini A, Tran TNT, LaVan DA, Langer R. Nanopartide-aptamer bioconjugates: A new approach for targeting prostate cancer cells. *Cancer Res*. 2004 Nov 1;64(21):7668-72.

107. Cho HJ, Yoon HY, Koo H, Ko SH, Shim JS, Lee JH, et al. Self-assembled nanoparticles based on hyaluronic acid-ceramide (HA-CE) and Pluronic (R) for tumor-targeted delivery of docetaxel. *Biomaterials*. 2011 Oct;32(29):7181-90.

108. Cho HJ, Yoon IS, Yoon HY, Koo H, Jin YJ, Ko SH, et al. Polyethylene glycol-conjugated hyaluronic acid-ceramide self-assembled nanoparticles for targeted delivery of doxorubicin. *Biomaterials.* 2012 Feb;33(4):1190-200.

109. Ma M, Chen HR, Chen Y, Zhang K, Wang X, Cui XZ, et al. Hyaluronic acid-conjugated mesoporous silica nanoparticles: excellent colloidal dispersity in physiological fluids and targeting efficacy. *J Mater Chem.* 2012;22(12):5615-21.

110. Forster MD, Ormerod MG, Agarwal R, Kaye SB, Jackman AL. Flow cytometric method for determining folate receptor expression on ovarian carcinoma cells. *Cytom Part A.* 2007 Nov;71A(11):945-50.

111. Yu JM, Xie X, Wu JZ, Liu YH, Liu PJ, Xu XY, et al. Folic acid conjugated glycol chitosan micelles for targeted delivery of doxorubicin: preparation and preliminary evaluation in vitro. *J Biomat Sci-Polym E.* 2013 Apr 1;24(5):606-20.

112. Majd MH, Asgari D, Barar J, Valizadeh H, Kafil V, Abadpour A, et al. Tamoxifen loaded folic acid armed PEGylated magnetic nanoparticles for targeted imaging and therapy of cancer. *Colloid Surface B.* 2013 Jun 1;106:117-25.

113. Zong H, Thomas TP, Lee KH, Desai AM, Li MH, Kotlyar A, et al. Bifunctional PAMAM Dendrimer Conjugates of Folic Acid and Methotrexate with Defined Ratio. *Biomacromolecules.* 2012 Apr;13(4):982-91.

114. Molek P, Strukelj B, Bratkovic T. Peptide Phage Display as a Tool for Drug Discovery: Targeting Membrane Receptors. Molecules. 2011 Jan;16(1):857-87.

115. Pan LM, He QJ, Liu JN, Chen Y, Ma M, Zhang LL, et al. Nuclear-Targeted Drug Delivery of TAT Peptide-Conjugated Monodisperse Mesoporous Silica Nanoparticles. *J Am Chem Soc.* 2012 Apr 4;134(13):5722-5.

116. Pearce TR, Shroff K, Kokkoli E. Peptide Targeted Lipid Nanoparticles for Anticancer Drug Delivery. *Adv Mater.* 2012 Jul 24;24(28):3803-22.

117. Moghimi SM, Hunter AC, Murray JC. Long-circulating and target-specific nanoparticles: Theory to practice. *Pharmacol Rev.* 2001 Jun;53(2):283-318.

118. Stoddart A. Corona creation. *Nat Mater.* 2013 Nov;12(11):946-.

119. Lynch I, Salvati A, Dawson KA. Protein-Nanoparticle Interactions What Does the Cell See? *Nat Nanotechnol.* 2009 Sep;4(9):546-7.

120. Thiele L, Diederichs JE, Reszka R, Merkle HP, Walter E. Competitive adsorption of serum proteins at microparticles affects phagocytosis by dendritic cells. *Biomaterials.* 2003 Apr;24(8):1409-18.

121. Karmali PP, Simberg D. Interactions of nanoparticles with plasma proteins: implication on clearance and toxicity of drug delivery systems. *Expert Opin Drug Del.* 2011 Mar;8(3):343-57.

122. Salvati A, Pitek AS, Monopoli MP, Prapainop K, Bombelli FB, Hristov DR, et al. Transferrin-functionalized nanoparticles lose their targeting capabilities when a biomolecule corona adsorbs on the surface. *Nat Nanotechnol.* 2013 Feb;8(2):137-43.

123. Moghimi SM, Hunter AC. Poloxamers and poloxamines in nanoparticle engineering and experimental medicine. *Trends Biotechnol.* 2000 Oct;18(10):412-20.

124. Moghimi SM, Muir IS, Illum L, Davis SS, Kolbbachofen V. Coating Particles with a Block-Copolymer (Poloxamine-908) Suppresses Opsonization but Permits the Activity of Dysopsonins in the Serum. *Biochim Biophys Acta*. 1993 Nov 7;1179(2):157-65.

125. Hong W, Chen D, Zhang X, Zeng J, Hu H, Zhao X, et al. Reversing multidrug resistance by intracellular delivery of Pluronic(R) P85 unimers. *Biomaterials*. 2013 Dec;34(37):9602-14.

126. Saxena V, Hussain MD. Polymeric Mixed Micelles for Delivery of Curcumin to Multidrug Resistant Ovarian Cancer. *J Biomed Nanotechnol*. 2013 Jul;9(7):1146-54.

127. Flens MJ, Zaman GJR, vanderValk P, Izquierdo MA, Schroeijers AB, Scheffer GL, et al. Tissue distribution of the multidrug resistance protein. *Am J Pathol*. 1996 Apr;148(4):1237-47.

128. Owens DE, Peppas NA. Opsonization, biodistribution, and pharmacokinetics of polymeric nanoparticles. *Int J Pharmaceut*. 2006 Jan 3;307(1):93-102.

129. Abuchowski A, Vanes T, Palczuk NC, Davis FF. Alteration of Immunological Properties of Bovine Serum-Albumin by Covalent Attachment of Polyethylene-Glycol. *J Biol Chem*. 1977;252(11):3578-81.

130. Perry JL, Reuter KG, Kai MP, Herlihy KP, Jones SW, Luft JC, et al. PEGylated PRINT Nanoparticles: The Impact of PEG Density on Protein Binding, Macrophage Association, Biodistribution, and Pharmacokinetics. *Nano Lett*. 2012 Oct;12(10):5304-10.

131. Lee H. Molecular Dynamics Studies of PEGylated Single-Walled Carbon Nanotubes: The Effect of PEG Size and Grafting Density. *The Journal of Physical Chemistry* C. 2013.

132. Rodriguez PL, Harada T, Christian DA, Pantano DA, Tsai RK, Discher DE. Minimal "Self" Peptides That Inhibit Phagocytic Clearance and Enhance Delivery of Nanoparticles. *Science*. 2013 Feb 22;339(6122):971-5.

133. DiMasi JA, Hansen RW, Grabowski HG. The price of innovation: new estimates of drug development costs. *J Health Econ*. 2003 Mar;22(2):151-85.

134. Hofheinz RD, Gnad-Vogt SU, Beyer U, Hochhaus A. Liposomal encapsulated anti-cancer drugs. *Anti-Cancer Drug*. 2005 Aug;16(7):691-707.

135. Miele E, Spinelli GP, Miele E, Tomao F, Tomao S. Albumin-bound formulation of paclitaxel (Abraxane (R) ABI-007) in the treatment of breast cancer. *Int J Nanomed*. 2009;4(1):99-105.

136. Kim TY, Kim DW, Chung JY, Shin SG, Kim SC, Heo DS, et al. Phase I and pharmacokinetic study of Genexol-PM, a cremophor-free, polymeric micelle-formulated paclitaxel, in patients with advanced malignancies. *Clin Cancer Res*. 2004 Jun 1;10(11):3708-16.

137. Wagner V, Dullaart A, Bock AK, Zweck A. The emerging nanomedicine landscape. *Nat Biotechnol*. 2006 Oct;24(10):1211-7.

138. Davis SS, Washington C, West P, Illum L, Liversidge G, Sternson L, et al. Lipid Emulsions as Drug Delivery Systems. *Ann Ny Acad Sci*. 1987 Dec 22;507:75-88.

139. Uson N, Garcia MJ, Solans C. Formation of water-in-oil (W/O) nano-emulsions in a water/mixed non-ionic surfactant/oil systems prepared by a low-energy emulsification method. *Colloid Surface A.* 2004 Dec 10;250(1-3):415-21.

140. Wang LJ, Li XF, Zhang GY, Dong JF, Eastoe J. Oil-in-water nanoemulsions for pesticide formulations. *J Colloid Interf Sci.* 2007 Oct 1;314(1):230-5.

141. Mason TG, Wilking JN, Meleson K, Chang CB, Graves SM. Nanoemulsions: formation, structure, and physical properties. *J Phys-Condens Mat.* 2006 Oct 18;18(41):R635-R66.

142. Anton N, Vandamme TF. The universality of low-energy nano-emulsification. *Int J Pharmaceut.* 2009 Jul 30;377(1-2):142-7.

143. Anton N, Vandamme TF. Nano-emulsions and Micro-emulsions: Clarifications of the Critical Differences. *Pharm Res-Dordr.* 2011 May;28(5):978-85.

144. Anton N, Benoit JP, Saulnier P. Design and production of nanoparticles formulated from nano-emulsion templates - A review. *J Control Release.* 2008 Jun 24;128(3):185-99.

145. Lopez-Montilla JC, Herrera-Morales PE, Pandey S, Shah DO. Spontaneous emulsification: Mechanisms, physicochemical aspects, modeling, and applications. *J Disper Sci Technol.* 2002;23(1-3):219-68.

146. Jumaa M, Muller BW. Parenteral emulsions stabilized with a mixture of phospholipids and PEG-660-12-hydroxy-stearate: evaluation of accelerated and long-term stability. *Eur J Pharm Biopharm.* 2002 Sep;54(2):207-12.

147. Young TJ, Johnston KP, Pace GW, Mishra AK. Phospholipid-stabilized nanoparticles of cyclosporine A by rapid expansion from supercritical to aqueous solution. *Aaps Pharmscitech.* 2004;5(1).

148. Ortega-Vinuesa JL, Bastos-Gonzalez D. A review of factors affecting the performances of latex agglutination tests. *J Biomat Sci-Polym* E. 2001;12(4):379-408.

149. HidalgoAlvarez R, Martin A, Fernandez A, Bastos D, Martinez F, delasNieves FJ. Electrokinetic properties, colloidal stability and aggregation kinetics of polymer colloids. *Adv Colloid Interfac.* 1996 Sep 2;67:1-118.

150. Lopez-Leon T, Carvalho ELS, Seijo B, Ortega-Vinuesa JL, Bastos-Gonzalez D. Physicochemical characterization of chitosan nanoparticles: electrokinetic and stability behavior. *J Colloid Interf Sci.* 2005 Mar 15;283(2):344-51.

151. Lazaridis N, Alexopoulos AH, Chatzi EG, Kiparissides C. Steric stabilization in emulsion polymerization using oligomeric nonionic surfactants. *Chem Eng Sci.* 1999 Aug;54(15-16):3251-61.

152. Mollet H, Grubenmann A, Payne H. Formulation Technology: Emulsions, Suspensions, Solid Forms. 2008.

153. Grigoriev DO, Miller R. Mono- and multilayer covered drops as carriers. *Curr Opin Colloid In.* 2009 Feb;14(1):48-59.

154. He W, Lu Y, Qi JP, Chen LY, Hu FQ, Wu W. Nanoemulsion-templated shell-crosslinked nanocapsules as drug delivery systems. Int J Pharmaceut. 2013 Mar 10;445(1-2):69-78.

155. Kothamasu P, Kanumur H, Ravur N, Maddu C, Parasuramrajam R, Thangavel S. Nanocapsules: the weapons for novel drug delivery systems. *Bioimpacts.* 2012;2(2):71-81.

156. Derjaguin B, Landau L. Theory of the Stability of Strongly Charged Lyophobic Sols and of the Adhesion of Strongly Charged-Particles in Solutions of Electrolytes. *Prog Surf Sci.* 1993 May-Aug;43(1-4):30-59.

157. Verwey EJW. Theory of the Stability of Lyophobic Colloids. *J Phys Colloid Chem.* 1947;51(3):631-6.

158. Quesada M, Puig J, Delgado JM, Hidalgo-Alvarez R. Modelling the kinetics of antigen-antibody reactions at particle enhanced optical immunoassays. *J Biomat Sci-Polym E.* 1998;9(9):961-71.

159. Fuchs NZ. *Physica.* 1984;89:736.

160. Parshley RM. Hydration forces between mica surfaces in electrolyte solutions. *Adv Colloid Interface Sci.* 1982;16:57.

161. Lopez-Leon T, Santander-Ortega MJ, Ortega-Vinuesa JL, Bastos-Gonzalez D. Hofmeister Effects in Colloidal Systems: Influence of the Surface Nature. *J Phys Chem C.* 2008 Oct 16;112(41):16060-9.

162. Molina-Bolivar JA, Ortega-Vinuesa JL. How proteins stabilize colloidal particles by means of hydration forces. *Langmuir.* 1999 Apr 13;15(8):2644-53.

163. Martins S, Sarmento B, Ferreira DC, Souto EB. Lipid-based colloidal carriers for peptide and protein delivery - liposomes versus lipid nanoparticles. *Int J Nanomed.* 2007;2(4):595-607.

164. Porter CJH, Pouton CW, Cuine JF, Charman WN. Enhancing intestinal drug solubilisation using lipid-based delivery systems. *Adv Drug Deliver Rev.* 2008 Mar 17;60(6):673-91.

165. Muller RH, Schmidt S, Buttle I, Akkar A, Schmitt J, Bromer S. SolEmuls (R) - novel technology for the formulation of i.v. emulsions with poorly soluble drugs. *Int J Pharmaceut.* 2004 Jan 28;269(2):293-302.

166. Mason TG, Wilking JN, Meleson K, Chang CB, Graves SM. Nanoemulsions: formation, structure, and physical properties (vol 19, pg 079001, 2007). *J Phys-Condens Mat.* 2007 Feb 21;19(7).

167. Cevc G, Vierl U. Nanotechnology and the transdermal route A state of the art review and critical appraisal. *J Control Release.* 2010 Feb 15;141(3):277-99.

168. Souto EB, Nayak AP, Murthy RS. Lipid nanoemulsions for anti-cancer drug therapy. *Pharmazie.* 2011 Jul;66(7):473-8.

169. Shakeel F, Baboota S, Ahuja A, Ali J, Shafiq S. Celecoxib nanoemulsion: Skin permeation mechanism and bioavailability assessment. *J Drug Target.* 2008;16(10):733-40.

170. Tiwari SB, Amiji MM. Improved oral delivery of paclitaxel following administration in nanoemulsion formulations. *J Nanosci Nanotechnol.* 2006 Sep-Oct;6(9-10):3215-21.

171. Elnaggar YSR, El-Massik MA, Abdallah OY. Self-nanoemulsifying drug delivery systems of tamoxifen citrate: Design and optimization. *Int J Pharmaceut.* 2009 Oct 1;380(1-2):133-41.

172. Elsheikh MA, Elnaggar YSR, Gohar EY, Abdallah OY. Nanoemulsion liquid preconcentrates for raloxifene hydrochloride: optimization and in vivo appraisal. *Int J Nanomed.* 2012;7:3787-802.

173. Alayoubi AY, Anderson JF, Satyanarayanajois SD, Sylvester PW, Nazzal S. Concurrent delivery of tocotrienols and simvastatin by lipid nanoemulsions potentiates their antitumor activity against human mammary adenocarcenoma. *European Journal of Pharmaceutical Sciences.* 2013 Feb 14;48(3):385-92.

174. Zhao H, Lu H, Gong T, Zhang ZR. Nanoemulsion loaded with lycobetaine-oleic acid ionic complex: physicochemical characteristics, in vitro, in vivo evaluation, and antitumor activity. *Int J Nanomed.* 2013;8:1959-73.

175. Minta JO, Pambrun L. Invitro Induction of Cytologic and Functional-Differentiation of the Immature Human Monocyte-Like Cell-Line U-937 with Phorbol-Myristate Acetate. *Am J Pathol.* 1985;119(1):111-26.

176. Liu MY, Wu MC. Induction of Human Monocyte Cell-Line U937 Differentiation and Csf-1 Production by Phorbol Ester. *Exp Hematol.* 1992 Sep;20(8):974-9.

Chapter 2. Hypotheses and objectives

Hypotheses

- Lipid nanocapsules based on a core-shell structure, could efficiently encapsulate, transport and deliver hydrophobic drugs such as docetaxel, increasing its cytotoxic effect due to the oily core and the shell composed of phospholipids that could favor their interaction with cell membranes.

- The modification of the surface of lipid nanocapsules with folic acid could enhance their selective uptake by cancer cells that overexpress receptors for this molecule and, thus, to increase the delivery of drugs toward these target cells.

- The functionalization of lipid nanoparticles with monoclonal antibodies that recognize specific antigens presented in cancer cell membranes, could facilitate the selective targeting of these nanosystems. As an example, herceptin, an antibody with medical applications, immobilized onto lipid nanocapsules could enhance their

uptake in HER2 positive cancer cells, compared with cells with a low expression of HER2 receptors.

- The nature of the surfactant that composes the shell of the lipid nanocapsules could affect how they interact with the biological environment. The use of hydrophilic surfactants such as pluronics in the shell could decrease their opsonization and recognition by immune cells.

Main objectives

The main goal of this study is to evaluate the potential of different nanocapsule systems (nanoemulsions) to transport and deliver lipophilic anticancer drugs such as docetaxel, with the aim of improving their cytotoxicity in cancer cells, focusing in the surface characteristics and shell composition and the manner in which they influence the behaviour of the nanoparticles in physiological conditions. To achieve this goal several steps were followed:

- To synthesize lipid nanocapsules based on a core-shell structure, with the desire properties such as colloidal stability, particle size, monodispersity, and surface charge, and to carry out an in-depth physico-chemical characterization with particular emphasis on the influence of the shell composition in their colloidal stability and electrophoretic mobility.

- To encapsulate in the oily core of the nanoemulsions an hydrophobic dye (Nile red) and an anticancer drug (docetaxel) in order to study the uptake and cytotoxic effect of the nanocapsules in breast cancer cells as well as its effect in the cell cycle and apoptosis.

- To modify the surface of nanocapsules with folic acid in the interest of designing targeted nanoparticles against cancer cells that overexpress folate receptors such as some colon cancer cell lines, comparing the biological effect in folate receptor-negative-cells. Moreover, to carry out a complete physico-chemical characterization of these systems to analyze their properties before the development of biological studies.

- To synthesize a new formulation of lipid nanocapsules and to establish a method of functionalization of their surfaces with monoclonal antibodies which have different isoelectric points. This study implies the immobilization of a monoclonal antibody used currently in cancer therapy, herceptin, to target the nanocapsules against HER2 positive breast cancer cells and to study differences in uptake and cytotoxicity comparing the results of these cells with HER2 negative cancer cells and healthy ones.

- Finally, to study the influence of the surfactant, located in the nanocapsule shell, on the protein adsorption, macrophage association, uptake and cytotoxic effect in cancer cells, since understanding this should help us to modulate the surface architecture to control the environmental interactions and, thus, to optimize functionality of nanosystems in an environment specific way.

Chapter 3. Brief summary of the presented papers

In this thesis, the results are presented in five different papers according to a chronological criterion. A brief summary of the main results and their interrelationships is presented below.

Paper I. In this work different protocols to establish a simple, reproducible, and non-expensive procedure to synthesize lipid nanocapsule systems with an oily core and different surface characteristics were developed by using phospholipid molecules, a poloxamer, and chitosan. Special attention was paid to design nanocapsules in which antibody molecules could be covalently attached on the surface (e.g. particles with an enriched carboxylic surface). They were analyzed in order to acquire a fuller knowledge concerning the physicochemical properties examining the role played by their components. These experiments showed that the nanosystems presented an appropriate size, monodispersity and colloidal stability for parenteral administration. In addition, a polyclonal IgG was immobilized on the surface of the particles and the immunological response of this new system against the specific ligand was quantified showing specific recognition properties. Finally

the potential use of these nanocapsules was evaluated by studying the *in vitro* the uptake of Nile red-loaded systems by breast cancer cells, being the results modulated by the surface characteristics.

Paper II. A fuller biological *in vitro* study of the nanoparticles presented in the paper I was developed in this second article. An hydrophobic anticancer drug, docetaxel, was encapsulated in three lipid nanocapsule systems with different shell composition, and their cytotoxic effect, apoptosis and cell cycle effect in a breast cancer cell line was evaluated. The anti-tumor effect of docetaxel was improved by its encapsulation in lipid nanocapsules, which significantly decreased the IC_{50} rate with evidence of apoptosis and premature cell cycle progression from G(1) to G(2)-M phase.

Paper III. Once bare lipid nanoparticles were characterized and their cytotoxic effect evaluated (paper I and II), next step was to vectorize these systems to facilitate selective targeting against cancer cell lines that overexpress membrane folate receptors. Thus, nanocapsules coated with folate-chitosan conjugates at varying folate concentrations were synthesized and characterized. They were loaded with Nile red and docetaxel, and evaluated in four tumor cell lines with different expression of folate receptors, demonstrating that the folate-mediated internalization of the particles in the cancer cells was improved when the nanocapsules were coated by folate-chitosan conjugates.

Paper IV. Another strategy of vectorization of lipid nanoparticles was developed and optimized. In this paper a standardization of a simple method to obtain targeted nanocapsules with monoclonal antibodies was established. Three different antibodies were covalently immobilized on an enriched carboxylic surface of lipid nanocapsules by using deoxycholic acid molecules. One of these antibodies was trastuzumab (herceptin®), a specific HER2 oncoprotein antibody. After the

complete physico-chemical characterization, immunological analyses verified the expected specific immuno-response of the systems. Moreover herceptin-modified nanocapsules with Nile red enclosed were evaluated by *in vitro* assays analyzing the uptake in different breast cancer cell lines, which overexpress low and high levels of HER2, and a healthy breast cell line as a negative control. Cytotoxic effect was studied by encapsulating docetaxel and both biological studies showed that these immuno-nanocapsules present specific recognition properties.

Paper V. Finally, a study to deeply understand how lipid nanocapsules interact with the highly complex surrounding biological milieu was carried out. Surfactants with markedly different nature (poloxamer and phospholipids) were used as components of the shell in diverse combinations to provide different surface properties. Protein adsorption on the surfaces was determined showing that poloxamer significantly reduces such adsorption. Moreover the influence of these differences on cellular uptake and cytotoxicity in a lung cancer cell line was analyzed by encapsulating a hydrophobic fluorescent dye (Coumarin 6) or a lipophilic drug (docetaxel) respectively, observing quantitative dissimilarities: as the concentration of poloxamer increases in the shell of the particles, both the cytotoxicity and the uptake decrease. The trend of uptake was similar when particles were studied when working with cells of the immune system such as macrophages.

Chapter 4: Results

Paper I: Characterization of Different Functionalized Lipid Nanocapsules as Potential Drug Carriers

Paola Sánchez Moreno [1], Juan Luis Ortega Vinuesa [1], Antonio Martín Rodríguez [1], Houria Boulaiz [2], Juan Antonio Marchal Corrales [2] and José Manuel Peula García [3]

[1] *Biocolloid and Fluid Physics Group, Department of Applied Physics, University of Granada, 18071 Granada, Spain*

[2] *Human Anatomy and Embryology Department, Regenerative Biomedicine Institute (IBIMER), Campus de la Salud, University of Granada, 18071 Granada, Spain*

[3] *Department of Applied Physics II, University of Málaga, 29071 Málaga, Spain*

Published in:

International Journal of Molecular Sciences

Int. J. Mol. Sci. **2012**, *13*(2), 2405-2424

Abstract

Lipid nanocapsules (LNC) based on a core-shell structure consisting of an oil-filled core with a surrounding polymer layer are known to be promising vehicles for the delivery of hydrophobic drugs in the new therapeutic strategies in anti-cancer treatments. The present work has been designed as basic research about different LNC systems. We have synthesized – and physico-chemically characterized – three different LNC systems in which the core was constituted by olive oil and the shell by different phospholipids (phosphatidyl-serine or lecithin) and other biocompatible molecules such as Pluronic® F68 or chitosan. It bears remarking that the olive-oil-phosphatidyl-serine LCN is a novel formulation presented in this work and was designed to generate an enriched carboxylic surface. This carboxylic layer is meant to link specific antibodies, which could facilitate the specific nanocapsule uptake by cancer cells. This is why nanoparticles with phosphatidyl-serine in their shell have also been used in this work to form immuno-nanocapsules containing a polyclonal IgG against a model antigen (C-reactive protein) covalently bounded by means of a simple and reproducible carbodiimide method. An immunological study was made to verify that these IgG-LNC complexes showed the expected specific immune response. Finally, a preliminary *in vitro* study was performed by culturing a breast-carcinoma cell line (MCF-7) with Nile-Red-loaded LNC. We found that these cancer cells take up the fluorescent Nile-Red molecule in a process dependent on the surface properties of the nanocarriers.

1. Introduction

Nanomedicine, an emerging new field created by the fusion of nanotechnology and medicine, has become one of the most promising pathways for developing effective targeted therapies with particular impact on oncology. This is because these new therapeutic strategies could supply the tools necessary to improve inherent limitations of classical pharmacotherapy [1-4].

In recent years, different colloidal systems such as nanoparticles and nanocapsules have been reported as potential carriers for drug delivery [5, 6]. Structured nanocapsules are generally described as colloidal systems with a core-shell structure [1, 2], where the core acts as a liquid reservoir for several molecules or drugs, and the shell as a protective membrane. These nanosystems present promising applications as carriers of drugs, proteins or DNA chains, or in diagnosis applications as contrast agents [7, 8]. Their useful properties include biocompatibility and biodegradability, low toxicity, controlled release of drugs and the ability to target specific tissues [5].

In particular, lipid nanocapsules (LNC), consisting of an oil-filled core with a surrounding polymer shell have special use for encapsulating and delivering hydrophobic drugs. The versatility of these LNC for an efficient encapsulation in their oily core of several anti-cancer drugs has been previously demonstrated [9, 10]. It should be noted that, due to the hydrophobic character of many of these drugs, current pharmacotherapy must use solubilizer agents for their intravenous administration [11], which in turn is another foreign substance that has to be added in the blood stream. This is why LNC offer a promising system and an excellent alternative to emulsions or microemulsions for pharmaceutical application of hydrophobic drugs [7, 12, 13]. Thanks to the drug protection and their controlled release on cancer cells, these kinds of nanoparticles provide an ideal solution,

leading to selective cytotoxicity, minimizing the serious and unpleasant side effects of cancer drugs and preventing damage to healthy tissues [14, 15].

The shell of LNC can be formed by a wide variety of polymers/surfactants with hydrophilic segments such as polyethylene glycol (PEG), polyethylene oxide, poloxamers, poloxamines, polysorbates, chitosan, etc. [16-19]. These types of polymers, in addition to enhancing the intrinsic colloidal stability of the system, may help to avoid their recognition by the mononuclear phagocyte system (MPS), a major drawback that often arises after intravenous injection of drug carriers, causing a decrease in circulating LNC as well as undesirable accumulation of these colloids in the liver or the spleen. Therefore, the nature of the polymeric shell is crucial to minimize the MPS action by repelling plasma proteins [16] and achieving the so-called *Stealth*® nanosystems [5, 11, 20-22]. This would increase the *in vivo* long-term stability of the nanoparticles, and it would also facilitate their ability to cross certain biological barriers. For example, nanoparticles coated with polysorbates or poloxamers have been reported to successfully pass the blood-brain-barrier and other physiological barriers [23].

On the other hand, although LNC represent an important class of nanocarriers capable of efficiently encapsulating and delivering a variety of drugs, their typical pathway to act on cancer tissues is through the so-called *enhanced permeability and retention effect*. This means passive targeting with non-specific delivery and the inability to cross several biological barriers based on molecular recognition processes [7, 10, 15]. Thus, it would be advisable to improve the efficacy of chemotherapy as well as to decrease the systemic toxicity of these drugs by using tailor-made tumor-targeted drug carriers, thereby reducing — although not completely avoiding — unspecific passive delivery.

Vectorization and targeting capacities of these systems can be implemented by surface modification with specific biomolecules (e.g. antibody fragments, folic acid) conjugated to LNC and enhancing the cell-targeting through molecular recognition processes such as ligand-receptor or antigen-antibody reactions [6, 10, 24-26]. Today, it is possible to form a LNC surface with several agents bearing diverse functional groups capable of covalently binding a variety of biochemically active groups. Shell polymers are generally synthesized with pendant functional groups such as hydroxyl, carboxyl, amine or thiol groups (-OH, -COOH, $-NH_2$, or –SH). As a result, these tailored-LNCs would deliver a given drug specifically towards a targeted malignant tumor [4].

Within this scenario, the main objective of the present work focuses on developing a simple, reproducible, and non-expensive procedure to synthesize LNCs systems, paying special attention to designing nanocapsules in which antibody molecules can be covalently attached on the surface. Thus, several lipid nanosystems with different surface characteristics have been obtained and analyzed in order to acquire a fuller knowledge concerning the physicochemical properties of these colloidal particles, closely examining the role played by the components. Thus, a thorough characterization was made, including size, electrokinetic behavior, and colloidal stability.

Specifically, we have synthesized three different core-shell lipid nanosystems by using a simple process with commercially available biocompatible components. In all cases, the hydrophobic core was constituted by olive oil, while the hydrophilic shell nature was varied by adding different molecules in order to generate different (and desirable) surface properties. The molecules used in the surface modification were phospholipid molecules, a poloxamer, and chitosan. Thus, we have two typical reference systems previously reported [18] with an anionic and a cationic surface charge respectively, and a novel nanosystem (not

described in the literature yet) in which the shell was constituted by phosphatidyl-serine and a poloxamer producing a carboxyl-functionalized nanosystem.

In the second step, we developed the chemical immobilization of a classical polyclonal IgG antibody on the carboxylated nanocapsules by means of a reproducible and simple method. For this, a well-established procedure based on the carbodiimide (CDI) method was used [27-30]. All the antibody-LNC systems were physico-chemically characterized and compared with bare LNC. The immunological response of our colloidal immune-nanocapsules was also quantified against the specific ligand of the antibody molecules, the C-reactive protein (CRP). The goal of this part was to check whether this new LNC system enriched by phosphatidyl-serine could efficiently link antibodies for future vectorization purposes, and whether these antibodies kept their intrinsic immuno-reactivity once they were immobilized on the LNC surface.

The work finishes with an *in vitro* study to evaluate the potential use of our LNC. In this last part, Nile-Red-loaded lipid nanocapsules were prepared to make a quantitative study of particle uptake by a breast-carcinoma cell line (MCF-7), Nile-Red being a commercially available hydrophobic fluorescent molecule.

2. Experimental section

Reagents

Olive oil, poloxamer 188 (Pluronic® F68), Nile Red and phosphatidyl-L-serine were obtained from Sigma Aldrich. The olive oil was purified with activated magnesium silicate (Florisil, Fluka) in order to eliminate free fatty acids. Epikuron 145V, which is a deoiled, wax-like, phosphatidyl-choline-enriched fraction of soybean lecithin, was kindly provided by Cargil Ibérica SL. Protasan® Cl 113, and

medium-molecular-weight chitosan chloride salt with a deacetylation degree of 85%, was supplied from FMC Biopolymer Novamatrix (Norway). For the study of the electrophoretic mobility and colloidal stability at different pH values, several buffered solutions with a low ionic strength (I = 0.002 M) were prepared: pH 4 and 5 were buffered with acetate, pH 6 and 7 with phosphate, and pH 8 and 9 with borate. Additionally, in some cases, stability was evaluated in phosphate buffer saline (PBS) and different culture mediums: Dulbecco's Modified Eagle's Medium (DMEM) supplemented with fetal bovine serum. Other chemicals and electrolytes used were of analytical grade and purchased from Sigma, Merck, and Scharlau. Deionized Milli-Q water was used throughout.

Nanocapsules preparation

The nanosystems studied were prepared by a solvent-displacement technique following the procedure of Prego *et al.* [50]. This is a well-known technique widely reported for the preparation of nanocapsules, where hydrophilic surfactants are usually dissolved in the aqueous phase before emulsion formation. Briefly, an organic phase was prepared containing 125 µl of olive oil and phospholipids: 40 mg of Epikuron 145V (EPI nanocapsules) or 10 mg of phosphatidyl-L-serine (PhS nanocapsules) dissolved in 0.5 ml ethanol and 9.5 ml of acetone. This organic phase was immediately poured over an aqueous phase containing 50 mg of Pluronic® F68 or 10 mg of chitosan oligomers. The mixture turned milky immediately because of the formation of the nanoemulsion. Then, the organic solvents were evaporated under vacuum to a final volume of 15 ml. Figure 1 shows a scheme of the synthesis procedure.

All nanosystems presented olive oil in their hydrophobic core and, depending on the composition of the organic and aqueous phases, the final sample showed different interface properties. Thus, three different systems were

formulated: EPI nanocapsules with a surface shell composed by epikuron and Pluronic® F68; CS nanocapsules with epikuron and chitosan oligomers; and finally, PhS nanocapsules with phosphatidyl-L-serine and Pluronic® F68.

Fluorescent LNCs were formulated by dissolving Nile Red in the olive oil phase at a concentration of 0.025% (w/w). The encapsulation of this fluorescent molecule was confirmed by using a SPEX Fluoromax-2 spectrofluorometer. The emission fluorescence spectra were determined from 550 to 700 nm previous excitation of the sample at a wavelength of 485 nm, with a scanning speed of 100 nm/min and a wavelength accuracy of ±1 nm.

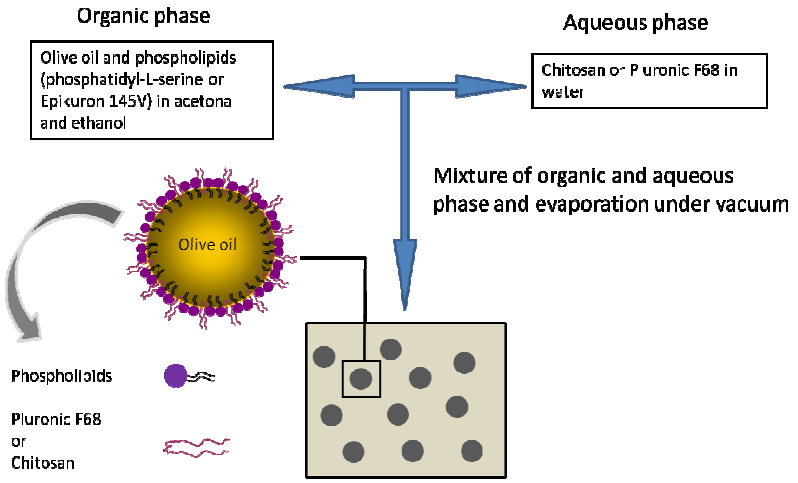

Figure 1. Scheme detailing the preparation of the particles.

Nanocapsule characterization

Size, morphology, and storage stability. The average size of the nanosystems was determined by combining a high-performance-particle-sizer technology with a non-

invasive-backscattering method, where the measurement is taken at an angle of 173º. This technique minimizes multiple scattering [51] and the light detected is processed by a digital correlator (ALV 5000/E), providing information on the average diffusion coefficient of the particles, which can be easily related to the mean diameter (∅) by using the Stokes-Einstein equation for spheres. The morphological characterization of the nanosystems was developed using transmission electron microscopy (TEM) in the Scientific Instrumentation Centre, Granada University (Spain).

Electrophoretic mobility. A Zetasizer-nano (Malvern Instruments, UK) was used to measure the electrophoretic mobility (μ_e). The study was focused on measuring the μ_e as a function of pH while maintaining a constant low-ionic-strength value (0.002 M). Each μ_e mobility datum was the average of 6 individual measurements.

Colloidal stability. Colloidal stability was spectrophotometrically studied (Beckman DU 7400 spectrophotometer) working at physiological pH in simple saline media. The salts used in these stability studies were NaCl and $CaCl_2$. As described in detail in reference [52], it is possible to derive the "critical coagulation concentration" (CCC) and the "critical stabilization concentration" (CSC) values. These parameters are fundamental in colloidal-stability studies, since they give valuable information about certain surface characteristics. For example, CCC is related to the surface charge density, while the CSC is associated to the surface hydrophilicity [51]. In addition to measuring the colloidal stability of our nanocapsules with NaCl and $CaCl_2$, we also evaluated stability in PBS and in DMEM supplemented with fetal bovine serum by monitoring the variation of optical absorbance of the nanocapsules as a function of time.

Immuno-nanocapsules

Conjugation of IgG antibodies with LNC. C-reactive protein (CRP) and polyclonal immunoglobulin G-anti-CRP (aCRP-IgG) from rabbit were obtained, purified, and kindly donated by Biokit S.A. (Spain). The covalent attachment of αCRP-IgG to the PhS nanoparticles was performed according to the well-established carbodiimide method [27]. In this method, 1 ethyl-3-(3-dimethyl aminopropyl) carbodiimide (CDI) was used to bind the antibody via its amino groups to the carboxyl groups of the PhS nanoparticles. Briefly, a sample of PhS system having 0.2 m^2 of total surface was incubated at pH 8 with CDI (100 μl of a solution of 15 mg/ml) for 30 min at 25ºC. Subsequently, activated nanoparticles were incubated with two different amounts of αCRP-IgG, 1mg/m^2 and 2.5 mg/m^2, overnight. All the immuno-nanocapsules were cleaned by means of a dialysis process in pH 8 buffer solution in order to separate the non-coupled αCRP-IgG molecules.

Immunological study. The immunoassays were performed in saline BSA borate buffer: pH 8, borate (15 mM), NaCl (150 mM), NaN_3 as preservative (1 mg/ml), and bovine serum albumin from Sigma-Aldrich (1 mg/ml). The immuno-nanoparticles were diluted in this solution to provide a working LNC reagent. A series of CRP solutions was prepared in the saline BSA medium, the antigen concentration ranging from 0.25 μg/ml to 40 μg/ml. Turbidimetric curves of absorbance vs. time were plotted using a simple spectrophotometer (Beckman DU 7400). Absorbance measurements were collected at 570 nm for 300 sec at 25ºC, after mixing 50 μl of each antigen solution with 150 μl of the immuno-LNC solution.

Cell line and culture conditions

A breast-carcinoma cell line (MCF-7) was supplied by the Scientific Instrumentation Centre, Granada University (Spain). Cells were grown at 37ºC in an atmosphere containing 5% CO_2, with DMEM (Gibco, Grand Island, NY, USA) supplemented with 10% (v/v) heat-inactivated fetal bovine serum (FBS), 2% L-glutamine, 2.7% sodium bicarbonate, 1% Hepes buffer, and 1% of penicillin/streptomycin solution.

The intracellular uptake of fluorescence-labeled nanoparticles was performed as follows. MCF-7 cells ($3x10^4$) were seeded into 24-well plates under the culture conditions detailed above. After 24 h, cells were fed with fresh medium and treated with Nile-Red-nanocapsules. After incubation for 30 min and 2 h with particles labeled with Red Nile the cells were washed with PBS to remove free nanocapsules. Then the cells were harvested by PBS-ethylenediamine-tetraacetid acid (PBS-EDTA), washed twice with cold PBS, and pelleted by centrifugation at 1500 rpm for 5 min. Living cells were resuspended in PBS and analyzed for red fluorescence by flow cytometry in a FACScan (Becton Dickinson, USA). The fluorescent pulses were analyzed by CellQuest Pro software. Instrument settings, such as the photomultiplier voltage and compensation, were adjusted in such a way that the difference in background fluorescence of cells without internalized nanocapsules became insignificant. SPSS (Statistical Package for the Social Sciences) version 7.5 (Chicago, IL, USA) was used for the statistical analysis in cell culture studies. The results were compared by means of the Student's *t* test. Differences were considered statistically significant at a *P* value of < 0.05.

3. Results and Discussions

The first part of this work includes a complete physicochemical and morphological characterization of our colloidal systems. Their synthesis procedures are shown in experimental section.

The shell of the simplest system (referred to as EPI) was constituted by a commercial mixture of phospholipid molecules (Epikuron) and a poloxamer (Pluronic® F68), both acting as colloidal stabilizers. A second system (referred to as CS) was formulated by substituting the poloxamer by chitosan oligomers. Finally, in the third formulation Epikuron was substituted by phosphatidyl-serine (referred to as pHS).

Particle size and size distribution are key variables to determine the *in vivo* distribution of the nanoparticles, the drug release, the targeting ability, and their colloidal stability [31, 32]. Generally, a sub-micron size is recommended in the literature. It is advisable to formulate nanoparticles with an optimal size depending on their specific use, normally under 200-300 nm of diameter, and preserving, at the same time, the colloidal stability of the system [16]. In our case, the synthesis procedure yielded to spherical nanocapsules with an average diameter in the nanometric scale, Table 1. It should be noted that the size of all the formulations remained at a constant value under the storage conditions (pure water, 4ºC) for at least four months, which is a good indication of their intrinsic stability in water.

The morphology of the nanocarriers was analyzed by TEM. The three LNC systems showed a spherical shape and a size consistent with the values previously found using light back-scattering measurements. Figure 2 shows a TEM micrograph of the EPI nanocapsules.

Table 1. Particle size of the different lipid nanocapsule and immuno-nanocapsule systems

Nanosystem	**Diameter (nm)**
EPI	170 ± 20
CS	330 ± 30
PhS	210 ± 20
PhS-1mgIgG/m^2	200 ± 20
PhS-2.5mgIgG/m^2	204 ± 14

Given the size differences among the EPI and PhS nanoparticles, the "epikuron-poloxamer" pair appears to be a better emulsifier than the "PhS-poloxamer" one, in that the former produces particles with a smaller diameter than the latter. Previous results have shown that the presence of poloxamer together with lecithin increases the particle size in comparison to the case in which lecithin was the only component of the shell [18]. This feature could be extrapolated to the PhS nanoparticles (with a larger diameters) suggesting a greater incorporation of poloxamer when this surfactant is added together with phosphatidyl-serine, producing nanoparticles with a larger diameter. Results of electrokinetic measurements and colloidal stability (shown in the following sections) appear to support this idea. Nevertheless, the most significant result was the size increment found when chitosan was added together with epikuron. In this case, positive chitosan chains can interact electrostatically with negative phospholipid molecules, reducing the effective concentration of this latter emulsifier and, consequently, producing larger nanocapsules [18].

With regard to the immuno-nanocapsules, we will firstly explain why our PhS-LNCs were sensitized with a partial coating of IgG. It is well known that the presence of polyclonal IgG molecules linked onto colloidal particles causes a

significant alteration of their surface properties, changing the electrokinetic behavior and reducing significantly the colloidal stability at neutral pH [28].

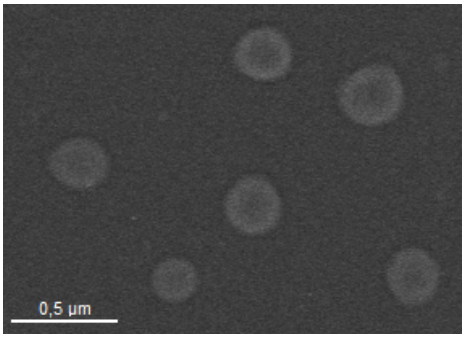

Figure 2.Transmission electron microscopy of the EPI nanocapsules.

The development of colloidally stable nanosystems is a prerequisite for successful future applications of drug carriers in biological media. Taking into account that a low stability has been found working with other nanoparticles of similar size as ours when their surfaces were saturated with IgG molecules (5 mgIgG/m^2) [33], we developed systems with a low to medium IgG coverage: 1 mgIgG/m^2, and 2.5 mgIgG/m^2. The covalent coupling was developed by means of the CDI method, described in detail in the experimental section, and no aggregation was noted over the experimental period.

After coupling, immuno-nanocapsules were separated from unbound protein by a dialysis procedure. An analysis of the eluted solution volume from dialysis by means of spectrophotometric measurements did not detect any presence of protein molecules in the solution, which would indicate very high coupling efficiency. The size of these antibody-nanocapsule complexes (at pH 8 and low-ionic-strength medium) is shown in Table 1. Diameters remain similar to those of the original PhS-system regardless of the antibody amount on the surface. This is a

good indication that the appropriate selection was made with our antibody density values, since an increase in the hydrodynamic diameter has been reported for several nanosystems having a high density of antibodies immobilized on them, meaning low stability and a strong tendency to aggregate [25, 34].

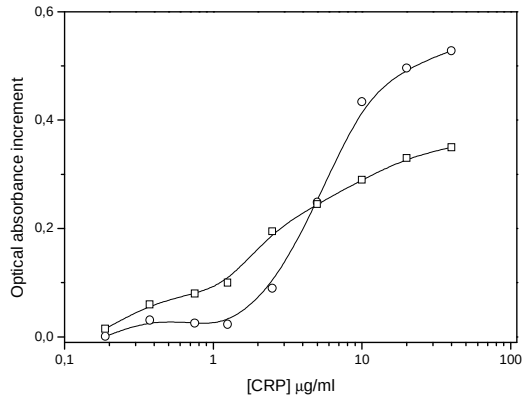

Figure 3. Absorbance change after 300 s (λ = 570 nm) due to aggregation induced by different CRP concentrations: (○) PhS-1mgIgG/m²; (□) PhS-2.5mgIgG/m². Reaction medium: 13 mM borate (pH 8.0), 150 mMNaCl, 1 mg/ml NaN_3, 1 mg/ml BSA. The starting point of optical absorbance for all experiments was 0.5.

Prior any further physico-chemical characterization of the immuno-complexes, it was necessary to test whether the immobilized IgG maintained its antigenic activity. Previous results working with hard nanospheres in which IgG was covalently linked with the CDI method showed good immuno-activity [27, 28]. However, we are now working with soft liquid particles where IgG might denature when located in the oil/water interface and/or may change the preferential orientation of the adhered IgG molecules– especially when surfactant molecules (e.g. poloxamer) are placed on the surface [35]. Therefore, we quantified the immuno-reactivity by spectrophotometrically measuring the agglutination extent when our immuno-nanocapsules were mixed with the corresponding antigen (CRP). These experiments are determinant to test the feasibility and potential

applicability of these soft lipid immuno-nanocapsules in future active targeting strategies. Figure 3 shows the changes in the optical absorbance vs. the CRP concentration for both immuno-complexes. It should be noted that at low CRP concentrations, those particles with a higher IgG coating were more reactive, while at [CRP] < 5 μg/ml the highest increment of absorbance was found with the 1 mgIgG/m^2 complex. Nevertheless, the immuno-agglutination extent was significant in both cases and it indicates an adequate surface disposition of the antibody molecules for specific recognition.

The next set of experiments was focused on determining the electrical state of the nanocapsules at different pH values. A magnitude commonly used to gain information about the surface state of charge of colloidal particles is electrophoretic mobility (μ_e). This is an experimental parameter directly related with the zeta potential existing in the shear plane of the particles [28, 36]. The electrophoretic mobility data, gathered from low-ionic-strength media, are shown in Figure 4. The μ_e values depend on the electrical potential at the shear plane, which is ultimately governed by the composition of the LNC surface and by the salinity and pH conditions of the medium in which the particles are dispersed. The μ_e results agree with the nature of the shell of our nanocapsules and they confirm the presence of the different molecules used in their synthesis. That is, the EPI and PhS nanocapsules showed typical behavior of colloids with weak acid groups, giving lower μ_e values at acidic pH values than those found at neutral and basic pH.

In addition, Figure 4 shows a peculiar nuance related with the nature of the surface-charged groups. These groups come exclusively from the Epikuron molecules in the EPI nanocapsules, in which phosphatidyl-choline is the major component. Thus, the phosphatidic acid – with a pK_a between 3 and 4 – is the main charged group in these LNC. However, the PhS-nanoparticles present only phosphatidyl-serine as phospholipidic molecules; that is, in this case there are two

different surface charged groups: phosphatidic and carboxylic (pK_a= 4.8). This is also reflected in the electrokinetic behavior, since the reduction in the mobility value begins at pH 5 for the PhS system while it is at pH 4 for the EPI particles (see Figure 4).

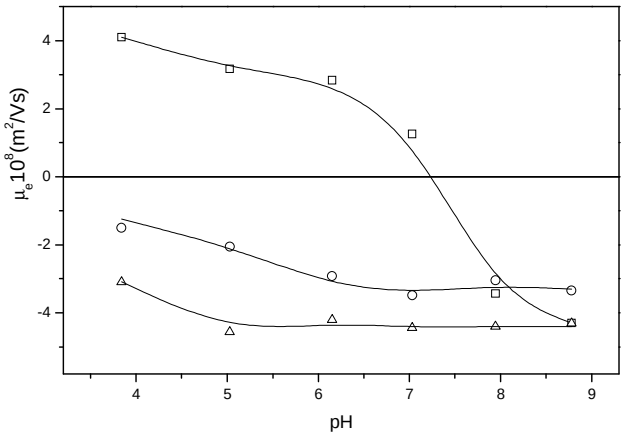

Figure 4. Electrophoretic mobility vs. pH for (△) EPI, (□) CS, and (○) PhS nanocapsules.

This subtle difference in our experimental μ_e measurements agrees with other data gathered with similar colloidal systems formed by both phosphatidic [18] and carboxylic [37] surface groups. The presence of Pluronic F68 molecules on the surface does not alter the electrical state of the surface, since this poloxamer is a non-ionic surfactant [18, 35]. However, a μ_e reduction (in absolute value) could be expected after the incorporation of this non-ionic surfactant onto the nanoparticle surface, since the presence of polyethylene oxide (PEO) chains would cause an outward shift of the shear plane where the ζ-potential is defined, and this would subsequently diminish the electrophoretic mobility. At least for polystyrene or polylactic-co-glycolic acid particles the μ_e reduction was significant and directly related to the poloxamer coating [35, 38]. The results shown in Figure 4 for both EPI and PhS systems would indicate a higher incorporation of poloxamer for the PhS nanoparticles with an appreciable decrease of the absolute μ_e values

throughout the pH range studied, as experimentally observed. As will be shown, the stability experiments corroborate this assumption related to the higher incorporation of Pluronic F68 in the PhS-LNC.

On the other hand, the μ_e behavior of the CS nanocapsules becomes radically different. These CS-LNC show mobility data very similar to those found with pure chitosan nanogels [38] and they practically coincide with previously results found for similar chitosan nanocapsules [18]. The μ_e confirms that the incorporation of chitosan was clearly effective when this polysaccharide was added to the formulation. It can be seen that mobility goes from positive values at acidic pH to large negative values at more basic pH, presenting an isoelectric point (i.e.p.) at pH 7. The positive charge of nanocapsules is provided by the glucosamine groups of chitosan, which present a weak basic character. At basic pH, chitosan chains are uncharged, so that the negative μ_e comes from the lecithin phosphatidic groups. This μ_e behavior indicates a clear incorporation of this polycationic polymer into the nanocapsule shell yielding to a surface structure practically formed (in its outer part) by a chitosan layer.

Usually, the presence of IgG molecules on the surface of colloidal particles causes a significant alteration of the μ_e values in comparison with the same bare surfaces. Therefore, the electrokinetic behavior of our immuno-nanocapsules can also be useful to determine the presence of such active material (IgG) linked on the LNC surface. Figure 5 shows the mobility of our immuno-nanocapsules as a function of the medium pH. These data support the presence of antibody molecules in the particle surface. Also, a clear correlation is found between the mobility data and the amount of surface protein.

It is known that, when colloidal particles are coated by a protein, the original isoelectric point of bare particles moves towards the isoelectric point of the pure protein. In the case of our immuno-capsules, they inverted the original PhS-LNC μ_e sign at acidic pH 4 (due to the positive electrical charge of IgG molecules at these pH values [28, 37, 40]), shifting the isoelectric points of the complexes at pH 4.6 and 5.1 for the 1 mgIgG/m^{2}and 2.5 mgIgG/m^2 systems, respectively [41, 42]. On the other hand, analyzing the μ_e values at neutral and basic pH, we found another important difference among bare nanocapsules and immuno-nanocapsules, with a clear μ_e decrease (in absolute value) when the antibody coating increased. In these conditions, the surface charge density of the surface protein layer became significantly low, which translated as a reduction of the original negative surface electrostatic potential. It is worth remembering that μ_e values are usually indicative of the colloidal stability of the particles. Therefore, a reduction in μ_e values at neutral and basic pH values would imply decreased colloidal stability. As shown below, these complexes present low colloidal stability at physiological pH.

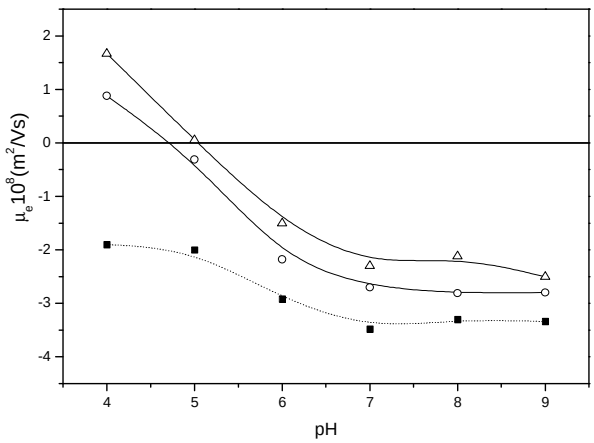

Figure 5. Electrophoretic mobility vs. pH for (■) PhS, (○) PhS-1 mg IgG / m^2, and (△) PhS-2.5 mg IgG /m^{2}IgG.

In the next set of experiments, the colloidal stability was studied at a pH value which matched that of culture media (7.4) used in the *in vitro* experiments in order to analyze the stability/instability of the nanocapsules when incubated with cells. Aggregations were induced by salinity using NaCl and $CaCl_2$ independently. The corresponding CCC and CSC values for all the systems–nanocapsules and immuno-nanocapsules– are shown in Table 2. With regard to the CCC data, calcium exerts a much higher destabilizing effect than sodium does, as expected. This is due to the double valence of calcium, which screens the nanocapsule surface charge much better than sodium does. Consequently, the CCC values are consistently lower for $CaCl_2$ than for NaCl.

Table 2. Critical coagulation concentration (CCC) and critical stabilization concentration (CSC) data (in mM units), at pH 7.4, using NaCl and $CaCl_2$ as aggregating salts.

pH 7,4	**EPI**		**CS**	
	CCC	CSC	CCC	CSC
NaCl	stable	stable	aggreg	161
$CaCl_2$	61	77	aggreg	14

PhS		**PhS-IgG ($1mgm^{-2}$)**		**PhS-IgG ($2.5\ mgm^{-2}$)**		**pH 7,4**
CCC	CSC	CCC	CSC	CCC	CSC	
stable	stable	stable	Stable	38	56	**NaCl**
stable	stable	12	22	9	12	**$CaCl_2$**

Next, we examine the results found for bare nanocapsules. The CCC and CSC data gathered for the EPI nanocapsules are similar to those previously obtained for nanocapsules formulated with the same shell composition [18]. The incorporation of poloxamer into the shell confers a more hydrophilic character ascribed to the PEO fragments. The CSC data corresponding to $CaCl_2$ confirm the

presence of poloxamer molecules on the surface, showing a restabilization process typical of surfaces with hydrophilic character. This stability observed at moderate and high ionic strengths is governed by repulsive hydration forces that are explained in detail in references [43, 44].

With regard to the NaCl, the EPI sample became completely stable in the entire NaCl-concentration range. This is due to the fact that the CCC is higher than the CSC, overlapping both critical concentrations in this highly hydrophilic system. That is, the restabilization mechanism based on hydration forces begins to act at a salt concentration in which the classical DLVO potential barrier still has not been definitively eliminated by the screening effect of the electrolyte concentration [18].

When we analyzed the colloidal stability of PhS nanocapsules, a completely stable system was found, since it was impossible to coagulate at any NaCl or $CaCl_2$ salt concentration. This feature, characteristic of sterically stabilized colloids, clearly indicates a higher incorporation of Pluronic F68 molecules into the PhS system in contrast to the EPI case. Furthermore, this result agrees with previous electrokinetic data, in which a reduction in μ_e values has been related to the incorporation of PEO chains on the surface shell, which (consequently) shifted the shear plane where the zeta potential is defined outward.

Performing the experimental study of the stability of the CS system was a difficult task, because these LNC coagulated –even before adding any salt concentration– as soon as the nanocapsules were immersed in the buffer at pH 7.4. This high instability at neutral pH is consistent with the isoelectric point shown in the μ_e experiments (see Fig. 4), and it indicates that repulsive electric forces are the main factor responsible for the stability of the CS system at low ionic strength. Nevertheless, our deacetylated chitosan is a hydrophilic material, and therefore repulsive hydration forces should be expected to act under high-salinity conditions.

This is why we immersed the CS particles in a pH 7.4 buffer, but previously adding a moderate or high NaCl concentration. It bears highlighting that this saline-system was totally stable. This is why the CSC data shown in Table 2 for the CS-LNC were gathered from a high-salinity solution and making successive dilutions that reduced the ionic strength and, consequently, triggered coagulation at a given low-salinity value.

In summary, the stability patterns of our systems comes from a combination of the destabilizing power exerted by salinity (which screens the electrical repulsion existing in low-ionic-strength media), and the stabilizing effect given by hydration forces in hydrophilic surfaces when salinity increases. When the electrolyte concentration is not too high (and hydration forces can be neglected), the CCC values correlate with the μ_e data in the less hydrophilic systems (EPI and CS), the stability being governed mainly by the surface electrical charge (which in turn depends on the nature of the shell molecules). For high-salinity conditions or for highly hydrophilic surfaces (i.e. PhS-LNC) both repulsive steric and hydration forces keep stable the systems.

With regard to the colloidal stability of our immuno-complexes, Figure 6 shows a typical experiment in which the stability factor (W) is evaluated at different $CaCl_2$ concentrations. The W-stability factor is an experimental parameter that provides information on the coagulation probability: it is related to the number of collisions that two colliding particles must undergo before they remain definitively stuck. Therefore, $W = 1$ signifies a completely unstable system, while $W = \infty$ means total stability. The corresponding CCC values (calculated when W reduces to 1) are given in Table 2. These CCC data correlate properly with the mobility data at neutral pH (see Fig. 4).

The stability decreased when the IgG coating was increased. Although both systems presented quite low stability (CCC with $CaCl_2$ ~10 mM), it was even lower when the IgG load was higher. It should be noted that the total stability found with the 1 mgIgG/m² system in NaCl solutions disappeared when the IgG coating increased up to 2.5 mgIgG/m². There is no doubt that the stability behavior of the PhS system significantly changed when the IgG molecules were linked to the bare PhS nanoparticles: A completely stable system in both salt solutions reduces its colloidal stability when protein molecules are bounded on its surface. This phenomenon has been also found when working with other nanoparticles-protein complexes totally or partially covered by polyclonal IgG molecules [28, 33, 45]. Beduneau et al., working with lipid nanocapsules conjugated with antibody molecules, detected an aggregation of the immuno-nanoparticles with a high density of antibodies [10], while Koning et al. detected the same stability when a high density of antibodies was grafted onto liposomes [34].

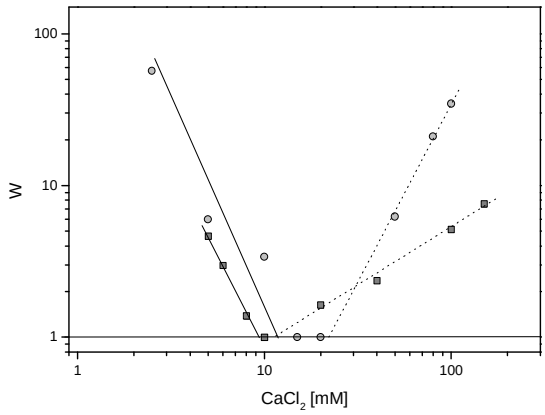

Figure 6. Stability factor vs. calcium chloride concentration (mM) at pH 7.4: (■)1mg/m²IgG-PhS; (●) 2.5 mg/m²IgG-PhS. Solid lines help to locate the CCC values, while dashed lines point to the CSC data.

Once the stability was evaluated in simple pH 7.4 media, it was analyzed in the cell-culture medium (DMEM) supplemented with FBS, used to develop the *in*

vitro uptake experiments in order to ensure that our different nanosystems preserve their colloidal stability in this complex medium. Figure 7 shows the time evolution of optical absorbance when nanocapsules were introduced in the cell-culture medium. The absorbance remained constant, indicating that no aggregation took place. Taking into account the CSC values shown in Table 2, the high stability of all our LNC systems in this culture medium must be governed by the intrinsic hydrophilic character of their respective surfaces, since DMEM is a medium enriched with different cations that strengthen hydration forces enough to keep all of our nanoparticles stable.

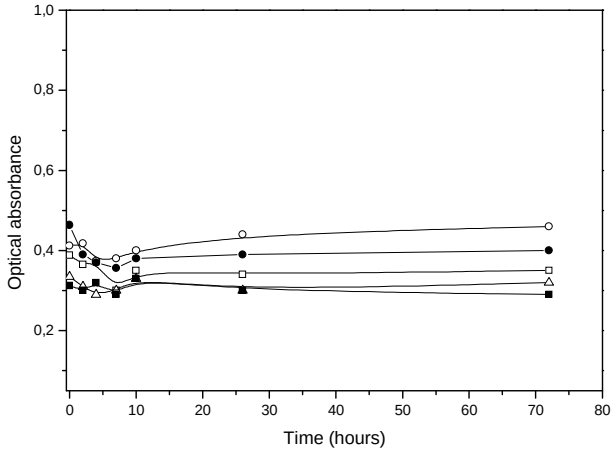

Figure 7. Aggregation kinetics of the (□) EPI, (○) CS, (△) PhS, (■) PhS-1mg/m²IgG, and (●) PhS-2.5mg/m² IgG nanocapsules when immersed in DMEM medium supplemented with FBS.

The final experiments were focused on analyzing the uptake of our different nanocapsules by a cancer-cell line (MCF-7). To quantify this cell uptake, we worked with nanocapsules loaded by Nile Red. The presence of Nile Red in the oily core of our nanoparticles was previously checked by means of fluorescent measurements. It should be noted that Nile Red presents a very different emission fluorescent spectrum as a function of the medium in which it is dissolved [46]. Figure 8 shows the emission fluorescent spectrum of the different nanoparticle

systems. For all of them, the spectrum was similar to those found for Nile Red dissolved in olive oil. Comparing these results with the Nile Red emission spectrum dissolved in an aqueous solution, we found that the presence of this fluorescent molecule in the hydrophobic oil core of our LCN was, therefore, clearly confirmed. On the other hand, as expected, the encapsulation of Nile Red hardly changed the size or charge of LNC.

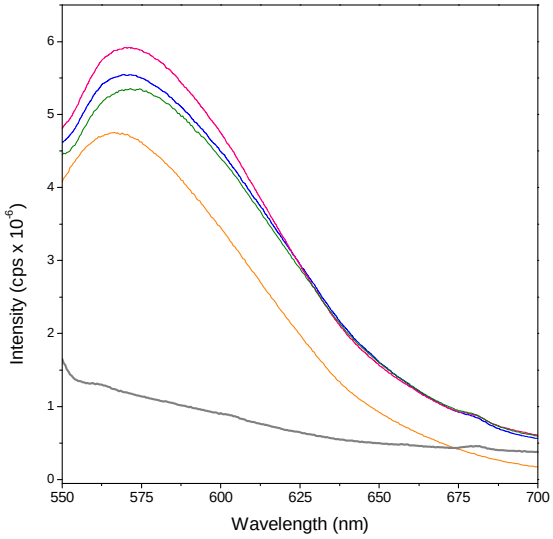

Figure 8. Emission spectrum of Red Nile in olive oil and water, and inside different nanoparticles: EPI (pink line); CS (blue line); PhS (green line); olive oil (orange line) and water (grey line).

The cell uptake of these fluorescent nanocapsules was analyzed by flow cytometric assays. Figure 9 shows the fluorescence intensity of the cell cultures containing different nanosystems after 30 min and 2 h of incubation time. The results led us to perform a quantitative analysis of the different nanocapsules, showing that the internalization efficacy was significantly changed by the nature and properties of the different shells. A combination of surface charge and hydrophilicity plays the major role in affinity in the endocytosis pathway [47]. Results with CS nanocapsules showed the highest fluorescent intensity, in

agreement with the enhanced mucoadhesion properties reported for chitosan nanosystems [9, 48]. The lower fluorescent response observed with the EPI and PhS systems appeared to be related both to the negative surface charge of these nanocapsules as well as to the hydrophilic character provided by poloxamer molecules –which produce more biocompatible systems but at the same time reducing their cellular uptake [10, 49]. The higher hydrophilicity of the PhS surface (which presents an enriched Pluronic F68 layer according to the mobility and stability data) could be responsible for the low fluorescent intensity shown by these nanocapsules in comparison with the EPI ones.

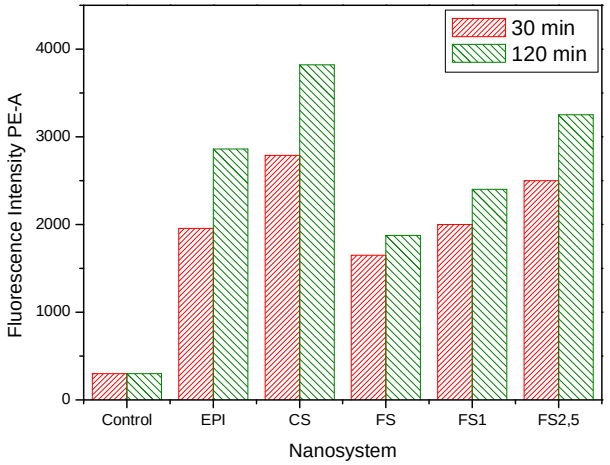

Figure 9. Relative fluorescent intensity of the MCF7 cell line when incubated with Nile-Red-loaded nanocapsules for 30 min and 2 h. Control refers to that incubation performed only with cells.

Finally, Figure 9 also shows an increment of the fluorescence intensity when the IgG coverage increased. Since our aCRP-IgG molecules did not recognize any specific ligand of the cell membrane, a change in the cell uptake of immuno-nanocapsules with regard to the bare nanocapsules must have been caused by both the surface charge and hydrophilic characteristics, which in turn were modulated by

the protein coating. Actually, the results agree with the surface characteristics discussed above for our immuno-nanocapsules, considering their electrophoretic and stability behavior. That is, the electric charge and hydrophilic character decreased when the amount of bounded IgG was increased, yielding to a situation in which the LNC endocytosis was enhanced.

Conclusions

The present work constitutes basic research aimed mainly at analyzing certain surface characteristics (i.e. charge and hydrophilicity) of different lipid nanocapsules. Colloidal properties of a novel LNC system, in which the shell was enriched by carboxyl groups supplied by phosphatidyl-serine molecules, was compared to two standard LNC systems: an anionic one formed by Epikuron and Pluronic F68, and a cationic system coated by chitosan.

Electrokinetic mobility and classical studies of colloidal stability lead us to conclude that the incorporation of Pluronic F68 on the PhS shell was higher than in the EPI case. Additionally, the original PhS surface was successfully modified by linking (covalently) IgG molecules. The presence of these antibodies conferred specific recognition properties to these nanocapsules, showing clear binding of a specific antigen (CRP). In addition, the adhered antibody layer altered the original surface properties of the bare PhS particles, since both surface charge density and hydrophilicity were reduced by the IgG coating.

With regard to the cell-culture incubation studies, all our systems were colloidally stable in the incubation medium thanks to the stabilizing role played by the hydration forces. The cellular uptake was modulated by the surface characteristics of the LNC, and the highest uptake was found with the CS cationic particles, while the lowest intracellular incorporation was found with the most

hydrophilic negative surface (PhS). In the latter case a great amount of poloxamer molecules existed in the outer shell, hampering such uptake. In summary, we have developed a novel LNC system capable of linking antibodies by using a simple procedure yielding to active immuno-nanocapsules that may be useful for future potential applications in anti-cancer therapies.

Acknowledgements

The authors wish to express their appreciation for the financial support granted by the Ministerio de Educación y Ciencia (MEC, Spain), projects MAT2010-20370 (European FEDER support included),the Consejería de Innovación, Ciencia y Tecnología de la Junta de Andalucía (Spain), projects of excellence P07-FQM-2496 and P07-FQM03099, and PI10/02295 (Instituto de Salud Carlos III, Fondo de Investigación Sanitaria, Spain). Also we wish to express our gratitude to Dr. Josep Puig from Biokit S.A. for the kindly donation of antibody samples.

References

1. Duncan, R. Nanomedicines in action. *Pharm. J.*2004, *273,* 485–488.

2. Royal Society & Royal Academy of Engineering. Nanoscience and Nanotechnologies: Opportunities and Uncertainties; Royal Society, London, United Kingdom, 2004.

3. European Science Foundation. Nanomedicine. An ESF–European Medical Research Councils (EMRC) Forward Look Report. European Science Foundation, Strasbourg, France, 2005.

4. Kateb B.; Chiu K.; BlackK .L.; Yamamoto V.; Khalsa B.; Ljubimova J.Y.; Ding H.; Patil R.;Portilla-Arias J.A.; Modo M; Moore D.F.; Farahani K.; Okun M.S.; Prakash N.; Neman J.; Ahdoot D.; Grundfest W.; Nikzadand S.; Heiss J.D., Nanoplatforms for constructing new approaches to cancer treatment, imaging, and drug delivery: What should be the policy?, *NeuroImage* 2011, *54(1)*, 106-124.

5. Malan Y.; Loizidou M.; Seifalian A.M., Liposomes and nanoparticles: nanosized vehicles for drug delivery in cancer. *Trends in Pharmacological Science,* 2009, *30(11)*, 592-599.

6. Peer D.; Karp J.M.; Hong S.; Farokhzad O.C.; Margalit R.; Langer R. Nanocarriers as an emerging platform for cancer therapy. *Nature nanotechnology*, 2007, *2*, 751-760.

7. Huynh N.T.; Passirani, C.; Saulnier P.; Benoit J.P. Lipid nanocapsules: A new platform for nanomedicine. *International Journal of Pharmaceutics,* 2009, *379*, 201-209.

8. Prego C.; Torres D.; Fernandez-Megia E.; Novoa-Carballal R.; Quiñoá E.; Alonso M.J. Chitosan–PEG nanocapsules as new carriers for oral peptide delivery: Effect of chitosan pegylation degree. *J. Control. Rel.*,2006, 111, 299- 308.

9. Lozano M.V.; Torrecilla D.; Torres D.; Vidal A.; Dominguez F.; Alonso M.J., Highly efficient system to deliver taxanes into tumor cells: docetaxel-loaded chitosan oligomer colloidal carriers. *Biomacromolecules,* 2008, *9*, 2186-2193.

10. Beduneau A.; Saulnier P.; Benoit J.P., Active targeting of brain tumors using nanocarriers. *Biomaterials,* 2007, *28*, 4947-4967.

11. Khalid M.N.; Simard P.; Hoarau D.; Dragomir A.; Leroux J.C. Long Circulating Poly (Ethylene Glycol)-Decorated Lipid Nanocapsules Deliver Docetaxel to Solid Tumors. *Pharmaceutical Research*, 2006, *23*, 752-758.

12. Gaucher G.; Marchessault R.H.; Leroux J.C. Polyester-based micelles and nanoparticles for the parenteral delivery of taxanes, *J. Control. Release*, 2010, *143*, 2-12 (2010).

13. Abdel-Mottaleb M.M.A.; Neumann D.; Lamprecht A. Lipid nanocapsules for dermal application: A comparative study of lipid-based versus polymer-based nanocarriers, *Int. J. Pharm.,*2011, *79,* 36-42.

14. Haley B.; Frenkel E., Nanoparticles for drug delivery in cancer treatment. *Urol. Oncol.,* 2008, *26*, 57-64.

15. Mailänder V.; Landfester K., Interaction of nanoparticles with cells, *Biomacromolecules,* 2009, *10*, 2379-2400.

16. Mohanraj V.J.; Chen Y.Nanoparticles – A Review, *Trop J Pharm Res*, 2006, *5 (1),* 561-573.

17. Lee S.H.; Choi S.H.; Kim S.H.; Park T.G., Thermally sensitive cationic polymer nanocapsules for specific cytosolic delivery and efficient gene silencing of siRNA: Swelling induced physical disruption of endosome by cold shock*, J. Control. Rel.*,2008,*125*, 25-32.

18. Santander-Ortega M.J.; Lozano-Lopez M.V.; Bastos-Gonzalez D.; Peula-Garcia J.M; Ortega-Vinuesa J.L., Novel core–shell lipid-chitosan and lipid-poloxamer

nanocapsules: stability by hydration forces, *Colloid and Polymer Science,* 2010, *288*, 159–172.

19. Santander-Ortega M.J.; Peula-García J.M.; Goycoolea F.M.; Ortega-Vinuesa J.L. Chitosan nanocapsules: Effect of chitosan molecular weight and acetylation degree on electrokinetic behaviour and colloidal stability, *Colloid and Surfaces B: Biointerfaces,* 2011, *82*, 571-580.

20. Mosqueira V.C.F.; Philippe L.; Barratt G.. Surface-modified and conventional nanocapsules as novel formulations for parenteral delivery of halofantrine. *J. Nanosci. Nanotechnol.*, 2006, *6*, 3193-3202.

21. Kwon G.S.; Okano T. Polymeric micelles as new drug carriers. *Adv. Drug Deliv. Rev.*, 1996, *21*, 107-116.

22. Goutayer M.; Dufort S.; Josserand V.; Royère A.; Heinrich E.; Vinet F.; Bibette J.; Coll J.; Texier I., Tumor targeting of functionalized lipid nanoparticles: Assessment by *in vivo* fluorescence imaging, *Eur. J. Pharm. Biopharm.*,2010,*75*, 137-147.

23. Ambrousi, A.; Gelperina S.; Khalansky A.; Tanski S.; Theisen A.; Kreuter J., Influence of surfactants, polymer and doxorubicin loading on the anti-tumour effect of poly(but*yl cyan*oacrylate) nanoparticle*s* in a rat glioma model, *J. Microencapsulation,* 2006, *23*, 582-592.

24. Torchilin V.P., Multifunctional nanocarriers, *Avd. Drug Deliv. Rev.*, 2006, *58*, 1532-1555.

25. Beduneau A.; Saulnier P.; Hindré F.; Clavreul A.; Leroux J.C.; Benoit J.P. Active targeting of brain tumors using nanocarriers, *Biomaterials,* 2007, *28*, 4978-4967.

26. Rata-Aguilar A.; Sánchez-Moreno, P.; Jódar-Reyes A.B.; Martín-Rodríguez A.; Boulaiz H.; Marchal-Corrales J.A.; Peula-García J.M.; Ortega-Vinuesa J.L., Colloidal stability and "*in vitro"* antitumor targeting ability of lipid nanocapsules coated by folate-chitosan conjugates, *J. Bioactive and Compatible Polymers,* send to publish.

27. Ortega-Vinuesa J.L.; Hidalgo-Alvarez R.; de las Nieves F.J.; Davey C.; Newman D.J.; Price C.P., Characterization of immunoglobulin G bound to latex particles using surface Plasmon resonance and electrophoretic mobility. *J. Colloid Interface Sci.* 1998*, 204*, 300-311.

28. Ortega-Vinuesa J.L.; Bastos-González D., A review of factors affecting the performances of latex agglutination tests, *J. Biomater. Sci., Polym. Ed.*, 2001, *12*, 379-408.

29. Gupta A.K.; Curtis A.S.G., Lactoferrin and ceruloplasmin derivatized superparamagnetic iron oxide nanoparticles for targeting cell surface receptors*, Biomaterials,* 2004,*25*, 3029-3040.

30. Zhang K.; Rossin R.; Hagooly A.; Chen Z.; Welch M.J.; Wooley K.L., Folate-mediated cell uptake of shell-cross linked spheres and cylinders, *J. Polym. Sci. Part A Polymer Chem.,* 2008, *46*, 7578-7583.

31. Desai M.P.; Labhasetwar V.; Walter E.; Levy R.J.; Amidon G.L., The mechanism of uptake of biodegradable microparticles in Caco-2 cells is size dependent, *Pharm. Res.,* 1997, *14*, 1568-1573.

32. Panyam J.; Labhasetwar V., Biodegradable nanoparticles for drug and gene delivery to cells and tissue. *Adv. Drug Deliv. Rev.,* 2003, *55,* 329-347.

33. Martin A.; Puig J.; Galisteo F.; Serra J.; Hidalgo-Alvarez R., On some aspects of the adsorption of immunoglobulin-G molecules on polystyrene microspheres, *J. Dispersion Sci. Technol.*, 1992, *13*, 399–416.

34. Koning G.A.; Morselt H.W.M.; Scherphof G.L.; Kamps J.A.A.M.; Gorter A.; Allen T.M., Interaction of differently designed immunoliposomes with colon cancer and Kupffer cells. an in vitro comparison, *Pharmaceut. Res.,* 2003, *20(8)*, 1249-1257.

35. Torcello-Gómez A.; Santander-Ortega M.J.; Peula-García J.M; Maldonado-Valderrama J.; Gálvez-Ruiz M.J.; Ortega-Vinuesa J.L.; Martín-Rodríguez A., Adsorption of antibody onto Pluronic F68-covered nanoparticles: link with surface properties, *SoftMatter*, 2011, *7*, 8450-8461.

36. Couvreur P.; Barratt G.; Fattal E.; Legrand P.; Vauthier C., Nanocapsule technology: a review. *Crit. Rev. Ther. Drug Carrier Syst.,* 2002; *19*, 99-134.

37. Peula J.M.; Santos R.; Forcada J.; Hidalgo-Álvarez R.; de las Nieves F.J., Study on the colloidal stability mechanisms of acetal-functionalized latexes, *Langmuir,* 1998, *14*, 6377-6384.

38. Santander-Ortega M.J.; Jódar-Reyes A.B.; Csaba N.; Bastos-González D.; Ortega-Vinuesa J.L., Colloidal Stability of Pluronic F68-coated PLGA nanoparticles: A variety of stabilization mechanism, *J. Colloid Interface Sci.,* 2006, *302*, 522-529.

39. López-León T.; Carvalho E.L.S.; Seijo B.; Ortega-Vinuesa J.L.; Bastos-González D., Physicochemical characterization of chitosan nanoparticles: electrokinetic and stability behavior, *J. Colloid Interface Sci.,* 2005*, 283,* 344-*3*51.

40. Peula J.M.; Hidalgo-Alvarez R.; de las Nieves F.J., Covalent binding of proteins to acetal-functionalized latexes. I. Physics and chemical adsorption and electrokinetic characterization, *J. Colloid Interface Sci.,* 1998, *201*, 132-138.

41. Peula J.M.; Hidalgo-Alvarez R.; de las Nieves F.J., Coadsorption of IgG and BSA onto sulfonated polystyrene latex: Sequential and competitive coadsorption isotherms, *J. Biomat. Sci. PolymerEdn.*, 1995, *7*, 231-240.

42. Ortega-Vinuesa J.L.; Galvez-Ruiz M.J.; Hidalgo-Alvarez R., F(ab')$_2$-Coated polymer carriers: Electrokinetic behavior and colloid stability, *Langmuir*, 1996,*12*, 3211–3220.

43. Molina-Bolívar J.A.; Galisteo-González F.; Hidalgo-Álvarez R., The role played by hydration forces in the stability of protein-coated particles: non-classical DLVO behaviour. *Colloids Surf.B Biointerfaces,* 1999, *14*, 3-17.

44. Molina-Bolívar J.A.; Ortega-Vinuesa J.L., How proteins stabilize colloidal particles by means of hydration forces. *Langmuir,* 1999, *15*, 2644-2653.

45. Peula J.M.; Hidalgo-Alvarez R.; de las Nieves F.J.. Covalent binding of proteins to acetal-functionalized latexes. II. Colloidal Stability and Immunoreactivity, *J. Colloid Interface Sci.,* 1998, *201,* 139-145.

46. Greenspan P.; Fowle S.D., Spectrofluorometric studies of the lipid probe nile red, *Journal of Lipid Research*, 1985, 26, 781-789

47. Florence A.T., Hussain N., Transcytosis of nanoparticle and dendrimer delivery systems: evolving vistas. *Adv. Drug Deliv. Rev.,* 2001,*50(1),*69-89.

48. Hafner A.; Lovric J.; Voinovich D.; Filipovic-Grcic J., Melatonin-loaded lecithin/chitosan nanoparticles: Physicochemical characterization and permeability through Caco-2 cell monolayers, *Int. Journal of Pharmaceutics*, 2009, *381*, 205-213.

49. Vonarbourg A.; Passirani C.; Saulnier P.; Benoit J.P., Parameters influencing the stealthiness of colloidal drug delivery systems, *Biomaterials*, 2006, *27*, 4356-4373.

50. Prego C.; Fabre M.; Torres D.; Alonso M.J., Efficacy and mechanims of action of chitosan nanocapsules for oral peptide delivery, *Pharm. Res*., 2006, *23,*549-556.

51. Wulff-Pérez M.; Torcello-Gómez A.; Gálvez-Ruíz M.J.; Martín-Rodríguez A., Stability of emulsions for parenteral feeding: Preparation and characterization of o/w nanoemulsions with natural oils and pluronic F68 as surfactant, *Food Hydrocolloids*, 2009, *23*, 1096-1102.

52. Peula-García J.M.; Ortega-Vinuesa J.L.; Bastos-González D., Inversion of Hofmeister series by chanching the surface of colloidal particles from hydrophobic to hydrophilic, *J. Phys. Chem.,* 2010, *114*, 11133-11139.

Paper II: Novel Drug Delivery System Based on Docetaxel-Loaded Nanocapsules as a Therapeutic Strategy against Breast Cancer Cells

Paola Sánchez Moreno [1§], Houria Boulaiz [2§], Juan Luis Ortega Vinuesa [1], José Manuel Peula García [3] and Antonia Aránega[2]

[1] *Biocolloid and Fluid Physics Group, Department of Applied Physics, University of Granada, 18071 Granada, Spain*

[2] *Human Anatomy and Embryology Department, Regenerative Biomedicine Institute (IBIMER), Campus de la Salud, University of Granada, 18071 Granada, Spain*

[3] *Department of Applied Physics II, University of Málaga, 29071 Málaga, Spain*

[§] *Both authors contributed equally to this work*

Published in:

International Journal of Molecular Sciences

Int. J. Mol. Sci. **2012**, *13*(4), 4906-4919

Abstract

In the field of cancer therapy, lipid nanocapsules based on a core-shell structure are promising vehicles for the delivery of hydrophobic drugs such as docetaxel. The main aim of this work was to evaluate whether the docetaxel-loaded lipid nanocapsules improved the anti-tumor effect of free docetaxel in breast cancer cells. Three docetaxel-loaded lipid nanocapsules were synthesized by a solvent displacement method. Cytotoxic assays were evaluated in breast carcinoma (MCF-7) cells treated with the sulforhodamine B colorimetric method. Cell cycle was studied by flow cytometry and Annexin V-FITC, and apoptosis was evaluated by using propidium iodide assays. The anti-proliferative effect of docetaxel appeared much earlier when the drug was encapsulated in lipid nanoparticles than when it was free. Docetaxel-loaded lipid nanocapsules significantly enhanced the decrease in IC_{50} rate, and the treated cells evidenced apoptosis and a premature progression of the cell cycle from G(1) to G(2)-M phase. The chemotherapeutic effect of free docetaxel on breast cancer cells is improved by its encapsulation in lipid nanocapsules. This approach has the potential to overcome some major limitations of conventional chemotherapy and may be a promising strategy for future applications in breast cancer therapy.

1. Introduction

Breast cancer is the most common malignant tumor and the first cause of morbidity and mortality among women worldwide [1, 2]. The past century witnessed the maturation of chemotherapy as a viable, adjuvant therapeutic modality for the treatment of cancer. Furthermore, in the case of breast disease, there have been advances in its early detection as well as in surgery, radiotherapy, hormone therapy. The majority of women (>75%) with breast cancer are diagnosed at an early stage or are operable [3], and these patients require adjuvant chemotherapy to reduce the risk of recurrence [4-5].

Taxanes (paclitaxel or docetaxel) are active cytotoxic agents that promote the polymerization of tubulin and the stabilization of microtubules by preventing their disassembly. Adjuvant chemotherapy with taxanes reduces the risk of cancer recurrence and death in patients with early or operable breast cancer and has shown benefits in patients with high-risk, node-negative breast cancer. However, although these novel chemotherapeutics have led to improvements in survival, they are associated with numerous drug-related toxicities [6]. Thus, docetaxel has been associated with a significant increase in neutropenia, febrile neutropenia, leucopenia, stomatitis, edema, fatigue and/or asthenia, and diarrhea [6]. These effects are due in part to the high doses used to achieve the desired anti-tumor effect, which are necessary because of the non-specific distribution of both novel and traditional chemotherapies, with only a small fraction of drugs reaching the tumor.

It is well known that injected materials suffer from sequestration by the reticuloendothelial system, a system comprised of monocytes and macrophages that clear foreign materials [7]. The drugs can accumulate in healthy organs, and there is

a fine line between tolerability and severe morbidity, e.g., in the case of doxorubicin, a DNA intercalator that produces cardiotoxicity [8]. Moreover, the commercial formulation of docetaxel, Taxotere®, is formulated with a high concentration of Tween 80 (40 g/L), which has been found to have severe side effects, including hypersensitivity reactions, cumulative fluid retention, and nausea and has shown incompatibility with commonly used polyvinyl chloride intravenous administration sets [9]. Taken together, these factors compromise the curative potential of anticancer drugs, and more effective methods for their delivery to tumors are required [10].

Therefore, novel therapeutic approaches and alternative formulations of docetaxel with no (or low concentration) of Tween 80 are urgently needed to improve the efficacy of treatment in breast cancer patients with a poor prognosis. In this context, liposomes and polymer-drug conjugates were developed in the 1960s and 1970s [11] in attempts to apply Paul Ehrlich's "magic bullet" concept to chemotherapy [12]. These are now mainstay platforms in nanomedicine, a multidisciplinary field that aims to utilize nanoscale (1–100 nm) constructs to improve the delivery of chemotherapeutics [13].

Primarily, these carriers assist in drug solubilization and protect the drug from degradation. Their nanoscale size range and the frequently ubiquitous presence of poly (ethylene glycol) (PEG) or Pluronic ® F68 on their surface aids evasion of the reticuloendothelial system, allowing drugs to accumulate in tumors through enhanced permeability and retention, the result of tumor blood vessel leakiness [14-15]. Lower sequestration rates in healthy organs coupled with higher accumulation and retention rates in tumors would improve the effectiveness of treatments and minimize adverse effects. Lipid nanocapsules based on a core-shell structure are promising vehicles for the delivery of hydrophobic drugs such as docetaxel.

The main aim of this work was to evaluate whether docetaxel-loaded lipid nanocapsules improve the anti-tumor effect of free docetaxel in MCF-7 breast cancer cells. Indeed, we found a greater reduction in IC_{50} rate when the docetaxel was encapsulated in lipid nanoparticles, with evidence of apoptosis and a premature cell cycle progression from G(1) to G(2)-M phase.

2. Experimental section

Cell Lines and Culture Conditions

The human breast cancer MCF-7 cell line was grown at 37ºC in an atmosphere containing 5% CO_2 with Dulbecco's modified Eagle Medium (DMEM) (Gibco, Grand Island, NY, USA) supplemented with 10% (v/v) heat-inactivated fetal bovine serum (FBS) (Gibco) 2% L-glutamine, 2.7% sodium bicarbonate, 1% Hepes buffer, and 1% penicillin/streptomycin solution (GPS, Sigma).

Lipid Nanocapsule Preparation

Lipid nanosystems were prepared and characterized as described in [16]. Three systems were formulated: EPI nanocapsules, with surface shell composed of Epikuron and Pluronic® F68; CS nanocapsules, with shell of Epikuron and chitosan oligomers; and PhS nanocapsules, with shell of phosphatidyl-L-serine and Pluronic® F68. For nanosystem characterization, the average size was determined by combining a high-performance-particle-sizer technology with a non-invasive-backscattering method, in which the measurement is taken at an angle of 173°. A Zetasizer-Nano analyzer (Malvern Instruments, UK) was used to measure the electrophoretic mobility (μ_e). Zeta potential was calculated from this experimental magnitude in physiological medium conditions.

Fluorescent lipid nanocapsules were formulated by dissolving Nile Red in the olive oil phase at a concentration of 0.025% (w/w). Encapsulation of this fluorescent molecule was confirmed by using a SPEX Fluoromax-2 spectrofluorometer. Emission fluorescence spectra were determined from 550 to 700 nm at excitation wavelength of 485 nm, with a scanning speed of 100 nm/min and wavelength accuracy of ±1 nm.

Docetaxel-loaded lipid nanocapsules were formulated by dissolving docetaxel in the olive oil phase at a concentration of 0.1% (m/w). The encapsulation efficiency was calculated by HPLC at the Scientific Instrumentation Center of the University of Granada, using a SHIMADZU LC-20AC chromatograph with SPD-M20A diode array detector and C8 Nova-Pak Cartridge column (4 microns, 4.6 × 150 mm); detection was performed at a wavelength of 230 nm.

Uptake Studies

MCF-7 cells (5×10^4) were seeded into 24-well plates under the culture conditions detailed above. After 24 h, cells were fed with fresh medium and treated with Nile Red nanocapsules. Cells were incubated with Nile Red labeled particles for 1 h and 5 h and then washed twice with acidic phosphate saline buffer (PBS) to remove free nanocapsules. Fresh PBS was added and living cells were analyzed by fluorescent microscopy (Nikon Eclipse Ti-S). Cells treated with empty nanoparticles were used as controls.

Cytotoxicity Assays in vitro

MCF-7 cells (1×10^3) were plated into 24-well plates under the culture conditions detailed above. The cells were fed with fresh medium and increased concentrations of free and encapsulated drug every alternate day up to the end of the experiment. After 6 days of treatment, cells were counted using sulforodamine-B (SRB) colorimetric assay as previously described [44] using a Titertek Multiscan apparatus (Flow, Irvine, California) at 492 nm. We evaluated the linearity of the SRB assay with cell number using stock MCF-7 cells before each cell growth experiment. IC_{50} values were calculated from semi-logarithmic dose-response curves by linear interpolation. All experiments were plated in triplicate wells and were carried out at least twice.

Apoptosis Detection by Staining with Annexin V-FITC and Propidium Iodide

The Annexin V-FITC Apoptosis Detection kit I (Pharmingen, San Diego, CA, USA) was used to detect apoptosis by flow cytometry. MCF-7 cells (5×10^4 cells) were plated onto 24 well plates and cultured overnight, followed by incubation with IC_{50} values of free or encapsulated docetaxel for 24 h. Cells were harvested by PBS-EDTA, washed twice in cold PBS (1.4 M NaCl, 27 mM KCl, 100 mM KH_2PO_4/K_2HPO_4, pH 7.2), and pelleted by centrifugation at 500 g for 10 min. They were then resuspended at 10^6 cells/100 μL in a binding buffer (Hepes buffer, 10 mM, pH 7.4, 150 mM NaCl, 5 mM KCl, 1 mM $MgCl_2$, 1.8 mM $CaCl_2$), stained with annexin V incubation reagent (1 μL annexin V-FITC (25 μg/mL), 10 μL binding buffer, 10 μL PI (50 μg/mL), and 79 μL H_2O) and incubated in the dark for 15 min at room temperature. Then, 500 μL binding buffer was added and the cells (10,000 cells per sample) were immediately analyzed using a FACScan flow cytometer (Becton Dickinson, San Jose, CA, USA). All experiments were performed in triplicate and yielded similar results.

Cell Cycle Distribution Analysis

Cells at 70% of confluence were treated with the half maximal inhibitory concentration (IC_{50}) of free or encapsulated docetaxel. Cells in monolayer culture were harvested, washed twice with sample buffer (100 mg glucose; 100 mL PBS without Ca^{2+} or Mg^{2+}), and fixed in 70% (vol/vol) cold ethanol for up to 1 week. Cells were pelleted, washed once with sample buffer, and resuspended in PI solution (50 μg/mL PI, 0.5 mg/mL RNase in sample buffer, pH 7.4) for 30 min in the dark. Fluorescence activated cell sorting (FACS) analysis was performed after 24 h of treatment. All experiments were performed in triplicate and yielded similar results.

3. Results and Discussion

In cancer therapy, most proposed formulations present certain drawbacks related to low drug loading, toxicity, and/or an unsuitable release pattern [17]. Furthermore, as previously noted, docetaxel is formulated using Tween 80 (polysorbate 80) and ethanol (50:50, v/v), and acute hypersensitivity reactions have been noted in the majority of patients treated in phase I clinical trials, [18–20]. Fluid retention and hypersensitivity, among other reactions, are also associated with some other drugs with Tween 80 in their formulation [17]; therefore, this excipient may be partially responsible for some of the toxic effects observed with docetaxel [21, 22]. An ideal formulation should provide biocompatible nanosized particles and high drug loading with sustained-release characteristics, allowing drug release in the target site at a therapeutic concentration, thereby minimizing drug inefficiency and adverse effects. Various approaches have been investigated in this line [21, 23, 24].

In the present study, we reformulated docetaxel in a better-tolerated and less-toxic vehicle to avoid premedication with corticosteroids and antihistamines, which is usually prescribed to reduce adverse reactions associated with docetaxel in Tween 80. Three previously obtained and characterized nanocapsule systems (16) were used to encapsulate docetaxel. All of them have a hydrophobic core constituted by olive oil, but they differ in their shell components.

The shell of the simplest system (EPI), with an average diameter of 170 ± 20 nm, comprised a mixture of phospholipid molecules (Epikuron) and a poloxamer (Pluronic® F68), which both act as colloidal stabilizers. Pluronic® F68 possesses the capacity to avoid opsonin adsorption, thereby preventing the triggering of a cascade of immune system reactions that would eliminate the nanocapsules from the bloodstream [15]. Furthermore, because this poloxamer is not toxic, it can be used in nanoemulsions for the release of drugs and genes [25].

A second system (CS), with an average diameter of 330 ± 30 nm, was formulated by replacing the poloxamer with chitosan oligomers. Chitosan is a polysaccharide obtained from the deacetylation of chitin, which is a structural element of the exoskeleton of crustaceans. It is hydrophilic, biocompatible, and biodegradable and has low toxicity, and its effectiveness as an adsorption-enhancing agent has been demonstrated by various authors [26].

Finally, a third formulation (PhS), with an average diameter of 210 ± 20 nm, was designed to create a nanosystem in which Epikuron was replaced with phosphatidyl-serine, producing a carboxyl-functionalized nanosystem that offers the possibility of the efficient attachment of antibody molecules for future vectorization purposes [16].

The surface electrical state of the different nanocapsules was analyzed by measuring their electrophoretic mobility as a function of the pH in low ionic strength media. Electrophoretic mobility is an experimental parameter directly related with the zeta potential and the surface potential, which is dependent of the surface composition and the salinity and pH of the medium. The zeta potential values at neutral pH agree with the nature of the shell of the nanocapsules showing a positive surface charge (16.3 mV) for CS nanosystem, and a negative surface charge for EPI and PhS nanosystems (−56.4 mV and −44.4 mV respectively).

Uptake Analysis

Fluorescence microscopy studies were conducted to test the intensity of uptake by MCF-7 cells of the encapsulated Nile red. The uptake was significantly faster for Nile Red-CS nanocapsules than for the other two types. After only 1 hr, CS particles showed the highest uptake, followed by EPI and then PhS particles (Figure 1). Uptake increased with longer incubation time, preserving these differences among particles until 5 hours, when the cells showed the same amount of fluorescence, and no differences among the three types of nanoparticles could be detected. At 3 hours of incubation, the Nile red was localized in the cytoplasm of cells (Figure 1), indicating that these nanosystems are effective vehicles to transport the molecules within MCF-7 cells by endocytosis and can avoid efflux by cell membrane MDR transport proteins such as p-glycoprotein (P-gp) [25,27,28].

The variation in internalization among the different nanoparticles may be attributable to a combination of surface charge and hydrophilicity, which play a major role in affinity in the endocytosis pathway [29]. The CS nanocapsules showed the highest fluorescence intensity, related to their positive superficial charge, which increases the affinity between nanoparticle and negatively-charged cell membrane [30]. This finding is consistent with the enhanced mucoadhesive properties reported

for chitosan nanosystems [31,32]. The lower fluorescence response observed with the EPI and PhS systems appears attributable to the size and negative surface charge of these nanocapsules as well as to the hydrophilic nature of the poloxamer molecules,

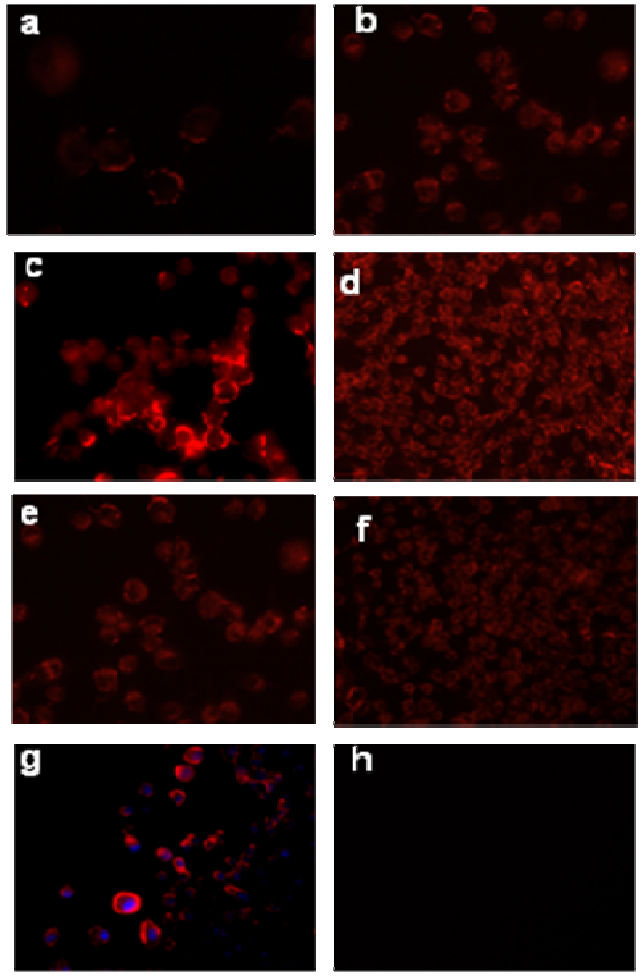

Figure 1. MCF-7 cells treated with: Nile Red- EPI nanocapsules for (a) 1 h and (b) 3 h; Nile Red-CS nanocapsules for (c) 1 h and (d) 3 h (f); or Nile Red- Phs nanocapsules for (e) 1 h and (f) 3 h; (g) Localization of Nile Red in the cytoplasm; the cell nucleus is stained with DAPI; (h) Blank: cells treated with empty nanocapsules. (a, c, e , f and g: x40 magnification; b, d: x 20 magnification).

which produce systems that are more biocompatible but have a lower cell uptake [33, 34]. The lower fluorescence intensity of PhS *versus* EPI nanocapsules may be attributable to the lesser hydrophilicity of the former. Nevertheless, given that these differences disappear after 5 hours of treatment, all three systems achieve similar uptake efficacy (data not shown).

Synthesis, Encapsulation Efficiency, and Cytotoxicity Assays of Docetaxel-Loaded Nanoparticles

Docetaxel-loaded nanoparticles were prepared by using a solvent-displacement technique. For encapsulation, docetaxel was dissolved in olive oil from the organic phase of the emulsion before it was mixed with the aqueous phase. High-performance liquid chromatography (HPLC) study of the encapsulation efficiency of docetaxel showed that the organic phase of CS, EPI, and PhS nanoparticles contained 86%, 80%, and 80% of the drug, respectively.

In cytotoxicity assays, MCF-7 cells were treated with free docetaxel or increasing concentrations of the different docetaxel-loaded nanocapsules for 6 days, followed by calculation of the inhibitory concentration 50 (IC_{50}) in each case. No significant differences in growth patterns were found between parental MCF-7 cells and MCF-7 cells treated with empty CS, EPI, or PhS nanoparticles (data not shown). With equivalent drug loading in the culture medium, a markedly lower proliferation rate was observed in the MCF-7 cells treated with docetaxel-loaded nanoparticles than in the parental MCF-7 cells treated with free docetaxel (Figure 2). A 20 nM dose of free docetaxel had no cytotoxic effect on cells, whereas 20 nM of docetaxel-loaded CS, EPI, or PhS nanoparticles induced a significant decrease of 94.65%, 89.27%, or 51.01%, respectively, in their survival rate ($P < 0.001$) (Figure 2A). IC_{50} values were 45 nM for free docetaxel, 9 nM for docetaxel-loaded CS and EPI nanoparticles, and 20 nM for docetaxel-loaded PhS nanoparticles (Figure 2B).

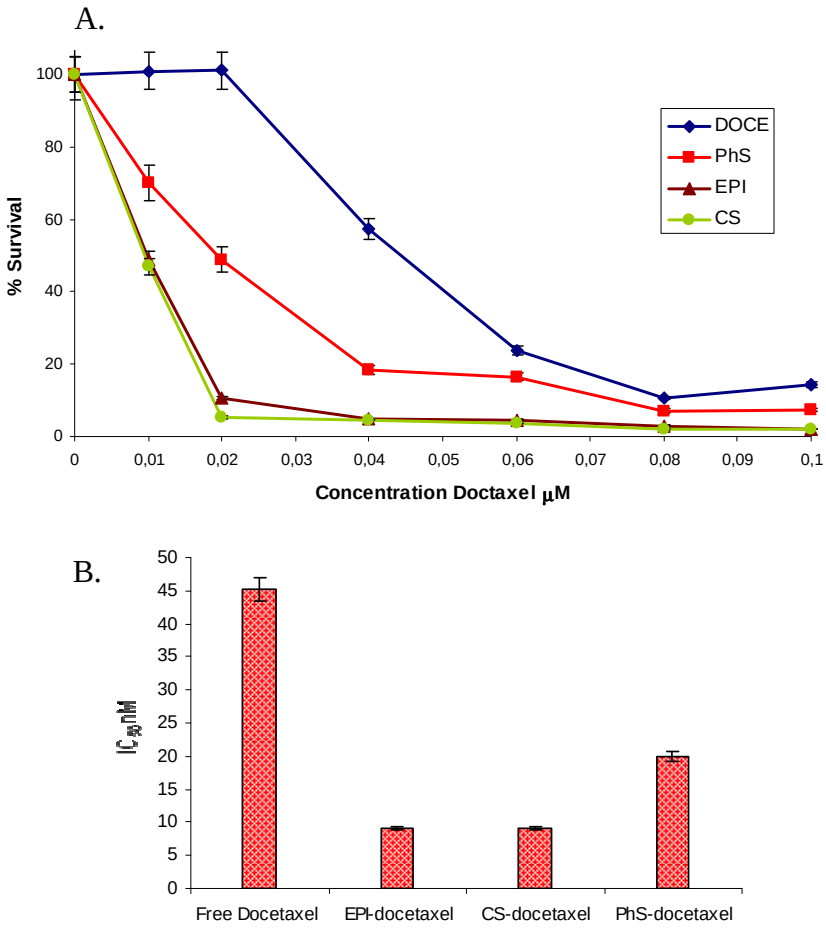

Figure 2. (**A**) Growth-in hibition curves of MCF-7 cells after 6 days of exposure to free docetaxel and to the three docetaxel-loaded nanoparticles (EPI, CS and PhS). Values are the mean of four independent experiments; (**B**) IC_{50} values (drug concentration producing 50% reduction in absorbance in control cells) of free docetaxel and the three docetaxel-loaded nanoparticles, expressed in nM and estimated as described in Material and Methods. ***** statistically significant.

Recent studies reported similar effects with high-dose docetaxel in oily core nanocapsules. Youm *et al.* [35] observed that the bioactivity against SUM 225 cells was higher for free *versus* encapsulated docetaxel at lower concentrations (2.5 µM) but was significantly higher for the encapsulated form at the highest concentration (5

μM). Likewise, Li *et al.* [36] found that cell death was greater in drug-resistant MCF-7/ADR cells when doxorubicin was delivered in LA-TPGS nanoparticles at high drug concentrations. Importantly, EPI, CS, and PhS nanocapsules described in the present study induced high cell death levels even at low concentrations, exerting a five-fold (EPI and CS) and 2.26-fold (PhS) more potent cytotoxic effect *versus* free docetaxel. These data indicate that the sustained release of the drug and its enhanced drug internalization by MCF-7 cells when in this nanocapsule formulation may increase the biological response to docetaxel and allow a decrease in the dose, thereby reducing its side effects.

Apoptosis Determinations and Cell Cycle Analysis

Apoptosis is considered the main cell death mechanism in response to taxanes. Docetaxel targets tubulin, stabilizing microtubules and thereby inducing cell-cycle arrest and apoptosis [37]. We therefore studied these well-documented effects on cell cycle distribution and apoptosis in the tumor cells. When undergoing apoptosis, cells externalize phosphatidylserine, a lipid found on the inner surface of the cell membrane that can be labeled with fluorochrome-conjugated annexin V. It is therefore possible to distinguish between intact cells (stained negative for both annexin V-FITC and propidium iodide [PI]), early apoptosis (stained positive for annexin V-FITC and negative for PI), late apoptosis or cell death (stained positive for both annexin V-FITC and PI), and necrosis (stained positive for PI).

Our flow cytometry study with annexin V assay showed that 94.30% of control MCF-7 culture cells were viable, 1.05% were early apoptotic, 0.35% were in late or final stages of apoptosis, and 4.30% were necrotic ($P < 0.001$) (Figure 3). No significant differences *versus* control cells were found in MCF-7 cells treated for 24 hours with empty nanoparticles (data not shown). No apoptosis was detected in cells treated with 45.2 nM free docetaxel for 24 h. Significant apoptosis levels were

observed in cells treated with docetaxel-loaded nanoparticles, and the highest apoptosis level (16.19%) was in the cells treated with 9.1 nM of EPI docetaxel-loaded nanoparticles (Figure 3 a-e).

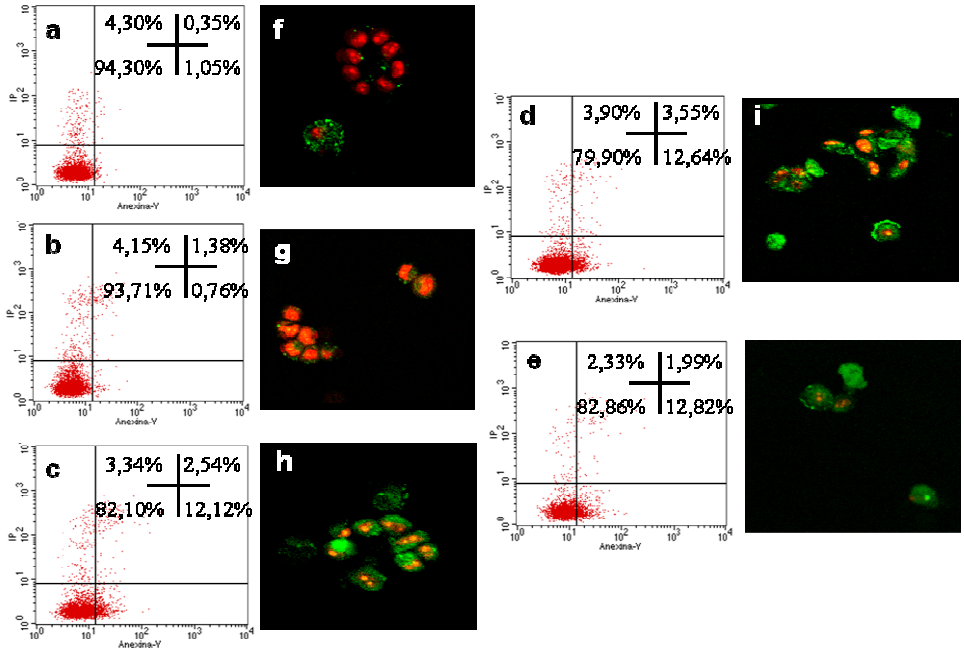

Figure 3. Quantification of *docetaxel*-induced apoptosis in MCF-7 cells by flow cytometry (a, b, c, d and e) and confocal laser scanning microscopy (f, g, h, i, and j). Cells were incubated with free docetaxel or docetaxel-loaded EPI, CS, or PhS nanoparticles for 24 h. Untreated cells served as controls. Cells were stained with annexin V and PI to evaluate apoptotic cell death (see Materials and Methods): (a and f) MCF-7 control cells, (b and g) free docetaxel, (c and h) docetaxel-loaded EPI, (d and i) docetaxel-loaded CS, (e and j) docetaxel-loaded PhS. On confocal laser scanning, early apoptosis (stained positive for annexin V-FITC and negative for PI), late apoptosis or cell death (stained positive for both annexin V-FITC and PI) and necrosis (stained positive for PI) can be observed; viable cells are not visible (stained negative for both annexin V-FITC and PI). Data are representative of four separate experiments.

The confocal microscopy study confirmed these results (Figure 3f-j). In fact, it is known to be difficult to demonstrate programmed cell death by known apoptosis-inducing agents in the MCF-7 human breast cancer cell line, and only a few cytotoxic agents have been found to act preferentially *via* an apoptotic mechanism in human breast cancer cells [38, 39].

A.

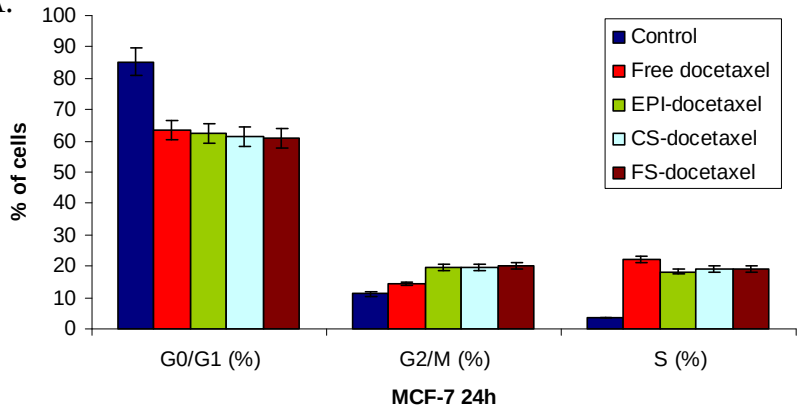

B.

Cell cycle phases	Control	Free docetaxel	EPI-docetaxel	CS-docetaxel	PhS-docetaxel
G0/G1 (%)	85.21 ± 4.18	63.32 ± 1.04	62.15 ± 3.07	61.49 ± 2.5	60.87 ± 1.05
G2/M (%)	11.12 ± 0.2	14.44 ± 0.18	19.57 ± 0.15	19.55 ± 0.09	20.23 ± 1.17
S (%)	3.67 ± 0.01	22.24 ± 0.2	18.29 ± 1.0	18.97 ± 1.01	18.91 ± 1.19

Figure 4. Representative flow cytometry profiles of the cell cycle phase distribution of MCF7 cells (A, B). Cells were incubated with free docetaxel or docetaxel-loaded EPI, CS, or PhS nanoparticles for 24 h. Untreated cells served as controls. Cells were subsequently fixed and stained with propidium iodide for DNA content analysis. Data are representative of four separate experiments.

It has also been reported that docetaxel acts at molecular level by impairing mitosis and inducing cell-cycle arrest [40]. We performed flow cytometry studies to determine differences in cell cycle distribution among the treatments. Figure 4 depicts the results of treating MCF-7 cells for 24 horus with free or nanocapsule-loaded docetaxel at IC_{50} values. All treatments induced accumulation in G_2/M and S phases, with a significant decrease in G_0/G_1 phase *versus* control cells. The accumulation was significantly greater in cells treated with docetaxel-loaded nanoparticles than in cells treated with the free drug (Figure 4). The rapid decrease in cell cycle progression, evidenced by the increased percentage of cells in S and G_2/M phase, is in agreement with previous reports that docetaxel treatment induces a G_2 cell cycle buildup in several cell lines, including MCF-7 [41–43].

Conclusions

In conclusion, our three lipid core-shell nanocapsules appear to be excellent platforms for the encapsulation and delivery of docetaxel into human cancer cells, especially in cancers that are drug-resistant through efflux pump activity. Our carriers, especially the CS and EPI nanoparticles, favor a fast and efficient uptake of the encapsulated drug into tumor cells. Moreover, the encapsulated docetaxel maintained its full activity and preserved its mechanism of action, characterized by apoptosis and premature cell cycle progression from G(1) to G(2)-M phase. Our results suggest that the use of lipid nanocapsules may allow doses of docetaxel to be decreased without loss of therapeutic effect, thereby reducing the drug toxicity. It also avoids any adverse effect of excipients (e.g., Tween 80), and may constitute a promising strategy for future applications in breast cancer therapy.

Acknowledgements

The study was supported in part by grants from the Science and Innovation Ministry through the project REF: SAF2009-12295 and MAT2010-20370 (European FEDER support included), the "Instituto de Salud Carlos III" (Fondo de Investigación Sanitaria project n°. P07-FQM03099) and the "Consejería de Innovación, Ciencia y Tecnología de la Junta de Andalucía" (Spain), by projects of excellence P07-FQM-2496 and P07-FQM03099. The authors also wish to express their gratitude to A. Martín-Rodríguez from the Department of Applied Physics, University of Granada, for his scientific assistance and to Pablo Álvarez from the Regenerative Biomedicine Institute for his technical assistance.

References

1. Ferlay, J.; Shin, H.R.; Bray, F.; Forman, D.; Mathers, C.; Parkin, D.M. Estimates of worldwide burden of cancer in 2008: GLOBOCAN 2008. *Int. J. Cancer* 2010, *127*, 2893–2917.

2. Jemal, A.; Bray, F.; Center, M.M.; Ferlay, J.; Ward, E.; Forman, D. Global cancer statistics. *CA Cancer J. Clin.* 2011, *61*, 69–90.

3. Verma, S.; Lavasani, S.; Mackey, J.; Pritchard, K.; Clemons, M.; Dent, S.; Latreille, J.; Lemieux, J.; Provencher, L.; Verma, Sh.; *et al.* Optimizing the management of her2-positive early breast cancer: The clinical reality. *Curr. Oncol.* 2010, *17*, 20–33.

4. Early Breast Cancer Trialists' Collaborative Group (EBCTCG). Effects of chemotherapy and hormonal therapy for early breast cancer on recurrence and 15-year survival: An overview of the randomised trials. *Lancet* 2005, *365*, 1687–1717.

5. Early Breast Cancer Trialists' Collaborative Group (EBCTCG). Polychemotherapy for early breast cancer: An overview of the randomised trials. Early Breast Cancer Trialists' Collaborative Group. *Lancet* 1998, *352*, 930–942.

6. Qin, Y.Y.; Li, H.; Guo, X.J.; Ye, X.F.; Wei, X.; Zhou, Y.H.; Zhang, X.J.; Wang, C.; Qian, W.; Lu, J.; *et al.* Adjuvant Chemotherapy, with or without Taxanes, in Early or Operable Breast Cancer: A Meta-Analysis of 19 Randomized Trials with 30698 Patients. *PLoS One*2011, *6*, e26946.

7. Peer, D.; Karp, J.M.; Hong, S.; Farokhzad, O.C.; Margalit, R.; Langer, R. Nanocarriers as an emerging platform for cancer therapy. *Nat. Nanotechnol.* 2007, *2*, 751–760.

8. Olson, R.D.; Mushlin, P.S. Doxorubicin cardiotoxicity: Analysis of prevailing hypotheses. *FASEB J.* 1990, *4*, 3076–3086.

9. Ma, Y.; Zheng, Y.; Zeng, X.; Jiang, L.; Chen, H.; Liu, R.; Huang, L.; Mei, L. Novel docetaxel-loaded nanoparticles based on PCL-Tween 80 copolymer for cancer treatment. *Int. J. Nanomed.* 2011, *6*, 2679–2688.

10. Blanco, E.; Hsiao, A.; Mann, A.P.; Landry, M.G.; Meric-Bernstam, F.; Ferrari, M. Nanomedicine in cancer therapy: Innovative trends and prospects. *Cancer Sci.* 2011, *102*, 1247–1252.

11. Duncan, R. The dawning era of polymer therapeutics. *Nat. Rev. Drug Discov.* 2003, *2*, 347–360.

12. Strebhardt, K.; Ullrich, A. Paul Ehrlich's magic bullet concept: 100 years of progress. *Nat. Rev.* 2008, *8*, 473–480.

13. Boulaiz, H.; Alvarez, P.J.; Ramirez, A.; Marchal, J.A.; Prados, J.; Rodríguez-Serrano, F.; Perán, M.; Melguizo, C.; Aranega, A. Nanomedicine: Application areas and development prospects. *Int. J. Mol. Sci.* 2011, *12*, 3303–3321.

14. Maeda, H. The enhanced permeability and retention (EPR) effect in tumor vasculature: The key role of tumor-selective macromolecular drug targeting. *Adv. Enzyme Regul.* 2001, *41*, 189–207.

15. Couvreur, P.; Barratt, G.; Fattal, E.; Legrand, P.; Vauthier, C. Nanocapsule technology: A review. *Crit. Rev. Ther. Drug Carrier Syst.* 2002, *19*, 99–134.

16. Sánchez-Moreno, P.; Ortega-Vinuesa, J.L.; Martín-Rodríguez, A.; Boulaiz, H.; Marchal, J.A.; Peula-García, J.M. *Characterization of different functionalized lipidic nanocapsules as potential drug carriers. Int. J. Mol. Sci.* 2012, *13*, 2405–2424.

17. Immordino, M.L.; Brusa, P.; Arpicco, S.; Stella, B.; Dosio, F.; Cattel, L. Preparation, characterization, cytotoxicity and pharmacokinetics of liposomes containing docetaxel. *J. Control. Release* 2003, *91*, 417–429.

18. Earhart, R.H. Docetaxel (taxotere): Preclinical and general clinical information. *Semin. Oncol.* 1999, *26*, 8–13.

19. Verweij, J. Docetaxel (taxotere™): A new anti-cancer drug with promising potential? *Br. J. Cancer* 1994, *70*, 183–184.

20. Piccart, M.J.; Di Leo, A. Future perspectives of docetaxel (taxotere) in front-line therapy. *Semin. Oncol.* 1997, *24*, S10–27–S10–33.

21. Lee, S.W.; Yun, M.H.; Jeong, S.W.; In, C.H.; Kim, J.Y.; Seo, M.H.; Pai, C.M.; Kim, S.O. Development of docetaxel-loaded intravenous formulation, Nanoxel-PM™ using polymer-based delivery system. *J. Control. Release* 2011, *155*, 262–271.

22. Weiszhár, Z.; Czúcz, J.; Révész, C.; Rosivall, L.; Szebeni, J.; Rozsnyay, Z. Complement activation by polyethoxylated pharmaceutical surfactants: Cremophor-EL, Tween-80 and Tween-20. *Eur. J. Pharm. Sci.* 2011, *45*, 492–498.

23. Zhao, M.; Su, M.; Lin, X.; Luo, Y.; He, H.; Cai, C.; Tang, X. Evaluation of docetaxel-loaded intravenous lipid emulsion: Pharmacokinetics, tissue distribution, antitumor activity, safety and toxicity. *Pharm. Res.* 2010, *27*, 1687–1702.

24. Gao, K.; Sun, J.; Liu, K.; Liu, X.; He, Z. Preparation and characterization of a submicron lipid emulsion of docetaxel: Submicron lipid emulsion of docetaxel. *Drug Dev. Ind. Pharm.* 2008, *34*, 1227–1237.

25. Sahu, A.; Kasoju, N.; Goswami, P.; Bora, U. Encapsulation of curcumin in Pluronic block copolymer micelles for drug delivery applications. *J. Biomater. Appl.* 2011, *25*, 619–639.

26. Ray, S.D. Potential aspects of chitosan as pharmaceutical excipient. *Acta Pol. Pharm.* 2011, *68*, 619–622.

27. Wasan, K.M. The biological functions of lipid excipients and the implications for pharmaceutical products development. *J. Pharm. Sci.* 2009, *98*, 379–382.

28. Anbharasi, V.; Cao, N.; Feng, S.S. Doxorubicin conjugated to D-alpha-tocopheryl polyethylene glycol succinate and folic acid as a prodrug for targeted chemotherapy. *J. Biomed. Mater. Res. A* 2010, *94*, 730–743.

29. Florence, A.T.; Hussain, N. Transcytosis of nanoparticle and dendrimer delivery systems: Evolving vistas. *Adv. Drug Deliv. Rev.* 2001, *50*, 69–89.

30. Sandri, G.; Bonferoni, M.C.; Rossi, S.; Ferrari, F.; Gibin, S.; Zambito, Y.; Di Colo, G.; Caramella, C. Nanoparticles based on N-trimethylchitosan: Evaluation of absorption properties using in vitro (Caco-2 cells) and ex vivo (excised rat jejunum) models. *Eur. J. Pharm. Biopharm.* 2007, *65*, 68–77.

31. Lozano, M.V.; Torrecilla, D.; Torres, D.; Vidal, A.; Dominguez, F.; Alonso, M.J. Highly efficient system to deliver taxanes into tumor cells: Docetaxel-loaded chitosan oligomer colloidal carriers. *Biomacromolecules* 2008, *9*, 2186–2193.

32. Hafner, A.; Lovric, J.; Voinovich, D.; Filipovic-Grcic, J. Melatonin-loaded lecithin/chitosan nanoparticles: Physicochemical characterization and permeability through Caco-2 cell monolayers. *Int. J. Pharm.* 2009, *381*, 205–213.

33. Vonarbourg, A.; Passirani, C.; Saulnier, P.; Benoit, J.P. Parameters influencing the stealthiness of colloidal drug delivery systems. *Biomaterials* 2006, *27*, 4356–4373.

34. Beduneau, A.; Saulnier, P.; Benoit, J.P. Active targeting of brain tumors using nanocarriers. *Biomaterials* 2007, *28*, 4947–4967.

35. Youm, I.; Yang, X.Y.; Murowchick, J.B.; Youan, B.B. Encapsulation of docetaxel in oily core polyester nanocapsule intended for breast cancer therapy. *Nanoscale Res. Lett.* 2011, *6*, 630.

36. Li, P.Y.; Lai, P.S.; Hung, W.C.; Syu, W.J. Poly(l-lactide)-vitamin E TPGS nanoparticles enhanced the cytotoxicity of doxorubicin in drug-resistant MCF-7 breast cancer cells. *Biomacromolecules* 2010, *11*, 2576–2582.

37. Montero, A.; Fossella, F.; Hortobagyi, G.; Valero, V. Docetaxel for treatment of solid tumours: A systematic review of clinical data. *Lancet Oncol.* 2005, *6*, 229–239.

38. Chadderton, A.; Villeneuve, D.J.; Gluck, S.; Kirwan-Rhude, A.F.; Gannon, B.R.; Blais, D.E.; Parissenti, A.M. Role of specific apoptotic pathways in the restoration of paclitaxel-induced apoptosis by valspodar in doxorubicin-resistant MCF-7 breast cancer cells. *Breast Cancer Res. Treat.* 2000, *59*, 231–244.

39. Marchal, J.A.; Núñez, M.C.; Suárez, I.; Díaz-Gavilán, M.; Gómez-Vidal, J.A.; Boulaiz, H.; Rodríguez-Serrano, F.; Gallo, M.A.; Espinosa, A.; Aránega, A.; *et al.* A synthetic uracil derivative with antitumor activity through decreasing cyclin D1 and Cdk1, and increasing p21 and p27 in MCF-7 cells. *Breast Cancer Res. Treat.* 2007, *105*, 237–246.

40. Hernández-Vargas, H.; Palacios, J.; Moreno-Bueno, G. Molecular profiling of docetaxel cytotoxicity in breast cancer cells: Uncoupling of aberrant mitosis and apoptosis. *Oncogene* 2007, *26*, 2902–2913

41. Liu, D.; Liu, Z.; Wang, L.; Zhang, C.; Zhang, N. Nanostructured lipid carriers as novel carrier for parenteral delivery of docetaxel. *Colloids Surf. B Biointerfaces* 2011, *85*, 262–269.

42. Sharma, R.I.; Welch, A.E.; Schweiger, L.; Craib, S.; Smith, T.A. [F]fluoro-2-deoxy-d-glucose incorporation by MCF-7 breast tumour cells in vitro is modulated by treatment with tamoxifen, Doxorubicin, and docetaxel: Relationship to chemotherapy-induced changes in ATP content, hexokinase activity, and glucose transport. *Int. J. Mol. Imaging* 2011, *2011*, 874585.

43. Ghawanmeh, T.; Thunberg, U.; Castro, J.; Murray, F.; Laytragoon-Lewin, N. miR-34a expression, cell cycle arrest and cell death of malignant mesothelioma cells upon treatment with radiation, docetaxel or combination treatment. *Oncology* 2012, *10*, 330-335.

44. Villalobos, M.; Olea, N.; Brotons, J.A.; Olea-Serrano, M.F.; Ruiz de Almod´ovar, J.M.; Pedraza, V. The E-Screen assay: A comparison of different MCF-7 cell stocks. *Environ. Health Perspect.* 1995, *9*, 844–849.

Paper III. Colloidal stability and in vitro antitumor targeting ability of lipid nanocapsules coated by folate-chitosan conjugates

Azahara Rata-Aguilar[1§], Paola Sánchez-Moreno[1§], Ana Belén Jódar-Reyes[1], Antonio Martín-Rodríguez[1], Houria Boulaiz[2], Juan Antonio Marchal-Corrales[2], José Manuel Peula-García[3], and Juan Luis Ortega-Vinuesa[1]

[1]Department of Applied Physics, University of Granada, Granada, 18071 (Spain)

[2] Human Anatomy and Embryology Department, Regenerative Biomedicine Institute (IBIMER), University of Granada, Campus de la Salud, 18071, Granada, Spain

[3]Department of Applied Physics, University of Malaga, Malaga, 29071 (Spain)

§ Both authors contributed equally to this work

Published in:

JOURNAL OF Bioactive and Compatible Polymers: Biomedical Applications

J. Bioact. Compat. Pol.. **2012**, *27*(4), 388-404

Abstract

In this study, the synthesis and characterization of lipid nanocapsules coated with folate–chitosan conjugates at varying folate concentrations are reported; these nanocapsules have a potential application as anticancer drug carriers. The main goal of this study was to evaluate (a) the colloidal stability of the particles and (b) their cell targeting. A classical colloidal characterization of the nanocapsules was carried out by analyzing size, electrokinetic charge, and stability in different saline solutions, including cell culture media. At neutral pH, the stability was improved by the presence of folate due to electrical interactions. In addition, folate modulated the hydrophilic/ phobic nature of the surface, which became critical to keep the systems stable (or not) under physiological saline conditions due to the action of short-range repulsive hydration forces. The cellular uptake of our nanocapsules was evaluated by working with four tumor cell lines. Both fluorescent analyses with particles colored by Nile Red, and antitumor activity of our systems loaded with docetaxel, demonstrated that the folate-mediated internalization of the particles in the cancer cells was improved when the nanocapsules were coated by folate–chitosan conjugates.

1. Introduction

In recent years, many nanosystems with functional properties have been developed and used in a broad range of bioapplications: tissue engineering [1], vaccine, drug, and gene delivery [2–6] as well as diagnosis and therapeutics [7,8]. An exciting challenge for science today is to formulate intelligent antitumor drug nanocarriers. If targeted nanoparticles could deliver a drug directly to cancer cells, it would render better efficacy and less toxic side effects for chemotherapy patients [9–11]. This challenge is interdisciplinary, since physicists, chemists, biologists, pharmacologists, and so on must closely collaborate to develop such ideal colloidal delivery systems.

Among the different colloidal systems used for biological applications, cationic nanocapsules are promising. The hydrophobic core serves as a reservoir for hydrophobic drugs, protecting the content during transport to the target cell [12]. The hydrophilic shell can be modified physicochemically to have desirable properties, such as targeting or the evasion of scavenging by the mononuclear phagocyte system [13].

Additionally, the cationic charge favors an easy approach to cell membranes for rapid internalization. Although artificial cationic lipids have previously been used in the synthesis of cationic nanocapsules, the current tendency is to use natural biocompatible substances. Chitosan seems to have a strong potential applicability in pharmaceutical and medical areas for its accessibility (it is the second most plentiful biomass produced by deacetylation of chitin), low cost, and biological properties such as biocompatibility, biodegradability (under certain conditions), low toxicity, and mucoadhesivity. Also, it is hemostatic, bacteriostatic, fungistatic, anticarcinogenic, and anticholesteremic, [14] without inducing allergic reactions or immunorejections. There is a plethora of articles in which chitosan is

used as a surface component in drug delivery systems. The abundance of free amino groups in its linear structure promotes ionic cross-linkage with multivalent anions to form nanogels [18,19], allowing chemical links with different molecules that may act as vectors. For example, folate can be conjugated to chitosan to achieve targeting properties.

The folate conjugation to chitosan may improve gene transfection or drug–cell internalization efficiency due to promoted uptake of folate receptor-bearing tumor cells. Folate receptors, though overexpressed in various cancer cells, are rarely found on the normal cell surface or are located at the apical surfaces of polarized epithelia [20]. Also, folate conjugates covalently derived via their γ-carboxyl group can retain the high-affinity ligand-binding property of folate and the kinetics of cellular uptake of conjugated folate compounds by folate receptors resemble to those of free folate [21]. Different studies have reported on folate-mediated targeting of antitumor drugs and genes by conjugating folic acid onto polymeric micelles [22], macromolecules [23], nanoparticles [10,11,24] and liposomes.[25] Other folate conjugates such as protein toxins, chemotherapy or radioimaging agents, anti-T-cell receptor antibodies, and gene-transfer vectors have also demonstrated receptor-specific delivery properties [20]. However, conjugation between chitosan and folic acid to create effective targeted drug delivery vehicles has been developed only in recent years [26–29] and oily core–shell nanocapsules coated with chitosan–folate conjugates have still not been reported, being a novel colloidal system in need of evaluation.

The development of colloidally stable nanosystems is a prerequisite for successful drug delivery in biological media. The poor solubility of both chitosan and folic acid at neutral pH might compromise nanocapsule stability in physiological fluids, once such nanostructures are coated with folate–chitosan conjugates. The inherent hydrophobic nature of folic acid clashes with the

hydrophilic character of chitosan. Therefore, a special effort to analyze and explain the forces acting between these kinds of particles, that is, forces responsible for preventing or provoking spontaneous aggregation of the system. In addition to the two classical forces described by the well-known Derjaguin–Landau–Verwey–Oberbeek (DLVO) theory (i.e. the repulsive one coming from electrostatic interactions and the attractive one arising from London–van der Waals interactions), there is a key repulsive interaction that should be taken into account: the short-range hydration force. In previous studies on nanocapsules coated by chitosan molecules with different properties (i.e. molecular weight and degree of acetylation) [30,31] we demonstrated that hydration forces are crucial in the stability of such systems when immersed in simulated biological fluids. This hydration force is a structural interaction that gives anomalous stability to many hydrophilic colloids in aqueous media with moderate or high ionic strength [32–36]. Microscopically, it arises from the structure of water molecules as well as hydrated ions located near hydrophilic surfaces [37–39].

Within this scenario, this article focuses on the synthesis and physicochemical characterization of core–shell nanocapsules coated by folate–chitosan conjugates, paying special attention to their colloidal stability in different saline media. In addition, these nanocapsules are evaluated in vitro by analyzing their uptake by four different cancer cell lines (A549, MCF-7, HT-29, and Caco-2), three of which overexpress folate receptors. To determine their targeting and uptake efficiency, we quantified their fluorescence emission as well as antitumor activity by working with Nile Red and docetaxel-loaded nanocapsules, respectively. Both substances are hydrophobic and thus adequate to be encapsulated inside our particles. The hydrophobic fluorescent stain Nile Red is a solvatochromic dye with absorption bands that vary in shape, position, and intensity, depending on the nature of the solvent [40]. Docetaxel, a well-known anticancer drug, has been successfully encapsulated in lipid nanocapsules [41], since it is poorly water soluble.

It is a potent taxane that inhibits microtubule polymerization/depolymerization and cell replication. To reduce the side effects of this cytotoxic agent for better tolerance to treatment, recent approaches have aimed at reformulating docetaxel with recently developed colloidal carriers [41].

2. Materials and methods

Reagents

The nanocapsule hydrophobic core was constituted by olive oil (Sigma, Madrid, Spain) purified by stirring with ionic interchange resins—activated magnesium silicate, Florisil (Fluka, Madrid, Spain) — at room temperature for 3 h and subsequent centrifugation. The first shell layer was composed of Epikuron 145V, a deoiled wax-like phosphatidylcholine-enriched fraction of soybean lecithin, kindly donated by Cargill (Barcelona, Spain). Protasan® C1 113, a medium-molecular-weight chitosan chloride salt with a deacetylation degree of 85%, was supplied by FMC BioPolymer NovaMatrix (Sandvika, Norway). Folic acid and phosphate-buffered saline (PBS) were purchased from Sigma. Different salts used to prepare buffered solutions for electrophoretic mobility measurements or for colloidal aggregation studies were of analytical grade and purchased from Sigma, Merck (Madrid, Spain), and Scharlau (Barcelona, Spain). Deionized Milli-Q water was used throughout the experiment.

Synthesis and purification of folate-chitosan conjugates

The conjugation process was described by Dube et al. [42], although these authors did not use chitosan; they used a copolymer of *N*-isopropylacrylamide and amino-*N*-ethylenedioxy-bis(ethylacrylamide) instead. Briefly, in our case, a solution

of folate (FOL) and 1-(3-dimethylaminopropyl)-3-ethylcarbodiimide hydrochloride (ECDI) at molar ratio of 1:1.2 in anhydrous dimethyl sulfoxide (DMSO) was prepared and stirred at room temperature until folate was definitively dissolved. It was then added to a solution of 0.5% (w/v) chitosan (CS) in acetate buffer (0.1 M, pH 4.7) and stirred in the dark for 16 h. The resulting product was precipitated by drop addition of diluted NaOH up to pH 9.0, followed by centrifugation at 2500 r/min for 10 min at room temperature. The precipitate was purified by suction filtration using a Buchner funnel. Folate–chitosan conjugates were then washed thoroughly using diluted aqueous NaOH and finally deionized water. The product was vacuum-dried at room temperature for 48 h.

Two conjugates with different folate/chitosan ratios (0.1% and 0.2% w/w) were formulated, referred to as CS-FOL-1 and CS-FOL-2, respectively. The yield of the coupling was determined, after calibration, by measuring the intensity of absorbance at 285 nm of the formulations being 73.9% for CS-FOL-1 and 63.25% for CS-FOL-2. The presence of folate residues successfully conjugated to the chitosan backbone was confirmed by proton nuclear magnetic resonance (^{1}HNMR) in the Scientific Instrumentation Centre, Granada University (Spain) using a diluted deuterium acetic acid solution as a solvent.

Nanoparticle Preparation

Nanocapsules were prepared following a procedure originally developed by Calvo et al. [43], slightly modified to avoid any poloxamer in the formulation; this omission was explained in Ref. [30]. Briefly, 40 mg of Epikuron 145V was dissolved in 500 μL of ethanol, 125 μL of olive oil were added, and then 9 mL of acetone. Subsequently, this organic phase was poured under agitation into 20 mL of an acidulated aqueous solution containing pure chitosan or the folate–chitosan conjugates (0.5 mg/mL). Nanocapsules were formed immediately, as the solution

rapidly turned milky after mixing the organic and aqueous phases. Organic solvents (acetone and ethanol) plus a portion of the volume of water were evaporated in a Rotavapor (Rotary evaporator, Barloworld Scientific Limited Stone, Staffordshire, UK) at 40°C for 8 h, giving a final volume corresponding to 3/4 of the original one.

Size and electrophoretic mobility

The hydrodynamic mean diameter of the nanocapsules was determined by photon correlation spectroscopy (PCS), using a 4700C light-scattering device (Malvern Instruments, Worcestershire, UK) that used a He–Ne laser (10 mW). The light scattered by the samples was detected at 90°. The temperature was set at 25°C. Electrophoretic mobility (μe) was measured with a nanozeta dynamic light-scattering analyzer (ZetaSizer NanoZ, Malvern Instruments). Our study focused on measuring the μe values as a function of pH, maintaining a constant low ionic strength equal to 0.002 M.

Colloidal stability

Colloidal stability was initially analyzed at neutral pH in simple saline media (varying the salt concentration with NaCl or $CaCl_2$). From these studies we were able to calculate the "critical coagulation concentration" (CCC) and the "critical stabilization concentration" CSC. These parameters are fundamental in colloidal stability studies, and the way they have been derived is explained in the introduction of the dissertation (1.7 Colloidal stability of nanoemulsions). We encourage readers to read it in order to clarify the information given by the CCC and CSC values about both the charge density and hydrophilicity of the nanoparticle surface.

In addition to measuring the colloidal stability of our nanocapsules with NaCl and $CaCl_2$, we also evaluated stability in PBS, the cell-culture medium (Dulbecco's modified Eagle's médium (DMEM)), and DMEM supplemented with fetal bovine serum (FBS) by monitoring the hydrodynamic mean diameter of the nanocapsules as a function of time by PCS.

Cell lines and culture conditions

Four human tumor-cell lines, MCF-7, HT-29, A549, and Caco-2, were supplied by the Scientific Instrumentation Centre, Granada University (Spain). All cell lines were grown at 37ºC in an atmosphere containing 5% CO2, with Dubelcco's modified Eagle Medium (DMEM) (Gibco, Grand Island, NY, USA) supplemented with 10% (v/v) heat-inactivated fetal bovine serum (FBS), 2% L-glutamine, 2.7% sodium bicarbonate, 1% Hepes buffer, and 1% of penicillin/streptomycin solution. Three cell lines (MFC-7, HT-29 and Caco-2) overexpress folate receptors [28, 44]. The lung-cancer cell line (A549) served as a negative control, as it does not overexpress folate receptors in the cell membrane [45].

Cell culture with fluorescence-labeled nanoparticles

A549, MCF-7, HT-29, and Caco-2 cells ($5x10^4$) were seeded into 24-well plates under the culture conditions detailed above. After 24 h, cells were fed with fresh medium and treated with Nile Red-nanocapsules. Nanocapsules were formulated by loading Red Nile dissolved in the olive oil at a concentration of 0.025% (w/w). The cells were incubated with Red Nile labeled particles for 1 and 4 h in media with and without free folic acid addition (5mM), respectively, and then washed with PBS to remove free nanocapsules. Cells were harvested by PBS-ethylenediamine-tetraacetid acid (PBS-EDTA), washed twice with cold PBS, and

pelleted by centrifugation at 1500 r/min for 5 min. Living cells were resuspended in PBS and analyzed for red fluorescence by flow cytometry in a FACScan (Becton Dickinson, San Jose, CA, USA). The fluorescent pulses were analyzed by CellQuest Pro software. Instrument settings, such as photomultiplier (PMT) voltage and compensation, were adjusted in such a way that the difference in background fluorescence of cells without internalized nanocapsules became insignificant.

Intracellular uptake of docetaxel-loaded nanocapsules

A549, MCF-7, HT-29, and Caco-2 cells ($5x10^3$) were plated into 24-well plates under the culture conditions detailed above. The cells were fed with fresh medium supplemented with 0.1 μM of free and encapsulated docetaxel. After 24 h of treatment, cells were counted using the sulforhodamine-B (SRB) colorimetric assay as described in reference [46] using a Titertek Multiscan apparatus (Flow, Irvine, CA, USA) at 492 nm. We evaluated the linearity of the SRB assay with the cell number for each cell line stock before each cell-growth experiment. All experiments were plated in triplicate wells and replicated at least twice.

Statistical analysis

Statistical Package for the Social Sciences (SPSS) version 7.5 (Chicago, IL, USA) was used for the statistical analysis in cell culture studies. The results were compared by means of the Student's *t*-test. All data are expressed as means ±standard deviations (SDs). Differences were considered statistically significant at a p value of < 0.05.

3. Results

1H NMR characterization of folate-chitosan conjugates

After synthesizing and purifying the folate/chitosan conjugates the presence of chemically linked residues of folate was corroborated by the ^{1}H NMR analysis. Corresponding spectra are shown in Figure 1. The signals located in the 1 - 5 ppm range are assigned to the resonance of the chitosan residue protons. Peak assignment of the different chemical groups are indicated in the signal appearing at δ 4.7 ppm in Fig. 1 (a) is ascribed to traces of hydrogen in the deuterated water. This peak does not appear in Figs. 1(b) and (c) because in these cases the spectra were obtained using a *double pulsed field gradient spin-echo* (DPFGSE) treatment that removed the D_2O signal. In addition, an acetic acid peak appears in the CS-FOL-1 and CS-FOL-2 samples because, although the chitosan was able to dissolved in water, the folate-chitosan conjugates were completely insoluble in water, (which may be considered as another experimental evidence of the effective coupling of folate with chitosan). In these cases, addition of deuterated acetic acid in D_2O (ratio 1:4) was necessary to solubilize the conjugates, and this is why an acetic peak appears at 2.2 ppm in the CS-FOL-1 and CS-FOL-2 systems. In Figs. 1 (b) and (c), those signals found at 7.3–8.7 ppm are attributed to the resonance of the folate aromatic protons (29). Therefore not only the por solubility in water, but also the ^{1}H NMR data confirm that the couple of folate residues to the chitosan was successfully carried out via the carbodiimide method.

Characterization of nanoparticles

The synthesis procedure yielded nanocapsules with an average diameter of approximately 300 nm: CS = 330 ± 90, CS-FOL-1 = 215 ± 50, and CS-FOL-2 =

245 ± 70. The size of all the formulations (CS, CS-FOL-1, and CS-FOL-2, with or without Red Nile or docetaxel loads) remained a constant value under the storage conditions (pure water, 4ºC) for at least four months.

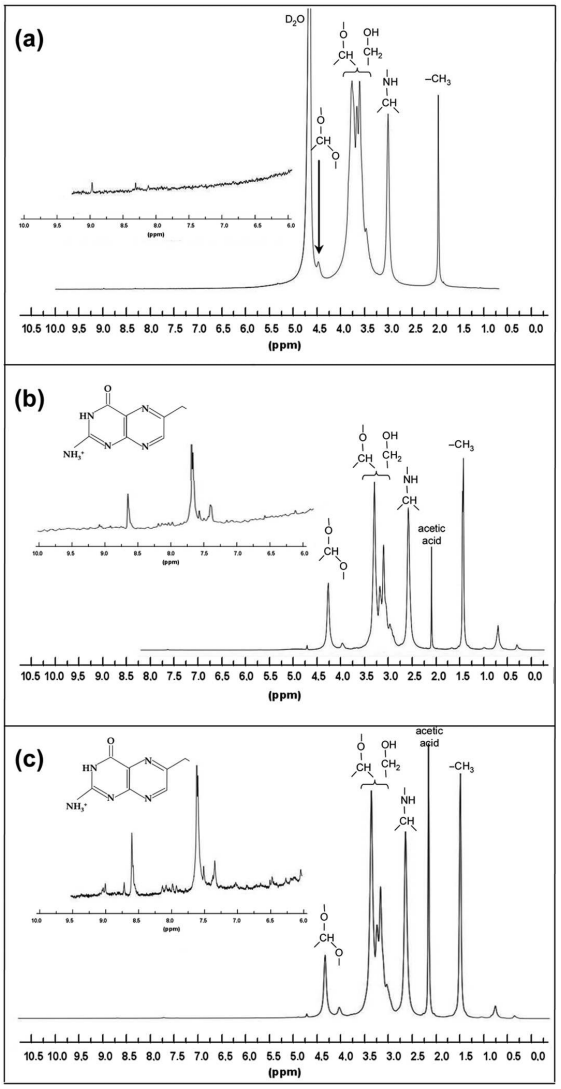

Figure 1. 1H-NMR spectrum of (a) pure chitosan, (b) CS-FOL-1, and (c) CS-FOL-2 conjugates. 1H-NMR: proton nuclear magnetic resonance.

Electrophoretic mobility

The electrical state of the particles was evaluated by electrophoretic mobility (μ_e) measurements. Mobility as a function of pH in buffered media shown in figure 2 indicates the same ionic strength (0.002 M). The electrokinetic behavior of the CS sample coincided with other similar formulations shown in reference [31]. However, clear differences appear when folate is linked to the particle surface, being the μ_e-shift with regard to the CS sample more significant for the CS-FOL-2 case.

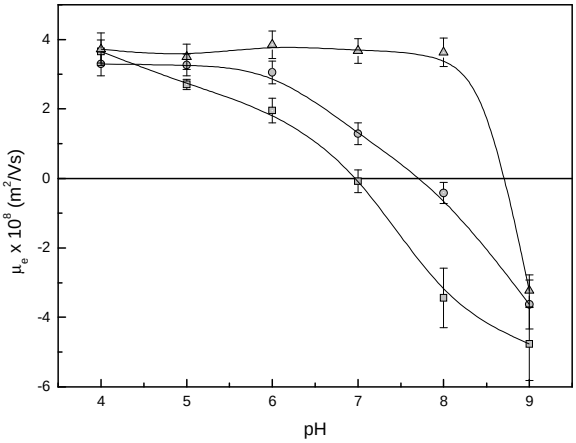

Figure 2. Electrophoretic mobility versus pH in buffered media of low salinity (ionic strength equal to 0.002 M) for the CS (squares), CS-FOL-1 (circles), and CS-FOL-2 (triangles) nanocapsules.

Colloidal stability

The colloidal stability was initially studied in simple saline solutions. Nanocapsules dissolved at pH 7.0 (Bis-Tris) were forced to aggregate by adding increasing concentrations of NaCl and, independently, $CaCl_2$. The aggregation kinetics enabled us to analyze the stability factor "W" as a function of the electrolyte concentration (Figure 3), and the corresponding CCC and CSC values

were determined (Table 1). Again, the stability patterns were dependent on the surface characteristics, since the presence of folate modulated the CCC and CSC values as explained in the "Discussion" section.

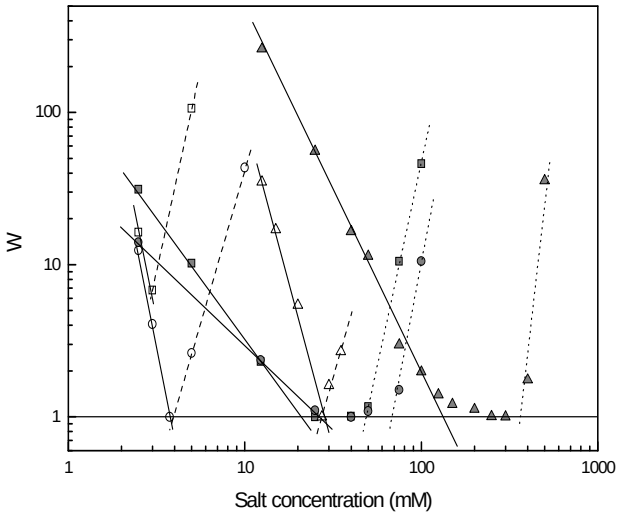

Figure 3. Stability factor (*W*) as a function of salt concentration (filled symbols for NaCl and empty symbols for CaCl2) for our CS (squares), CS-FOL-1 (circles), and CS-FOL-2 (triangles) nanocapsules. Information about "*W*" is described in Introduction of the thesis. (1.7. Colloidal stability of nanoemulsions).

Table 1. CCCs and CSCs of our three nanocapsule systems in saline media (NaCl and CaCl2) buffered at pH 7.0

		NaCl		$CaCl_2$	
	Diameter(nm)	CCC (mM)	CSC (mM)	CCC (mM)	CSC (mM)
CS	330	20	50	-4	-4
CS-FOL-1	215	27	70	-3	-3
CS-FOL-2	245	130	370	27	27

Stability was subsequently analyzed in more complex media, that was, PBS and cell-culture medium (DMEM) supplemented with FBS; the aggregation kinetics are shown in Figure 4.

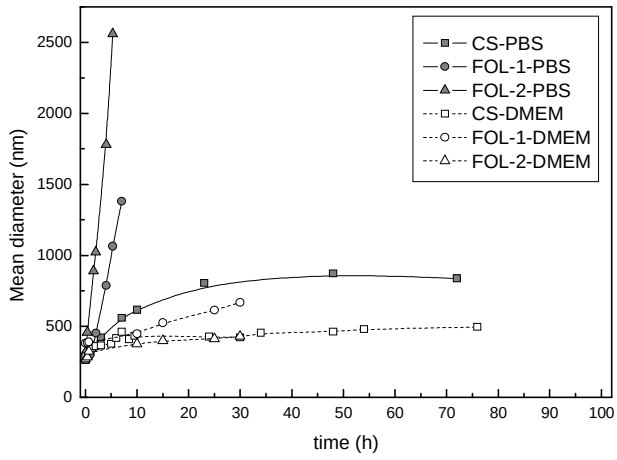

Figure 4. Aggregation kinetics of the CS (squares), CS-FOL-1 (circles), and CS-FOL-2 (triangles) nanocapsules when immersed in PBS (dark symbol) and DMEM medium supplemented with FBS (White symbols). PBS: phosphate-buffered saline; DMEM: Dulbecco's modified Eagle's medium; FBS: fetal bovine serum.

Intracellular uptake of Red Nile-loaded nanocapsules

Flow cytometry was employed to study the behavior of our nanocapsules loaded by Red Nile for targeting the four cancer-cell lines. In these experiments, the cell cultures were performed in non-supplemented DMEM medium at two incubation times, 1h and 4h. To determine whether nanocapsules were taken up by membrane folate receptors, experiments were conducted, on one hand, in a medium without free folic acid, and, on the other hand, in a medium in which free folic acid was added 10 min before addition of the nanocapsules. In this latter case, folate receptors in the cell membranes were blocked by the free folic acid

molecules, preventing the intracellular uptake of the nanocapsules with folate-chitosan conjugates on their surface. Results after 1 h and 4 h of incubation are shown in Figure 5(a) and 5(b), respectively. In each cell line, the relative fluorescent intensity detected by flow cytometry was designated as 100% for the brightness emission by the CS nanocapsules incubated 4 h without free folic acid.

The results after 1h-incubation (Figure 5(a)) show a general (but weak) trend in which increased fluorescence correlates with the folate concentration in the nanocapsule surface in cell lines overexpressing folate receptors (MCF-7, HT-29, and Caco-2). The most effective uptake appeared in the MCF-7 breast cancer cell line with the CS-FOL-2 system. This (weak) global uptake profile changed when membrane folate receptors were previously blocked with free folic acid. The differences among the blocked and nonblocked folate receptor experiments were mainly manifested when nanocapsules had folate-chitosan conjugates in their shells, above all with the CS-FOL-2 complexes in the MCF-7 cell line. Finally, the cell line that does not overexpress the folate receptor (A549) had very low fluorescence, practically coinciding with all the complexes (CS, CS-FOL-1, and CS-FOL-2) regardless of whether free folic acid was previously added.

The general tendency observed in the 1-h experiments was reinforced with the 4-h assays 4 h (Figure 5(b)), where differences between the blocked and nonblocked experiments or between the CS and CS-FOL-2 samples were much clearer. For example, in the MCF-7 cell line, the relatively greater fluorescence with regard to the CS sample was equal to 25% for the CS-FOL-1 system, and almost doubled (92%) in the CS-FOL-2 case. Similarly, in the HT-29 cell line, increments were 10% and 63% for CS-FOL-1 and CS-FOL-2, respectively, and 15% and 50% in the Caco-2 cell line. These global increments totally disappeared when free folic acid was added to block folate receptors. Finally, the A549 line gave, in general, a significant fluorescence when compared to the uptake kinetics shown by this same

cell line in the 1-h incubation experiment, although no specificity with regard to folate concentration in the shell particle is observed.

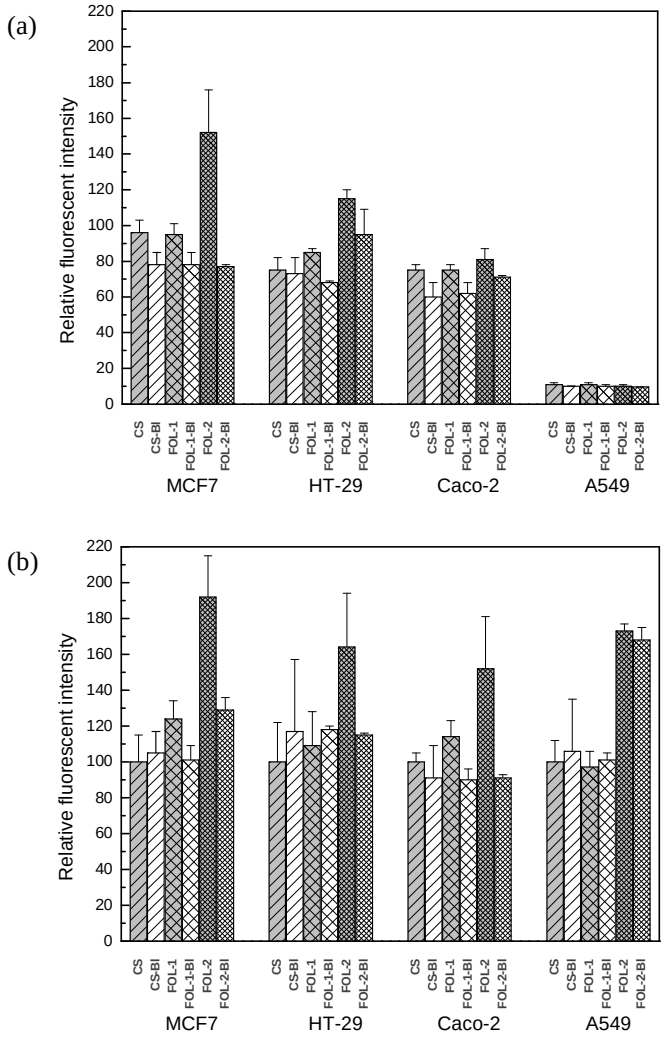

Figure 5. Relative fluorescent intensity of our four cell lines when incubated with Nile Red–loaded nanocapsules for (a) 1 h and (b) 4 h. The gray columns represent incubations without free folic acid in the medium. The columns with a white back represent experiments in which the membrane folate receptors had previously been blocked with free folic acid; in addition, these columns have been given a final "-Bl" notation.

Anti-tumor activity of docetaxel-loaded nanocapsules

The last set of experiments was designed to quantify the anti-tumor activity of docetaxel-loaded nanocapsules. Cytotoxicity was evaluated by culturing the four cancer-cell lines for 24 h in DMEM without FBS and supplemented with 0.1 μM of docetaxel-loaded nanocapsules. Cells treated with the same concentration of docetaxel in a free form that was used as control. The internalization of this drug clearly improved when using a cationized nanocarrier (compared with the free docetaxel case), regardless of whether the nanocarrier had folate or not (Figure 6).

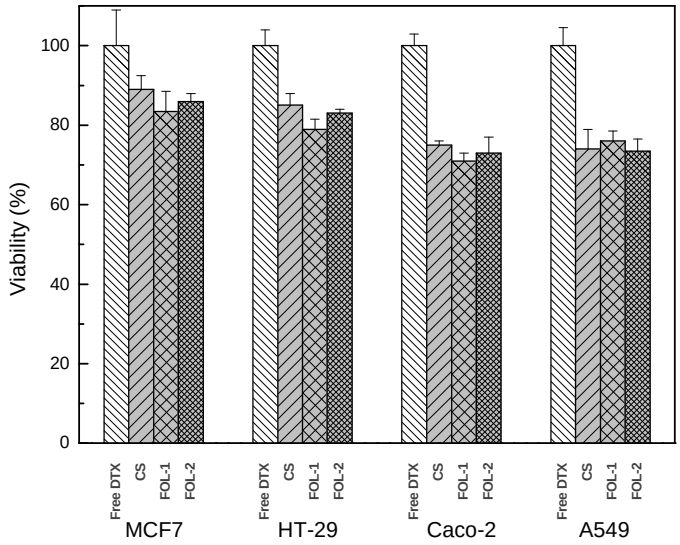

Figure 6. Percentage of cells remaining alive after incubation with 0.1 μM of docetaxel for 24 h. The White back column represents the pool in which docetaxel was added in a free form. The gray columns show the results when docetaxel was previously encapsulated in our nanocapsules. DTX: docetaxel.

This greater capture when folate is on the particle surface yielded to a cell-death increment up to 7% (i.e. see the CS-FOL-1 case compared to the CS system

in the HT-29 line). Unfortunately, the results did not correlate appropriately with the folate concentration in the nanocapsule surface, because the percentage of live cells after 24 h is always higher in the CS-FOL-2 samples than in the CS-FOL-1 ones.

4. Discussion

The size of the nanocapsules was rather similar among the different formulations, that is, it was independent of the folate concentration. This was because the nanocapsule formation was led by the surfactant properties of lecithin. Once the oil-lecithin nanocapsules were formed the folate-chitosan conjugates adhered to the lecithin shell by electrostatic interactions [47]. In addition, the inherent folate hydrophobicity also favored the shell adhesion onto the oily core by attractive hydrophobic forces [48]. Notably, the average size was identical to the original nanocapsules even in cases where Red Nile or docetaxel were added to the apolar phase of the synthesis procedure to attain loaded nanosystems.

The presence of folate in the nanocapsules surface was clearly corroborated by the μ_e data (Figure 2), as the isoelectric point of the original CS particles significantly shifted toward more basic pH values, this shift being greater at higher folate concentrations. When folate was covalently linked to chitosan, a positive charge of the original chitosan backbone was replaced by one carboxylic group, one primary amine, one secondary amine, and two amide groups. All these organic groups supplied by the folate molecule provided a basic net character yielding to a positive polymer under most of the pH conditions. Given that the cell-culture pH was almost neutral, the presence of folate converted a practically uncharged nanocapsule (the CS case) into a significantly charged system, perhaps improving the intrinsic stability of the system when immersed in the cell culture media.

Regarding colloidal stability, we first analyzed the NaCl data (Table 1). The CCC values correlated properly with the mobility data at neutral pH. The CS sample presented quite low stability (CCC = 20 mM), which was slightly improved when some folate was attached to the chitosan backbone (the CS-FOL-1 case). However, the improvement became significant when the folate concentration was increased even more (CS-FOL-2) reaching a CCC value equal to 130 mM.

Information on the surface hydrophilicity is provided by the CSC data. The chitosan hydrophilicity is clearly manifested by a low CSC value (50 mM), signifying that, at NaCl concentrations higher than 50 mM, the hydrated ions located near the hydrated chitosan shell supplied a protective structural layer that prevented aggregation under further salinity increase. Folate is relatively hydrophobic, and therefore the CSC value increased when folate was conjugated with the chitosan, reaching a high value (370 mM) for the CS-FOL-2 sample. This change from a high hydrophilic surface (CS sample) to a partially hydrophobic one (CS-FOL-2), as well as the electrophoretic mobility behavior, clearly indicates that folate molecules were effectively linked to the chitosan structure during conjugation.

Similar patterns to those found with NaCl were detected with $CaCl_2$. Calcium, a divalent ion with a voluminous hydration layer, exerted a strong effect on both the CCC and CSC values. Due to its high hydration number, this cation gave lower CSC values when compared to monovalent cations, as a lower ionic concentration is needed to create the protective hydration shell around hydrophilic colloidal particles [32-36]. Therefore, the CCC values of the most hydrophilic systems (CS and CS-FOL-1) were difficult to determine with $CaCl_2$, since the repulsive hydration forces started to act even at very low salt concentrations. In such cases, the initial W decline caused by the electric double-layer screening was rapidly overlapped by the re-stabilization induced by hydration forces, finding

systems that hardly aggregate. Therefore, the CCC values given in Table 1 for the most hydrophilic nanocapsules are only as indicative.

Finally, the conjugate with the highest folate concentration (CS-FOL-2) registered a higher CCC and CSC (27 mM), corroborating NaCl data, that is, the average surface charge increases (higher CCC values with regard to the CS surface) because of the presence of folate molecules, while the hydrophilicity decreases (higher CSC data).

Contrary to initial expectations, the most stable system in PBS had the lowest surface-charge density (CS), while the most charged one (CS-FOL-2) rapidly aggregated. The DLVO theory fails to explain these results, because hydration forces caused this anomalous stabilization. The PBS ionic strength surpassed the CCC values of our three systems (Table 1), and thus the potential barrier predicted by the DLVO theory disappeared. However, chitosan hydrophilicity favored the repulsive hydration forces, which, although not totally avoiding aggregation, was significantly slowed. This repulsion was absent in the most hydrophobic systems (CS-FOL-2), while CS-FOL-1 behavior is intermediate between that of CS and CS-FOL-2.

The aggregation patterns changed dramatically when the samples were immersed in DMEM with FBS the most unstable system in PBS (CS-FOL-2) became the most stable one, perhaps because of the adsorption of proteins (mainly albumin) at hydrophobic surfaces. Protein adsorption is generally favored by hydrophobic interactions between the surface and these macromolecules. In fact, hydrophobic interaction is one of the key controls in protein adsorption [49]. It is usually higher for large, soft proteins, such as albumin. This is why the most hydrophobic system adsorbs more albumin molecules, giving this protein great stability due to its high charge density at neutral pH and its highly hydrophilic

character responsible for hydration forces [33, 50, 51]. Similar results in folate-conjugated polymer micelles were found [27], when the positive zeta potential was inverted into negative values after the micelles were dissolved in the cell-culture medium. This inversion was ascribed to the adsorption of albumin molecules. We found this behavior in the CS-FOL-1 sample, although the albumin adsorption appeared to be lower than the CS-FOL-2 case, since the surface hydrophobicity was lower in the former than in the latter. The hydrophilic character of our CS sample probably did not promote protein adsorption as much as most hydrophobic nanocapsules (CS-FOL-2) did. The high stability of CS in supplemented DMEM medium may be ascribed to the intrinsic hydrophilic surface, since a medium enriched with different cations strengthens hydration forces enough to keep the CS particles practically stable.

The increase in fluorescence correlated with the folate concentration in the nanocapsule surface in cell lines that overexpress membrane folate receptors (Figure 5(a)). A comparison of the colorectal cancer cell lines indicated that fluorescence intensity increased more clearly in the HT-29 cells than in the Caco-2 one because the former had 1.5-fold higher expression of folate receptors than the latter [29]. This reinforced the positive results found with the other lines overexpressing folate receptors; that is, the presence of folate–chitosan conjugates on the nanocapsule surface enhanced the cell uptake of such nanocapsules. Similar results were obtained by Pan and Feng [52] using a multifunctional nanoparticle system to provide a sustained, controlled, and targeted codelivery of quantum dots. The particles with folate conjugated on the surface had higher celular uptake than those with no folate conjugation in MCF-7 cells while no significant targeting effect was observed for the NIH 3T3 (a standard fibroblast cell line) cells.

Our results obtained after 4 h (Figure 5(b)) reinforced those found after the 1 h of incubation, although the cell uptakes were much higher. These differences,

however, disappeared when free folic acid was added to block folate receptors. This indicated that the greater uptake by folate–chitosan conjugates was caused by the specific recognition of folate bonded to the nanocapsules by its membrane receptor. The A549 line, despite showing low uptake kinetics after 1 h of incubation (Figure 5(a)), gave significantly more fluorescence at 4 h. Nevertheless, the nanocapsule uptake by the A549 cells was clearly not mediated by folate receptors, as fluorescent intensity was coincident whether or not free folic acid was added to the medium.

The most striking result is that docetaxel antitumor efficiency was enhanced when enclosed within the nanocapsules. The cationized nanocarriers clearly improved the internalization of this drug, regardless of whether the nanocarrier had folate or not. It is likely that CS, CS-FOL-1, and CS-FOL-2 improved the internalization of the drug due to the attractive electrostatic interactions between the cell membrane and the positive surface of the nanocapsules. Although differences are not as marked as those found when working with Nile Red–loaded particles, the results with docetaxel follow the same direction: the folate linked to the external shell of the nanocapsules improved their capture by the folate receptors in the cell membrane.

The greater capture yielded to a cell death increment, however did not correlate appropriately with the folate concentration in the nanocapsule surface, since the efficiency of the CS-FOL-1 samples is always better than that of the CS-FOL-2 ones. This may be due to two different effects that are counterbalanced. The presence of folate on the nanocapsule surface enhanced the targeting (as shown with the Nile Red experiments), which favored the uptake of docetaxel-loaded nanocapsules by the tumor cells. However, with the toxic drug, we provided folate molecules to the cell which the surviving cells use to proliferate. Therefore, an increase in folate concentration in the nanoparticle surface may be

counterproductive. For example, after 48 h with the two colon cancer lines, we found that the differences among the CS, CS-FOL-1, and CS-FOL-2 were higher than those at 24 h, the live cells were 76% (CS), 73% (CS-FOL-1), and 84% (CS-FOL-2) in both HT-29 and Caco-2 pools. Nevertheless, the cell death was consistently more effective in short-time incubations when folate was present (irrespective of concentration) in cell lines overexpressing folate receptors than that in the A549 line, where the CS, CS-FOL-1, and CS-FOL-2 samples did not differ.

Conclusions

Folate–chitosan conjugates bearing different folate concentrations were successfully synthesized. These conjugates were used to coat oil–lecithin nanocapsules capable of delivering hydrophobic molecules in their core, forming a novel nanosystem for developing targeting strategies. The folate increased the positive charge of the particles, although the surfaces were changed from hydrophilic to partially hydrophobic. This change in hydrophilicity caused coloidal instability in the cell culture medium due to the medium salinity. Nevertheless, the in vitro experiments were designed to last few hours, and thus, the nanocapsule uptake by the cell culture was more effective than any eventual aggregation. The specificity by the nanocapsule for folate receptors was manifested in three cell lines (MCF-7, HT-29, and Caco-2) that overexpressed such receptors. Thanks to the observed specific intracellular uptake of these folic– chitosan-coated nanocapsules indicate a potential for applications in anticancer drug delivery, and they may constitute an important base for future generations of drug nanocarriers for in vivo studies.

Funding

This work was supported by the following research projects: MAT2007-66662-C02-01 and MAT2010-20370 - European FEDER support included - (MICINN, Spain), P07-FQM3099 (Junta de Andalucía, Spain), and PI10/00592 (Instituto de Salud Carlos III, Fondo de Investigación Sanitaria, Spain).

References

1. Marin RV, Ng CH , Wilke M, Tiersch B, Fratzl P and Peter MG. Size-controlled hydroxyapatite nanoparticles as self-organized organic–inorganic composite materials. *Biomaterials* 2005; 26: 5414-5426.

2. Vyas SP and Gupta PN. Implication of nanoparticles/microparticles in mucosal vaccine delivery. *Expert Rev. Vaccines* 2007; 6: 401-418.

3. Lozano MV, Torrecilla D, Torres D, Vidal A, Domínguez F and Alonso MJ. Highly efficient system to deliver taxanes into tumor cells: docetaxel-loaded chitosan oligomer colloidal carriers. *Biomacromolecules* 2008; 9: 2186-2193.

4. Luo D and Saltzman WM. Synthetic DNA delivery systems. *Nat Biotechnol* 2000; 18: 33-37.

5. Pack DW, Hoffman AS, Pun S and Stayton PS. Design and development of polymers for gene delivery. *Nat Rev Drug Discov* 2005; 4: 581-593.

6. Mishra B, Patel BB and Tiwari S. Colloidal nanocarriers: a review on formulation technology, types and applications toward targeted drug delivery. *Nanomedicine: NBM* 2010; 6: 9-24.

7. Yang SJ, Shieh MJ, Lin FH, Lou PJ, Peng CL, Wei MF, et al. Colorectal cancer cell detection by 5-aminolaevulinic acid-loaded chitosan nano-particles. *Cancer Lett* 2009; 273: 210-220.

8. Faraji AH and Wipf P. Nanoparticles in cellular drug delivery. *Bioorg Med Chem* 2009; 17: 2950-2962.

9. Feng SS. Nanoparticles of biodegradable polymers for new-concept chemotherapy. *Expert Rev Med Devices* 2004; 1: 115-125.

10. Bhattacharya R, Patra CR, Earl A, Wang S, Katarya A, Lu L, et al. Attaching folic acid on gold nanoparticles using noncovalent interaction via different polyethylene glycol backbones and targeting of cancer cells. *Nanomedicine: NBM* 2007; 3: 224-38.

11. Ebrahimnejad P, Dinarvand R, Sajadi A, Jaafari MR, Nomani AR, Azizi E, et al. Preparation and in vitro evaluation of actively targetable nanoparticles for SN-38 delivery against HT-29 cell lines. *Nanomedicine: NBM* 2010; 6: 478-485.

12. Yoo HS and Park TG. Biodegradable polymeric micelles composed of doxorubicin conjugated PLGA-PEG block copolymer. *J Control Release* 2001; 70: 63-70.

13. Kwon GS and Okano T. Polymeric micelles as new drug carriers. *Adv Drug Deliv Rev* 1996; 21: 107-116.

14. Hejazi R and Amiji M. Chitosan-based gastrointestinal delivery systems. *J Control Release* 2003; 89: 151-165.

15. Chen H and Fan M. Novel thermally sensitive pH-dependent chitosan/carboxymethyl cellulose hydrogels. *J Bioact Compat Polym* 2008; 23: 38-48.

16. Chen X, Ding S, Qu G and Zhang C. Synthesis of novel chitosan derivatives for micellar solubilization of cyclosporine A. *J Bioact Compat Polym* 2008; 23: 563-578.

17. Kavaz D, Odabas S, Güven E, Demirbilek M and Denkbas EB. Bleomycin loaded magnetic chitosan nanoparticles as multifunctional nanocarriers. *J BioactCompat Polym* 2010; 25: 305-318.

18. Calvo P, Remuñán-López C, Vila-Jato JL and Alonso MJ. Novel hydrophilic chitosan-polyethylene oxide nanoparticles as protein carriers. *J Appl Polym Sci* 1997; 63: 125-132.

19. López-León T, Carvalho EL, Seijo B, Ortega-Vinuesa JL and Bastos-González D. Physicochemical characterization of chitosan nanoparticles: electrokinetic and stability behavior. *J Colloid Interface Sci* 2005; 283: 344-351.

20. Lu Y and Low PS. Immunotherapy of folate receptor-expressing tumors: review of recent advances and future prospects. *J Control Release* 2003; 91: 17-29.

21. Wang S, Luo J, Lantrip DA, Waters DJ, Mathias CJ, Green MA, et al. Design and synthesis of [111In]DTPA-folate for use as a tumor-targeted radiopharmaceutical. *Bioconjug Chem* 1997; 8: 673-679.

22. Park EK, Kim SY, Lee SB and Lee YM. Folate-conjugated methoxy poly(ethylene glycol)/poly(epsilon-caprolactone) amphiphilic block copolymeric micelles for tumor-targeted drug delivery. *J Control Release* 2005; 109: 158-168.

23. Lu Y and Low PS. Folate-mediated delivery of macromolecular anticancer therapeutic agents. *Adv Drug Deliv Rev* 2002; 54: 675-693.

24. Mansouri S, Cuie Y, Winnik F, Shi Q, Lavigne P, Benderdour M, et al. Characterization of folate-chitosan-DNA nanoparticles for gene therapy. *Biomaterials* 2006; 27: 2060-2065.

25. Gabizon A, Shmeeda H, Horowitz AT and Zalipsky S. Tumor cell targeting of liposome-entrapped drugs with phospholipid-anchored folic acid-PEG conjugates. *Adv Drug Deliv Rev* 2004; 56: 1177-1192.

26. Chan P, Kurisawa M, Chung JE and Yang YY. Synthesis and characterization of chitosan-g-poly(ethylene glycol)-folate as a non-viral carrier for tumor-targeted gene delivery. *Biomaterials* 2007; 28: 540-549.

27. You J, Li X, de Cui F, Du YZ, Yuan H and Hu FQ. Folate-conjugated polymer micelles for active targeting to cancer cells: preparation, in vitro evaluation of targeting ability and cytotoxicity. *Nanotechnology* 2008;19: 045102.

28. Sahu SK, Mallick SK, Santra S, Maiti TK, Ghosh SK and Pramanik P. In vitro evaluation of folic acid modified carboxymethyl chitosan nanoparticles loaded with doxorubicin for targeted delivery. *J Mater Sci Mater Med* 2010; 21: 1587-1597.

29. Yang SJ, Lin FH, Tsai KC, Wei MF, Tsai HM, Wong JM, et al. Folic acidconjugated chitosan nanoparticles enhanced protoporphyrin IX accumulation in colorectal cancer cells. *Bioconjug Chem* 2010; 21: 679-689.

30. Santander-Ortega MJ, Lozano-López MV, Bastos-González D, Peula-García JM and Ortega-Vinuesa JL. Novel core-shell lipid-chitosan and lipid-poloxamer nanocapsules: stability by hydration forces. *Colloid Polym Sci* 2010; 288: 159-172. 21

31. Santander-Ortega MJ, Peula-García JM, Goycoolea FM and Ortega-Vinuesa JL. Chitosan nanocapsules: Effect of chitosan molecular weight and acetylation degree on electrokinetic behaviour and colloidal stability. *Colloids Surf B Biointerfaces* 2011; 82: 571-580.

32. Molina-Bolívar JA, Galisteo-González F and Hidalgo-Álvarez R. The role played by hydration forces in the stability of protein-coated particles: non-classical DLVO behaviour. *Colloids Surf B Biointerfaces* 1999; 14: 3 17.

33. Molina-Bolívar JA and Ortega-Vinuesa JL. How Proteins Stabilize Colloidal Particles by Means of Hydration Forces. *Langmuir* 1999; 15: 2644-2653.

34. Dávalos-Pantoja L, Ortega-Vinuesa JL, Bastos-González D and Hidalgo-Álvarez R. A comparative study between the adsorption of IgY and IgG on latex particles. *J Biomater Sci Polym Ed* 2000; 11: 657-673.

35. Santander-Ortega MJ, Jódar-Reyes AB, Csaba N, Bastos-González D and Ortega-Vinuesa JL. Colloidal stability of pluronic F68-coated PLGA nanoparticles: a variety of stabilisation mechanisms. *J Colloid Interface Sci* 2006; 302: 522-529.

36. Peula-García JM, Ortega-Vinuesa JL and Bastos-González D. Inversion of Hofmeister Series by Changing the Surface of Colloidal Particles from Hydrophobic to Hydrophilic. *J Phys Chem C* 2010; 114: 11133-9.

37. Pashley RM. Hydration forces between mica surfaces in electrolyte solutions. *Adv Colloid Interface Sci* 1982; 16: 57-62.

38. Israelachvili JN. Solvation, Structural and Hydration Forces, in Intermolecular and Surface Forces, 2nd Ed., p. 260-288, Academic Press, London. 1992.

39. Faraudo J and Bresme F. Origin of the short-range, strong repulsive force between ionic surfactant layers. *Phys Rev Lett* 2005; 94: 077802.

40. Jores K, Haberland A, Wartewig S, Mäder K and Mehnert W. Solid lipid nanoparticles (SLN) and oil-loaded SLN studied by spectrofluorometry and Raman spectroscopy. *Pharm Res* 2005; 22: 1887-1897.

41. Khalid MN, Simard P, Hoarau D, Dragomir A and Leroux JC. Long circulating poly(ethylene glycol)-decorated lipid nanocapsules deliver docetaxel to solid tumors. *Pharm Res* 2006; 23, 752-758.

42. Dubé D, Francis M, Leroux JC and Winnik FM. Preparation and tumor cell uptake of poly(N-isopropylacrylamide) folate conjugates. *Bioconjug Chem* 2002; 13: 685-692.

43. Calvo P, Remuñán-López C, Vila-Jato JL and Alonso MJ. Development of positively charged colloidal drug carries: chitosan-coated polyester nanocapsules and submicron-emulsions. *Colloid Polym Sci* 1997; 275: 46-53.

44. Lee ES, Na K and Bae YH. Doxorubicin loaded pH-sensitive polymeric micelles for reversal of resistant MCF-7 tumor. *J Control Release* 2005; 103: 405-418.

45. Choi H, Choi SR, Zhou R, Kung HF and Chen IW. Iron oxide nanoparticles as magnetic resonance contrast agent for tumor imaging via folate receptor-targeted delivery. *Acad Radiol* 2004; 11: 996-1004.

46. Villalobos M, Olea N, Brotons JA, Olea-Serrano MF, Ruiz de Almodóvar JM and Pedraza V. The E-Screen assay: A comparison of different MCF-7 cell stocks. *Env Health Perspect* 1995; 9: 844-849.

47. Sonvico F, Cagnani A, Rossi A, Motta S, Di Bari MT, Cavatorta F, et al. Formation of self-organized nanoparticles by lecithin/chitosan ionic interaction. *Int J Pharm*. 2006; 324: 67-73.

48. Chandler D. Insight Review: Interfaces and the driving force of hydrophobic assembly. *Nature* 2005; 437: 640-647.

49. Norde W. Adsorption of proteins from solution at the solid-liquid interface. *Adv Colloid Interface Sci* 1986; 25: 267-340.

50. Peula JM and de las Nieves FJ. Adsorption of monomeric bovine serum albumin on sulfonated polystyrene model colloids 3. Colloidal stability of latex-protein complexes. *Colloids Surf A Physicochem. Eng Aspects* 1994; 90: 55-62.

51. Peula JM, Hidalgo-Alvarez R and de las Nieves FJ. Coadsorption of IgG and BSA onto sulfonated polystyrene latex: I. Sequential and competitive coadsorption isotherms. *J Biomater Sci Polym Ed* 1995; 7: 241-251.

52. Pan J and Feng SS. Targeting and imaging cancer cells by Folate-decorated, quantum dots (QDs)- loaded nanoparticles of biodegradable polymers. *Biomaterials* 2009; 30: 1176-1183.

53. Israelachvili JN. Electrostatic Forces between Surfaces in Liquids, in Intermolecular and Surface Forces, 2nd Ed., p. 213-259, Academic Press, London. 1992

Paper IV. Synthesis and Characterization of Lipid Immuno-Nanocapsules for Directed Drug Delivery: Selective Antitumor Activity against HER2 Positive Breast-Cancer Cells

Paola Sánchez-Moreno[1], Juan Luis Ortega-Vinuesa[1], Houria Boulaiz[2], Juan Antonio Marchal-Corrales[2], José Manuel Peula-García[3]

[1]Department of Applied Physics, University of Granada, Granada, 18071 (Spain)

[2] Human Anatomy and Embryology Department, Regenerative Biomedicine Institute (IBIMER), University of Granada, Campus de la Salud, 18071, Granada, Spain

[3]Department of Applied Physics, University of Malaga, Malaga, 29071 (Spain)

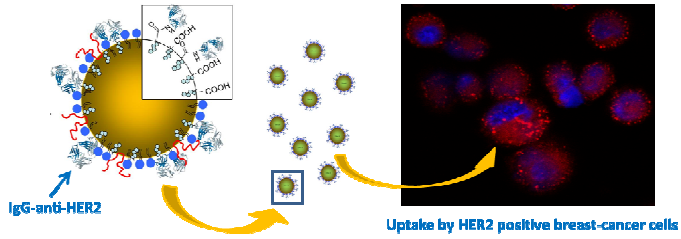

Published in:

Biomacromolecules **2013**, 14, 4248−4259

Abstract

Lipid nanocapsules (LNC) are usually developed as nanocarriers for lipophilic drug delivery. The surface characteristics of these colloidal particles are determinant for a controlled and directed delivery to target tissues with specific markers. We report the development of immuno-nanocapsules, in which some antibody molecules with different immuno-specificity are conjugated to the nanocapsule surface, offering the standardization of a simple method to obtain vectorized nanosystems with specific recognition properties. Nanocapsules were prepared by a solvent-displacement technique, producing an oily core coated by a functional shell of different biocompatible molecules and surface carboxylic groups. Three different antibodies (one a specific HER2 oncoprotein antibody) were conjugated with these nanoparticles by the carbodiimide method, which allows the covalent immobilization of protein molecules through carboxylic surface groups. The immuno-nanocapsules were completely characterized physico-chemically via electrokinetic and colloidal stability experiments, confirming the correct immobilization of these antibody molecules on the colloidal nanoparticles. Also, additional immunological analyses verified that these IgG-LNC complexes showed the expected specific immuno-response. Finally, different healthy and tumoral breast-cell lines were cultured *in vitro* with Nile-Red-loaded and docetaxel-loaded HER2 immuno-nanocapsules. The results indicate that our immuno-nanocapsules can increase their uptake in HER2 over-expressing tumoral cell lines.

1. Introduction

The development of targeted therapies, especially in anti-tumor treatments, is one of the main goals of nanomedicine today[1-3]. Conventional chemotherapy usually prompts modest tumor response and provokes undesirable side effects due to the non-specific action of drugs to all proliferating tissues[4]. To avoid these and other disadvantages, drug nanocarriers should be formulated to deliver the anti-tumor drug directly to the cancerous cells. This is a complex interdisciplinary task with too many variables to be controlled. These variables include the use of biocompatible materials, with simple but robust processes for biomaterial assembly, usually requiring different conjugation chemistries followed by some purification processes[5]. Therefore, current formulations based on complex nanostructures, such as polymer conjugates, polymeric micelles, liposomes, carbon nanotubes or nanoparticles[6-9], must be superficially modified to provide carriers with vectorization properties. Of course, such nanocomplexes must be biodegradable, non-toxic, and their laboratory production should be easy and reproducible[10].

In recent years, lipid nanocapsules have been developed as potential nanocarriers. The inner hydrophobic domain, encased in a hydrophilic outer shell, has been used to encapsulate hydrophobic drugs, these molecules being protected during their transport to the target cells[11]. Additionally, the external shell can be physico-chemically modified, for example by ligands such as antibodies, which can be linked to the surface of the nanocarriers to deliver a given drug specifically to target cells that overexpress the corresponding antigen receptor. These tailor-made vehicles would improve the effectiveness of the drug while minimizing undesirable side effects in healthy cells.[12,13]

With regard to the nature of the ligands, monoclonal antibodies have been extensively employed to develop targeted nanocarriers, referred to as immuno-

nanocarriers[14]. Some advantages of immuno-nanocarriers include the improvement of drug selectivity, high drug-loading efficiency, minor drug leakage, and protection of drugs from enzymatic degradation[15]. The design of immuno-nanocapsules requires not only the creation of well-defined structures, but also the optimization of appropriate antibody-conjugation chemistry.

In this study, we have optimized a method for covalently linking four different immuno-γ-globulines (IgG) with different isoelectric points on the surface of lipid nanocapsules. The chemical procedure for such linkage requires carboxylic groups to be present on the nanocapsule surface. Therefore, we have developed a novel system in which the nanoparticle shell has been enriched by deoxycholic acid. This amphiphilic molecule has been previously used as a component of different types of nanoparticles. Chemically conjugated with oligosaccharides, it has shown great potential to form both drug- and gene-carriers[16], and it increases the efficacy of oral bioavailability of different nanoparticles that encapsulate drugs[17]. However, the use of carboxylic groups of deoxycholic acid molecules for covalent immobilization of protein molecules on particle surfaces has not previously been described.

In the present study, we have selected different IgG molecules in order to optimize an adequate protocol to obtain immune-nanocapsules. The use of low-cost IgG molecules without therapeutic applications against cancer cells becomes useful to design the necessary initial and basic probes to develop stable and reproducible IgG-coated nanocapsules. In this way, we have used a polyclonal antibody reactive against the human C reactive protein (CRP), and additionally, two complementary monoclonal anti-human chorionic gonadotropin (hCG) antibodies. Thus, we achieved the optimal experimental conditions to link other anti-tumor specific antibodies, such as the anti-HER2 antibody used in this study: Trastuzumab (also known as Herceptin®), which is a humanized IgG1 against the

human epidermal growth factor receptor 2 (HER2) having selective anti-tumor activity.

HER2 or ErbB2 (Neu) is a trans-membrane receptor protein at the head of an intracellular tyrosine kinase signaling cascade responsible for increased proliferation, oncogenesis, metastasis, and possibly resistance to apoptosis-inducing therapeutic agents[18]. Between 15% and 20% of the cases of breast cancers show overexpression of HER2 and thus an adverse prognostic[19]. Some reports indicate that nanocarriers conjugated with Trastuzumab can recognize HER2/neu receptors and be internalized into cells via receptor-mediated endocytosis[19-21]. However, few studies examine the conjugation of Trastuzumab to nanoemulsions[22]. Furthermore, despite increasing interest in developing such systems, their complete physicochemical characterization is not included in most studies on biodegradable nanocarriers.

The present study focuses on the synthesis and physico-chemical characterization of core-shell lipid nanocapsules coated by different antibodies, with the aim of developing vectorized nanocarrier systems. For this, lipid nanocapsules were prepared by a simple process using a solvent-displacement technique with commercially available biocompatible components. The hydrophobic core was constituted by olive oil, while the hydrophilic shell presented phospholipidic molecules, a poloxamer (in order to confer structural stability and stealth properties[23,24]), and deoxycholic acid molecules to form a carboxylated surface. We achieved the chemical immobilization of the different IgG antibodies on the carboxylated surface by using a reproducible and simple method based on a carbodiimide molecule[25,26]. This method is currently used to bound proteins chemically on different nanosystems[27-29].

Subsequently, the different immuno-nanocapsules were physico-chemically characterized and compared with bare nanocapsules to assess the role played by the different antibody molecules. The characterization was based on size analysis, gel-electrophoresis measurements, electrokinetic behavior, and colloidal stability. The immunological response of the IgG-nanocapsules was also quantified against the specific ligand of the antibody molecules, CRP or hGC, by light-scattering agglutination assays. Finally, Trastuzumab-modified nanocapsules with a fluorescent molecule enclosed (Nile Red) were evaluated *in vitro*, analyzing the particle uptake by three different breast-cell lines: a healthy (MCF-10A) one, and two cancer-cell lines that over-express low (MCF-7) and high (SK-BR3) levels of HER2. Moreover, the anti-tumor activity of the Transtazumab-sensitized carriers was evaluated using docetaxel-loaded nanocapsules.

2. Experimental section

Materials

Poloxamer 188 (Pluronic F-68®), deoxycholic acid (DC), Nile Red, N-(3-dimethylaminopropyl)-N'-ethyl-carbodiimide (ECDI), C-reactive protein (CRP), human chorionic gonadotropin (hCG), Brilliant Blue R250 and olive oil were purchased from Sigma-Aldrich (Spain). All of them, except the olive oil, were used as received. Olive oil was previously purified in our labs with Activated Magnesium Silicate (Florisil, Fluka) to eliminate free fatty acids. Docetaxel, with a purity ≥ 97.0%, was from Fluka (Spain). Epikuron 145V, which is a phosphatidylcholine-enriched fraction of soybean lecithin, was supplied by Cargill (Barcelona, Spain). A polyclonal anti-CRP-IgG from rabbit was obtained, purified and kindly donated by Biokit S.A. (Spain). Its isoelectric point (IEP) was 7.3 ± 0.9.[30] Two complementary monoclonal anti-hCG antibodies (referred to as anti-hCG-IgG-α and anti-hCG-

IgG-β) were purified and also donated by Operon S.A. (Zaragoza, Spain), with IEPs equal to 5.5 and 6.2, respectively[31]. Finally, Trastuzumab (Herceptin®), also referred to here as anti-HER2-IgG and with an IEP of 9.2[32], was purchased from Roche (Switzerland). 3-(4,5-dimethylthiazol-2-yl)-2,5-diphenol tetrazolium bromide (MTT) cell-proliferation assay was from Promega (USA). Water was purified in a Milli-Q Academic Millipore system. Other solvents and chemicals used were of the highest grade commercially available.

Methods

Preparation of antibody coated nanoparticles

Preparation of lipid nanoparticles

Nanoparticles were prepared by using a modified solvent-displacement technique of Calvo et al.[33]. Briefly, an organic phase composed of 125 μL of olive oil, 10mg of deoxycholic acid, 40mg of Epikuron 145V dissolved in 0.5 mL of ethanol, and 9.5 mL of acetone, was added to 20 mL of an aqueous phase containing 50 mg of Pluronic F68 under magnetic stirring. The mixture turned milky immediately due to the formation of a nanoemulsion. Organic solvents (acetone and ethanol) plus a portion of the volume of water were evaporated in a rotary evaporator at 40°C, giving a final volume of 18 mL. In some cases, we dissolved docetaxel or Nile Red fluorochrome in the olive-oil phase in order to synthesize nanocapsules loaded with these compounds inside.[29]

Covalent coupling of antibodies

Antibodies were immobilized on the nanoparticle surface by a carbodiimide method, which permits covalent binding of protein molecules to the

carboxylic groups supplied by the deoxycholic molecules. The antibody-coupling protocol was conducted at different pH values, depending on the IEP of each IgG, in such a way that the DC nanoparticles were firstly dialyzed against different activation buffers. A phosphate buffer (pH 7.0) was used prior to link the acid IgGs (anti-hCG-IgG-α and anti-hCG-IgG-β); a borate buffer (pH 8.0) for the neutral anti-CRP-IgG; and a borate buffer (pH 10.0) for the basic anti-HER2-IgG. In this way, we set a negative net charge with regard to the electrical state of the antibodies, which was required to properly link these molecules through the carbodiimide method.

Once the dialysis was finished, 45 μL of an aqueous ECDI solution (15 mg/mL) was added to the DC-nanoparticle solution having a total particle surface equal to 0.77 m^2. These samples were incubated at room temperature for 15 min. Subsequently, the antibody coverage was performed by adding, independently, two different theoretical IgG concentrations (2.5 mg/m^2 and 5 mg/m^2), and then the solutions were incubated at room temperature for 2 h. Finally, a new dialysis was performed against the same buffer to remove any IgG molecules that were not coupled to the nanocapsules.

Physico-chemical characterization

Size and electrophoretic mobility

The hydrodynamic mean diameter of the nanocapsules was determined by photon correlation spectroscopy (PCS), using a 4700C light-scattering device (Malvern Instruments, UK) and working with a He-Ne laser (10mW). The light scattered by the samples was detected at 173°, and the temperature was set at 25°C. The diffusion coefficient measured by dynamic light scattering can be used to calculate the size of the nanoparticles by means of the Stokes-Einstein equation.

The homogeneity of the size distribution is expressed as polydispersity index (PDI), which was calculated from the analysis of the intensity autocorrelation function.[34]

Electrophoretic mobility (μ_e) as a function of pH was measured after diluting a small volume of the nanocapsule stock (with a total surface equal to 0.05 m^2) in 1 mL of the desired buffered solution. It should be noted that all the buffers used in the μ_e studies had identical ionic strengths, being equal to 0.002M. The μ_e measurements were made in triplicate using a nano-zeta dynamic light-scattering analyzer (Zeta-Sizer NanoZ, Malvern Instruments, UK).

Protein separation by SDS-PAGE

The nanocapsule-protein complexes were separated and denatured by boiling for 5 min in the following buffer: 62.5 mM Tris-HCl (pH 6.8 at25°C), 2% (w/v) sodium dodecyl sulfate (SDS), 10% glycerol, 0.01% (w/v) bromophenol blue, 40 mM dithiothreitol (DTT). Samples were then separated by size in porous 10% polyacrylamide gel (1D SDS polyacrylamide gel electrophoresis), under the effect of an electric field. The electrophoresis was run under constant voltage (130 V, 45 min) and the gels were stained using a Coomassie Blue solution (0.1% Coomassie Brilliant Blue R-250, 50% methanol and 10% glacial acetic acid) and destained with the same solution lacking the dye.

Densitometry was performed using Image J analysis software (NIH). This technique allows a quantitative digital analysis of image data from electrophoresis gels[35], calculating in this way the final antibody coverage degree of every immuno-nanocapsule. Gels were scanned and band intensities were quantified by Image J densitometry analysis. The digital image of the gel was converted to a gray-scale image. We selected the lanes of the gel and plotted them to draw a profile plot for each lane getting peaks of each lane (higher peaks represent darker bands). For each

peak we got the size. With data we calculated the relative density of the peaks. We expressed the density of the selected bands relative to the control band, in which the protein concentration was equivalent to 2,5 mg/m^2.

Colloidal stability

Sample stability was studied spectrophotometrically at physiological pH (i.e. 7.4), and by using NaCl and Ca_2Cl independently as aggregating electrolytes. The turbidity of the system was monitored with a Beckman DU 7400 spectrophotometer, working at λ = 570 nm. The analysis of the aggregation kinetics served to calculate the critical coagulation concentration (CCC) and the critical stabilization concentration (CSC), these being fundamental parameters in colloidal-stability studies. Briefly, the CCC value provides information on the charge density of the nanoparticle surface, and the CSC on surface hydrophilicity. More details about these colloidal-stability parameters can be found below in Supporting Material.

Immunoassays

Immuno-agglutination reactions with our IgG-coated particles were monitored by using a Beckman DU 7400 spectrophotometer, working at λ = 570 nm. However, agglutination was triggered only by the presence of the specific antigen in solution, i.e. CRP for the anti-CRP-IgG tailored nanocapsules, and hCG for a combination of the complementary anti-hCG-IgG-α and anti-hCG-IgG-β coated particles. In this sense, it was not possible to perform immuno-agglutination assays for the anti-HER2-IgG case, as HER2 is a membrane protein. Therefore, the immuno-reactivity of Trastuzumab-coated nanocapsules was evaluated by means of cell-culture studies. The anti-CRP-IgG particles were immunoassayed at pH 7.4 and 150 mM $CaCl_2$. A series of CRP solutions were prepared in the same buffer

covering the 0.06-16.67 μg/mL range. After mixing equal volumes (0.3 mL) of sensitized nanocapsules and CPR solutions, the absorbance was monitored for 10 min. The final particle concentration in the cuvette was $2.7x10^{11}$ mL^{-1}, which gave an initial absorbance of c. 0.5. For the anti-HCG-IgG case, the reaction buffer was a TRIS solution (pH 8.0 and10 mM) and the hCG solutions were set in the 1-300 IU range.

Cell lines and culture conditions

The human breast-cancer cell lines MCF-10A, SK-BR3 and MCF-7 were supplied by the Scientific Instrumentation Center of the University of Granada (Spain). The culture medium was Dulbecco's modified Eagle medium (DMEM, Sigma, St Louis, MO, USA) for MCF-7, and McCoy's 5A medium for SK-BR3 , both of them supplemented with heat-inactivated 10% (v/v) fetal bovine serum (FBS, Sigma), 2% L-glutamine, 2.7% sodium bicarbonate, 1% Hepes buffer, and 1% of penicillin/streptomycin solution in a humidified atmosphere of 5% CO_2 at 37°C. The healthy MCF-10A cells were grown in Ham's F12 medium (Sigma Chemical Co., St. Louis, MO, USA) supplemented with 5% heat-inactivated horse serum, 10 μg/mL insulin, 100 ng/mL cholera toxin, 0.5 μg/mL hydrocortisone, 20 ng/mL EGF, and 100 μg/mL penicillin/streptomycin in a humidified atmosphere of 5% CO_2 at 37°C.

Uptake studies of Nile-Red-loaded nanocapsules

MCF-7, MCF-10A, and SK-BR3 cells ($1.5 X 10^5$) were seeded into 6-well plates under the culture conditions detailed above. After 24 h, cells were fed with fresh serum-free medium and treated with immuno-nanocapsules loaded by Nile Red. In the control groups, cells were treated with nonfluorescent nanocarriers. In this study, nanocapsules were formulated by adding Nile Red into the olive oil at a

concentration of 0.025% (w/w). Subsequently, the same protocol described above was used to coat the nanocapsule surfaces by our antibodies. After cell incubation, the wells were washed with PBS to remove free nanocapsules, which were harvested using phosphate-buffered saline-ethylenediamine-tetraacetic acid (PBS-EDTA), washed twice in cold PBS, and pelleted by centrifugation at 500 g for 10 min. Then the cells were fixed with 4% formalin for 20 min and then pelleted, resuspended in PBS, and analyzed for red fluorescence flow cytometry (FACScan, Becton Dickinson, San Jose, CA, USA). The fluorescence pulses were analyzed by the CellQuest Pro software.

Finally, the membrane binding and cell internalization of Nile-Red-labeled nanoparticles in MCF-7, MCF-10A, and SK-BR3 lines were also examined by laser-scanning confocal microscopy. Cells were imaged by a Leica TCS SP2 Confocal Spectral Microscope (UV–VIS) and the images were analyzed with Leica Confocal Software. All experiments were performed in triplicate and replicated at least twice. Sterility evaluations of all nanosystems were performed prior to develop nanocapsule uptake studies in order to exclude a possible biological contamination.

Cytotoxicity assays

The MCF-7, MCF-10A, and SK-BR3 cells (1 X 10^4) were plated into 96-well plates under the culture conditions detailed above. Cells were fed with fresh serum-free medium with 0.1 μM of free or encapsulated docetaxel for 24 h. Then cells were counted using the MTT colorimetric assay using a Titertek Multiscan apparatus (Flow, Irvine, California) at 492 nm. All the experiments were plated by triplicate wells and replicated at least twice.

Statistical analysis

SPSS 7.5 software (IBM, Chicago, IL, USA) was used for all data analyses. Results were compared with Student's t test. All data were expressed as means ± standard deviation (SD). Differences were considered statistically significant at a P value of < 0.05.

3. Results and discussions

Physico-chemical characterization of nanocapsules and immuno-nanocapsules

Particle size

The synthesis procedure yielded to a homogeneous population of nanocapsules with an average diameter of 180 ± 20 nm and a polydispersity index of 0.116. These results are similar to those previously reported using the same solvent displacement technique and similar shell components[29]. It is important to remark that the size of our nanosystem remained at a constant value under storage conditions, i.e. pure water and 4ºC for at least 3 months. Futhermore, this diameter is optimal for the use of our nanocapsules in potential *in vivo* applications where the size and size distribution is a decisive variable in ensure adequate bio-distribution by crossing biological barriers and minimizing the macrophageuptake[36].

Immuno-nanocapsules

Two different amounts of antibody molecules were initially incubated with our functionalized DC nanocapsules corresponding to medium and high protein

coverage. They were set theoretically at 2.5 mg/m^2 and 5.0 mg/m^2, respectively. This choice was based in previous research on colloidal nanoparticles. It is well established that the immobilization of antibody molecules on the surface of nanoparticles strongly alters their surface properties, notably affecting the colloidal stability of the nanosystem[37]. The development of immuno-nanoparticles for a successful use in the transport and directed delivery of drugs in biological systems requires equilibrium between colloidal stability and immuno-reactivity of the nanosystems. It was confirmed that colloidal particles of similar size with their surface saturated by IgG molecules (5 mgIgG/m^2) led to high levels of specific immunological detection but low colloidal stability, while a reduction of the IgG coverage increased the colloidal stability while diminishing the specific immunological recognition[38].

The covalent coupling was developed by means of the ECDI procedure, described in detail in the experimental section, and no aggregation of the nanosystem was observed during the experimental period. Figure 1 shows a schematic representation of the coupling process to produce the immuno-nanocapsules. After incubation time, the antibody-nanocapsule complexes were separated from unbound protein by a dialysis procedure, which is normally used when working with nanoemulsions and soft-particle systems[39], and has previously shown their efficacy working with the same type of nanocapsules.[29] These did not appreciably change in diameter after the covalent coupling of our antibodies. The size of each formulation (DC-anti-CRP-IgG, DC-anti-hCG-IgG-α [and β], and DC-anti-HER2-IgG) with both theoretical antibody coverages (medium and high) at pH 8.0 and low-ionic-strength medium remained similar to those of the original DC-systems regardless the antibody amount coupled on the surface.

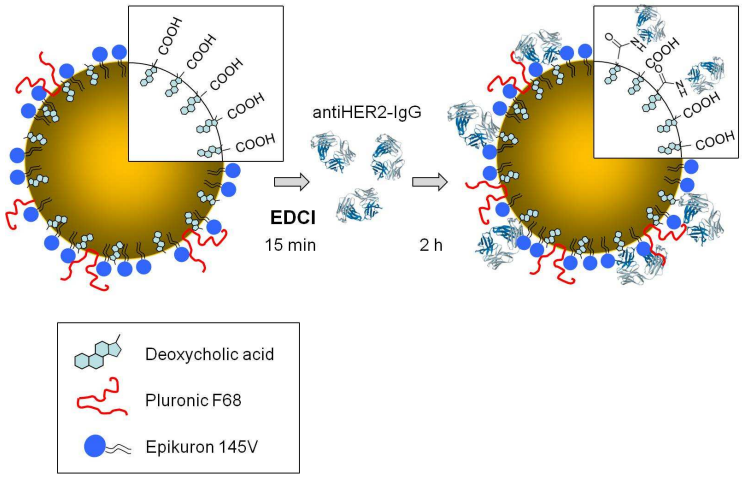

Figure 1. Schematic details of the preparation of our immuno-nanocapsules

The size stability with the anti-CRP-IgG sample may be interpreted as a first indication that all our particles possessed a medium coverage with regard to the surface antibody concentration, irrespective the theoretical anti-CRP-IgG load initially added. This statement is based on the fact that nanosystems with a high coverage of polyclonal antibodies on the surface usually show an notable size increase due to low colloidal stability and particle-aggregation processes, as reported elsewhere[26,40,41].

At this point, it becomes necessary to check first the presence of antibody molecules on the surface of the nanocapsules and then its final surface concentration. Subsequently, it would be also necessary to evaluate their colloidal and temporal stability, as well as the correct antigenic activity of the coupled antibody molecules, both of them being crucial properties for future biological applications. The presence of IgG on the nanocapsule surface was firstly estimated by gel-electrophoresis studies. The results from the analysis of the different systems

by SDS gel chromatography under reducing conditions confirm the immobilization of the different antibody molecules on the nanocapsules surface, showing a migration response typical for IgG antibodies, with two heavy and two light chains corresponding to an upper band at ~50 kDa (for the Fc fragment) as well as a lower band at ~25 kDa (for the Fab moieties)[42].

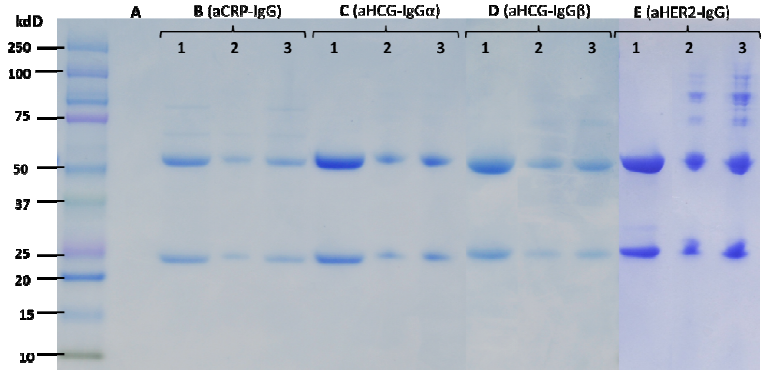

Figure 2. SDS-PAGE analysis under reducing conditions of different immuno-nanocapsules. *lane A*: Bared DC nanocapsules; *lanes B*: systems with anti-CRP-IgG; *lanes C*: systems with anti-hCG-IgG-α; *lanes D*: systems with anti-hCG-IgG-β; *lanes E*: systems with antiHER2-IgG. In all cases *number 1* corresponds to free antibody molecules, *number 2* corresponds to immuno-nanocapsules with an initial amount of 2.5 mg/m^2 of antibody, and *number 3* corresponds to immuno-nanocapsules with an initial amount of 5 mg/m^2 of antibody.

The image shown in Figure 2 corresponds to the analysis of the immuno-nanocapsules with our different antibody molecules coupled on the surface (lanes B to E), while lane A corresponds to the bare DC nanocapsules. Additionally, the final surface amount of antibody was evaluated using a densitometric procedure, and the coupling-efficiency results reached values of around 50-70% for the initial theoretical coverage of 2.5 mg/m^2 and around 30-40% with the 5 mg/m^2 coverage. The final coverage data for the different immuno-complexes are listed in Table 1.

These results are consistent with a low-medium final coverage for both initial situations, in which the final protein coverage of nanocapsules would be between 1,25mg/m^2 and 2 mg/m^2. As can discussed below, the results supplied by other physical properties of the immuno-complexes (i.e. electrophoretic mobility or colloidal stability) agree with this situation, which could be explained by the protective action of the PEO chains located in the nanocapsule shell against the protein approach. Beduneau et al. have indicated low coupling efficiency when working with monoclonal antibodies and Fab' fragment on functionalized nanocapsules as a consequence of the presence of PEG chains on the surface[39]. It is amply documented how the presence of PEO layers is frequently employed to reduce protein binding[43,44], and the effect on the protein adsoption processes is clearly reflected by a reduction in the amount of adsorbed proteins mediated by the presence of surface poloxamer molecules[45].

Table 1. Final antibody coverages for different immuno-nanocapsules and isoelectrics points (IEP) of the pure antibodies and the immuno-nanocapsules.

Initial theoretical coverage	**Final antibody coverage (mgIgG/m^2)**		**Antibody IEP**	**Complexes IEP**	
	2,5 mg/m^2	**5,0 mg/m^2**		**2,5 mg/m^2**	**5,0 mg/m^2**
DC-IgGαPCR	1,2	1,6	7,3	3,8	4,5
DC-IgGαhCG (Antibody α)	1,5	2,0	5,5	3,3	3,7
DC-IgGαhCG (Antibody β)	1,1	1,6	6,0	3,2	3,5
DC-IgGαHER2	1,7	2,1	9,2	7,0	7,4

Electrophoretic mobility

Electrophoretic mobility, μ_e, is an experimental parameter directly related to the zeta potential in the shear plane of the particles and is normally used to gain information concerning the surface electrical state of colloidal systems[26,46]. Thus,

the μ_e data reflect the composition of the nanocapsule surface and are influenced by both the ionic strength as well as the pH of the dispersion medium.

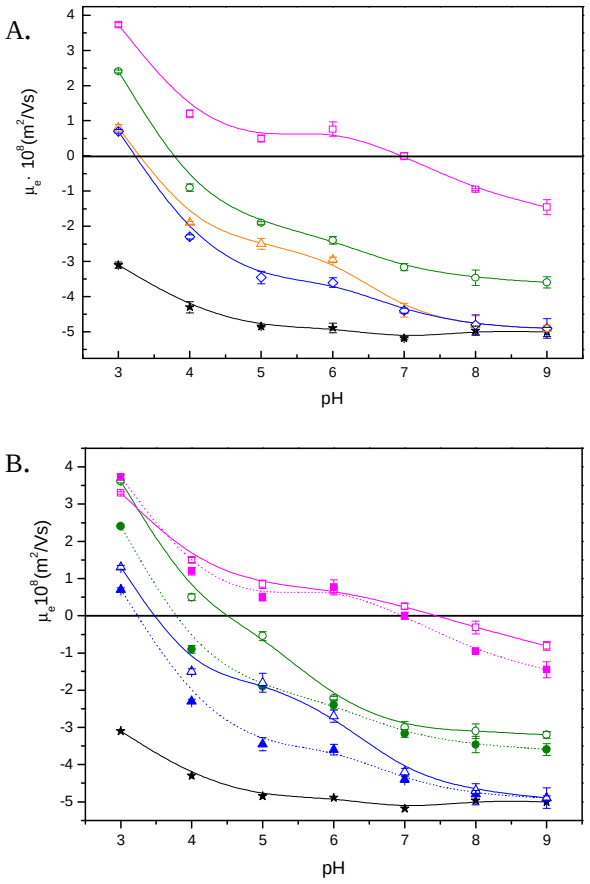

Figure 3 Electrophoretic mobility vs. pH in buffered media of low salinity (ionic strength equal to 0.002M) for the different nanosystems. **(A)** Immuno-nanocapsules with an initial theoretical antibody load of 2.5 mg/m². Bare DC (★), anti-HER2-IgG- (□), anti-PCR-IgG- (○), anti-hCG-IgG-α- (△), and anti-hCG-IgG-β- (◇) nanoparticles. **(B)** Immuno-nanocapsules with different initial theoretical antibody amounts. Bare DC (★), anti-HER2-IgG- (□, ■), anti-PCR-IgG- (○, ●), and anti-hCG-IgG-β- (△, ▲) nanoparticles. Dashed line with solid symbols correspond to a theoretical coverage of 2.5 mg/m² while solid lines with empty symbols are for 5.0 mg/m².

Usually, when colloidal particles are coated by protein molecules, the μ_e values change markedly compared with the same bare surfaces. In this way, the electrophoretic mobility was determined for all our systems in low-ionic-strength media at different pH values from 3.0 to 9.0 (see Figure 3A,B).

In terms of the electrokinetic behavior of bare DC nanocapsules, the μ_e results agree with the nature of the shell of these particles in which carboxylic groups predominate on the surface, showing the typical behavior of colloids with weak acid groups, that is, constant μ_e values at basic and neutral pH values that begin to fall to acidic pH around the pK_a (4.8) [47]. However, the most important aspect of the μ_e results is related to the presence of IgG molecules immobilized onto the nanocapsule surface, which significantly alters the mobility data. The μ_e results reflect the presence of antibody molecules on the nanocapsule surfaces and indicate a clear correspondence with the kind of adhered antibody and its respective IEP, as shown in Figure 3A. Clear differences appear depending on the antibody nature, revealing that the original IEP of the linked IgG molecules modulates the final IEP of the nanocomplex in which the antibody was immobilized. That is, for every system, the μ_e sign inverted at different pH values, being consistently below the IEP of the respective coupled antibody due to the change in surface charge of the nanoparticles by the positive electrical charge of the IgG molecules[37].

Additionally, it is well known that when a protein covers colloidal particles, the IEP of such complexes also depends on the degree of protein coverage, so that it gradually tends to the pure protein IEP when the protein load on the nanoparticles increases[38,39]. For an analysis of this point, Figure 3B presents the electrokinetic response of the immuno-complexes as a function of the theoretical initial coverage. As can be seen, little difference is found in the entire pH range when we compare the two coatings for each type of immuno-nanocapsule. In fact, from this figure we can estimate the IEP of the different systems for which the

values are shown in Table 1 together with the corresponding pure antibody IEPs. The IEP of our immuno-nanocapsules tends to the IEP of the respective pure antibody when their protein coverage increases. However, the minor differences between the two coverage situations appear to indicate that, in fact, the surface antibody density for both theoretical protein coverages is only slightly higher for the 5.0 mg/m^2 case compared to that of 2.5 mg/m^2 and, in all cases, it might correspond to a low-medium coverage degree. Several experimental results for polymeric colloidal particles partially coated by a polyclonal anti-CRP-IgG present an electrokinetic response very similar to that of our immuno-nanocapsules[26, 47].

Finally, another conclusion can be drawn taking into account the μ_e values shown in Figure 3B at neutral and basic pH, where we found a significant difference among the different immuno-nanocapsules related to the charge density of the antibody-layer surface. The antibodies with neutral and basic IEPs, i.e. anti-HER2-IgG and anti-CRP-IgG, cause sharp declines in the μ_e values due to the low charge densities of these two antibodies that screen the original negative surface charge of the DC nanocapsules. However, the complexes with the hCG specific antibody on their surface display mobility values close to those of the bare nanocapsules as a consequence of the higher negative net charge of these antibody molecules at neutral and basic pH. Given that μ_e values are usually indicative of the colloidal stability of the nanoparticles, their decrease at neutral and basic pH would represent a reduction of this important parameter.[26, 47] As shown below, the immuno-nanocapsules with anti-HER2 and anti-CRP antibodies present low colloidal stability at physiological pH.

It would be worthwhile to make a final discussion about the mobility data extracted at those pH values in which nanocomplexes were unstable, that is, at their corresponding IEPs. It should be noted that every mobility datum was taken from a stable nanocapsule pool that was buffered in the same solution used for the

covalent coupling of the antibodies, that is, pH 7 for the anti-hCG-IgG (α and β), pH 8 for the anti-CRP-IgG, and pH 10 for anti-HER2-IgG. In all cases, the average diameter was 180 nm. From these stable pools, a small volume (few μLs) was taken and poured into a 5 mL low salinity solution containing the desired buffer just before measuring the electrophoretic mobility. Dilution was so high that the final pH value was that supplied by the most volumetric solution. Subsequently, we waited for the stabilization of the particle charge in the new pH value during 5 minutes, and then the mobility datum was obtained. Even in those cases in which the pH coincides with the isoelectric point of the system, that is, pH where $\zeta \approx 0$, the aggregation kinetics were so slow due to the high dilution conditions that it was perfectly possible to extract mobility data in early times (the mentioned 5 minutes) before the system aggregates.

In summary, except for those cases in which the pH coincides with the isoelectric points of the nanocapsules, the size of the particles remains constant at around 180 nm. In the isoelectric points, the lack of net surface charge in the particle would provoke aggregation (see Table 2 for the anti-HER2 case). Nevertheless, the mobility data are always collected in the few first minutes of an aggregation process that takes place in high dilution conditions. That is, in an extremely slow process that permits to extract the mobility datum before aggregates start forming.

Colloidal stability

Colloidal stability was studied by analyzing the aggregation process of our particles dissolved at physiological pH (7.4) and using, independently, two different electrolytes (NaCl and $CaCl_2$) to trigger the aggregation. The analysis of the coagulation kinetics allows us to calculate an important parameter for colloidal stability: the stability factor, W, which is defined in the Introduction of the thesis

(1.7 Colloidal stability of nanoemulsions). Figure 4 shows the W dependence on the electrolyte concentration for bare DC and anti-HER2-IgG nanocapsules. From these experiments, we can estimate the CCC and CSC values following the procedure detailed in the introduction. The corresponding values for all the systems with both electrolytes are shown in Table 2. These data highlight two general points. On the one hand, the CCC values are always lower for $CaCl_2$ than for NaCl, due to the better screening power of the surface charge shown by divalent cations. On the other hand, the stability patterns clearly depended on the surface characteristics, and the presence of antibody molecules on the surface of the nanocapsules strongly modulated the CCC and CSC values.

In this scenario, we can start analyzing the results found for bare DC nanocapsules. The CCC values agree with the high electric potential previously observed in the electrokinetic experiments (see Fig. 3A and 3B). The high colloidal stability at any NaCl concentration is comparable to those previously found working with nanocapsules with a similar shell composition[33]. This stable situation is also influenced by the incorporation of poloxamer molecules into the shell, which increases the surface hydrophilicity attributed to the PEO fragments. In this way, a re-stabilization process at high or moderate salinity media –typically found with hydrophilic surfaces– has also been found working with $CaCl_2$, as reflected by the CSC value. This re-stabilization pattern is based on repulsive hydration forces that appear at medium and high ionic strengths on hydrophilic surfaces. With regard to the NaCl, the overlap of both CCC and CSC concentrations induces a completely stable system in which the repulsive hydration forces offset the decrease of the repulsive electrostatic interaction that takes place when the electrolyte concentration increases. [24]

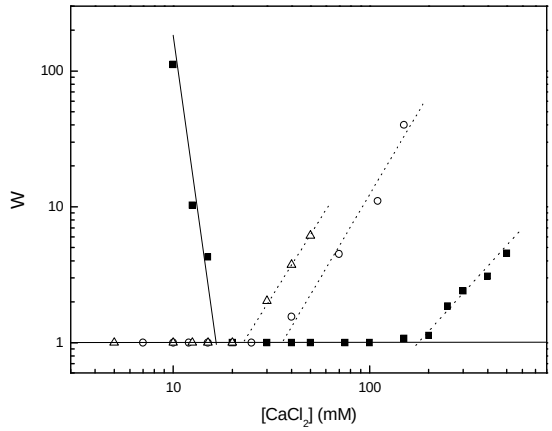

Figure 4. Stability factor vs. calcium chloride concentration at pH 7.4: Bare DC nanocapsules (■), 2.5mg/m²-anti-HER2-IgG particles (○), and 5mg/m²-anti-HER2-IgG ones (△). The solid line helps to locate the CCC value, while dashed lines point to the CSC data.

Analyzing the colloidal stability of immuno-nanocapsules under the same experimental conditions, we find significant differences. The colloidal stability of several nanoparticles-protein complexes are known to be dramatically modified depending of the kind of protein molecule and the degree of coverage.[26] The IEP of the adsorbed protein is key. Our polyclonal IgG molecules partially or completely coat the surface of latex nanoparticles, provoking a total destabilization of the colloidal system at neutral pH.[37,47] However, the use of other proteins as monoclonal antibodies, bovine serum albumin, or $F(ab`)_2$ fragments, all with acid IEPs, yields immuno-complexes that are colloidally stable under physiological conditions.[26,38] Therefore, a good correlation between the electrokinetic behavior and the colloidal stability was observed (see the CCC values in Table 2). Complexes covered by anti-hCG-IgG (α and β) showed, at neutral and basic pH, a electrophoretic mobility value similar to that of the DC bare nanocapsules, resulting in immuno-nanocapsules with practically the same CCC values, i.e. completely stable systems with the NaCl electrolyte and a CCC value of 20 mM for $CaCl_2$.

However, when the anti-CRP-IgG coated nanocapsules, colloidal stability sharply reduced with the NaCl electrolyte, and a very low CCC value was found with the $CaCl_2$ one. Finally, taking into account that immuno-nanocapsules with anti-HER2-IgG present a zero net electrical charge around neutral pH, we should expect completely unstable complexes, as shown in Table 2 for any situation, with systems completely aggregated at physiological pH.

Fortunately, the presence of antibody molecules coupled with the immuno-nanocapsule shell increases their hydrophilic character, as reflected in the re-stabilization processes at salt concentrations beyond the CSC values. As seen in Table 2, all the immuno-complexes showed CSC values lower than those of the DC nanocapsules due to a change from a partially hydrophilic surface to a highly hydrophilic one, clearly indicating again the presence of antibody molecules linked to the surface. This is a decisive point, given the biological application of our immuno-nanocapsules with anti-HER2-IgG.

As displayed in Figure 4, both anti-HER2-IgG complexes present an aggregation pattern in which the W-stability factor is equal to unity at an extremely low salt concentration, signifying complete instability at physiological pH. However, this parameter starts to rise in value for $CaCl_2$ concentrations above 20 mM, indicating re-stabilization phenomenon that could make these systems stable under usual physiological conditions of moderate salinity. The formation of a repulsive hydration shell around colloidal particles covered by protein molecules is a common process[48] previously noted working with similar lipid nanocapsules partially covered by antibody molecules[29]. Culture medium for *in vitro* studies and real physiological medium are composed of different electrolytes that generate hydration forces strong enough to maintain the colloidal stability of our immuno-nanoparticles. In this way, the time course of the stability was evaluated in the cell-culture medium (DMEM) and DMEM supplemented with fetal bovine serum, used

to develop the *in vitro* experiments, and all of our nanosystems remained stable, i.e. without aggregation, at least for 96 h.

On the other hand, the degree of coverage is another important variable to consider, since the colloidal stability normally decreases when the antibody coating increases and, in fact, several examples verify this situation working with lipid nanocapsules[29,41] or other colloidal systems, such as liposomes[40]. However, in view of the data in Table 2, the CCC and CSC values changed only slightly for the two initial theoretical coatings (2.5 to 5 mg/m^2), suggesting again that, in our nanocapsules, the final amount of protein linked to the surface was not very different, implying that the surface protein saturation corresponds to a medium degree of coverage, as discussed above regarding the electrokinetic results (see Fig. 3B).

Table 2. Critical coagulation concentrations (CCC) and critical stabilization concentration (CSC) of our different nanocapsules.

pH 7.4	**NaCl**				**$CaCl_2$**			
	2.5mg/m^2		**5mg/m^2**		**2.5mg/m^2**		**5mg/m^2**	
	CCC (mM)	**CSC (mM)**	**CCC (mM)**	**CSC (mM)**	**CCC (mM)**	**CSC (mM)**	**CCC (mM)**	**CSC (mM)**
Bared DC	stable				CCC: 18		CSC: 160	
DC-IgGαPCR	40	32	15	31	6	23	2	11
DC-IgGαhCG (Antibody 1)	stable	stable	stable	stable	23	43	20	38
DC-IgGαhCG (Antibody 2)	stable	stable	stable	stable	21	39	18	36
DC-IgGαHER2	aggr.	34	aggr.	33	aggr.	34	aggr.	24

Immunoreactivity

To complete the characterization of the immuno-nanoparticles, it is necessary to study the adequate disposition of the antibody molecules on the surface shell in order to check their potential use for bio-technological applications as directed drug carriers. Therefore, two of the three systems was used with this

aim, those with anti-CRP-IgG and anti-hCG-IgG (α and β). Many studies working with polystyrene nanoparticles and these antibodies demonstrate the validity of the EDCI covalent attachment method in order to produce nanosystems that have adequate immunological behavior[26,49]. Recently, in a previous study using the same procedure, soft immuno-nanocapsules were made using similar lipid nanocapsules and anti-CRP-IgG, with satisfactory immunological results [29].

The immunological agglutination of our immuno-nanocapsules was studied spectrophotometrically. Figures 5A and 5B show the optical absorbance change caused by the specific agglutination of our samples in the presence of the antigenic molecules, i.e. CRP and hCG molecules, respectively. Regarding the results from these figures, we should highlight two considerations: firstly, the immuno-agglutination reaction proceeds with satisfactory results for both systems, indicating that the EDCI procedure yields to an adequate surface disposition of the different antibody molecules for specific recognition; and secondly, there is little difference between the two initial theoretical coverages, again confirming that both complexes differ only slightly in the final surface protein density.

It is necesary to remark an important result shown in the last immunoreactivity figures. In order to confirm the covalent attachment of the different antibody molecules, the same coupling procedure in absence of EDCI was developed. Thus, the protein molecules physically interact with the surface shell of the DC soft lipidic nanocapsules. After the dialysis step, these new immuno-complexes were characterized in the same way showing a surprising result. While electrokinetics experiments confirms the presence of antibody molecules adsorbed on the surface, the immunoreactivity experiments did not show any optical aggregation, which could be related with a denaturation and/or an inadequate orientation of the surface antibody molecules. This is a situation that can happen

when surfactant molecules (e.g. poloxamer) presents on the surface shell interact with the antibody molecules[43].

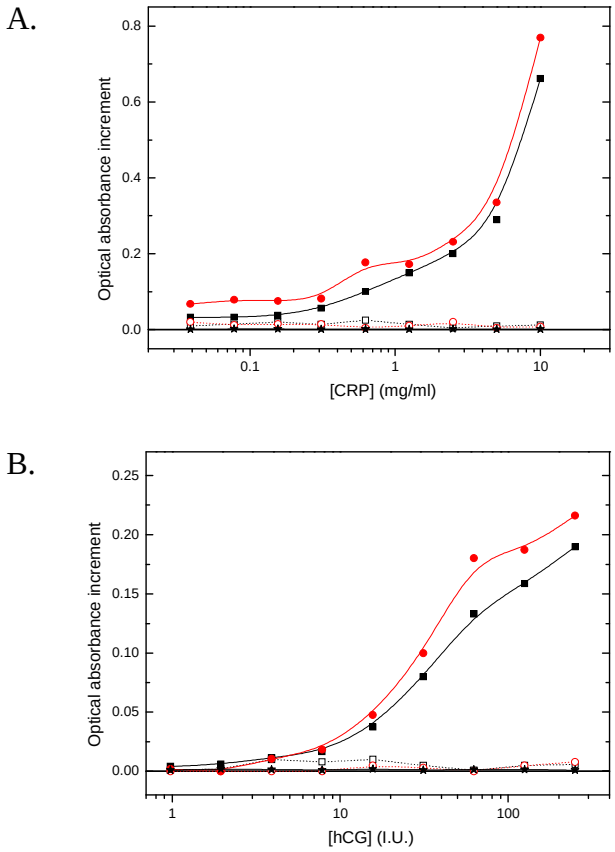

Figure 5. Absorbance increments after 5 min (λ = 570 nm) due to immunological aggregation. **(A)** Aggregation induced by different CRP concentrations: anti-CRP-IgG, 2.5 mg/m² (■,□); anti-CRP-IgG, 5.0 mg/m² (●,○); anti-hCG-IgG, 5.0 mg/m² (★). **(B)** Aggregation induced by different hCG concentrations: anti-hCG-IgG, 2.5 mg/m² (■, □); anti-hCG-IgG, 5.0 mg/m² (●,○); anti-CRP-IgG, 5.0 mg/m2 (★). Open symbols correspond to immuno-nanocapsules obtained without using the EDCI protocol.

Additionally, in order to check the immunological specificity, the immuno-agglutination of each type of immuno-nanocapsule was studied using three different antigens, CRP, hCG and human serum albumin (HSA). In all the cases, the experiment did not show any optical aggregation which represents an absence of cross reactions. As can be seen in figures 5A and 5B, immuno-agglutination was only observed when a sensitized nanocapsule system was incubated with its corresponding especific antigen. This is an important result, specially for the nano-system with antiHER2-IgG, that will be used later in the in vitro experiments.

Specific cellular uptake of trastuzumab-modified immuno-nanoparticles

The next set of experiments based on *in vitro* cell-culture studies will serve to demonstrate whether or not our anti-HER2-IgG nanocapsules can specifically recognize the HER2 receptors located in the cellular membrane of certain cell lines.

Breast-cancer cell lines have been used extensively in basic research and they have provided valuable insight into many aspects of breast-cancer biology. Cell lines are one of the most critical components in studying tumor carcinogenesis[50,51] and new therapeutic targets for breast carcinoma.[52,53] In our experiment, to assess whether our anti-HER2-IgG nanoparticles were properly vectorized, we selected three breast-cell lines: one non-tumorigenic cell line with low or no expression of HER2, MCF-10A and two human breast adenocarcinoma cell lines with low (MCF-7) and high (SK-BR3) levels of HER2 expression.[18,54] Moreover, these cell lines were used to study the cytotoxicity of the two docetaxel loaded immuno-nanoparticles formulations in comparison with free docetaxel as well as with the same drug carried into non-targeted DC nanoparticles.

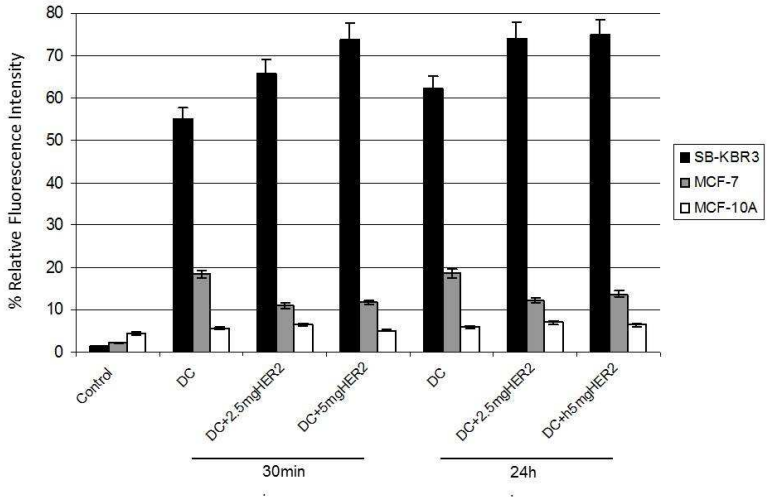

Figure 6. Quantitative study of cellular uptake efficiency for the bare DC particles, the 2.5mg/m^2-anti-HER2-IgG and the 5mg/m^2-anti-HER2-IgG immuno-nanocapsules loaded by Nile Red in SK-BR3 , MCF-7 and MCF-10A cells after 30 min and 24h.

Trastuzumab is used as a targeting ligand for breast-cancer cells overexpressing HER2[55]. In order to analyze whether the conjugation of Trastuzumab is an effective method for specific targeting nanocarriers towards HER2-positive breast-cancer cells, we used flow citometry to determine the cell uptake of the anti-HER2-IgG nanocapsules loaded by Nile Red. We compared the cellular uptake efficiency between the DC nanoparticles with or without Herceptin® conjugation to show that the Herceptin-conjugated nanoparticles were selective against breast-cancer cells with high HER2 expression. Figure 6 shows the fluorescence intensity of the cell cultures containing different nanosystems after 30 min. and 24h of incubation.

The results led us to perform a quantitative analysis of the different nanocapsules, showing that the internalization efficacy significantly changed by the nature and properties of the different shells. Our results indicate that our anti-

HER2-IgG immuno-nanocapsules, at both theoretical coverages (2.5 and 5.0 mg/m^2) were able to achieve a specific uptake in HER2-positive breast-cancer cells such as SK-BR3, whereas in the normal breast-cell line MCF10A no significant difference was detected in the uptake of the Trastuzumab modified and the non-targeted DC nanoparticles when compared to the control. That is, the 5mg/m^2-anti-HER2-IgG nanocapsules showed the highest fluorescent intensity (73.8%) in SK-BR3 cells in comparison to the 2.5mg/m^2-anti-HER2-IgG ones (65.65%) and DC particles (54.9%) ($P<0.01$). Moreover, the 5mg/m^2-anti-HER2-IgG nanocapsules uptake by SK-BR3 were 62.05% and 73.8% more intense than MCF-7 and MCF-10A, respectively ($P<0.01$). In MCF-7, we observed that both types of anti-HER2-IgG immuno-nanocapsules (2.5 and 5.0 mg/m^2) were able to decrease the uptake of Nile Red by 6.6% and 7.35%, respectively compared to the non-targeted DC nanoparticles ($P<0.01$). This is because the MCF-7 cell line is classified as luminal A subtype breast-cancer cells characterized by low levels or a lack of HER2 receptors on their surface[54], which impedes the entry of a large amount of nanoparticles. However, the non-targeted DC nanoparticles, having no Herceptin® on their surface, enter these cells more easily.

The same trend was observed after 24 h of exposure with the only difference that the uptake of 2.5mg/m^2- and 5mg/m^2-anti-HER2-IgG nanoparticles were similar in the SK-BR3 cell line. Our results confirmed that the anti-HER2-IgG immuno-nanocapsules specifically bind to the membrane HER2 molecules and are internalized by the cancer cells. These results are consistent with previous findings showing that Trastuzumab attachment increases internalization of different types of nanoparticles by HER2+ cells.[19,56,57] Moreover, Mi et al. (2012) demonstrated that the internalization of multimodality treatment nanoparticles with or without Herceptin conjugation into SK-BR3 cells after 30 min of incubation was 26.70% and 20.72%, respectively[57]. Therefore, greater uptake reported here compares favorably with these results.

Cellular uptake efficiency of non-targeted and targeted nanoparticles by SK-BR3 and MCF-7 cell lines after 30 min of incubation was qualitatively evaluated using confocal laser scanning microscopy. Fig. 7A, B, and C shows the confocal images of SK-BR3 cells incubated with DC, 2.5mg/m^2-anti-HER2-IgG and 5mg/m^2-anti-HER2-IgG particles, respectively. This images show that DAPI(4',6-diamidino-2-phenylindole)-stained nuclei are circumvented by the Nile-Red-loaded nanoparticles, indicating that they have been internalized into the cytoplasm of the cells. A comparison between two types of confocal images shows that the red-fluorescence intensity in Fig. 7B and C is higher than that in Fig. 7A, indicating higher cellular uptake efficiency of the Herceptin-conjugated nanoparticles. Moreover, the MCF-7 cell line clearly shows a much lower intensity level of Nile Red than do the SK-BR3 cells, and in this case the MCF-7 cells treated with DC without targeting properties display more uptake of Nile Red than the 2.5mg/m^2-anti-HER2-IgG and 5mg/m^2-anti-HER2-IgG nanoparticles.

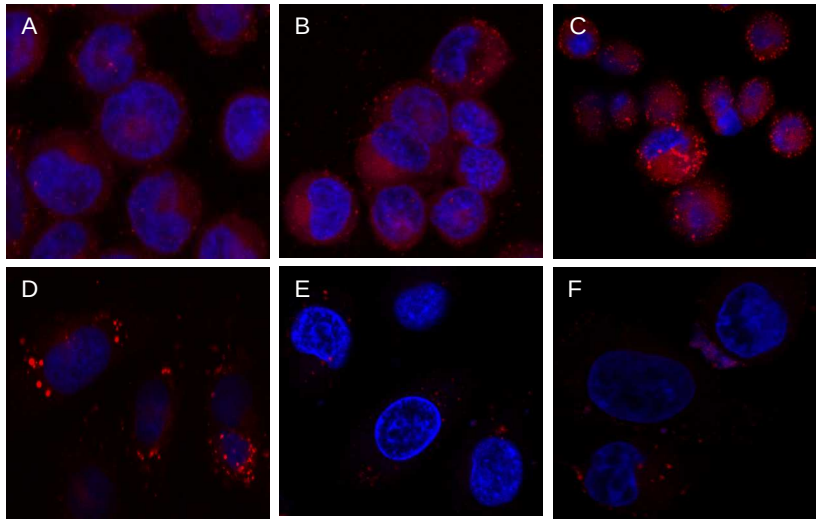

Figure 7. Confocal microscopy of SKBR-3 and MCF-7 cells after 30 min of exposure to DC particles (A, D), 2.5mg/m^2-anti-HER2-IgG (B, E), and 2.5mg/m^2-anti-HER2-IgG (C, F) immuno-nanocapsules, respectively.

Our results indicate that Tratuzumab could serve not only as a biological therapeutic agent but also as a targeting ligand to enhance the internalization of the nanoparticles into the HER2 overexpressed cancer cells. Indeed, these dual functions of Herceptin constitute another advantage of our DC nanoparticles. Nanoparticle uptake without a Trastuzumab coating may be a result of nonspecific binding interactions, e.g. hydrophobic binding of DC nanoparticles to the cell membrane.[58]

Cytotoxicity Assays of Docetaxel-loaded immuno-nanoparticles

The specific transport of the cytostatic drug docetaxel, their release, and biological activity were demonstrated in the last set of experiments. In addition to the cellular uptake of the immuno-nanoparticles, the therapeutic effect of these formulations was determined by MTT colorimetric assay.

The analysis of the encapsulation efficiency of docetaxel by high-performance liquid chromatography (HPLC) showed that the organic phase of the nanoparticles contained 85% of the drug. According to the data shown in Figure 8, after a 24h of incubation with 0.1μM of free docetaxel, the SK-BR3 cells showed a viability of 79.30% compared to 66.50%, 59.60%, and 62% for cells incubated with the same concentration of the drug encapsulated in the DC particles, the 2.5mg/m^2-anti-HER2-IgG ones, and the 5mg/m^2-anti-HER2-IgG nanocapsules, respectively. In this case, no difference in the cellular uptake as well as cytotoxic activity was observed between the 2.5mg/m^2-anti-HER2-IgG and the 5mg/m^2-anti-HER2-IgG immuno-nanocapsules. These results have the same tendency as those reported by Zhang et al.[59], who found 70% cell viability in SK-BR3 cells using nanoparticle-antibody bioconjugates for docetaxel delivery.

To demonstrate the specificity of our nanoparticle system, we incubated the weakly HER2-expressing control cell lines MCF-10A and MCF-7 with docetaxel-loaded Trastuzumab-modified nanoparticles and untreated DC nanoparticles. In the MCF-10A cell line, docetaxel-loaded DC nanoparticles showed more cytotoxicity (27.79%) than docetaxel-loaded 2.5mg/m²-anti-HER2-IgG particles (24.93%), 5mg/m²-anti-HER2-IgG nanocapsules (14.54%), and free docetaxel (5.5%). In the MCF-7 cell line, similar levels of cytotoxicity were induced by free (19.17%) and docetaxel-loaded DC nanoparticles (19.72%). However, the 2.5mg/m²-anti-HER2-IgG and 5mg/m²-anti-HER2-IgG immuno-nanocapsules showed lower levels of cytotoxicity 14.85% and 16.64%, respectively, which may be due to a specific nanoparticle uptake (Fig. 8). These results agree with those found with the Nile Red uptakes and verify the specificity and the biological activity of our newly designed ligand-targeted nanoparticles.

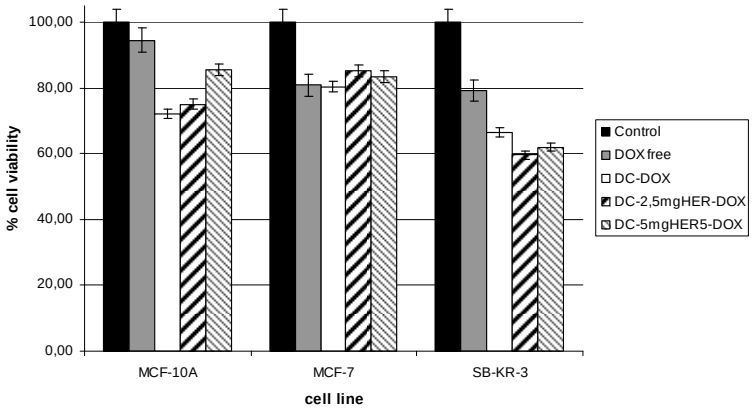

Figure 8. Cell-viability assay: Effect of free docetaxel and docetaxel-loaded DC particles, 2.5mg/m²-anti-HER2-IgG, and 5mg/m²-anti-HER2-IgG immuno-nanocapsules in SK-BR3, MCF-7- and MCF-10A cell lines. Untreated cells set the 100% standard.

Conclusions

The present work constitutes basic research aimed at optimizing a procedure to develop lipidic nanocapsules with specific recognition properties required nanosystems used in directed and controlled drug-delivery processes. A novel LNC system has been established, in which the shell was composed of phospholipids and Pluronic F68, and functionalized by carboxyl groups supplied by deoxycholic acid molecules.

We show the optimization of a successful procedure to covalently bind antibody molecules to these functionalized nanocapsules by means of a simple and reproducible EDCI method. The adhering antibody layer altered the original surface properties of the bare DC nanocapsules, changing their physico-chemical characteristics, as reflected in the results of electrophoretic mobility and colloidal-stability experiments. Additionally, the final surface hydrophilicity of the different immuno-nanocapsules favours the appearance of hydration repulsive forces allowing all immuno-nanoparticle systems to remain colloidally and temporally stable in saline solutions and in typical cell-culture media. Furthermore, the immunological recognition of specific antigen molecules and *in vitro* studies reveals the adequate surface disposition of the antibody molecules immobilized on the nanocapsule surfaces, suggesting their ability to deliver drugs selectively towards target cells.

Acknowledgments

The authors appreciate the financial support from the projects MAT2010-20370 (European FEDER support included, MICINN, Spain), PI10/02295 (Instituto de Salud Carlos III, Fondo de Investigación Sanitaria, FEDER funds)

and P07-FQM2496, P10-CTS-6270 and P07-FQM3099 (Junta de Andalucía, Spain). Also we wish to express our gratitude to Biokit S.A. for kindly donating the antiCRP antibody samples and to Operon S.A. for the kind donation of the anti-hCG antibody samples.

References

1. Duncan R. *Pharm J*. 2004, *273,* 485-488.

2. Foundation ES. Nanomedicine. An ESF–European Medical Research Councils (EMRC) Forward Look Report. *European Science Foundation*, Strasbourg. 2005.

3. Ferrari, M. *Nat. Rev. Cancer* 2005, *5*, 161-171.

4. Zhukov, N.V.; Tjulandin, S.A. *Biochemistry* 2008, *73(5)*, 605-618.

5. Gu, F.; Zhang, L.; Teply, B.A.; Mann, N.; Wang, A.; Radovic-Moreno, A.F.; Langer, R.; Farokhzad, O.C. *Proc. Natl. Acad. Sci. USA* 2008, *105(7)*, 2586-2591.

6. Heath, J.R.; Davis, M.E. *Annu. Rev. Med.* 2008, *59*, 251-265.

7. Peer, D.; Karp, J.M.; Hong, S.; Farokhzad, O.C.; Margalit, R.; Langer, R. *Nat. Nanotechnol.* 2007, *2(12),*751-760.

8. Delogu, L.G.; Venturelli, E.; Manetti, R.; Pinna, G.A.; Carru, C.; Madeddu, R.; Murgia, L.; Sgarrella, F.; Dumortier, H.; Bianco, A. *Nanomedicine* 2012 *7(2)*, 231-243.

9. Pescatori, M.; Bedognett, D.; Venturelli, E.; Ménard-Moyon, C.; Bernardini, C.; Muresu, E.; Piana, A.; Maida, G.; Manetti, R.; Sgarrella, F.; Bianco, A.; Delogu, L.G. *Biomaterials* 2013, *34*, 4395-4403

10. Lozano, M.V.; Torrecilla, D.; Torres, D.; Vidal, A.; Dominguez, F.; Alonso, M.J. *Biomacromolecules* 2008, *9(8),* 2186-2193.

11. Yoo, H.S.; Park, T.G. *.J Controlled Release* 2001, *70,* 63-70.

12. Allen, T.M. *Nat. Rev. Cancer* 2002, *10,*:750-763.

13. Torchilin, V.P. *Nat. Rev. Drug Discov.* 2005, *4,* 145-160.

14. Thierry, B. *Curr. Drug Deliv.* 2009, *6,* 391-403.

15. Moghimi, S.M.; Hunter, A.C.; Murray, J.C. *Pharmacol Rev.* 2001, *53,* 283-318.

16. Zhou, H.; Yu, W.; Guo, X.; Liu, X.; Li, N.; Zhang, Y.; Ma, X. *Biomacromolecules* 2010, *11*, 3480-3486.

17. Samstein, R.M.; Perica, K.; Balderrama, F.; Look, M.; Fahmy, T.M. *Biomaterials* 2008, *29*, 703-708.

18. Steinhauser, I.; Spankuch, B.; Strebhardt, K.; Langer, K *Biomaterials* 2006, *27*, 4975-4983.

19. Anhorn, M.G.; Wagner, S.; Kreuter, J.; Langer, K.; von Briesen, H. *Bioconjug. Chem.* 2008, *19*, 2321-2331.

20. Gao, J.; Kou, G.; Wang, H.; Chen, H.W.; Li, B.H.; Lu, Y.; Zhang, D.; Wang, S; Hou, S.; Qian, W.; Dai, J.; Zhao, J.; Zhong, Y.; Guo Y. *Breast Cancer Res. Tr.* 2009, *115*, 29-41.

21. Yang, H.M.; Park, C.W.; Woo, M.A.; Kim, M.I.; Jo, Y.M.; Park, H.G.; Park, H.G.; Kim; J.D. *Biomacromolecules* 2010, *11*, 2866-2872.

22. Goldstein, D.; Sader, O.; Benita, S. *Biomed. Pharmacother.* 2007, *61*, 97-103.

23. Malan, Y.; Loizidou, M.; Seifalian, A.M. *Trends Pharmacol. Sci.* 2009, *30(11)*, 592-599.

24. Santander-Ortega, M.J.; Lozano-Lopez, M.V.; Bastos-Gonzalez, D.; Peula-García, J.M; Ortega-Vinuesa, J.L. *Colloid and Polym Sci.* 2010, *288*, 159–172.

25. Ortega-Vinuesa, J.L.; Bastos-González, D. *J. Biomater. Sci., Polym. Ed.* 2001, *12*, 379-408.

26. Gupta, A.K.; Curtis, A.S.G. *Biomaterials* 2004, *25*, 3029-3040.

27. Pu, K.Y.; Shi, J.; Cai, L.; Li, K.; Liu, B. *Biomacromolecules* 2011, *12*, 2966-2974.

28. Salvati, A.; Pitek, A.S.; Monopol, M.P.; Prapainop, K.; Bombelli, F.B.; Hristov, D.R.; Kelly, P.M.; Åberg, C.; Mahon, E.; Dawson, K.A. *Nat. Nanotechnol.*, 2013, *8*, 137-143.

29. Sánchez-Moreno, P.; Ortega-Vinuesa, J.L.; Martín-Rodríguez, A.; Boulaiz, H.; Marchal, J.A. and Peula-García, J.M. *Int. J. Mol. Sci.* 2012, *13(2)*, 2405-2424.

30. Dávalos-Pantoja, L.; Ortega-Vinuesa, J.L.; Bastos-González, D.; Hidalgo-Álvarez, R. *Colloids Surf., B* 2001, 20, 165–175.

31. Xu, H.; Lu, J.R.; Williams, D.E. *J. Phys. Chem. B* 2006, 110, 1907-1914.

32. Choi, J.; Credit, K.; Henderson, K.; Deverkadra, R.; He, Z.; Wiig, H.; Vanpelt, H.; Flessner, M.F. Clin. *Cancer Res.* 2006; 12, 1906-1912.

33. Calvo, P.; Remuñán-López, C.; Vila-Jato, J.L.; Alonso, M.J. *J. Appl. Polym. Sci.* 1997, 63, 125-32.

34. Delgado Calvo-Flores, J.M.; Peula-García, J.M.; Martínez-García, R.; Callejas-Fernández J. *J. Colloid Interface Sci.* 1997, 189, 58-65.

35. L. Miller, 2012, http://lukemiller.org/index.php/2010/11/analyzinggels-and-western-blots-with-image-j/.

36. Panyam, J.; Labhasetwar, V. *Adv. Drug Deliv. Rev.,* 2003, *55,* 329-347.

37. Martin, A.; Puig, J.; Galisteo, F.; Serra, J.; Hidalgo-Alvarez, R. *J. Dispersion Sci. Technol.*, 1992, *13*, 399–416.

38. Peula, J.M.; Hidalgo-Alvarez, R.; de las Nieves, F.J. *J. Biomat. Sci. Polymer Edn.*, 1995, *7*, 231-240.

39. Goldstein, D.; Gofrit, O.; Nyska, A; Benita, S. *Cancer Res.*, 2007, 67, 269-275.

40. Koning, G.A.; Morselt, H.W.M.; Scherphof, G.L.; Kamps, J.A.A.M.; Gorter, A.; Allen, T.M. *Pharmaceut. Res.*, 2003, *20(8),* 1249-1257.

41. Beduneau, A.; Saulnier, P.; Hindré, F.; Clavreul, A.; Leroux, J.C.; Benoit, J.P. *Biomaterials*, 2007, *28*, 4978-4967

42. Nebija, D; Kopelent-Frank, H.; Urban, E.; Noe, C.R.; Lachmann, B. *J. Pharm. Biomed. Anal.,* 2011, *56*, 684-691.

43. Pop-Georgievski, O.; Popelka, S.; Houska, M.; Chvostova, D.; Proks, V.; Rypacek, F. *Biomacromolecules*, 2011, *12*, 3232-3242.

44. Delcroix, M.F.; Huet, G.L.; Conard, T.; Demoustier-Champagne, S.; Du Prez, F.E.; Landoulsi, J.; Dupont-Gillian, C.C. *Biomacromolecules*, 2013, *14*, 215-225.

45. Torcello-Gómez, A.; Santander-Ortega, M.J.; Peula-García, J.M; Maldonado-Valderrama, J.; Gálvez-Ruiz, M.J.; Ortega-Vinuesa, J.L.; Martín-Rodríguez, A. *Soft Matter*, 2011, 7, 8450-8461.

46. Couvreur, P.; Barratt, G.; Fattal, E.; Legrand, P.; Vauthier, C. *Crit. Rev. Ther. Drug Carrier Syst.*, 2002; *19*, 99-134.

47. Peula, J.M.; Hidalgo-Alvarez, R.; de las Nieves, F.J. *J. Colloid Interface Sci.*, 1998, *201*, 132-13.

48. Molina-Bolívar, J.A.; Ortega-Vinuesa, J.L. *Langmuir*, 1999, *15*, 2644-2653.

49. Stoll, S.; Ouali, L.; Pefferkorn, E. in *Colloidal Biomolecules, Biomaterials, and Biomedical Applications*, Ed. by Elaissari, A., CRC press 2003, *2*.

50. Peng, J.; Jordan, V.C. *Int. J. Oncol.* 2010, *36*, 451–458.

51. Martin, F.T.; Dwyer, R.M.; Kelly, J.; Khan, S.; Murphy, J.M.; Curran, C.; Miller, N.; Hennessy, E.; Dockery, P.; Barry, F.P.; O'Brien, T.; Kerin, M.J. *Breast Cancer Res. Treat.* 2010, *124(2)*,317-326.

52. Bonelli, M.A.; Fumarola, C.; Alfieri, R.R.; La Monica, S.; Cavazzoni, A.; Galetti, M.; Gatti, R.; Belletti, S.; Harris, A.L.; Fox, S.B.; Evans, D.B.; Dowsett, M.; Martin, L.A.; Bottini, A.; Generali, D.; Petronini, P.G. *Breast Cancer Res. Treat.* 2010, *124(1)*, 79-88.

53. Pietkiewicz, J.; Zielinska, K.; Saczko, J.; Kulbacka, J.; Majkowski, M.; Wilk, K.A. *Eur. J. Pharm. Sci.* 2010. 18, *39(5)*, 322-335.

54. Subik, K.; Lee, J.F.; Baxter, L.; Strzepek, T.; Costello, D.; Crowley, P.; Xing, L.; Hung, M.C.; Bonfiglio, T.; Hicks, D.G.; Tang, P. *Breast Cancer: Basic Clin. Res.* 2010, *4*, 35-41.

55. Sun, B.; Fena, S.S. *Nanomedicine.* 2009, *4*, 431–445.

56. Wuang, S.C.; Neoh, K.G.; Kang, E.T.; Pack, D.W.; Leckband, D.E. *Biomaterials.* 2008, *29(14)*, 2270–2279.

57. Mi, Y.; Liu, X.; Zhao, J.; Ding, J.; Feng, S.S. *Biomaterials.* 2012, *33(30)*, 7519–7529.

58. Nel, A.E.; Mädler, L.; Velegol, D.; Xia, T.; Hoek, E.M.; Somasundaran, P.; Klaessig, F.; Castranova, V.; Thompson, M. *Nat. Mater.* 2009, *8(7)*, 543–557.

59. Zhang, L.; Radovic-Moreno, A.F.; Alexis, F.; Gu, F.X.; Basto, P.A.; Bagalkot, V.; Jon. S.; Langer, R.S.; Farokhzad, O.C. *ChemMedChem.* 2007, *2,* 1268–1271

Paper V. Poloxamer functionalized lipid nanocapsules: the influence of the surface composition on cytotoxicity, protein adsorption, macrophage association and uptake by cancer cells

Paola Sánchez Moreno[1,2], Houria Boulaiz[2], José Manuel Peula García[1,3], Juan Luis Ortega Vinuesa[1], Pedro Buzón[4] , Irene Luque[4], Juan Antonio Marchal Corrales[2].

[1]Biocolloid and Fluid Physics Group, Department of Applied Physics, University of Granada, 18071 Granada, Spain; paolasm@ugr.es; jlortega@ugr.es

[2]Human Anatomy and Embryology Department, Regenerative Biomedicine Institute (IBIMER), University of Granada, Campus de la Salud, 18071, Granada, Spain; hboulaiz@ugr.es; jmarchal@ugr.es

[3]Department of Applied Physics II, University of Málaga, 29071 Málaga, Spain

[4]Department of Physical Chemistry, University of Granada, 18071 Granada, Spain; pbuzon@ugr.es; iluque@ugr.es

(Submitted)

Abstract

Different studies have shown the potential of lipid nanocapsules as hydrophobic drug delivery systems, especially in the field of cancer. To date, there are only few studies that offer a complete knowledge concerning to the physicochemical properties of this type of colloidal particles, examining the role played by their components and their impact on different cell lines. The aim of this study is to probe the ability of two surfactants of industrial interest with a markedly different nature, poloxamer Pluronic F127 (non-ionic) and Epikuron 145V (phospholipids), to provide different surface properties that influence the interaction of the lipid nanocapsules with the biological environment and cells. Four different systems have been formulated presenting an oily core and different shell compositions combining these two surfactants. A complete physicochemical characterization has been carried out and their ability to prevent protein adsorption onto the surface has been studied by different techniques such as electrophoresis or Isothermal Titration Calorimetry (ITC). Cellular uptake and cytotoxicity assays have been performed in a human lung cancer cell line and an additional uptake study has been carried out in an activated monocytic cell line. Our results demonstrated that poloxamer significantly reduces protein adsorption, compared to the other amphiphilic molecule, as well as the uptake and cytotoxicity is strongly dependent on the surface properties of the nanocarriers.

1. Introduction

The rapid advancement of nanomedicine has promoted the development of numerous nanosystems that can deliver drugs and other therapeutic agents to target tissues and that often possess complex structures and surface functionalizations (1-3).

Lipid nanocapsules have been studied in the pharmaceutical and medical fields, because they show promise as drug carriers as a result of their controlled and sustained release properties, subcellular size, and biocompatibility. Generally, these nanocapsules consist of a hydrophobic inner core which can incorporate lipophilic drugs and a hydrophilic outer shell that provides stabilization and offers the possibility of chemical modifications, among other important properties (4). Lipid nanocapsules play an increasingly important role for drug delivery in the field of cancer, showing greater advantages over other nanosystems such as liposomes in terms of leakage and drug loading, and have been shown by our group and others researchers to be effective carriers for delivering hydrophobic drugs like docetaxel (5-7). Due to their nanoscale size they can accumulate in tumor tissues more than they do in normal through enhanced permeability and retention effect (EPR) (8) and they can also been engineered and active targeted with different molecules against overexpressed receptors of cancer cells (9-11).

Following intravenous administration, a nanoparticle would be exposed to an evolved combinatorial system containing thousands of different proteins alongside lipids and sugars which can reconfigure nanoparticle dispersion and surface characteristics forming a "corona" (12-13). Recently has been shown that a biofunctional nanoparticle, quite basic in design, while it shows specific recognition of biological receptors in model *in vitro* conditions, it loses uptake and receptor specificity as the complexity of the environment is increased by introducing human

plasma (14). The proteins adsorbed onto the nanoparticle surface can interact with specific plasma membrane receptors on monocytes and various subsets of tissue macrophages, promoting rapid recognition and removing of the intravenously injected nanoparticles. Therefore, pharmacokinetics and biodistribution of nanoparticles are to a large extent governed by their surface properties dependent on the shell composition.

To prolong their half life in the bloodstream avoiding the recognition by the mononuclear phagocyte system (MPS), different coatings of grafting materials have been tailored in these nanosystems by using a variety of polymers such as poly (ethylene glycol) (PEG), poloxamers and poloxamines. PEG is a flexible, electrically neutral and hydrophilic polymer that has been commonly used to coat nanoparticles, to decrease the interaction of the surface with serum components and to prolong the particle circulation (15-19). Poloxamers (Pluronic®) and poloxamines (Tetronic®) have been used with the same purpose with different level of success (20-23). They are amphiphilic nonionic block polymers composed by hydrophobic propylene oxide (PO) fragments and hydrophilic ethylene oxide (EO) branches. Poloxamers consist of a central polyoxypropylene (POP) backbone, that is anchored onto the surface of the particles via hydrophobic interactions, which is flanked on both sides by two hydrophilic chains of polyoxyethylene (POE) that are extended outwards from the particles, yielding structures of the (POE) a (POP) b (POE) a type (24). Another important property presented by poloxamer and poloxamines is the inhibition of multidrug resistance (25, 26).

Within this scenario the goal of this study was to synthetize and physico-chemical characterize lipid nanocapsule systems, having as main objective to study how the surface physicochemical properties of these colloidal particles influence the protein adsorption, the macrophage association an the uptake by cancer cells. Thus, four lipid core-shell nanosystems have been obtained using a simple process

of synthesis. In all cases the hydrophobic core was constituted by olive oil, while the hydrophilic shell had a different composition. The commercially available and biocompatible surfactants composing the shell were pluronic F127, also known as poloxamer 407, which has been mainly choose because its properties of long term circulation and multidrug resistance, and Epikuron 145V (a mixture of phospholipid molecules), which provides negative charge to the surface of the nanocapsules.

Isothermal titration calorimetry (ITC) has been recently established as a method to characterize the interactions between molecules regarding thermodynamics, but only few publications describe the use of ITC to study the binding thermodynamics of nanoparticles with proteins (27,28). In this research, ITC has been used to asses the thermodynamics of binding of bovine serum albumin (BSA) and fetal bovine serum (FBS) onto the nanocapsule shells of the lipid nanosystem developed, which present different properties.

An additional uptake study in the human monocytic U937 cell line after activation with phorbol myristate acetate (human U937 macrophage-like) was performed to determine the resistance of these nanocapsules to the clearance by the immunitary system depending on their surface composition. Coumarin 6 was encapsulated in the hydrophobic core to carry out the *in vitro* uptake studies and docetaxel-loaded nanosystems were prepared to perform the cytotoxicity assay in the A549 cell line.

2. Materials

Poloxamer 407 (Pluronic F127) was purchased from Sigma-Aldrich (Spain). It is a triblock copolymer based on poly (ethylene oxide)-block-poly (propylene oxide)-block-poly (ethylene oxide) structure, expressed as PEOa–PPOb–PEOa being a= 100 and b= 65. The central hydrophobic block of PPO links to the oil while the two hydrophilic chains of PEO remain in the aqueous environment. Coumarin 6, Sulforhodamine-B and olive oil were also purchased from Sigma and all of them were used as received except olive oil that was previously purified with Activated Magnesium Silicate (Florisil, Fluka) to eliminate free fatty acids. Epikuron 145V, which is a highly purified deoiled phosphatidylcholine-enriched fraction of soybean lecithin, with an average molecular weight of 760 Da, was kindly supplied by Cargill Ibérica S. L. Docetaxel, with a purity ≥ 97.0%, was obtained from Fluka (Spain). Water was purified in a Milli-Q Academic Millipore system. Other solvents and chemicals used were of the highest grade commercially available.

3. Methods

Preparation of lipid nanoparticles

The nanosystems studied were prepared by a modified solvent-displacement technique following the procedure of Calvo et al. (29). Briefly, an organic phase composed of 125 μL of olive oil, dissolved in 0.5 mL of ethanol, and 9.5 mL of acetone, was added to 20 mL of an aqueous phase under magnetic stirring. Epikuron 145V and Pluronic F127 were dissolved in the organic phase and the aqueous phase respectively in different combinations. Organic solvents (acetone and ethanol) plus a portion of the volume of water were evaporated in a rotary evaporator at 40°C, giving a final volume of 18 mL. Finally, nanoparticles were

extensively cleaned by dialysis against ultrapure water for 24h to remove the unbound surfactant molecules.

The hydrophobic core of all the nanosystems were composed by olive oil and, depending on the composition of the organic and aqueous phases, the final sample showed different interface properties. Thus, four different systems were formulated: nanocapsules with a surface shell composed exclusively by epikuron 145V (referred as EP), nanocapsules with only pluronic F127 (PL) and two systems combining both surfactants in different proportion, nanocapsules with a predominance of pluronic F127 (MP) and nanocapsules with a predominance of epikuron 145V (ME) (see Table 1 and Figure 1).

Table 1. Concentration (mg/mL) of surfactant added in the synthesis of PL, EP, MP and ME nanocapsules

Nanocapsules	Pluronic F127	Epikuron 145V
PL	3,89	0
EP	0	2,22
MP	3,89	0,22
ME	0,39	2,22

Docetaxel-loaded lipid nanocapsules were formulated by dissolving docetaxel in the olive oil phase at a concentration of 0.7% (m/w). The concentration of docetaxel encapsulated in the particles during the different times of dialysis was determined by dissolving an aliquot of docetaxel loaded nanoparticles with acetonitrile. This sample was centrifuged during 20min at 4000 x g and the supernatant was measured in the Scientific Instrumentation Center of the University of Granada,

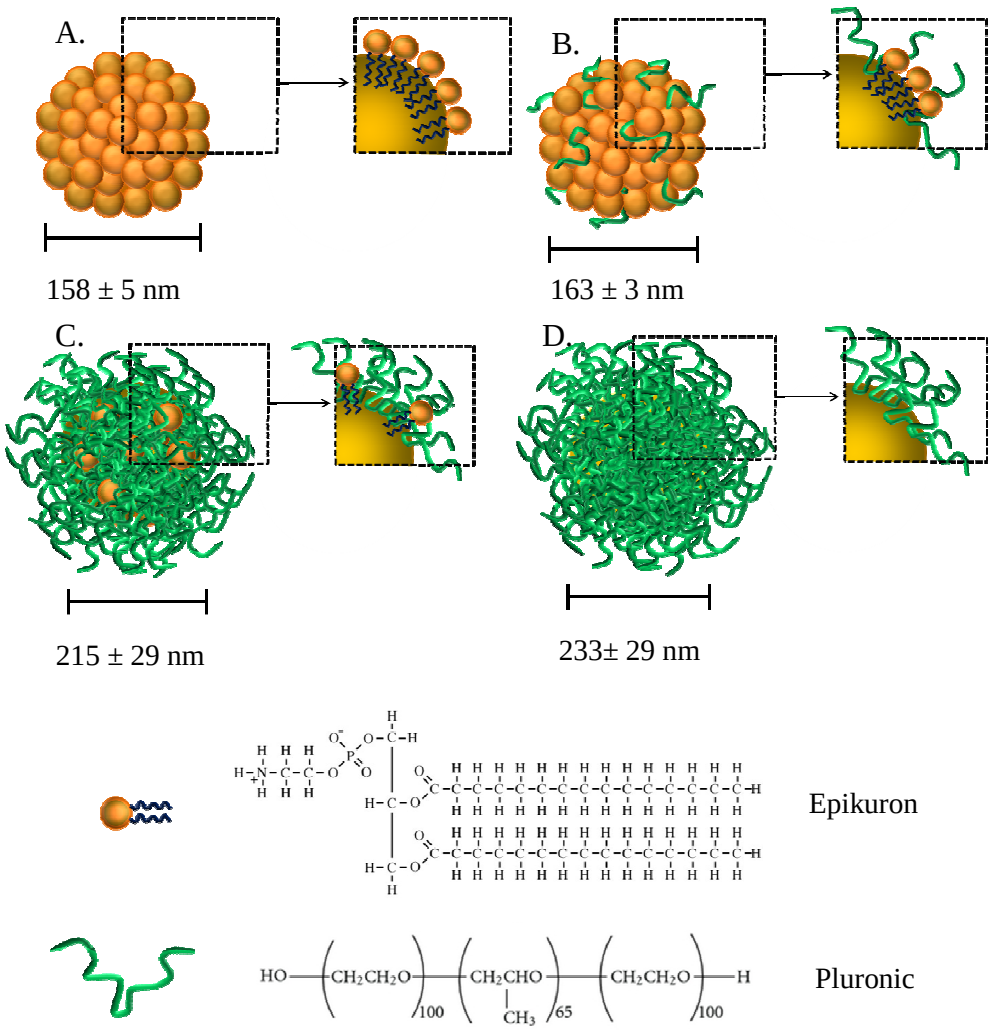

Figure 1. Schematic details of the composition and size of the four different nanosystems. A) EP nanocapsules. B) ME nanocapsules. C) MP nanocapsules. D) PL nanocapsules.

using a SHIMADZU LC-20AC chromatograph with SPD-M20A diode array detector and C8 Nova-Pak Cartridge column (4 microns, 4.6 x 150 mm); detection was performed at a wavelength of 230 nm. Coumarin 6 lipid nanocapsules were

formulated as before dissolving the dye in the olive oil phase at a concentration of 0.6% (m/v).

Physico-chemical characterization

Size and electrophoretic mobility

The hydrodynamic mean diameter of the nanocapsules and the electrophoretic mobility (μ_e) as a function of pH was determined using a nano-zeta dynamic light-scattering analyzer (Zeta-Sizer NanoZ, Malvern Instruments, UK).

The size and the homegeneity of the size distribution, expressed as polydispersity index (PDI), were obtained by means of the Stokes-Einstein equation using the diffusion coefficient measured by dynamic light scattering. The light scattered by the samples was detected at 173°, and the temperature was set at 25°C.

Electrophoretic mobility measurements were carried out after pouring a small volume of the nanocapsule stock (with a total surface equal to 0.05 m^2) into a 1 mL of a low salinity solution (0.002 M) containing the desired buffer, we waited for the stabilization of the particle charge in the new pH value during 5 minutes, and then the mobility datum was obtained in triplicate.

Colloidal stability

These experiments provide information related to the charge density of the nanoparticle surface, and the surface hydrophilicity. Sample stability was studied at physiological pH (i.e. 7.4) monitoring the turbidity of the systems with a Beckman

DU 7400 spectrophotometer, working at λ = 570 nm. NaCl and $CaCl_2$ were used as aggregating salts, independently.

From the analysis of aggregation kinetics results we were able to calculate the critical coagulation concentration (CCC) defined as the minimum salt concentration at which the system begins to re-stabilize when salinity is increased even more and related with the surface hydrophilicity (11).

Isothermal Titration Calorimetry (ITC).

ITC experiments were carried out using a high-precision ITC-200 titration calorimeter (Microcal Inc., Northampton, Massachusetts). The samples were extensively dialyzed against 2mM sodium phosphate buffer, pH 7.4, using 14,000 MWCO dyalisis membranes for nanocapsules and BSA, and 1,000 MWCO menbrane for FBS. Nanocapsule samples were placed in the cells and were progressively titrated with BSA or FBS. In all cases, a profile of injection volumes from 0.8 to 4 μl was used to better define the BSA and FBS titration curves. The heat evolved after each BSA or FBS injection was obtained from the integral of the calorimetric signal. The heat associated with the binding process was obtained as the difference between the heat of reaction and the corresponding heat of dilution, as obtained from independent titrations of BSA and FBS into the buffer.

The resulting binding isotherms were analyzed by non-linear least-squares fittings to a model corresponding to a single set of identical sites, according to the equation:

$$Q = \frac{V_0 \Delta H}{2K_a}\left[1 + K_a[L_t] + nK_a[M_t] + \sqrt{(1 + K_a[L_t] + nK_a[M_t])^2 - 4nK_a^2[M_t][L_t]}\right]$$

(equation 1)

where Q is the net heat of binding, n is the number of binding sites, □□H is the change in the enthalpy due to the binding process, K_a is the association constant, V_0 is the active cell volume, and $[M_t]$ and $[L_t]$ represent the total concentrations of nanocapsule and the titrant, respectively.

The binding isotherms corresponding to the titration of EP and ME nanocapsules with FBS, which could not be properly reproduced by this model, were analyzed according to a model of two sets of independent binding sites. According to this model, the net heat of binding can be expressed as:

$$Q = V_0[M_t]\left[\Delta H_1 \frac{n_1 K_1[L_t]}{1 + K_1[L_t]} + \Delta H_2 \frac{n_2 K_2[L_t]}{1 + K_2[L_t]}\right]$$

(equation 2)

where Q is the net heat of binding, n_1 and n_2 are the number of sites of each class, ΔH_1 and ΔH_2 are the change in the enthalpy due to the binding process for each site, K_1 and K_2 are the association constants for each site, V_0 is the active cell volume, and $[M_t]$ and $[L_t]$ are the total concentrations of nanocapsule and the titrant, respectively. In this case, the molar concentration of FBS was estimated considering a total protein concentration in FBS of 40 mg/mL and the molecular weight of BSA.

In all cases, the models were implemented in Origin 7.0 software (OriginLab Corporation, Northampton, MA). For the least-squares fit, the number

of binding sites, the association constant, and the binding enthalpy were considered as floating parameters.

Cell lines and culture conditions

The human lung-cancer cell line A549 was supplied by the Scientific Instrumentation Center of the University of Granada (Spain). Cells were maintained as monolayer cultures in DMEM (Sigma) and the human leukemic monocytes lymphoma cell line, U937, was maintained in a monocytic cell suspension in RPMI-1640 (Sigma) culture medium. Both cell lines were supplemented with heat-inactivated 10% (v/v) fetal bovine serum (FBS, Sigma), 2% L-glutamine, 2.7% sodium bicarbonate, 1% Hepes buffer, and 1% of penicillin/streptomycin solution in a humidified atmosphere of 5% CO_2 at 37°C. Treatment of U937 cells with phorbol 12-myristate 13-acetate (PMA) mimics the activation/differentiation of monocytes in vivo (175). Cells were activated to macrophages for 48 h with the addition of 10ng/mL PMA to the culture medium (176).

Uptake studies of Coumarin 6-loaded nanocapsules

U937 (1,5 X 10^5) were seeded into 6-well plates and activated with PMA for 48 h. A549 cells (1,5 X 10^5) were also seeded under the culture conditions detailed above. After 24 h, cells were fed with fresh medium and treated with nanocapsules loaded by Coumarin 6. In the control groups, cells were treated with nonfluorescent nanocarriers. After cell incubation, cells were washed three times with PBS to remove free nanocapsules, then harvested using phosphate-buffered saline-ethylenediamine-tetraacetic acid (PBS-EDTA) and pelleted by centrifugation. Then the cells were fixed at room temperature with a 4% formalin solution for 20 min and re-suspended in PBS before measuring the cell-associated fluorescence

(15,000 cells per sample) using a FacsCalibur flow cytometry device (Becton Dickinson). The results are reported by averaging the distribution of cell fluorescence intensity, working with three independent replicates. Error bars represent the standard deviation between replicates. Each experiment was performed at least three times.

In addition, uptake efficiency of Coumarin 6 loaded nanoparticles in the A549 cell line was qualitative studied by fluorescence microscopy. Cells were imaged by a Leica DM5500 microscope. All experiments were performed in triplicate and replicate at least twice.

Cytotoxicity assay

A549 cells (2×10^4) were plated into 24-well plates under the culture conditions detailed above. Cells were fed with fresh medium and increased concentrations of free and encapsulated docetaxel for 48 h. Then cells were counted using the sulforhodamine-B (SRB) colorimetric assay in a Titertek Multiscan apparatus (Flow, Irvine, California) at 492 nm. IC_{50} values were calculated from semi-logarithmic dose-response curves by linear interpolation. All experiments were performed in triplicate wells and were carried out at least three times.

Statistical analysis

SPSS 7.5 software (IBM, Chicago, IL, USA) was used for all data analyses. Results were compared with Student's t test. All data were expressed as means ± standard deviation (SD). Differences were considered statistically significant at a P value of < 0.05.

4. Results and discussion

Physico-chemical characterization of nanocapsules

Particle size

The synthesized nanoemulsions were stable under storage conditions, —pure water and 4ºC— for at least 3 months. The average diameter and PDI of the nanocapsules (see Figure 1) were 158± 5 nm and 0.108 for EP, 163± 3 nm and 0.110 for ME, 215± 29 nm and 0.125 for MP and 232± 29 nm and 0.146 for PL nanocapsules.These results are similar to those previously reported using the same solvent displacement technique and similar shell components (32). Futhermore, this diameter is optimal for the use of these nanocapsules in potential *in vivo* applications allowing these drug delivery systems to extravasate into tumor tissues, accumulate, and release the therapeutic drug locally through the "enhanced permeability and retention" (EPR) effect. (33). Considering the size differences among the systems, epikuron appears to be the best emulsifier, since the EP nanocapsules mean diameter was lower when this molecule acted by itself stabilizing the formulation, and even when it was mixed with pluronic F127 but remaining as the main component of the system (ME nanocapsules). When both types of molecules, epikuron 145V and pluronic F127, were mixed being poloxamer the main component of the shell and when the poloxamer acted by itself stabilizing the emulsion, the nanocapsules size increased. These results are concordant with previous data in which the presence of poloxamer together with lecithin increased the particle size in comparison to the case in which lecithin was the only component of the shell (34).

Electrophoretic mobility

The electric state of the different nanoparticles was determined by electrophoretic mobility (μ_e) measurements. The μ_e data reflect the composition of the nanocapsule surface and are influenced by both the ionic strength as well as the pH of the dispersion medium. The electrophoretic mobility was measured as a function of the pH of the medium. The electrophoretic mobility data, gathered from low ionic strength media, are shown in Figure. 2.

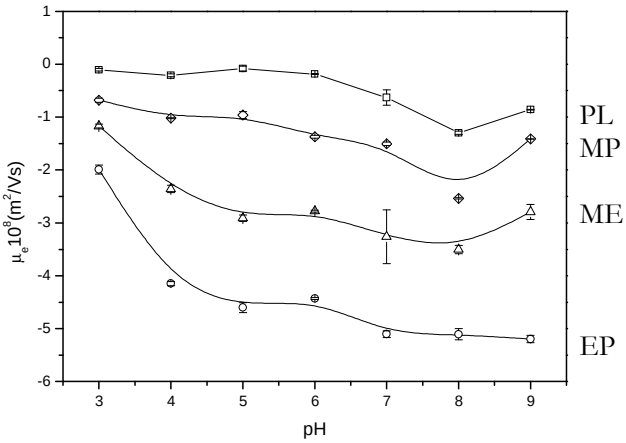

Figure 2: Electrophoretic mobility vs. pH in buffered media of low salinity (ionic strength equal to 0.002M) for the different nanosystems. PL (□), EP (○), ME (△) and MP (◇) nanocapsules.

EP nanocapsules showed the typical behavior of colloids with weak acid groups at the surface, giving lower electrophoretic mobility (in absolute value) at acid pH values than those obtained at neutral and basic pH. These groups come from the shell formed by Epikuron, in which phosphatidylcholine is the major component. The main effect when pluronic is present in the nanocapsules is the reduction (in absolute value) of μ_e in comparison with the pure epikuron nanocapsules, since the presence of polyethylene oxide (PEO) chains cause a

displacement of the shear plane of the diffuse layer resulting to lower mobility values. That is the case of ME nanocapsules in which the mobility remains negative but decreases in absolute value since the shell is formed mainly by epikuron but also by Pluronic and MP nanocapsules with even lower μ_e by increasing the Pluronic concentration and decreasing the Epikuron load. Finally PL nanoparticles with a shell constituted only by pluronic presented the lowest mobility values (neutral or nearly neutral). Mobility comes from a combination of electrical and frictional forces and the presence of this non ionic surfactant on the particles affects both forces (35).

In order to investigate the ability of the poloxamer molecules to alter the protein adsorption on lipid nanoparticles, all the system were incubated in 10% of fetal bovine serum at 37 °C. The presence of proteins molecules adsorbed onto the particles can be determine studing the electric state of the different nanoparticles since usually, when colloidal particles are coated by a protein, the original isoelectric point (IEP) of the bare particles moves towards the IEP of the proteins (13).

The μ_e results reflect the presence of proteins adsorbed on the nanocapsule surfaces and clear differences appear depending on the nanocapsules shell nature and the degree of protein coverage. The analyzed protein adsorption patterns are likely to be affected by both the type of surfactants and the charge being present (see Figure 3).

The presence of proteins adsorbed onto the EP particles caused a significant alteration of its original μ_e. In this case, the electrophoretic mobility even inverted its sign at pH 4, from -4,14 to 0,64 Adsorption on nanoparticles also resulted in changes in the surface charge of the nanocapsules with a combination of both surfactants: at pH 4 the μ_e values changed from -2,36 to 0,54 for ME nanocapsules, and from -1,01 to 0,10 for MP nanocapsules. An increase of the

poloxamer proportion in the shell reduced the difference between the mobility values of bare nanocapsules and complexes with protein on the surface by reducing the protein adsorption, in accordance with several studies (33, 35-36).

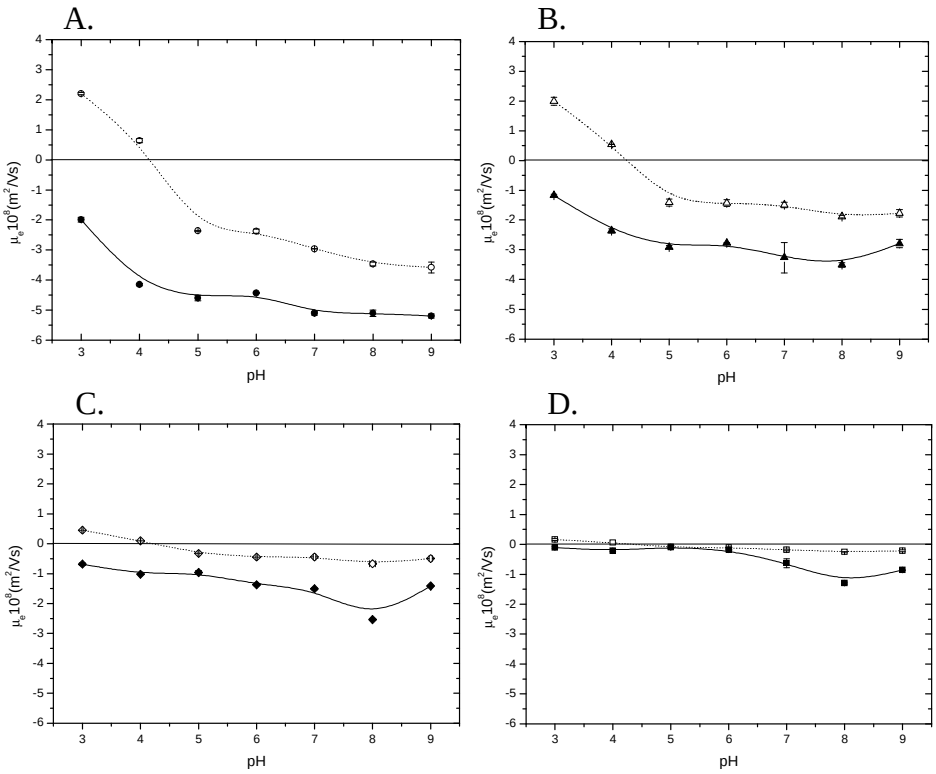

Figure 3 Bare nanocapsules and nanocapsules incubated with 10% FBS for 1hour at 37ºC, **A)** EP (○, ●), **B)** ME (△, ▲), **C)** MP (◇,◆) and **D)** PL (□, ■) nanoparticles. Dashed lines with solid symbols correspond to particles after the exposure with proteins while solid lines with empty symbols are for bare nanoparticles.

As can be seen, the lowest difference was found in the entire pH range when we compared the PL nanoparticles before and after the incubation with 10% FBS, indicating lesser extent of protein adsorption in this type of particle. In particular at pH 4 the electrophoretic mobility barely changed. Roser et al. showed that neutrally charged particles have a much lower opsonization rate than charged

particles, demonstrating a direct correlation between surface charge and protein binding (37). Therefore, the use of molecules such as poloxamers which can block the electrostatic and hydrophobic interactions is a good method to slow the adsortion of proteins

Calorimetric study of protein adsorption

Isothermal titration calorimetry was used to further investigate the differential protein adsorption potential of the different nanosystems. This technique provides a full thermodynamic characterization of the binding equilibrium in terms of binding affinity, number of binding sites and enthalpic and entropic contribution to the Gibbs energy of binding, reporting on the nature and magnitude of the forces driving the interaction. Upper panels in Figure 4 show the calorimetric titrations of the four types of nanocapsules with Bovine Serum Albumin (BSA). The corresponding binding isotherms are shown in the lower panels together with the best fit to a one set of sites model. The results of the thermodynamic analysis are summarized in table 2.

Nanocapsules bound to BSA with moderate dissociation constants in the low microMolar range. In all cases, protein binding was driven by a strongly favorable binding enthalpy that increased progressively with poloxamer content, suggesting that poloxamer strengthens the interaction with BSA. This increment in binding enthalpy was partially compensated by a parallel increase in unfavorable entropic contributions, resulting in a slight increase (of about 1 $kcal \cdot mol^{-1}$) in binding affinity for MP and PL particles with respect to ME and EP. Most interestingly, a high poloxamer content leads to a marked reduction in the number of binding sites that drops from $116x10^3$ sites per μm^{-2} for the EP particles to $24x10^3$ sites per μm^{-2} for PL particles.

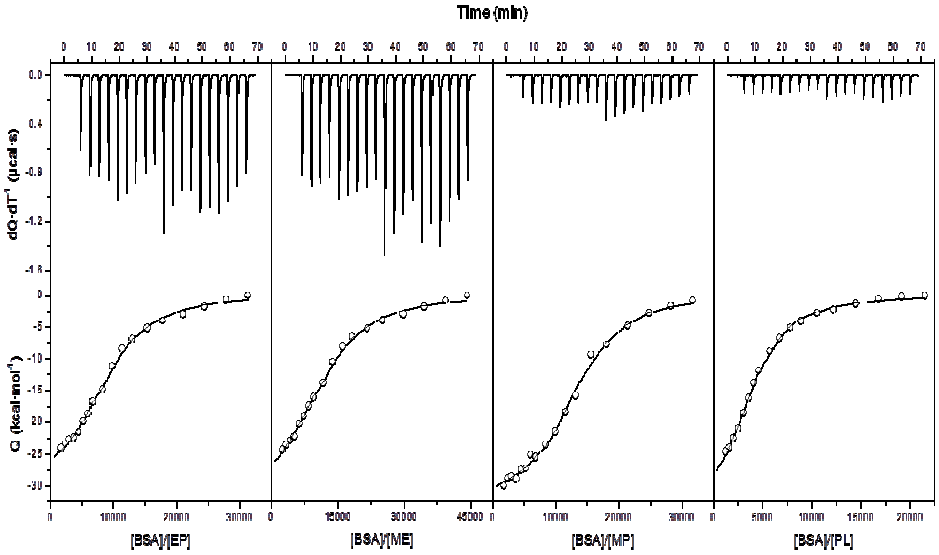

Figure 4. Isothermal titration calorimetry experiments for EP, ME, MP and PL nanoparticles with BSA at 25ºC in 2mM sodium phosphate pH 7.4. Upper panels show the heat effects associated with the injection of BSA into the calorimetric cell containing the the nanoparticle. Lower panels show the corresponding binding isotherm normalized for nanoparticle concentration and corrected for the heat of BSA dilution. Solid lines correspond to the best fit of data to a one-site model (equation 1).

A similar set of titration experiments were performed with Fetal Bovine Serum (FBS) in order to validate the results obtained with isolated BSA (see Figure 5). As before, the binding properties of the nanocapsules changed progressively as they were enriched in poloxamer. As illustrated in Figure 5, titrations of EP and ME nanocapsules show a more complex binding isotherms that cannot be described by a simple one-set of sites model but can be adequately reproduced by a model considering two different set of sites. This analysis reveals a tight binding event, characterized by dissociation constants in the nM range, superposed to another characterized by dissociation constant close to what was measured for the isolated BSA. This tight binding contribution is not observed for PL particles that is

perfectly described the one-set of sites model. In the case of MP particle, an intermediate behavior is observed. The curve can be fitted to a one-set of sites model, although slight systematic deviations are observed at high saturation.

Table 2. Binding thermodynamics of BSA and FBS to nanocapsules.

Protein Sample	Nanocapsule	n (10^3)	n / Area (10^3 n·µm^{-2})	Kd (µM)	ΔH_{ap} (kcal·mol^{-1})	$-T\cdot\Delta S_{ap}$ (kcal·mol^{-1})	ΔG_{ap} (kcal·mol^{-1})
BSA	**EP**	9.1	116.0	4.7	-30.1	22.9	-7.2
	ME	11.8	141.4	7.2	-32.9	25.9	-7.0
	MP	13.0	89.5	1.1	-32.6	24.4	-8.2
	PL	4.1	24.0	1.0	-35.0	26.8	-8.2
FBS	**EP**	53.5 16.8	682.1 214.2	3.6 0.057	-3.0 -11.4	-4.4 1.5	-7.4 -9.9
	ME	68.6 19.6	821.9 234.8	2.5 0.071	-1.9 -11.7	-5.7 1.9	-7.6 -9.8
	MP	32.7	225.2	1.8	-11.1	3.2	-7.9
	PL	11.0	64.5	3.9	-18.4	11.0	-7.4

For all particles, at least one binding event is identified with binding affinities very close to those measure for BSA, suggesting that the FBS context does not seem to alter significantly BSA binding. Because protein concentration cannot be determined exactly for BFS, the values for the number of binding sites obtained from these experiments cannot be quantitatively compared with those derived from the BSA titrations. Nonetheless, a similar trend is observed, with a significant reduction in the number of binding sites for MP particles that is even more pronounced for PL nanocapsules.

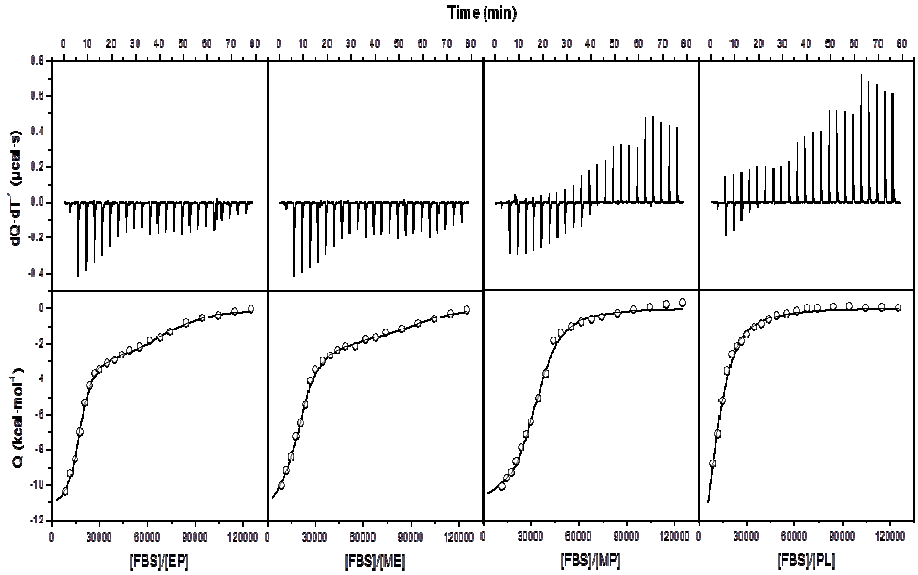

Figure 5. Isothermal titration calorimetry experiments for EP, ME, MP and PL nanoparticles with FBS at 25ºC in 2mM sodium phosphate pH 7.4. Upper panels show the heat effects associated with the injection of FBS into the calorimetric cell containing the nanoparticle. Lower panels show the corresponding binding isotherm normalized for nanoparticle concentration and corrected for the heat of FBS dilution. Solid lines correspond to the best fit of data to a one-site model (equation 1) in the experiments with MP and PL nanoparticles, and to a two sets of independent binding sites model (equation 2) in the experiments with EP and ME nanoparticles.

Taken together, these results clearly indicate that increasing poloxamer content results in a progressive modulation of the protein adsorption behavior of the nanocapsules, minimizing the protein binding capacity through a marked reduction in the number of binding sites.

Colloidal stability

The stability of the samples was studied at physiological pH (7.4) and at different concentrations of two different electrolytes (NaCl and $CaCl_2$) by analyzing the evolution of the diameter of the particles as a function of time.

From the analysis of the coagulation kinetics of the nanosystems it is possible to calculate the stability factor, logW, and hence the critical coagulation concentration (CCC) and the critical stabilization concentration (CSC) of the nanoparticles. Figure 6 shows the logarithm of the stability factor versus salt concentration. Studying CCC and CSC values we can estimate the effective surface charge and gain information about the hydrophilicity character of the surface of our nanosystems, both parameters modulated by the presence of proteins on the surface. It is noteworthy that CCC values with $CaCl_2$ are always lower than those with NaCl because divalent ions have a greater screening capacity favoring the aggregation of the system. Concerning CSC values, they are dependent on the hydration forces that appear at medium and high ionic strengths on hydrophilic nanoparticles when great amounts of hydrated ions are accumulated at the proximities of the surface. The repulsive hydration forces begin to act improving the stability of the nanosystem when the salinity value exceeds the CSC value (38,39). Again, calcium shows higher restabilization capacity compared to sodium. Respecting the stability of the system in NaCl, no aggregation of the particles was detected even at concentrations up to 4M because the overlap of both CCC and CSC concentrations induces completely stable systems.

Analyzing the colloidal stability in $CaCl_2$ (see table 3 and figure 6) we find that EP nanocapsules are the least stable of the systems studied presenting the lowest CCC value. The presence of poloxamer molecules adsorbed onto the shell of ME nanosystem is corroborated by reason of these particles are more stable than

pure Epikuron ones. No aggregation of MP and PL nanoparticles was detected because the concentration of poloxamer is higher on their shells and these molecules contribute to the stabilization of the systems by means of steric mechanism and increase the surface hydrophilicity attributed to the PEO fragments.

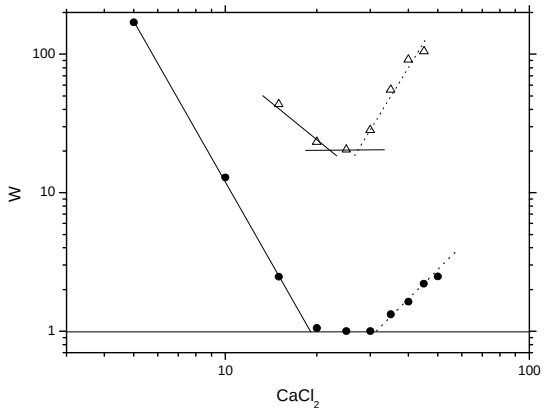

Figure 6. Stability factor vs. calcium chloride concentration at pH 7.4: EP nanocapsules (●), and ME ones (△). The solid line helps to locate the CCC value, while dashed lines point to the CSC data.

The presence of a protein corona after the incubation of the particles with 10%FBS can be also detected because the colloidal stability is modified. Proteins absorbed on the surface increase the hydrophilic character of the particles reflected in the restabilization processes. As in the previous case, all the nanosystems after the exposure to proteins were stable in NaCl.

Comparing CCC and CSC values of ME nanoparticles in calcium before and after the incubation with proteins, unlike the first case they aggregated, after the incubation they were as reflected in the electrophoretic mobility results. EP nanocapsules show also stable in all the concentrations confirming the presence of proteins absorbed on the surface significant stability differences, revealing a

different surface composition after the incubation with the FBS related with the presence of a protein corona surrounding the original shell of the particles. From these experiments no conclusions about the presence of a protein corona can be drawn about MP and PL nanoparticles because their behavior is the same. Surface differences cannot be detected due to the complete stability they showed in all the cases.

Table 3. Critical coagulation concentrations (CCC) and critical stabilization concentration (CSC) of our different nanocapsules before (bare nanoparticles) and after incubation with 10% FBS (nanoparticles + protein corona)

pH 7,4 $CaCl_2$	**Bare nanoparticles**		**Nanoparticles +protein corona**	
	Ccc (mM)	Csc (mM)	Ccc (mM)	Csc (mM)
EP	19	31	70	75
ME	22	25	stable	stable
MP	stable	stable	stable	stable
PL	stable	stable	stable	stable

In vitro uptake of nanocapsules by cancer cells

To understand the influence of the shell composition in the uptake by lung cancer cells, Coumarin 6, which has been extensively used as a fluorescent marker of lipid nanoparticles (40-42), was encapsulated in the core of the lipid nanosystems. We exposed the A549 cells, as a model of cancer cells, to our four types of nanocapsules and mesured their uptake by flow cytometry. Figure 7 shows the flow cytometry results obtained from cells treated for 3, 7, 24 and 48 h with the different nanoparticle systems.

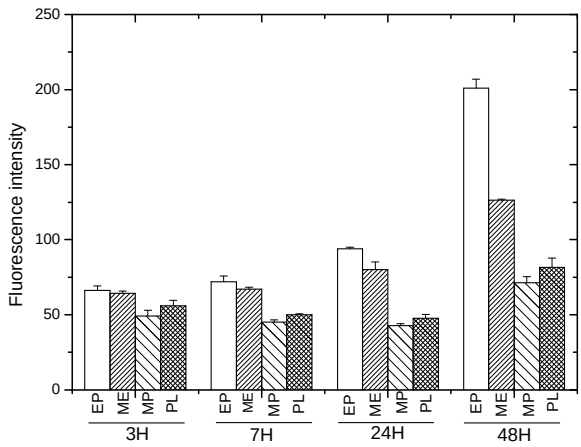

Figure 7. Quantitative study of cellular uptake efficiency for the EP,ME, MP and PL nanocapsules loaded by Coumarin 6 in A549 cells after 3, 7, 24 and 48h.

Significant variations in particle uptake result from the different composition of the shell. Thus for EP nanocapsules, at all the time points we investigated the uptake was higher. These particles are taken up to a much greater extent than those with a high concentration of poloxamer in the shell. This could be related with the fact that the protein corona is higher developed in EP nanocapsules and these proteins absorbed facilitate the uptake by the cells.

The data reported confirm that as the concentration of poloxamer increases in the shell of the particles, the uptake is less because the hydrophilicity of the surface is higher .This is present from early in the uptake profile but the differences between particles increase with the exposure time. Surface hydrophobicity has been considered as a major determinant of cellular response. Increasing the surface hydrophobicity the protein adsorption at the surface will increase, in accordance with the protein binding data from physico-chemical characterization experiments. Because there are a large number of proteins on the

cell surface, the interaction between the cell and nanocapsules become stronger and the uptake by the cells will be higher if the protein adsorption ability is strengthened. Comparable results were observed by Hu et al. and Allen et al. (43, 44).

Cellular uptake efficiency of nanoparticles by A549 cells was qualitatively evaluated using fluorescence microscopy after 24 hours of incubation. Figures 8 B, C, D and E show the fluorescence images of cells incubated with coumarin 6 loaded EP, ME, MP and PL nanoparticles respectively. Comparing the different nanocarriers, the green fluorescence intensity in cells treated with EP nanoparticles is higher than the cells incubated with the other nanosystems, as previous flow cytometry results showed, indicating a higher cellular uptake efficiency. The green fluorescence intensity surrounding DAPI stained nuclei decreases, and hence the uptake efficiency, as the concentration of poloxamer increases on the surface of the carriers. No green fluorescence was detected either when cells were incubated with the four types of blank particles (results not shown) and in the untreated control sample (Figure 8 A.), presenting the images only the blue fluorescence from the stained nuclei. The intensity of the cells incubated with free coumarin 6 was similar to the particles with poloxamer (MP and PL nanocapsules) than those composed by epikuron (ME and EP nanocapsules).

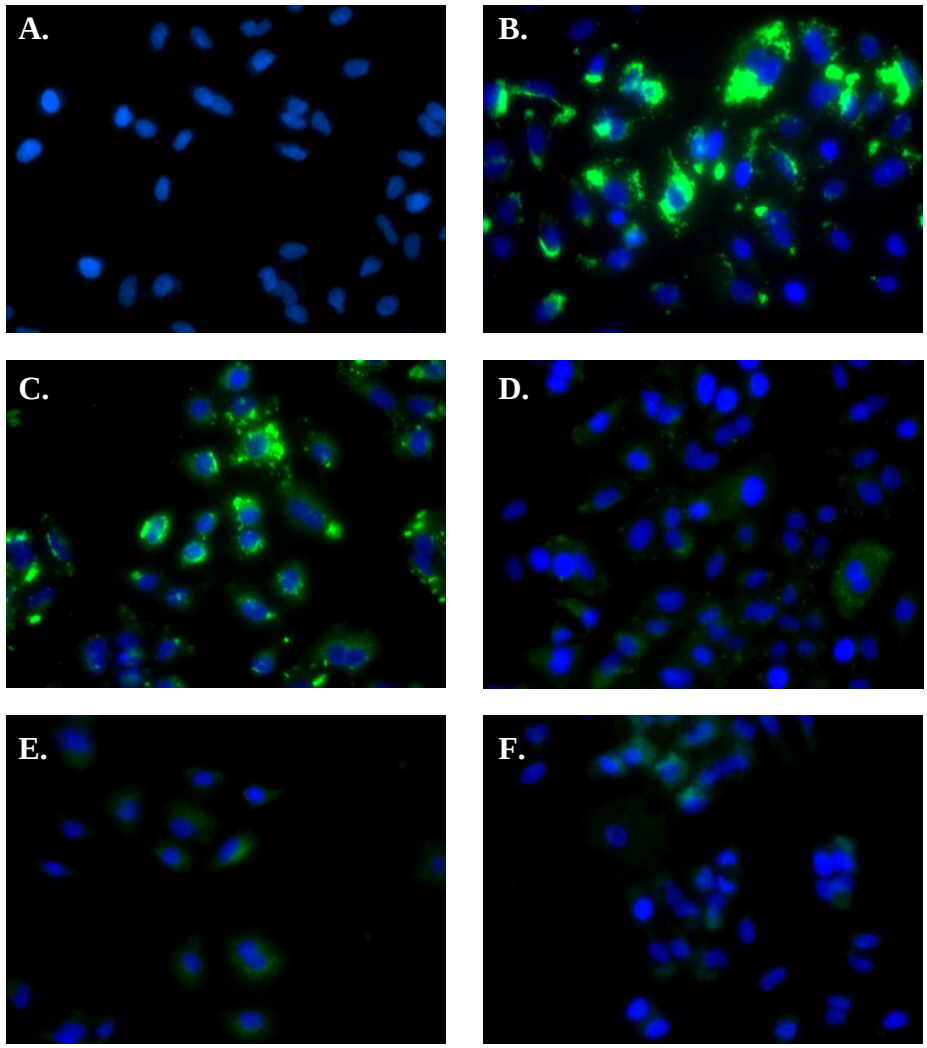

Figure 8. Fluorescence microscopy of A549 cells after incubation with free coumarin 6 (F) and coumarin 6 loaded EP (B), ME (C), MP (D) and PL (E) nanocapsules for 24h. The control of untreated cells is also showed (A).

Cytotoxicity Assays of Docetaxel-loaded nanoparticles

The therapeutic effect of docetaxel-loaded nanocapsules was determined by sulforhodamine-B colorimetric assay on the A549 cell line. Cell were treated with increasing concentrations of free docetaxel or the different docetaxel-loaded nanocapsules for 48 hours. The analysis of the encapsulation efficiency of docetaxel by high performance liquid chromatography (HPLC) showed that during first 5 hours of cleaning by dyalisis the 80% of the docetaxel which is in the core of the particles is released. From this time point untill 24 hours the 20% of docetaxel remained encapsulated in the oily core (see Figure 9).

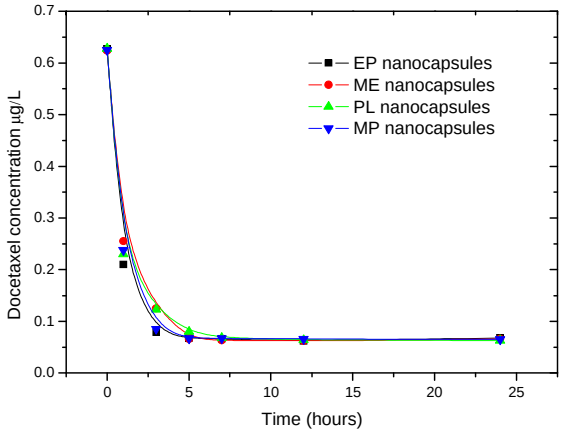

Figure 9. Concentration of docetaxel encapsulated in the particles after 1, 3, 5, 12 and 24 hours of dialysis.

Figure 10 shows the inhibitory concentration 50 (IC_{50}) in each case. A549 cells were also treated with empty EP, ME, MP or PL nanoparticles (data not shown) and no significant differences in growth patterns were found comparing with untreated A549 cells, meaning that empty nanocapsules were not toxic within the measured concentrations. It was found that DOC-MP and DOC-PL nanocapsules characterized by a higher amount of Pluronic F127 had lower cytotoxicity than the particles with less concentration of this molecule (DOC-ME

nanoparticles) and the pure epikuron ones (EP nanoparticles). A markedly lower proliferation rate was observed in A549 cells treated with docetaxel-loaded nanocapsules than those treated with free docetaxel. The four types of docetaxel loaded nanoparticles induced high cell death levels exerting 11.1-fold (DOC-EP), 8.0-fold (DOC-ME) and 3,2-fold (DOC-MP and DOC-PL) more potent cytotoxic effect *versus* free docetaxel. These results indicate that the treatment with docetaxel loaded nanocapsules enhanced drug internalization by A549 cells allowing a decrease in the dose. Similar results where showed in our group working with MCF 7 breast cancer cells exposed to lipid nanocapsules composed of a different shell but similarly loaded with docetaxel (5).

The data reported show that the most cytotoxic particles are those without Pluronic F127 (DOC-EP) and that as the concentration of poloxamer increase in the shell of the particles, the cytotoxicity decreases. This phenomenon appeared to correspond reasonably well to the cellular uptake efficiency, the protein adsorption and the hydrophilicity character of the surfaces.

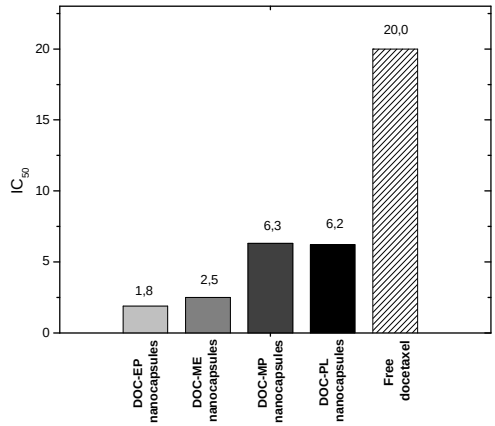

Figure 10. IC_{50} values (drug concentration producing 50% reduction in absorbance in control cells) of free docetaxel and docetaxel-loaded nanoparticles, expressed in nM

In vitro uptake of nanocapsules by monocytes and macrophages

Additionaly to the *in vitro* studies of the particles in A549 cells, an uptake assay was performed in the monocytic cell line U937 to determine if the immunitary clearance of these nanocapsules is affected by the shell composition. In the figure 11 are represented the fluorescence intensity detected by flow cytometry after 3, 7, 24 and 48h of exposure of monocytic U937 cell line and macrophage-like activated U937 cells to our different nanosystems loaded with coumarin 6.

The trend of this uptake study in activated U937 cells is the same than the one in A549. In both cases the uptake is higher in EP nanosystems and this uptake is reduced when the concentration of poloxamer increases on the surface. In both cases the steric repulsion effect produced by the extended PEO chains of pluronic F127 prevents protein adsorption and thus, interactions with macrophages and A549 cells. The concentration of pluronic may also play an important role because it has been reported that in general PEG chains, which have the same structure than PEO chains of poloxamer, form different structures on the surface of the particle for a low or a high surface coverage. The configuration adopted at low concentration is called "mushroom" where chains are located closer to the surface leaving gaps compared with the configuration adopted at high concentration of PEG and pluronic, known as "brush" because the motion of the chains is restricted, guaranteeing a complete coverage of the surface (45, 46). The surface of ME nanoparticles is composed by a low concentration of pluronic F127 while MP and PL present a high concentration. Stolnik et al working with polystyrene nanoparticles which were incubated with different concentrations of poloxamer obtaining different percentage of surface coverage showed a decrease in protein adsorption when the coverage by poloxamer was increased and improved circulation time in blood (47). Uptake by macrophages is also affected by the charge of particles (48). Particles bearing cationic or anionic surface charges are

phagocytated to a higher extent compared to neutral particles of the same size and they also present a higher uptake in non-phagocytic cells (49). According to electrophoretic mobility results EP nanoparticles are strong negatively charged as a result of the phospholipid molecules composition and this anionic charge may be related with the higher uptake of this nanosystem by macrophages. When the concentration or poloxamer increases in the surface the charged is reduced along with protein adsorption and uptake by cells.

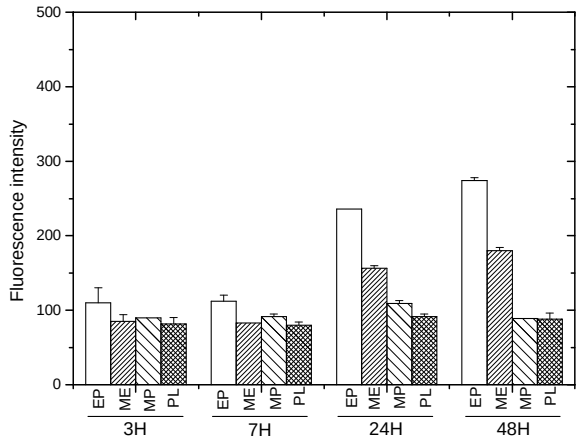

Figure 11. Quantitative study of cellular uptake efficiency for the EP,ME, MP and PL nanocapsules loaded by Coumarin 6 in activated U937 cells (A) after 3, 7, 24 and 48h.

Conclusions

In this study different techniques were used to investigate how the surface composition of lipid nanocapsules influences the protein adsorption and hence, the uptake and cytotoxicity by cancer cells, and the immune clearance by macrophages. ITC and electrophoresis were used to study the interactions between proteins and nanoparticle surfaces showing that the presence of poloxamer, a non-ionic surfactant, on the surface of lipid nanocapsules significantly reduced protein

adsorption when particles were dispersed in culture medium with proteins, by increasing the hydrophilicity of the surface and the steric hindrance. This affected their uptake by cancer cells and cytotoxicity, since both were decreased when the density of poloxamer in the shell was higher. Macrophage association was also significantly reduce upon functionalization of the lipid nanoparticles with poloxamer. Hence, the nature and concentration of the surfactant can be used to control the interactions of lipid nanocapsules with the biological environment.

References

1. Ojea-Jimenez I, Garcia-Fernandez L, Lorenzo J, Puntes VF. Facile Preparation of Cationic Gold Nanoparticle-Bioconjugates for Cell Penetration and Nuclear Targeting. *Acs Nano*. 2012 Sep;6(9):7692-702.

2. Senzer N, Nemunaitis J, Nemunaitis D, Bedell C, Edelman G, Barve M, et al. Phase I Study of a Systemically Delivered p53 Nanoparticle in Advanced Solid Tumors. *Mol Ther*. 2013 May;21(5):1096-103.

3.Xiao ZY, Levy-Nissenbaum E, Alexis F, Luptak A, Teply BA, Chan JM, et al. Engineering of Targeted Nanoparticles for Cancer Therapy Using Internalizing Aptamers Isolated by Cell-Uptake Selection. *Acs Nano*. 2012 Jan;6(1):696-704.

4. Huynh NT, Passirani C, Saulnier P, Benoit JP. Lipid nanocapsules: A new platform for nanomedicine. *Int J Pharmaceut*. 2009 Sep 11;379(2):201-9.

5. Sanchez-Moreno P, Boulaiz H, Ortega-Vinuesa JL, Peula-Garcia JM, Aranega A. Novel Drug Delivery System Based on Docetaxel-Loaded Nanocapsules as a Therapeutic Strategy Against Breast Cancer Cells. *International Journal of Molecular Sciences*. 2012 Apr;13(4):4906-19.

6. Khalid MN, Simard P, Hoarau D, Dragomir A, Leroux JC. Long circulating poly(ethylene glycol)-decorated lipid nanocapsules deliver docetaxel to solid tumors. *Pharm Res-Dordr.* 2006 Apr;23(4):752-8.

7. Lozano MV, Torrecilla D, Torres D, Vidal A, Dominguez F, Alonso MJ. Highly efficient system to deliver taxanes into tumor cells: Docetaxel-loaded chitosan oligomer colloidal carriers. *Biomacromolecules.* 2008 Aug;9(8):2186-93.

8. Maeda H. The enhanced permeability and retention (EPR) effect in tumor vasculature: The key role of tumor-selective macromolecular drug targeting. Adv *Enzyme Regul.* 2001;41:189-207.

9. Torrecilla D, Lozano MV, Lallana E, Neissa JI, Novoa-Carballal R, Vidal A, et al. Anti-tumor efficacy of chitosan-g-poly(ethylene glycol) nanocapsules containing docetaxel: Anti-TMEFF-2 functionalized nanocapsules vs. non-functionalized nanocapsules. *Eur J Pharm Biopharm.* 2013 Apr;83(3):330-7.

10. Rata-Aguilar A, Sanchez-Moreno P, Jodar-Reyes AB, Martin-Rodriguez A, Boulaiz H, Marchal-Corrales JA, et al. Colloidal stability and "in vitro" antitumor targeting ability of lipid nanocapsules coated by folate-chitosan conjugates. *J Bioact Compat Pol.* 2012 Jul;27(4):388-404.

11. Sanchez-Moreno P, Ortega-Vinuesa JL, Boulaiz H, Marchal JA, Peula-Garcia JM. Synthesis and Characterization of Lipid Immuno-Nanocapsules for Directed Drug Delivery: Selective Antitumor Activity against HER2 Positive Breast-Cancer Cells. *Biomacromolecules.* 2013 Dec 9;14(12):4248-59.

12. Stoddart A. Corona creation. *Nat Mater.* 2013 Nov;12(11):946-.

13. Lynch I, Dawson KA. Protein-nanoparticle interactions. *Nano Today*. 2008 Feb-Apr;3(1-2):40-7.

14. Salvati A, Pitek AS, Monopoli MP, Prapainop K, Bombelli FB, Hristov DR, et al. Transferrin-functionalized nanoparticles lose their targeting capabilities when a biomolecule corona adsorbs on the surface. *Nat Nanotechnol.* 2013 Feb;8(2):137-43.

15. Sheng Y, Yuan Y, Liu CS, Tao XY, Shan XQ, Xu F. In vitro macrophage uptake and in vivo biodistribution of PLA-PEG nanoparticles loaded with hemoglobin as blood substitutes: effect of PEG content. *J Mater Sci-Mater M.* 2009 Sep;20(9):1881-91.

16. Arnida, Janat-Amsbury MM, Ray A, Peterson CM, Ghandehari H. Geometry and surface characteristics of gold nanoparticles influence their biodistribution and uptake by macrophages. *Eur J Pharm Biopharm.* 2011 Apr;77(3):417-23.

17. Fang C, Bhattarai N, Sun C, Zhang MQ. Functionalized Nanoparticles with Long-Term Stability in Biological Media. *Small.* 2009 Jul 17;5(14):1637-41.

18. Shan XQ, Liu CS, Yuan Y, Xu F, Tao XY, Sheng Y, et al. In vitro macrophage uptake and in vivo biodistribution of long-circulation nanoparticles with poly(ethylene-glycol)-modified PLA (BAB type) triblock copolymer. Colloid Surface B. 2009 Sep 1;72(2):303-11.

19. Walkey CD, Olsen JB, Guo HB, Emili A, Chan WCW. Nanoparticle Size and Surface Chemistry Determine Serum Protein Adsorption and Macrophage Uptake. *J Am Chem Soc.* 2012 Feb 1;134(4):2139-47.

20. Muller RH, Wallis KH. Surface Modification of Iv Injectable Biodegradable Nanoparticles with Poloxamer Polymers and Poloxamine-908. *Int J Pharmaceut.* 1993 Jan 1;89(1):25-31.

21. Muller RH, Maassen S, Weyhers H, Mehnert W. Phagocytic uptake and cytotoxicity of solid lipid nanoparticles (SLN) sterically stabilized with poloxamine 908 and poloxamer 407. *J Drug Target.* 1996;4(3):161-70.

22. Goppert TM, Muller RH. Plasma protein adsorption of Tween 80-and poloxamer 188-stabilized solid lipid nanoparticles. *J Drug Target.* 2003 May;11(4):225-31.

23. Gaur U, Sahoo SK, De TK, Ghosh PC, Maitra A, Ghosh PK. Biodistribution of fluoresceinated dextran using novel nanoparticles evading reticuloendothelial system. *Int J Pharmaceut.* 2000 Jul 20;202(1-2):1-10.

24. Moghimi SM, Hunter AC. Poloxamers and poloxamines in nanoparticle engineering and experimental medicine. *Trends Biotechnol.* 2000 Oct;18(10):412-20.

25. Hong W, Chen D, Zhang X, Zeng J, Hu H, Zhao X, et al. Reversing multidrug resistance by intracellular delivery of Pluronic(R) P85 unimers. *Biomaterials.* 2013 Dec;34(37):9602-14.

26. Saxena V, Hussain MD. Polymeric Mixed Micelles for Delivery of Curcumin to Multidrug Resistant Ovarian Cancer. *J Biomed Nanotechnol.* 2013 Jul;9(7):1146-54.

27. Lindman S, Lynch I, Thulin E, Nilsson H, Dawson KA, Linse S. Systematic investigation of the thermodynamics of HSA adsorption to N-iso-

propylacrylamide/N-tert-butylacrylamide copolymer nanoparticles. Effects of particle size and hydrophobicity. *Nano Lett.* 2007 Apr;7(4):914-20.

28. Baier G, Costa C, Zeller A, Baumann D, Sayer C, Araujo PHH, et al. BSA Adsorption on Differently Charged Polystyrene Nanoparticles using Isothermal Titration Calorimetry and the Influence on Cellular Uptake. *Macromol Biosci.* 2011 May 12;11(5):628-38.

29. Calvo P, RemunanLopez C, VilaJato JL, Alonso MJ. Development of positively charged colloidal drug carriers: Chitosan coated polyester nanocapsules and submicron-emulsions. *Colloid Polym Sci.* 1997 Jan;275(1):46-53.

30. Minta JO, Pambrun L. Invitro Induction of Cytologic and Functional-Differentiation of the Immature Human Monocyte-Like Cell-Line U-937 with Phorbol-Myristate Acetate. *Am J Pathol.* 1985;119(1):111-26.

31. Liu MY, Wu MC. Induction of Human Monocyte Cell-Line U937 Differentiation and Csf-1 Production by Phorbol Ester. *Exp Hematol.* 1992 Sep;20(8):974-9.

32. Sanchez-Moreno P, Ortega-Vinuesa JL, Martin-Rodriguez A, Boulaiz H, Marchal-Corrales JA, Peula-Garcia JM. Characterization of different functionalized lipidic nanocapsules as potential drug carriers. *Int J Mol Sci.* 2012;13(2):2405-24.

33. Alexis F, Pridgen E, Molnar LK, Farokhzad OC. Factors affecting the clearance and biodistribution of polymeric nanoparticles. *Mol Pharm.* 2008 Jul-Aug;5(4):505-15.

34. Santander-Ortega MJ, Lozano-Lopez MV, Bastos-Gonzalez D, Peula-Garcia JM, Ortega-Vinuesa JL. Novel core-shell lipid-chitosan and lipid-poloxamer nanocapsules: stability by hydration forces. *Colloid Polym Sci.* 2010 Jan;288(2):159-72.

35. Gref R, Luck M, Quellec P, Marchand M, Dellacherie E, Harnisch S, et al. 'Stealth' corona-core nanoparticles surface modified by polyethylene glycol (PEG): influences of the corona (PEG chain length and surface density) and of the core composition on phagocytic uptake and plasma protein adsorption. *Colloids Surf B Biointerfaces.* 2000 Oct 1;18(3-4):301-13.

36. Karmali PP, Simberg D. Interactions of nanoparticles with plasma proteins: implication on clearance and toxicity of drug delivery systems. *Expert Opin Drug Del.* 2011 Mar;8(3):343-57.

37. Roser M, Fischer D, Kissel T. Surface-modified biodegradable albumin nano- and microspheres. II: effect of surface charges on in vitro phagocytosis and biodistribution in rats. *Eur J Pharm Biopharm.* 1998 Nov;46(3):255-63.

38. Molina-Bolivar JA, Galisteo-Gonzalez F, Hidalgo-Alvarez R. Particle enhanced immunoassays stabilized by hydration forces: a comparative study between IgG and F(ab ')(2) immunoreactivity. *J Immunol Methods.* 1998 Feb 1;211(1-2):87-95.

39. Molina-Bolivar JA, Ortega-Vinuesa JL. How proteins stabilize colloidal particles by means of hydration forces. *Langmuir.* 1999 Apr 13;15(8):2644-53.

40. Rivolta I, Panariti A, Lettiero B, Sesana S, Gasco P, Gasco MR, et al. Cellular Uptake of Coumarin-6 as a Model Drug Loaded in Solid Lipid Nanoparticles. *J Physiol Pharmacol.* 2011 Feb;62(1):45-53.

41. Liu YT, Li K, Pan J, Liu B, Feng SS. Folic acid conjugated nanoparticles of mixed lipid monolayer shell and biodegradable polymer core for targeted delivery of Docetaxel. *Biomaterials*. 2010 Jan;31(2):330-8.

42. Xu PF, Yin Q, Shen JN, Chen LL, Yu HJ, Zhang ZW, et al. Synergistic inhibition of breast cancer metastasis by silibinin-loaded lipid nanoparticles containing TPGS. *Int J Pharmaceut*. 2013 Sep 15;454(1):21-30.

43. Hu Y, Xie JW, Tong YW, Wang CH. Effect of PEG conformation and particle size on the cellular uptake efficiency of nanoparticles with the HepG2 cells. *J Control Release*. 2007 Mar 12;118(1):7-17.

44. Allen LT, Tosetto M, Miller IS, O'Connor DP, Penney SC, Lynch I, et al. Surface-induced changes in protein adsorption and implications for cellular phenotypic responses to surface interaction. *Biomaterials*. 2006 Jun;27(16):3096-108.

45. Storm G, Belliot SO, Daemen T, Lasic DD. Surface Modification of Nanoparticles to Oppose Uptake by the Mononuclear Phagocyte System. *Adv Drug Deliver Rev*. 1995 Oct;17(1):31-48.

46. Owens DE, Peppas NA. Opsonization, biodistribution, and pharmacokinetics of polymeric nanoparticles. *Int J Pharmaceut*. 2006 Jan 3;307(1):93-102.

47. Stolnik S, Daudali B, Arien A, Whetstone J, Heald CR, Garnett MC, et al. The effect of surface coverage and conformation of poly(ethylene oxide) (PEO) chains of poloxamer 407 on the biological fate of model colloidal drug carriers. Bba-*Biomembranes*. 2001 Oct 1;1514(2):261-79.

48. Thiele L, Merkle HP, Walter E. Phagocytosis and phagosomal fate of surface-modified microparticles in dendritic cells and macrophages. *Pharm Res-Dordr*. 2003 Feb;20(2):221-8.

49. Frohlich E. The role of surface charge in cellular uptake and cytotoxicity of medical nanoparticles. *Int J Nanomed*. 2012;7:5577-91.

Chapter 5. Conclusions

According to the objectives proposed, the conclusions of the more relevant results of this thesis are:

◇ Using a simple solvent displacement technique it was possible to prepare lipid nanocapsules with the required droplet size, monodispersity, and colloidal stability constituted by an olive oil core and a polymer shell of different surfactants, including phosphatidyl-serine, that let us to synthesized a novel lipid nanocapsule system in which the shell was enriched by carboxyl groups, capable of covalently linking antibodies.

◇ When a lipophilic molecule (e.g. Nile red, Coumarin 6 or docetaxel) was encapsulated in the oily core of lipid nanocapsules, its uptake by tumor cells was highly favored according to the *in vitro* studies. A markedly lower proliferation rate was observed in cancer cells treated with docetaxel-loaded nanoparticles than cells treated with free docetaxel. Encapsulated docetaxel maintained its full activity and

preserved its mechanism of action, suggesting that the use of lipid nanocapsules may allow decreased doses of docetaxel without loss of therapeutic effect.

◇ Folate-chitosan conjugates bearing different folate concentrations and lipid nanocapsules coated by these conjugates were successfully synthesized yielding to a novel functionalized nanosystem. When folate targeted nanosystems were studied *in vitro* they showed specific intracellular uptake in folate-receptor-positive cell lines.

◇ A novel lipid nanocapsule system composed, among other surfactants, by deoxycholic acid for covalent immobilization of protein molecules through carboxyl groups, was successfully prepared, and a simple method to vectorize these systems with monoclonal antibodies was established. The immunological recognition of specific antigen molecules revealed an adequate surface disposition of antibody molecules on the surface.

◇ Immuno-nanocapsules functionalized with herceptin, a monoclonal antibody against HER2 receptor, were obtained. *In vitro* studies suggested their ability to deliver drugs selectively toward target cells: HER2 positive breast cancer cells.

◇ The presence of poloxamer on the surface of lipid nanocapsules significantly reduced protein adsorption when particles were dispersed in culture medium with proteins. The presence of this non-ionic surfactant increased the hydrophilicity of the surface and the steric hindrance, which reduced the adhesion of proteins. Uptake and cytotoxicity was dependent on the surface properties of the nanocarriers, in such a way that when the concentration of poloxamer was increased in the shell of the particles the uptake was less effective and, therefore, the nanoparticles were less toxic because the protein corona was less developed. Uptake by cancer cells and macrophages was higher when the protein adsorption ability was strengthened. Hence, the nature and concentration of the surfactant can

be used to control the interactions of lipid nanocapsules with the biological environment.

◇ Characterization of nanocarriers in terms of electric state and colloidal stability agreed with the nature of the shell of nanocapsules and the electrophoretic results confirmed the presence of the different molecules used in their synthesis. When particles were functionalized with proteins, the original isoelectric point of bare particles moved towards the isoelectric point of the pure protein.

Conclusiones

En relación a los objetivos propuestos, las conclusiones extraídas de los resultados más relevantes de esta tesis son los siguientes:

◇ Mediante una técnica de desplazamiento de solvente se sintetizaron nanocápsulas lipídicas, con tamaño, estabilidad coloidal y monodispersidad adecuados, constituidas por un núcleo de aceite de oliva y una pared polimérica compuesta por diferentes surfactantes tales como la fosfatidilserina, entre otros. Mediante la utilización de este fosfolípido se preparó un nuevo sistema con una cubierta enriquecida en grupos carboxilo para permitir la unión covalente de anticuerpos a través de estos grupos.

◇ La captación de moléculas hidrofóficas tales como Rojo Nilo, Cumarina 6 o docetaxel por parte de distintas líneas celulares cancerígenas se incrementó cuando éstas fueron encapsuladas en el núcleo oleoso de las nanocapsules de acuerdo con los ensayos *in vitro*. Además, la tasa de proliferación de las líneas celulares cancerígenas que fueron tratadas con partículas que contenían docetaxel en su núcleo oleoso, se redujo en comparación con aquéllas tratadas con docetaxel sin encapsular. La encapsulación de docetaxel no alteró su mecanismo de acción ni

actividad. Esos resultados sugieren que gracias al uso de nanocapsulas lipídicas, las dosis de docetaxel se pueden reducir sin que se pierda su efecto terapéutico.

◇ Se consiguió sintetizar conjugados de quitosano y ácido fólico a distintas concentraciones, que se dispusieron adsorbidos en la pared de las nanocápsulas lipídicas, dando lugar a nanosistemas vectorizados frente a receptores de ácido fólico, que están sobreexpresados en algunas líneas celulares de cáncer. Se estudió la captación de dichos sistemas *in vitro* en células cancerígenas confirmando una mayor captación por aquellas células que sobreexpresaban receptors frente a dicha molécula.

◇ Se desarrolló un nuevo sistema compuesto por ácido desoxicólico, entre otros surfactantes, para permitir la inmobilización de proteínas a través de los grupos carboxilo aportados por dicha molécula, y se estableció un método sencillo de vectorización de estos sistemas con distintos anticuerpos monoclonales. Los ensayos inmunológicos de las partículas vectorizadas mostraron reconocimiento específico antígeno-anticuerpo, demostrando que la disposición de los anticuerpos en la superficie unidos covalentemente es adecuada.

◇ Se obtuvieron nanocápsulas funcionalizadas con herceptín, un anticuerpo monoclonal frente al receptor HER2, sobreexpresado en algunos tipos de cáncer. Los ensayos *in vitro* mostraron la capacidad de estos sistemas para liberar fármacos de forma selectiva frente a células cancerígneas HER2 positivas de cancer de mama.

◇ La presencia de poloxámero en la superficie de las nanocápsulas lipídicas redujo significativamente la adsorción proteica cuando las partículas estaban dispersas en medio de cultivo suplementado con suero bovino fetal. La presencia de este surfactante no iónico aumentó la hidrofilicidad de la superficie y el impedimento estérico lo que se tradujo en una menor adhesion de proteínas La captación de estas partículas y su citotoxicidad también fueron dependientes de la composición de la

superficie de modo que a medida que la concentración de poloxámero aumentó en la pared de las nanopartículas, la captación por parte de las células fue menos efectiva y por lo tanto las nanocápsulas portadoras de docetaxel menos citotóxicas. Por lo que la naturaleza y concentración del surfactante se puede modificar para controlar la interacción de las nanocápsulas lipídicas con el medio en el que se encuentran dispersas.

◇ Los resultados obtenidos de la caracterización físico-química de los nanosistemas, en relación al estado eléctrico y la estabilidad coloidal de las nanocápsulas, confirmaron la presencia de las distintas moléculas usadas en su síntesis. Cuanto se funcionalizaron las partículas con proteínas, el punto isoeléctrico original de las partículas sin vectorizar se acercó al de la proteína pura.